

**Oligosaccharides Prepared by Automated Glycan
Assembly as Basis for Structural Investigations of
Carbohydrates**

Inaugural-Dissertation
to obtain the academic degree
Doctor rerum naturalium (Dr. rer. nat.)

submitted to the Department of Biology, Chemistry, and Pharmacy
of Freie Universität Berlin

by

Andrew Kononov

(from Minsk, Belarus)

January 2018

This work was performed between November 2013 and October 2017 under the guidance of Prof. Dr. Peter H. Seeberger in the Department of Biomolecular Systems, Max Planck Institute of Colloids and Interfaces Potsdam, and the Institute of Chemistry and Biochemistry, Freie Universität Berlin.

1st reviewer: Prof. Dr. Peter H. Seeberger

2nd reviewer: Prof. Dr. Beate Kokschi

Date of oral defense: 15.11.2018

Declaration

This is to certify that the entire work in this thesis has been carried out by Mr. Andrew Kononov. The assistance and help received during the course of investigation have been fully acknowledged.

(Date, Place)

(Signature)

Acknowledgements

I am deeply thankful to Professor Dr. Peter H. Seeberger for giving me the opportunity to pursue my doctoral studies at the cutting edge of technology and innovation, as well as for his guidance and support over the past years.

I thank Prof. Dr. Beate Kokschi for agreeing to review this dissertation.

I am grateful to Dr. Martina Delbianco for fruitful discussions as well as successful and productive work on the collaborative project.

I thank Prof. Dr. Jesús Jiménez-Barbero, Dr. Ana Poveda, Yang Yu, Dr. Sebastian Götze, Dr. Jeyakumar Kandasamy for successful collaborations.

I am grateful to Dr. Richard Fair and Dr. Martina Delbianco for proofreading my thesis. I thank Renée Roller for proofreading the Zusammenfassung.

I also thank all the members of Biomolecular Systems department that I got to know over the past 4 years, especially automation subgroup members, for a friendly atmosphere and nice working environment.

Finally, I thank my parents for their support and belief in me.

List of publications

Scientific Publications

1. Yu Y., **Kononov A.**, Delbianco M., Seeberger P.H. A Capping Step During Automated Glycan Assembly Enables Access to Complex Glycans in High Yield, *in press*.
2. Delbianco M., **Kononov A.**, Poveda A., Yu Y., Jiménez-Barbero J. and Seeberger P.H. Tailor-made carbohydrate materials, *in preparation*.
3. Nonaka M., Bao X., Matsumura F., Götze S., Kandasamy J., **Kononov A.**, Broide D.H., Nakayama J., Seeberger P.H., and Fukuda M. Synthetic di-sulfated iduronic acid attenuates asthmatic response by blocking T-cell recruitment to inflammatory sites. *Proc. Natl. Ac. Sc.*, 2014, *111*, 8173-8178.

Scientific Conferences and Symposia

1. **Kononov A.**, Seeberger P.H., “Optimization of automated solid-phase synthesis”. // „1st Biomolecular Systems Conference”. **Poster Presentation**. Berlin, Germany. 11-13 November, 2016
2. **Kononov A.**, Seeberger P.H., “Automated solid-phase synthesis of glycosaminoglycans”. // 2nd International Symposium „Frontiers in Biomaterial Science”. **Poster Presentation**. Leipzig, Germany. 24-25 June, 2016
3. **Kononov A.**, Seeberger P.H., „Strategies of automated solid-phase synthesis of glycosaminoglycans”. // Conference “Glycoproteins and Glycolipids”. **Lecture**. Ringberg, Germany. 6-11 September 2015
4. **Kononov A.**, Seeberger P.H., „Toward automated solid-phase synthesis of glycosaminoglycans”. // Conference „Automation in Chemistry: Carbohydrate Synthesis and Continuous Flow”. **Lecture**. Ringberg, Germany. 21-25 September 2014
5. **Kononov A.**, Kandasamy J., Seeberger P.H. „Toward automated solid-phase synthesis of dermatan sulfate”. // Third Symposium of the Max Planck-RIKEN Joint Research Center. **Poster Presentation**. Ringberg, Germany. 21-24 Mai 2014

Contents

1	Introduction.....	17
1.1	General introduction.....	17
1.2	Structure of carbohydrates.....	17
1.2.1	Conformations of monosaccharides.....	17
1.2.2	Oligosaccharide conformations.....	19
1.3	Approaches to the synthesis of carbohydrates.....	20
1.3.1	Enzymatic synthesis of carbohydrates.....	20
1.3.2	Chemical synthesis of oligosaccharides.....	23
1.3.3	One-pot synthesis of oligosaccharides.....	26
1.3.4	Automated solution-phase synthesis of oligosaccharides.....	27
1.3.5	Automated solid-phase synthesis of carbohydrates.....	28
1.4	Aim of the thesis.....	34
2	Automated Solid-Phase Oligosaccharide Synthesis Optimization.....	35
2.1	Introduction.....	35
2.2	Photo cleavable Linker and Solid Support.....	36
2.2.1	Existing synthesis of photo cleavable linker and resin preparation.....	36
2.2.2	Investigation of resin loading and photo cleavage.....	37
2.2.3	The development of a new photo cleavable linker.....	46
2.3	Resin loading determination using different building blocks.....	50
2.4	Optimization of automated solid-phase synthesis.....	50
2.4.1	Acidic wash optimization.....	52
2.4.2	Glycosylation cycle.....	53
2.4.3	Deprotection cycle.....	57
2.5	Conclusions and perspectives.....	59
2.6	Experimental part.....	60

2.6.1	Synthesis of photo cleavable linkers and their derivatives.....	60
	Resin functionalization and resin loading determination.....	65
2.6.2	Photo cleavage of linkers and functionalized resin	68
2.6.3	Automated glycan assembly.....	72
3	Synthesis of oligosaccharides for structural investigations	76
3.1	Synthesis of building blocks.....	77
3.2	Synthesis of an oligosaccharide library	78
3.3	AGA of a mannose 50-mer.....	81
3.4	Molecular dynamics investigations	83
3.5	Toward tailor-made carbohydrate-based materials	85
3.6	Conclusions and perspectives	86
3.7	Experimental part	87
3.7.1	Automated glycan assembly.....	87
3.7.2	Synthesis of homopolymers	90
3.7.3	Synthesis of heteropolymers.....	102
4	Synthesis of Glycosaminoglycans	117
4.1	Introduction	117
4.2	Synthetic Strategies to Access GAGs.....	118
4.3	Synthesis of Building Blocks	123
4.3.1	Synthesis of galactosamine building blocks.....	123
4.3.2	Synthesis of iduronic acid building blocks.....	125
4.3.3	Synthesis of glucuronic acid building block	127
4.4	Testing synthetic strategies to access dermatan sulfate.....	127
4.5	Automated synthesis of dermatan sulfate oligosaccharides	129
4.6	Synthesis of disulfated iduronic acid.....	129
4.7	Conclusions and perspectives	131
4.8	Experimental Part	131

4.8.1	Synthesis of galactosamine building blocks.....	131
4.8.2	Synthesis of iduronic acid building blocks.....	137
4.8.3	Synthetic strategies for dermatan sulfate.....	140
4.8.4	Automated synthesis of dermatan sulfate oligosaccharides	144
4.8.5	Synthesis of disulfated iduronic acid.....	151
5	References.....	155

List of Abbreviations

Ac	Acetyl
Ac ₂ O	Acetic anhydride
AcOH	Acetic acid
ACN/CH ₃ CN	Acetonitrile
AGA	Automated glycan assembly
BB	Building block
BF ₃ .Et ₂ O	Boron trifluoride diethyl etherate
Bn	Benzyl
BnBr	Benzyl bromide
Bz	Benzoyl
BzCl	Benzoyl chloride
Bu	Butyl
PhCH(OMe) ₂	Benzaldehyde dimethyl acetal
Cap	Protecting group used for capping
CHCl ₃	Chloroform
CsOAc	Cesium acetate
Cs ₂ CO ₃	Cesium carbonate
CSA	Camphor sulfonic acid
δ	Chemical shift
d	doublet
DBU	1,8-diazabicycloundec-7-ene
DCM	Dichloromethane
DMF	Dimethylformamide
DMSO	Dimethyl Sulfoxide
Et	Ethyl
Et ₂ O	Diethyl ether
Et ₃ N	Triethylamine
ESI	Electrospray ionization
EtOH	Ethanol
Equiv	Equivalent
Fmoc	9-fluorenylmethoxycarbonyl

GAG	Glycosaminoglycan
GlcNAc	N-acetylglucosamine
Hal	Halogen
HPLC	High-performance liquid chromatography
N ₂ H ₄ .AcOH	Hydrazine acetate
HRMS	High resolution mass spectroscopy
I ₂	Iodine
Lev	Levulinoyl
Man	Mannose
MALDI	Matrix assisted laser desorption/ionization
m	Multiplet
Me	Methyl
NaOMe	Sodium methoxide
Nap	2-Naphthylmethyl bromide
NP	Normal phase
NIS	N-iodosuccinimide
NMR	Nuclear magnetic resonance
NPG	Non-participating protecting group
OPME	One-pot multienzyme synthesis
Pd/C	Palladium on activated charcoal
Ph ₃ P	Triphenylphosphine
Ph	Phenyl
PyBOP	Benzotriazol-1-yl-oxytripyrrolidinophosphonium hexafluorophosphate
TBAI	Tertabutylammonium iodide
ppm	Parts per million
PG	Protecting group
PPG	Participating protecting group
tPG	Temporary protecting group
Py	Pyridine
RT	Room Temperature
s	Singlet
TCA	Trichloroacetyl

THF

TfOH

TLC

TMSOTf

Tetrahydrofuran

Triflic Acid

Thin Layer Chromatography

Trimethylsilyltrifluoromethanesulfonate

List of Figures

Figure 1. Possible conformations of monosaccharides.	18
Figure 2. Representation of the anomeric effect using dipoles.	18
Figure 3. Orbital representation of the anomeric effect.	19
Figure 4. Angles determining conformations of glycosidic linkages.	19
Figure 5. Glycosyl donors that are used in chemical synthesis of oligosaccharides. ...	25
Figure 6. Structure of Merrifield resin.	30
Figure 7. The dependence of synthesis yield on oligosaccharide length	35
Figure 8. Overview of the oligosaccharides prepared by AGA.	81
Figure 9. HPLC trace of the crude 50-mer 60 compared with the potential deletion sequence 60a and uncapped 49-mer 60b.	83
Figure 10. The global minima conformations of oligosaccharides obtained by molecular dynamics simulations.	84
Figure 11. Definition of the torsion angles for every type of linkage	85
Figure 12. Types of glycosaminoglycans ¹⁴¹	117
Figure 13. Building blocks required for the synthesis of dermatan and chondroitin sulfate repeating units.....	119

List of Schemes

Scheme 1. Enzymatic synthesis of Le ^X -OBn. Modified from ref. 30	21
Scheme 2. One of the examples of the enzymatic synthesis of oligosaccharides. Modified from ref. 32.....	21
Scheme 3. A representative example of the OPME (One-pot multienzyme synthesis). Modified from ref. 33.....	22
Scheme 4. Linear approach to oligosaccharide synthesis.	23
Scheme 5. Convergent approach to oligosaccharide synthesis.	24
Scheme 6. General scheme of glycosylation reaction.	24
Scheme 7. Neighboring group participation.....	25
Scheme 8. An example of remote-group (C-4) participation (NPG – non-participating group).	26
Scheme 9. Solvent effects in glycosylation reactions.	26
Scheme 10. Iterative one-pot synthesis of oligosaccharides. Modified from ref. 72. ..	27
Scheme 11. General scheme of the automated solution-phase synthesis with electrochemical preactivation.....	28
Scheme 12. General scheme of automated glycan assembly (AGA). Reprinted (adapted) with permission from Seeberger, P. H., The logic of automated glycan assembly. Acc Chem Res 2015, 48 (5), 1450-63. Copyright (2015) American Chemical Society	29
Scheme 13 Linkers used in AGA. Modified from ref. 98	32
Scheme 14. Types of glycosylation donors used in AGA and promoters for their activation.	33
Scheme 15. Synthesis of photo cleavable linker.	37
Scheme 16. Modification of the Merrifield resin with the photo cleavable linker.....	37
Scheme 17. Methods of loading determination.....	39
Scheme 18. Testing the efficiency of resin functionalization.	41
Scheme 19. Photo cleavage of the standard photo cleavable linker.....	41
Scheme 20. The reactivity of different photo cleavable linker derivatives.....	42
Scheme 21. One possible mechanism of the photo cleavage process.....	44
Scheme 22. Structures of potential functionalized resins that can be used for photo cleavage.....	46
Scheme 23. Synthesis of model compounds for investigation of the photocleavage reaction.....	46

Scheme 24. Synthesis of new photocleavable linker.....	48
Scheme 25. Functionalization of the resin with the new linker.	48
Scheme 26. Photocleavage of the resin functionalized with the new photocleavable linker.....	49
Scheme 27. Possible explanation for the unexpected result with the new photocleavable linker.	49
Scheme 28. Resin loading determination using two different types of building blocks.	50
Scheme 29. Synthesis of mannoside dimer used as a model reaction for glycosylation cycle optimization.	54
Scheme 30. Synthesis of mannoside dimer as a model reaction for the deprotection cycle optimization.	57
Scheme 31. Retrosynthetic analysis of natural and unnatural oligosaccharides.	76
Scheme 32. Retrosynthetic analysis of the building blocks	77
Scheme 33. Synthesis of glucosamine building block.	78
Scheme 34. Scheme of oligosaccharide synthesis for compounds 52a-c.....	79
Scheme 35. Scheme of AGA for chitin hexasaccharide 54 (with capping).	80
Scheme 36. An example of block-coupling procedure	86
Scheme 37. Rearrangement of oxocarbenium ion to oxazoline in case of aminosugars.	119
Scheme 38. Strategy I for the synthesis of dermatan sulfate.....	121
Scheme 39. Strategy II for the synthesis of dermatan sulfate.	122
Scheme 40. Galactosamine BBs: retrosynthetic analysis.	123
Scheme 41. Synthesis of glucosamine derivative 75.....	124
Scheme 42. Synthesis of galactosamine BB 62a from 75. Mechanism of C-4 inversion.	124
Scheme 43. Synthesis of galactosamine building block 62b.....	125
Scheme 44. Retrosynthetic analysis of iduronic acid building blocks	125
Scheme 45. Synthesis of iduronic acid building blocks.	126
Scheme 46. Synthesis of iduronic acid building blocks	126
Scheme 47. Synthesis of glucuronic acid building block 65.....	127
Scheme 48. Synthesis of disaccharide 103	127
Scheme 49. Investigation of synthetic strategies on dermatan sulfate disaccharide ..	128

Scheme 50. Potential sulfation method	129
Scheme 51. AGA of dermatan sulfate oligosaccharides	129
Scheme 52. Synthesis of iduronic acid derivatives	130

List of Tables

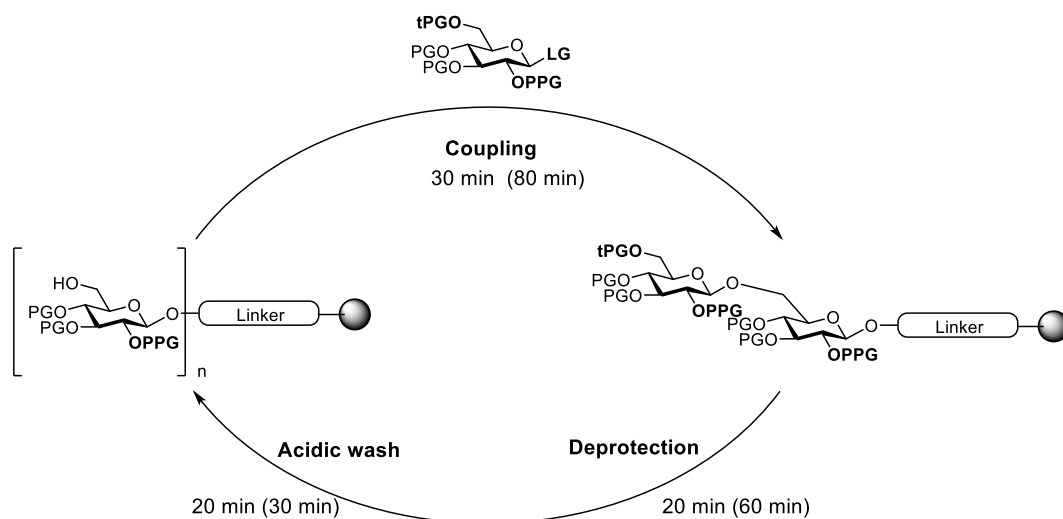
Table 1. Amount of solvent used for the synthesis of a 50-mer.....	36
Table 2. The influence of acidity on the photo cleavage reaction.....	43
Table 3. Time required for different steps in standard AGA.....	52
Table 4. Optimization of acidic wash cycle.	53
Table 5. Optimization of glycosylation conditions	55
Table 6. Optimization of glycosylation cycle.....	56
Table 7. Total amount of solvents used in the glycosylation cycle.....	56
Table 8. Optimization of the Fmoc-deprotection cycle.....	58
Table 9. Optimization of Fmoc-deprotection cycle.....	58
Table 10. Total amount of solvents used in the deprotection cycle	59
Table 11. AGA of mannose oligosaccharides	78
Table 12. Amount of solvents used for the synthesis of 50-mer.	82

Summary

Carbohydrates are the most abundant type of biomolecules. However, relatively little is known about the relation between the molecular structure of carbohydrates and their macroscopic properties. In order to shed light on this structure-properties correlation, the method that would enable an access to a variety of carbohydrate structures has to be developed. One of the most promising approaches to achieve this goal is automated solid-phase synthesis.

Chapter 2 of this dissertation covers the in-depth analysis and optimization of all the steps of automated glycan assembly, including resin functionalization, elongation cycle and photocleavage process. Several resin loading determination methods have been tested and the method with the best applicability has been chosen. New photo cleavable linkers have been designed and their potential applicability in automated glycan assembly has been investigated.

The optimization of the elongation cycle (acidic wash, glycosylation, deprotection steps) in automated glycan assembly has been performed. The time required for the cycle has been significantly reduced (from 170 min to 60 min), the amount of solvents and building blocks used has been decreased that made the overall automated process greener.



The scheme of automated glycan assembly. Time required for an elongation cycle before (in brackets) and after optimization.

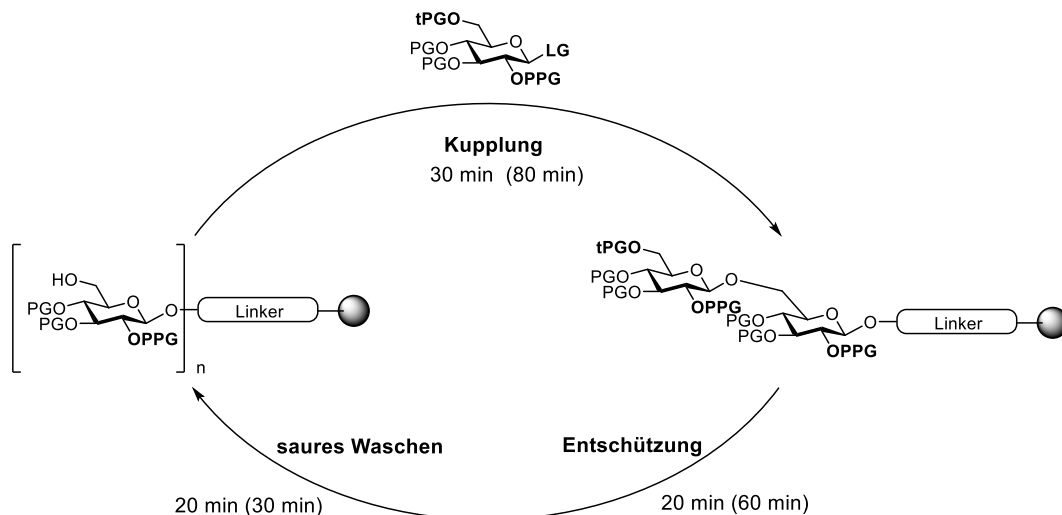
Chapter 3 describes the application of the optimized conditions to the synthesis of a library of oligo- and polysaccharides. It has been shown that these conditions can be applied

Zusammenfassung

Kohlenhydrate sind die häufigste Art von Biomolekülen. Über die Korrelation zwischen der Molekülstruktur von Kohlenhydraten und ihren makroskopischen Eigenschaften ist jedoch relativ wenig bekannt. Um dieses Verhältnis aufzuklären, muss eine Methode entwickelt werden, die Zugang zu einer Vielzahl von Kohlenhydratstrukturen ermöglicht. Einer der vielversprechendsten Ansätze zur Erreichung dieses Ziels ist die automatisierte Festphasensynthese.

Kapitel 2 dieser Dissertation behandelt die detaillierte Analyse und Optimierung aller Schritte der automatisierten Festphasensynthese von Oligosacchariden, einschließlich der Funktionalisierung von Harzen, des Elongationszyklus und des Photospaltungsprozesses. Mehrere Bestimmungsverfahren der Harzbeladung wurden getestet und das Verfahren mit der besten Anwendbarkeit wurde ausgewählt. Neue photospaltbare Linker wurden entwickelt und ihre mögliche Anwendbarkeit im Automated Glycan Assembly wurde untersucht.

Die Optimierung des Elongationszyklus (saure Wasch-, Glykosylierungs-, Entschützungs Schritte) beim Automated Glycan Assembly wurde durchgeführt. Die für den Zyklus benötigte Zeit wurde signifikant verkürzt (von 170 min auf 60 min), die Menge an verwendeten Lösungsmitteln und Bausteinen wurde verringert, wodurch der gesamte automatisierte Prozess umweltfreundlicher wurde.

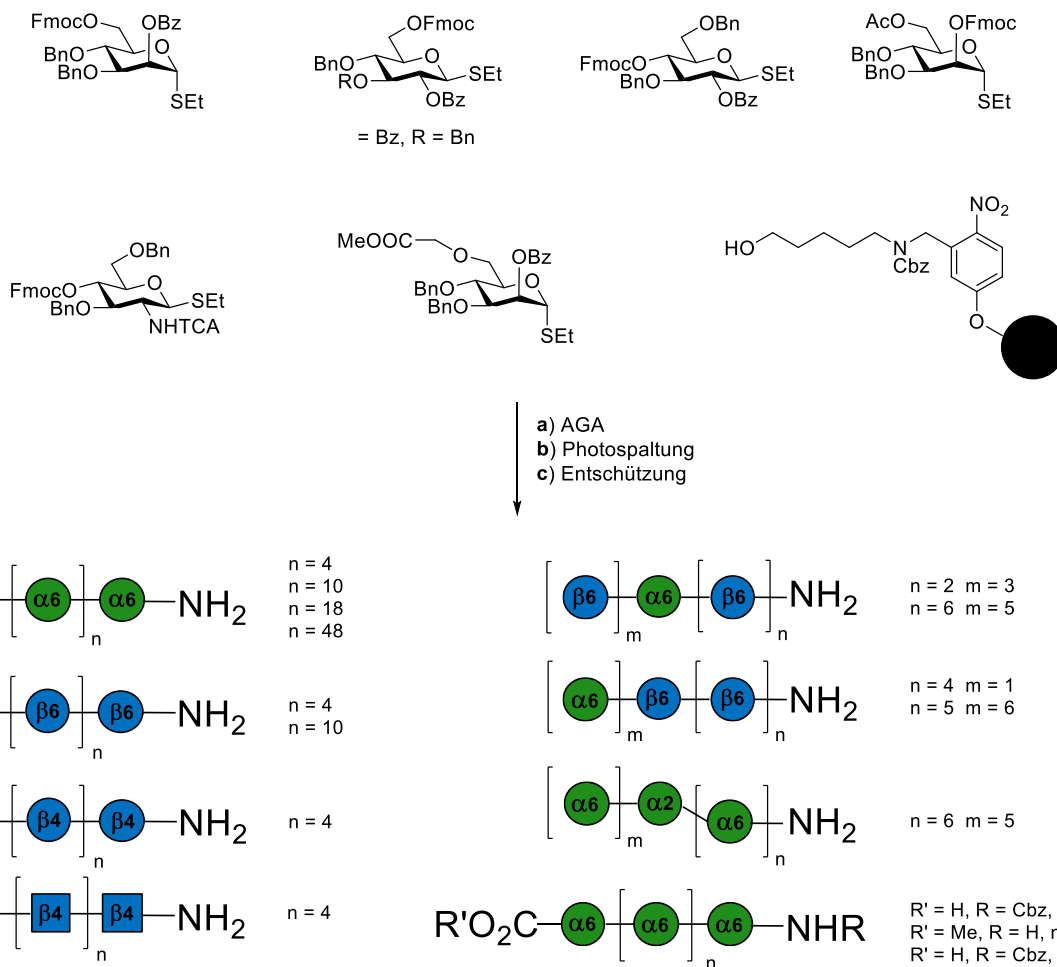


Das Schema des Automated Glycan Assembly. Zeit, die für einen Elongationszyklus vor (in Klammern) und nach der Optimierung benötigt wird

Kapitel 3 beschreibt die Anwendung der optimierten Bedingungen für die Synthese einer Bibliothek von Oligo- und Polysacchariden für Strukturuntersuchungen. Es wurde gezeigt, dass diese Bedingungen auf verschiedene Bausteine angewendet werden können und

einen modularen und schnellen Zugang zu einer Vielzahl von Strukturen (Mannoside, Glucoside, Glucosaminoside) ermöglichen.

Molekülmodellierungsstudien der synthetisierten Kohlenhydrate wurden durchgeführt. Es wurde gezeigt, dass Hexamere von Mannose, Glucose und Glucosamin unterschiedliche molekulare Formen haben, die zu Unterschieden in ihren makroskopischen Eigenschaften führen können.



Synthese von Oligosacchariden für Strukturuntersuchungen

Kapitel 4 beschreibt die Untersuchung möglicher Strategien zur Synthese von Glykosaminoglykanen. Die Synthese von Bausteinen, die für die Synthese von Dermatan- und Chondroitinsulfat-Oligosacchariden benötigt werden, wurde durchgeführt. Mehrere Strategien für die Synthese von vollständig entschützten Dermatan-sulfat-Oligosacchariden wurden getestet. Die automatisierte Synthese von mehreren Dermatan-sulfat-Oligosacchariden wurde durchgeführt. Die Synthese von mehreren Iduronsäure-Derivaten wurde durchgeführt. Die optimalen Synthesebedingungen für die disulfatierte Iduronsäure, die zuvor als potentieller

Inhibitor für die CCL20 - Heparinsulfat - Wechselwirkung identifiziert wurde, wurden ausgewählt.

Zusammenfassend wird gezeigt, dass die automatisierte Festphasensynthese einen Zugang zu der Bibliothek von Oligosacchariden ermöglicht, die für weitere Strukturuntersuchungen verwendet werden kann.

1 Introduction

1.1 General introduction

Carbohydrates are the most abundant type of biological molecules.¹ They are used by organisms as energy storage materials (like starch²⁻³ and glycogen⁴), as structural components (like cellulose⁵ and chitin⁶⁻⁷), they play an important role in cell-cell adhesion (like glycosaminoglycans)⁸⁻¹⁰ and are a part of glycoproteins¹¹ and glycolipids¹² that have various biological functions. It is also notable how small differences in structure of polysaccharides can lead to substantial differences in their macroscopic properties. For example, cellulose forms flexible structure of cotton,⁵ whereas chitin is a major component of a robust exoskeleton of crabs.⁷

Nevertheless, relatively little is known about the correlation between the molecular structure and macroscopic properties of carbohydrates.¹³⁻¹⁴ That is why the development of methods that enable fast and modular access to various carbohydrate structures is of a big importance.

1.2 Structure of carbohydrates

Polysaccharides are comprised of monosaccharides units connected together to form a chain. Therefore, the structure of polysaccharides is determined by the conformation of monosaccharides and by the geometry of glycosidic linkages. Some aspects of monosaccharides' conformations as well as the geometry of glycosidic linkages are discussed below.

1.2.1 Conformations of monosaccharides

Most of the monosaccharides have a rigid ring structure: they exist either as pyranoses (6-membered ring) or furanoses (5-membered ring). The 6-membered ring of monosaccharides can exist in different conformations (Figure 1).¹⁵⁻¹⁶ There are two chair conformations (¹C₄ and ⁴C₁), two boat conformations (B_{1,4}) and ^{1,4}B), one twisted boat (⁵S₀) and one half-chair conformation (⁰H₅). For most of the pyranoses ⁴C₁ chair conformation is the most favorable. For furanoses there are five possible conformations (three envelope ⁴E, ¹E and ⁰E as well as two twisted conformations ²T₃ and ³T₂).

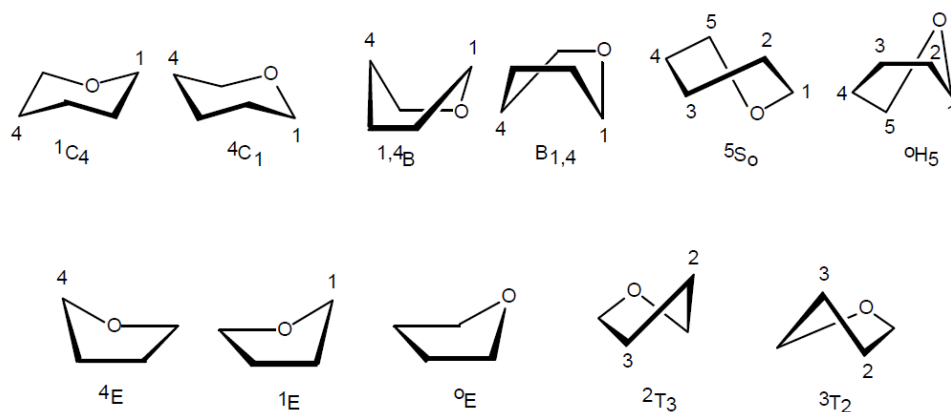


Figure 1. Possible conformations of monosaccharides.

There are several factors that determine monosaccharide conformation. As in the case with other cyclic molecules, equatorial substituents are favored in comparison with axial ones. The other aspect is the anomeric effect. It is a stereoelectronic phenomenon that describes the tendency of an anomeric substituent to prefer an axial orientation.¹⁷

This effect can be represented in two ways. In the first representation (Figure 2) partial dipole moments of the O-5 lone pairs and the bond between C-5 and an anomeric substituent are considered. In the equatorial anomer these dipoles are partially aligned and therefore repelling each other. In the axial anomer, on contrary, they are roughly opposing representing a more stable anomer. The other explanation of the anomeric effect (Figure 3) is following: an electron withdrawing axial substituent is stabilized via hyperconjugation owing to the coplanar orientation of both nonbonding orbital of O-5 and antibonding orbital of C-1. This does not occur with the other anomer, as the nonbonding orbital of O-5 and antibonding orbital of C-1 are in different planes and therefore are not able to interact.

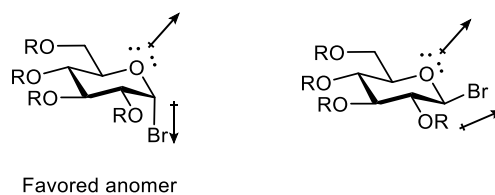


Figure 2. Representation of the anomeric effect using dipoles.

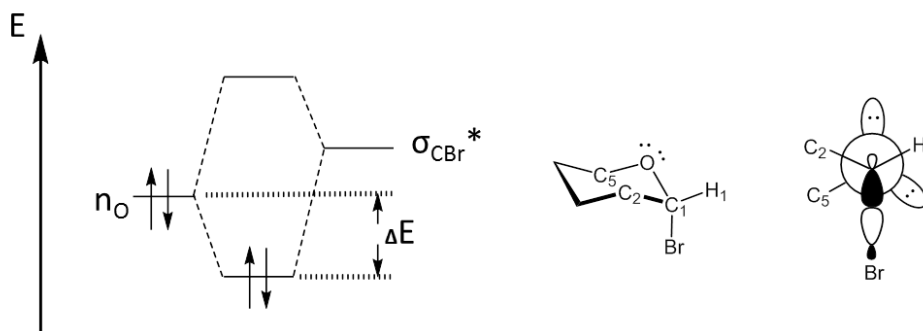


Figure 3. Orbital representation of the anomeric effect.

1.2.2 Oligosaccharide conformations

While monosaccharides generally represent a rigid ring structure, most of the glycosidic linkages are not rigid but flexible. For a characterization of a glycosidic linkage two or three torsion angles have to be determined (Figure 4).

The flexibility of glycosidic linkages makes the conformation characterization very difficult in case of oligosaccharides. Complete characterization of a glycosidic linkage requires knowledge of the number of conformers adopted by the linkage, the time spent in each conformer and the flexibility of each conformer.¹³

The torsion angle Φ is determined largely by the exo-anomeric effect.¹⁸ This is a stereoelectronic effect involving the lone pairs of the linkage oxygen. The torsion angle ψ is determined largely by the steric interactions and hydrogen bonding between residues and the solvent. The torsion angle ω exists only for 1-6 linkages and can adopt three staggered rotamers based on steric interactions.

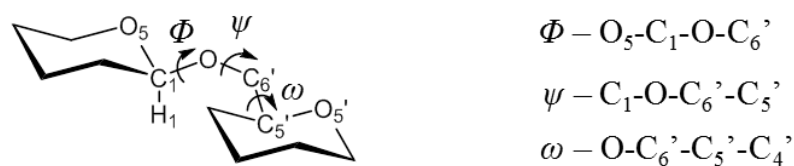


Figure 4. Angles determining conformations of glycosidic linkages.

There are several methods that can be used for characterization of the molecular shape of oligo- and polysaccharides: X-Ray crystallography, nuclear magnetic resonance (NMR) spectroscopy and molecular modelling. Although X-Ray crystallography is a powerful method for structural analysis of biomolecules, it has limited applicability in case of highly flexible oligosaccharide structures. NMR provides only time-averaged conformation data. This has led to the widespread use of molecular modelling for in determining linkage

conformations. However, theoretical calculations are limited by the accuracy of the theory used.

1.3 Approaches to the synthesis of carbohydrates

Extraction of carbohydrates from natural sources allows the access to relatively large variety of structures (like glycosaminoglycans,¹⁹⁻²⁴ plant carbohydrates,²⁵ capsular polysaccharides²⁶⁻²⁸ etc.), but it has a disadvantage: most of the polysaccharides obtained by this method are heterogeneous and this heterogeneity complicates to the large extent the further biological investigation and potential application of these molecules. Hence it is important to develop methods that will enable fast and modular synthesis of structurally-defined oligosaccharides. However, there are several challenges in the synthesis of carbohydrates. Unlike proteins and nucleic acids, carbohydrate molecules are often branched, monosaccharides units can be connected in different ways (for hexoses, for example, there are 5 possible connection points). Additionally, there are two types of linkages (α and β linkages) between monosaccharide units. From the nine monosaccharides found in humans more than 15 million tetrasaccharides can be assembled.²⁹

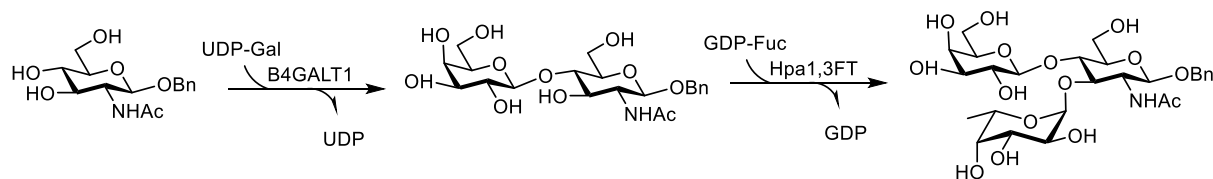
Glycan assembly can be performed using following approaches: enzymatic synthesis, chemical synthesis (manual or automated, solution-phase or on the solid support) or the combination of these methods.

1.3.1 Enzymatic synthesis of carbohydrates

The usage of enzymes for oligosaccharide synthesis enables relatively simple control of glycosylation stereo- and regioselectivity and makes it possible to perform reaction in mild conditions. Two types of enzymes can be used for the synthesis of carbohydrates: glycosyltransferases (enzymes that establish natural glycosidic linkages) and glycosidases (enzymes that hydrolyze glycosidic bonds).

Glycosyltransferases used in glycan synthesis generally catalyze the transfer of a glycosidic donor (in most of the cases nucleotide diphosphate) to a glycosyl acceptor. A representative example of the enzymatic synthesis using glycosyltransferases is the synthesis of Lewis^X derivative (Le^X-OBn) (Scheme 1).³⁰ Initially, benzyl glucosaminoside was glycosylated by uridine 5'-diphosphate-galactose (UDP-Gal) in the presence of β 1,4-galactosyltransferase from bovine milk (B4GALT1). Then, the resulting disaccharide was reacted with guanosine 5'-diphosphate-fucose (GDP-Fuc), in the presence of C-terminal 66

amino acids truncate α 1,3-fucosyltransferase from *Helicobacter pylori* (Hpa1,3FT), giving Le^X-OBn.

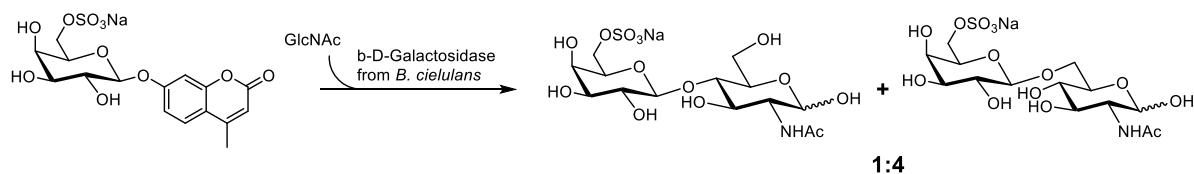


Scheme 1. Enzymatic synthesis of Le^X-OBn. Modified from ref. 30

Enzymatic synthesis using glycosyltransferases has several limitations. Firstly, glycosyltransferases are not readily available (they have to be cloned or overexpressed) and can be used for only a limited scope of substrates. Secondly, nucleotide glycosidic donors are often unstable and/or very expensive.³¹

Glycosidases are the other enzyme type that can be applied for the enzymatic synthesis of glycans. In nature glycosidases hydrolyze glycosidic bonds, therefore, in order to use them for synthetic purposes, their normal function must be reversed. As long as enzymatic reactions are (formally) equilibrium processes, it is possible to force a glycosidase to run in reverse by exposing the enzyme to a large excess of the reaction products and allowing the system to reach equilibrium. Replacing the anomeric hydroxyl group of the glycosyl donor fragment with a good leaving group, such as *para*-nitrophenol (PNP), shifts the equilibrium toward the glycosylation product.

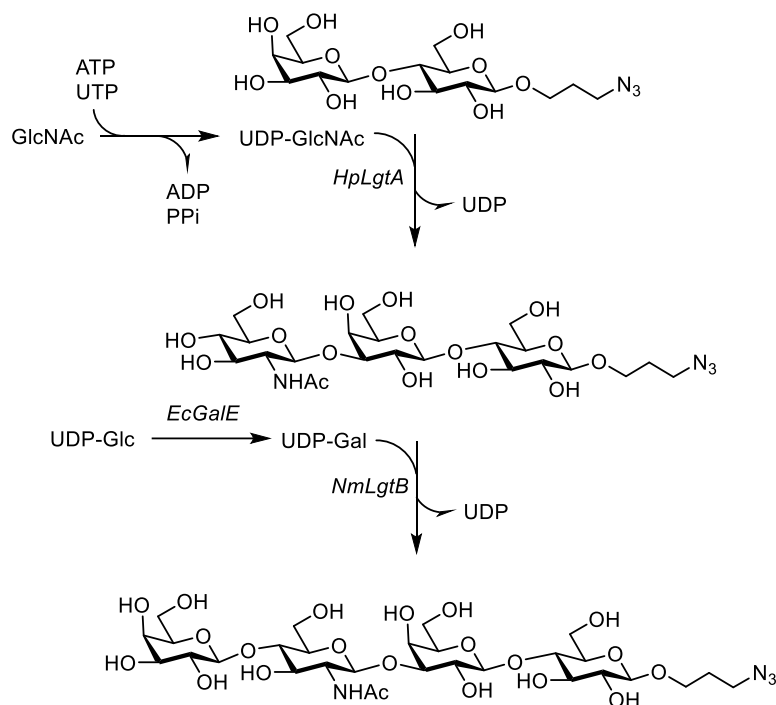
Synthesis of 6'-sulfated disaccharides is an example of glucosidase-catalyzed process (Scheme 2). It was found out that when 4-methylumbelliferyl 6-sulfo β -D-galactopyranoside was used as a glycosylating agent, the enzyme (β -D-galactosidase from *B. circulans*) induced the transfer of 6-sulfo galactosyl residue to a GlcNAc acceptor, giving the mixture of isomers 6'-Sulfo *N*-acetylglucosamine (S6Gal β 1-4GlcNAc) and 6'-Sulfo *N*-acetylglucosamine (S6Gal β 1-6GlcNAc), in a molar ratio 1:4.³²



Scheme 2. One of the examples of the enzymatic synthesis of oligosaccharides.

Modified from ref. 32.

Glycosidases are more stable and more readily accessible than glycosyltransferases. Glycosidase-based transformations can use much broader scope of potential substrates, but they result in lower yields, than glycosyltransferase-catalyzed processes.



Scheme 3. A representative example of the OPME (One-pot multienzyme synthesis).

Modified from ref. 33.

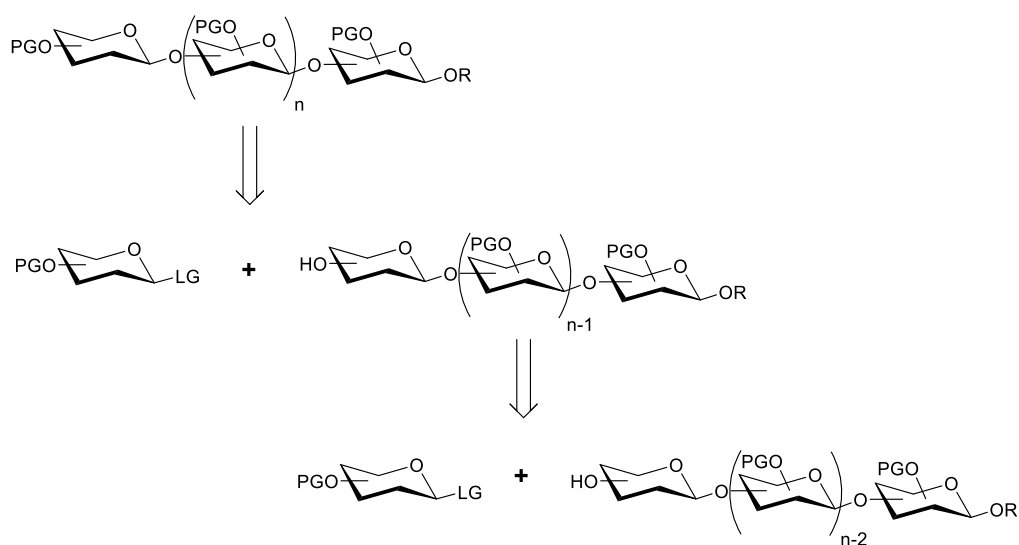
One-pot multienzyme synthesis (OPME) is an interesting modification of the enzymatic approach.³³⁻³⁵ In this method, simple monosaccharides or derivatives can be activated by one or more enzymes to form desired sugar nucleotides for glycosyltransferase-catalyzed formation of target elongated glycans in one pot. Each OPME process adds one monosaccharide or derivative with a desired glycosidic linkage defined by the glycosyltransferase used. Multiple OPME reactions can be carried out to build up more complex glycan targets.³⁶ One of the representative examples of this approach is the synthesis of Lacto-*N*-neotetraose from lactoside, *N*-acetylglucosamine (GlcNAc) and 5'-diphosphate-glucose (Scheme 3).³³ GlcNAc was activated to form UDP-GlcNAc in the presence of adenosine 5'-triphosphate (ATP), uridine 5'-triphosphate (UTP) and a fusion enzyme NahK-Glmu. The resulting UDP-GlcNAc was utilized by a *Helicobacter pylori* β1–3-*N*-acetylglucosaminyltransferase (HpLgtA) to form trisaccharide. At the next step, uridine 5'-diphosphate-galactose (UDP-Gal) was generated *in situ* from uridine 5'-diphosphate-glucose (UDP-Glu) using *Escherichia coli* UDP-galactose-4-epimerase (EcGalE) and utilized by

Neisseria meningitidis β 1–4-galactosyltransferase (NmLgtB) for β 1–4-galactosylation of trisaccharide giving Lacto-N-neotetraose.

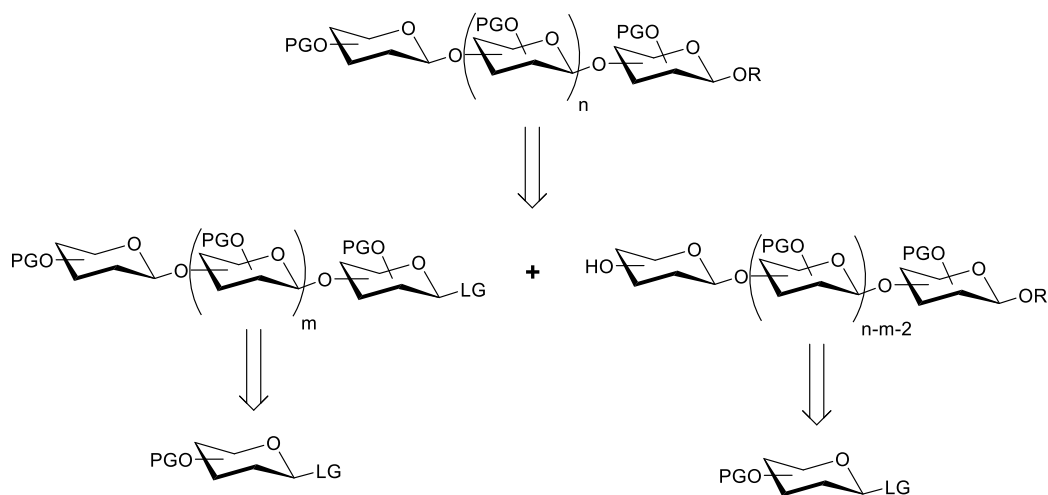
Overall, the usage of enzymes makes it possible to achieve excellent regio- and stereoselectivities in glycosylation transformations without extensive protecting group manipulation. Nevertheless, applicability of enzymatic oligosaccharide synthesis is limited by enzyme availability and the scope of possible enzymatic substrates.

1.3.2 Chemical synthesis of oligosaccharides

There are two approaches for chemical synthesis of oligosaccharides: linear synthesis (Scheme 4) and convergent (blockwise) synthesis (Scheme 5). In the linear approach (Scheme 4) oligosaccharide chain is step-by-step elongated by one unit using monosaccharide building blocks (that have protecting groups (PG) and a leaving group (LG)). In the convergent approach (Scheme 5), several oligosaccharide “blocks” are initially synthesized. Then, they are coupled together giving the desired oligosaccharide.

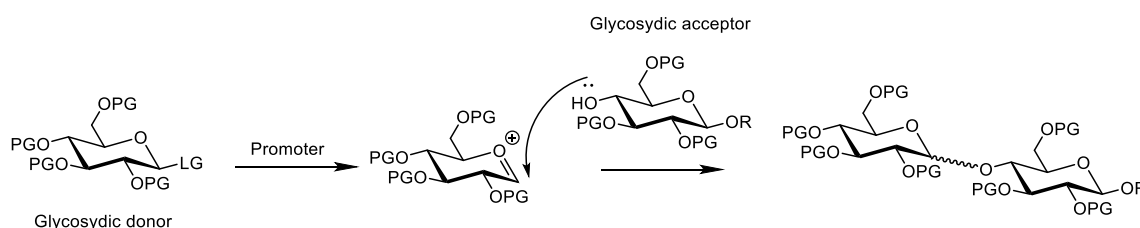


Scheme 4. Linear approach to oligosaccharide synthesis.



Scheme 5. Convergent approach to oligosaccharide synthesis.

The key step of chemical oligosaccharide synthesis are glycosylation reactions (Scheme 6). Glycosidic donor is generally activated by promoter forming a reactive intermediate (oxonium ion) that reacts further with a glycosidic acceptor (a molecule with a nucleophilic center, generally, free hydroxide group).



Scheme 6. General scheme of glycosylation reaction.

A lot of glycosylation donor types were developed (Figure 5). The first example was Koenigs-Knorr method, in which glycosyl halide are used as glycosylation donors. They are activated by silver or heavy metal salts.³⁷⁻³⁸ Among glycosylation donors that are used nowadays are phosphites,³⁹⁻⁴⁰ phosphates,⁴¹ trichloroacetimidates,⁴² thioimidates,⁴³ sulfoxides,⁴⁴ thioglycosides,⁴⁵ disulfides,⁴⁶ selenium glycosides,⁴⁷ thiocyanates,⁴⁸ pentenylglycosides,⁴⁹ glycosyl acetates,⁵⁰ silyl ethers,⁵¹ orthoesters,⁵² carbonates,⁵³ hydroxides,⁵⁴ glycols,⁵⁵ 2-pyridylthiocarbonates,⁵⁶ diazirines.⁵⁷

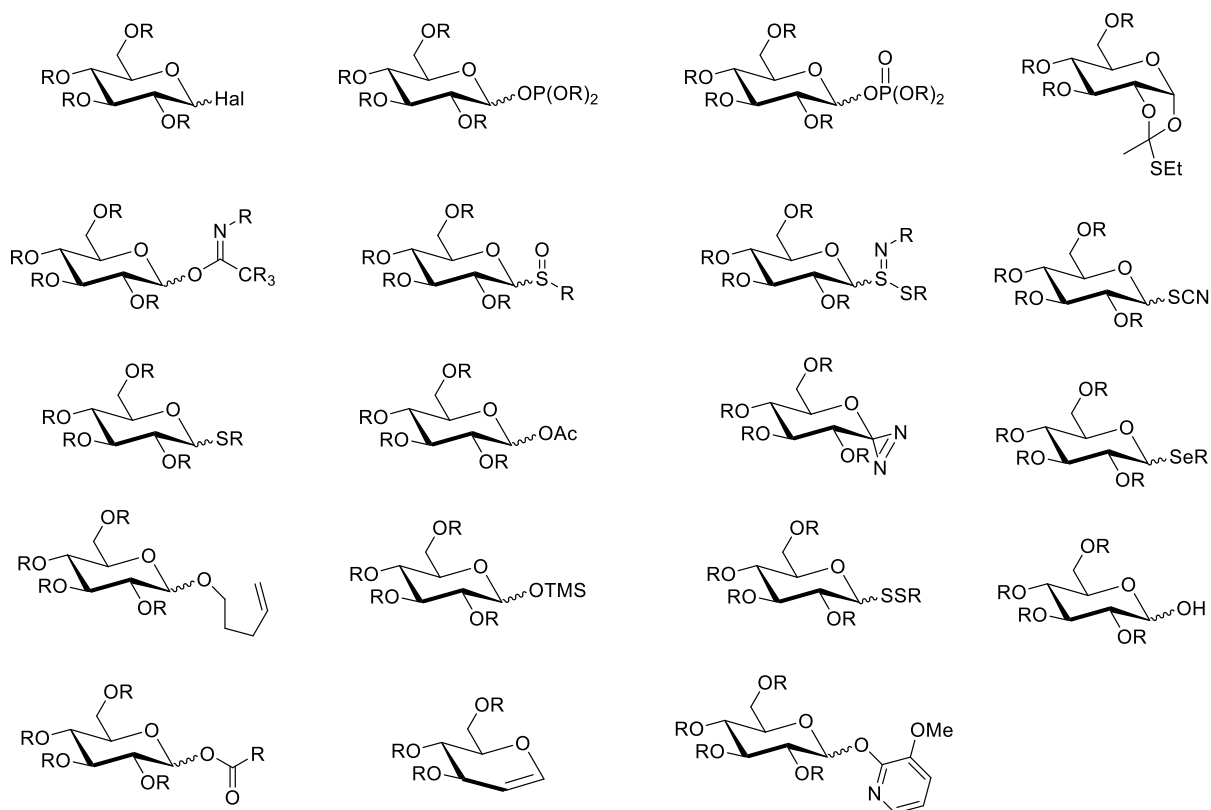
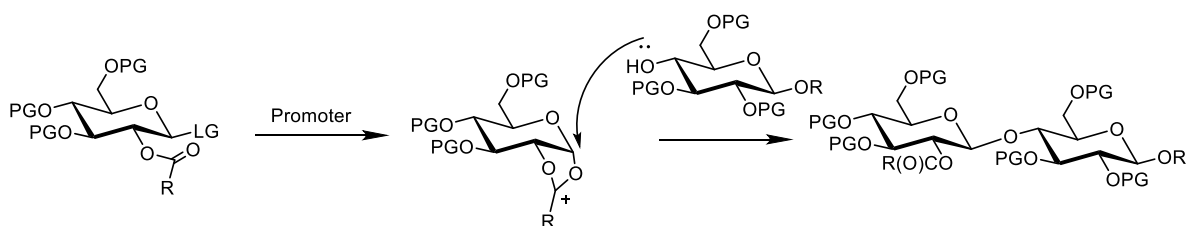


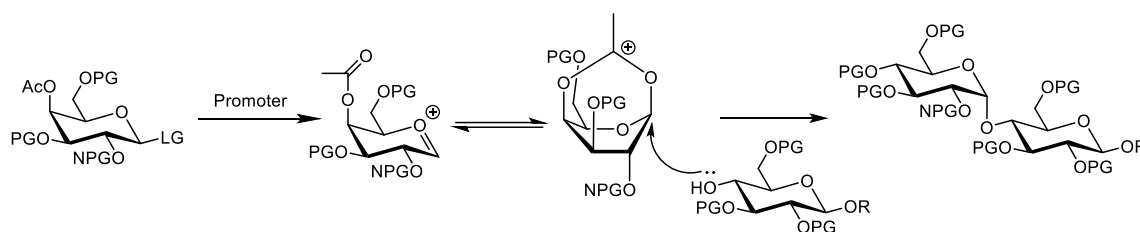
Figure 5. Glycosyl donors that are used in chemical synthesis of oligosaccharides.

The control of glycosylation stereoselectivity is a very important issue in the chemical synthesis of carbohydrates. There are several factors that influence stereoselectivity of glycosylations: structure of the glycosyl donor (protecting groups and the leaving group), structure of the glycosyl acceptor (protecting groups and position of the hydroxyl) and reaction conditions.

Neighboring-group participation is one of the most powerful tools to direct stereoselectivity toward the formation of a 1,2-trans-linked product.⁵⁸ In this case acyloxonium ion is formed and the further attack by a nucleophile is possible only from the trans-face (Scheme 7). Apart from neighboring-group participation, remote-group participation can influence glycosylation stereoselectivity (Scheme 8). Several examples of C-3, C-4 and C-6 participations are described in literature.⁵⁹⁻⁶⁰

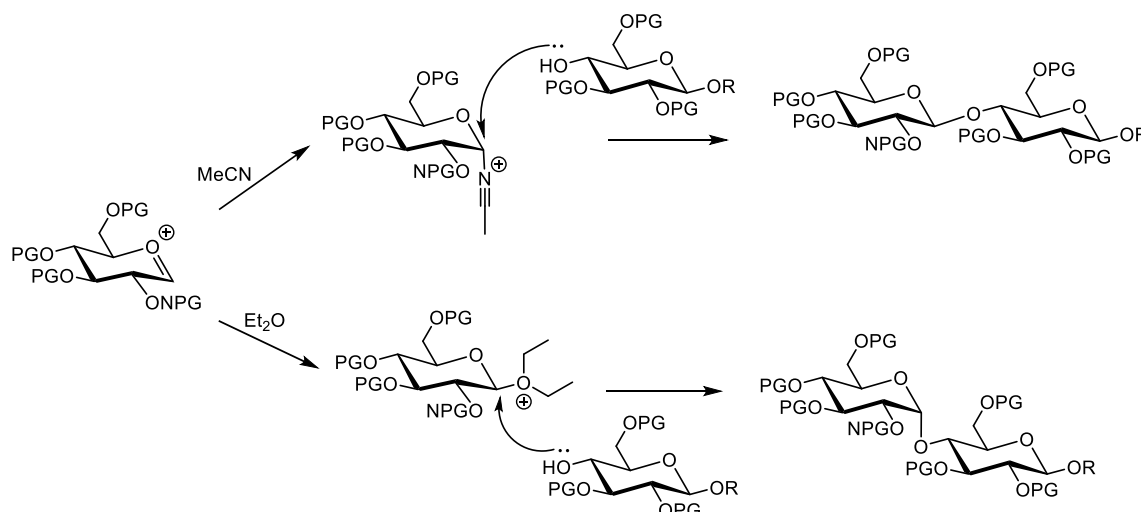


Scheme 7. Neighboring group participation.



Scheme 8. An example of remote-group (C-4) participation (NPG – non-participating group).

Stereoselectivity of glycosylation reactions can be regulated by the solvent effect (Scheme 9).⁶¹ One of the common examples of this effect is in using acetonitrile as a solvent. Acetonitrile can act as a nucleophile forming an intermediate that hinders the α -face and leads mainly to the β -product. The usage of diethyl ether, on contrary, results in α -product: it is assumed that equatorially-oriented oxonium ion is formed and subsequently attacked by glycosidic acceptor in S_N2 -type manner.⁶²



Scheme 9. Solvent effects in glycosylation reactions.

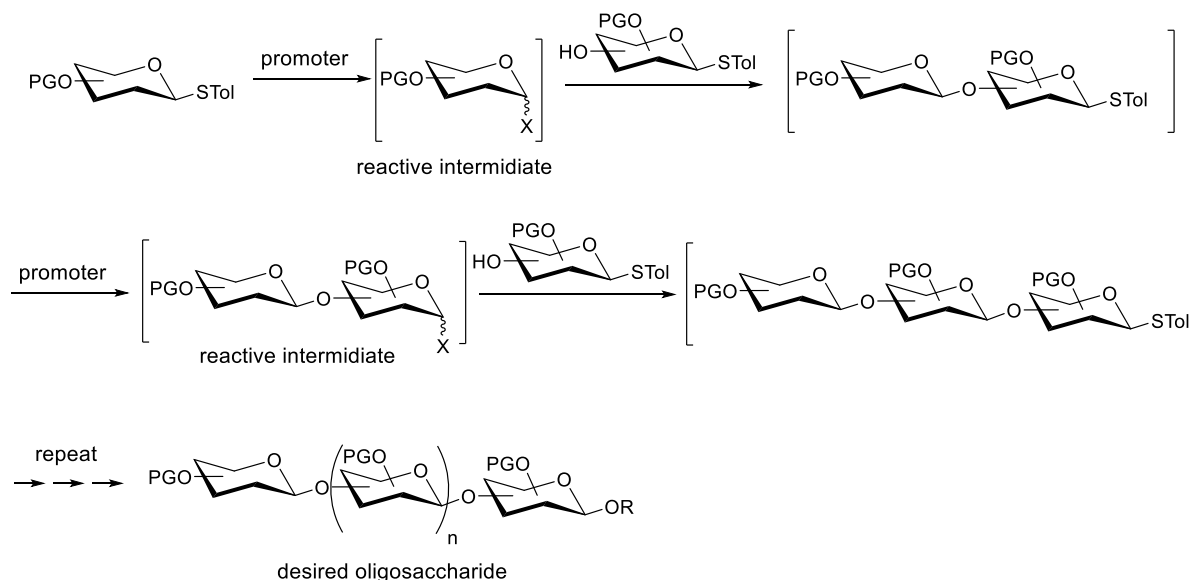
1.3.3 One-pot synthesis of oligosaccharides

The reactivity-based one-pot glycosylation is an interesting approach for the solution-phase synthesis of oligosaccharides. This method utilizes building blocks (glycosylation donors) with different reactivity that are allowed to react sequentially in a single reaction vessel. Varying electron-donating and electron-withdrawing protecting groups in glycosylation donors makes it possible to tune the reactivity of building blocks (within a specific glycosylation donor type, for example, phosphates).⁶³ The synthesis is planned so that the most reactive glycosylation donor is used for the reducing end, while the glycosylation

donor with the lowest reactivity is used for the non-reducing end of the target oligosaccharide.⁶⁴

This method has been applied to the synthesis of various glycans.⁶⁵⁻⁷¹ However, obtaining building blocks with different anomeric reactivities is in a lot of cases difficult and might require excessive synthetic manipulations.

The modification of this approach is iterative one-pot synthesis of oligosaccharides (Scheme 11).⁷² This method doesn't require the synthesis of glycosylation donors with different reactivities. It is based on the pre-activation procedure: glycosylation donor and a promoter are mixed together resulting in the formation of a reactive intermediate. Afterwards, glycosylation acceptor is added to the reaction mixture. This procedure can be repeated sequentially, resulting in the desired oligosaccharide.



Scheme 10. Iterative one-pot synthesis of oligosaccharides. Modified from ref. 72.

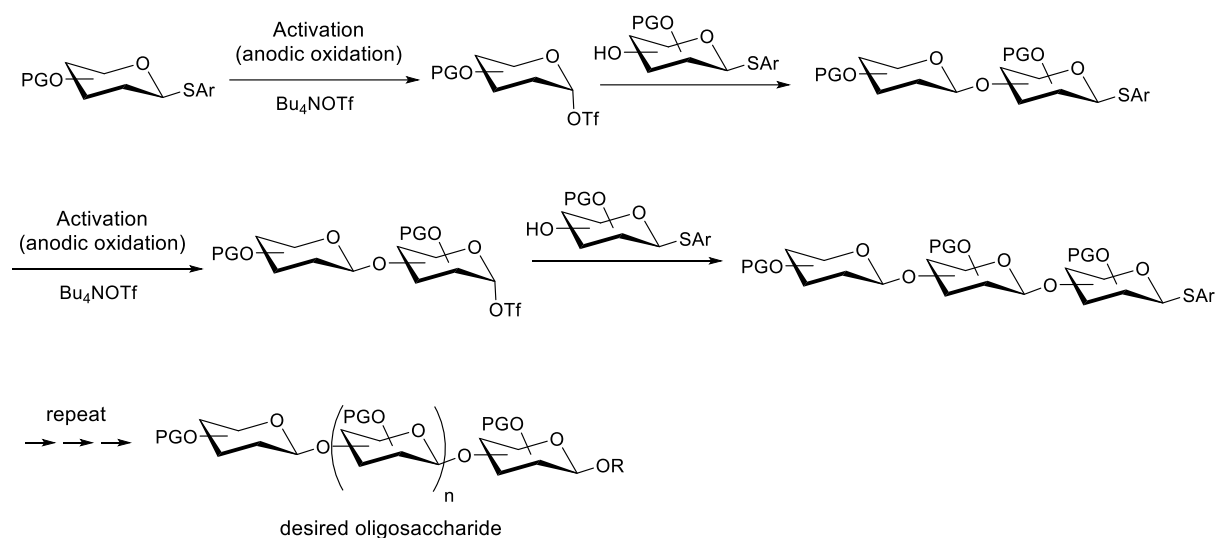
A variety of examples of utilization of this approach has been reported.⁷³⁻⁷⁶ It was also recently utilized for the synthesis of the longest oligosaccharide – arabino-galactan containing 92 monosaccharide units.⁷⁷ Despite the advantages that this method provides, it also has some limitations: this method is not automated, the variety of glycosylation donors that can be used for the synthesis is rather limited (even though several new glycosyl-donors have been developed for this synthetic method),⁷⁸⁻⁷⁹ it also lacks modularity.

1.3.4 Automated solution-phase synthesis of oligosaccharides

One-pot sequential glycosylation was used to develop an automated platform for solution-phase oligosaccharide synthesis.⁸⁰ This platform has been used for the synthesis of

several examples of biologically relevant molecules.⁸¹ Similar approaches have been used for the synthesis of oligomannosides⁸²⁻⁸⁴ as well as olimannuronates.⁸²

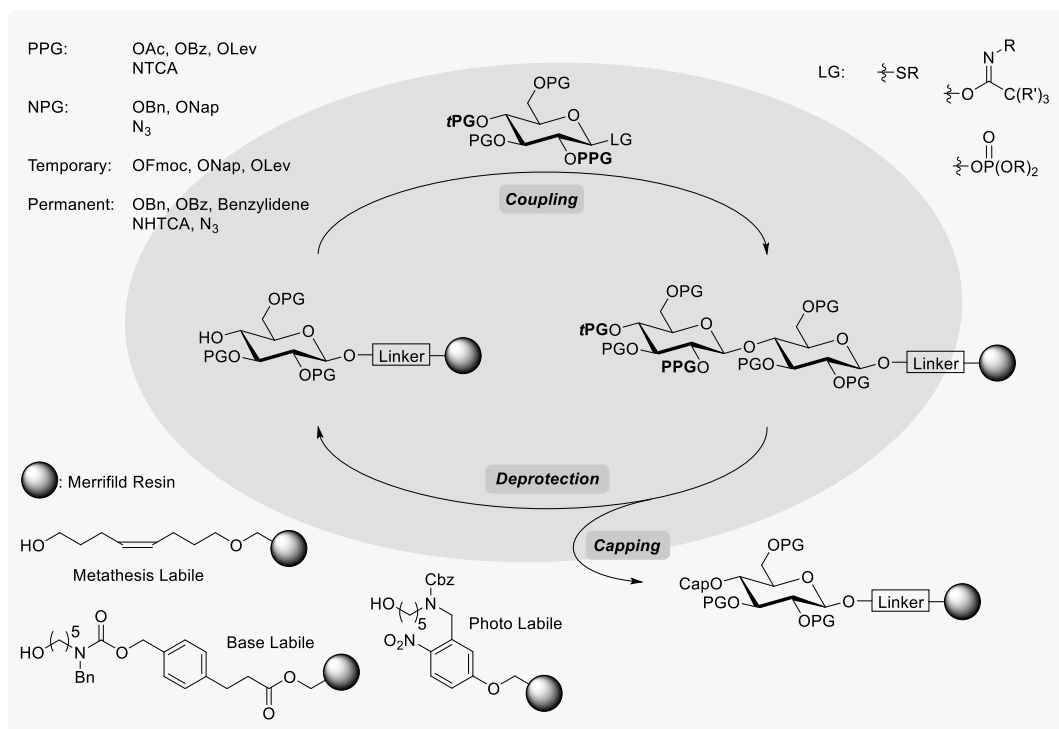
One of the modifications of iterative one-pot oligosaccharide synthesis is automated electrochemical assembly of thioglycosides (Scheme 12).⁸⁵ This method involves preactivation of glycosylation donors via electrochemical oxidation following by the addition of a glycosylation acceptor. In this way, oligosaccharide chain is built from the non-reducing to reducing end. This approach has been successfully applied to the synthesis of several glycans,⁸⁶⁻⁸⁷ including oligoglucosamines having 1,4- β -glycosidic linkages.⁸⁸



Scheme 11. General scheme of the automated solution-phase synthesis with electrochemical preactivation.

1.3.5 Automated solid-phase synthesis of carbohydrates

Automated glycan assembly (AGA) is a powerful method that was applied to the synthesis of a large variety of carbohydrate structures including glycosaminoglycans,⁸⁹⁻⁹¹ plant cell wall oligosaccharides⁹²⁻⁹⁴, glycans related to blood group determinants⁹⁵⁻⁹⁶, and tumor-associated glycans^{95, 97} among others.



Scheme 12. General scheme of automated glycan assembly (AGA). Reprinted (adapted) with permission from Seeberger, P. H., The logic of automated glycan assembly. *Acc Chem Res* 2015, 48 (5), 1450-63. Copyright (2015) American Chemical Society

Merrifield resin functionalized with a linker (metathesis⁹⁹, base¹⁰⁰, or photo labile^{91, 101}) is used as a solid support for automated glycan assembly. Free hydroxide groups of the linker are glycosylated with a building block (different types of glycosyl-donors can be used, Scheme 13). Building blocks have permanent protecting groups (PG, ex: benzyl (Bn), benzoyl (Bz), acetyl (Ac)) as well as temporary protecting groups (tPG, ex: 9-fluorenylmethyloxycarbonyl (Fmoc), levunoyl (Lev), 2-naphthyl (Nap)). The next step after glycosylation is a capping reaction, acetylation of the unreacted hydroxide groups, followed by deprotection of temporary protecting groups and further glycosylation with the next building block. This procedure is repeated several times before the synthesized oligosaccharide is cleaved from the solid support. The cleavage method depends on the linker that is used. Several important aspects of automated glycan assembly that will be discussed in the following sections include: 1) solid support; 2) linkers; 3) building blocks.

1.3.5.1 Solid support

Several properties of the resin are important for automated synthesis including: 1) type of the reactive groups on the surface on the resin; 2) resin loading capacity (the number of reactive groups per gram of resin); 3) solvent compatibility and resin swelling properties.

The type of reactive groups on the surface of the resin determines to a large extent the methods of resin functionalization as well as resin stability under storage conditions. The most common resin types used in automated synthesis have chloride groups on their surface that allows easy functionalization with nucleophiles.

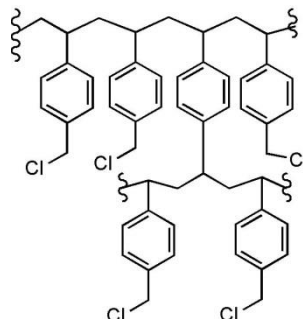


Figure 6. Structure of Merrifield resin.

Resin loading capacity is also an important consideration for automated synthesis. Low resin loading capacity may result in low synthesis productivity (the amount of produced material per gram of resin). With high resin loading some of the reaction sites may not be accessible for functionalization. Another factor that has to be considered when choosing the resin loading is the reaction concentration during automated glycan assembly (AGA). Low resin loading can require a very small reaction volume, which might be difficult to practically achieve. Conversely, high resin loading necessitates large reaction volumes that might require a more intense mixing or exceed the defined volume of the reaction vessel.

When choosing the resin, solvent compatibility and swelling properties of resins also have to be considered. Solvent absorption influences the reactivity of functional groups on the resin surface. Resin swelling also influences diffusion of reagents to the reactive sites. If resin swelling in a given solvent is not sufficient, the diffusion of reagents will also not be sufficient, possibly leading to poor reaction outcomes. Resin swelling properties also have to be considered while performing consecutive processes in different solvents. To completely remove solvent absorbed by the resin additional washing steps are required.

The most common resins for automated solid-phase synthesis are Merrifield resin and controlled pore glass (CPG).⁹⁸ For AGA, Merrifield resin (Figure 6) is the most commonly used solid support. As a cross-linked polymer resin, it is compatible with diverse solvents including DCM, THF, DMF, and dioxane. It also possesses good swelling properties. It allows for easy functionalization and has an optimal loading capacity for AGA as well.

Controlled pore glass is used frequently for oligonucleotide solid-phase synthesis. It is a non-swelling solid support, therefore it is compatible with a wide range of solvents for the

synthesis. However, there are several aspects of CPG that complicate its use for AGA: 1) handling of CPG beads may be difficult because of their mechanical instability (it is more fragile than Merrifield resin); 2) relatively low resin loading capacity compared to Merrifield resin; 3) incompatibility with silyl ether protecting groups that can be used as temporary protecting group in AGA.¹⁰²

1.3.5.2 AGA Linkers

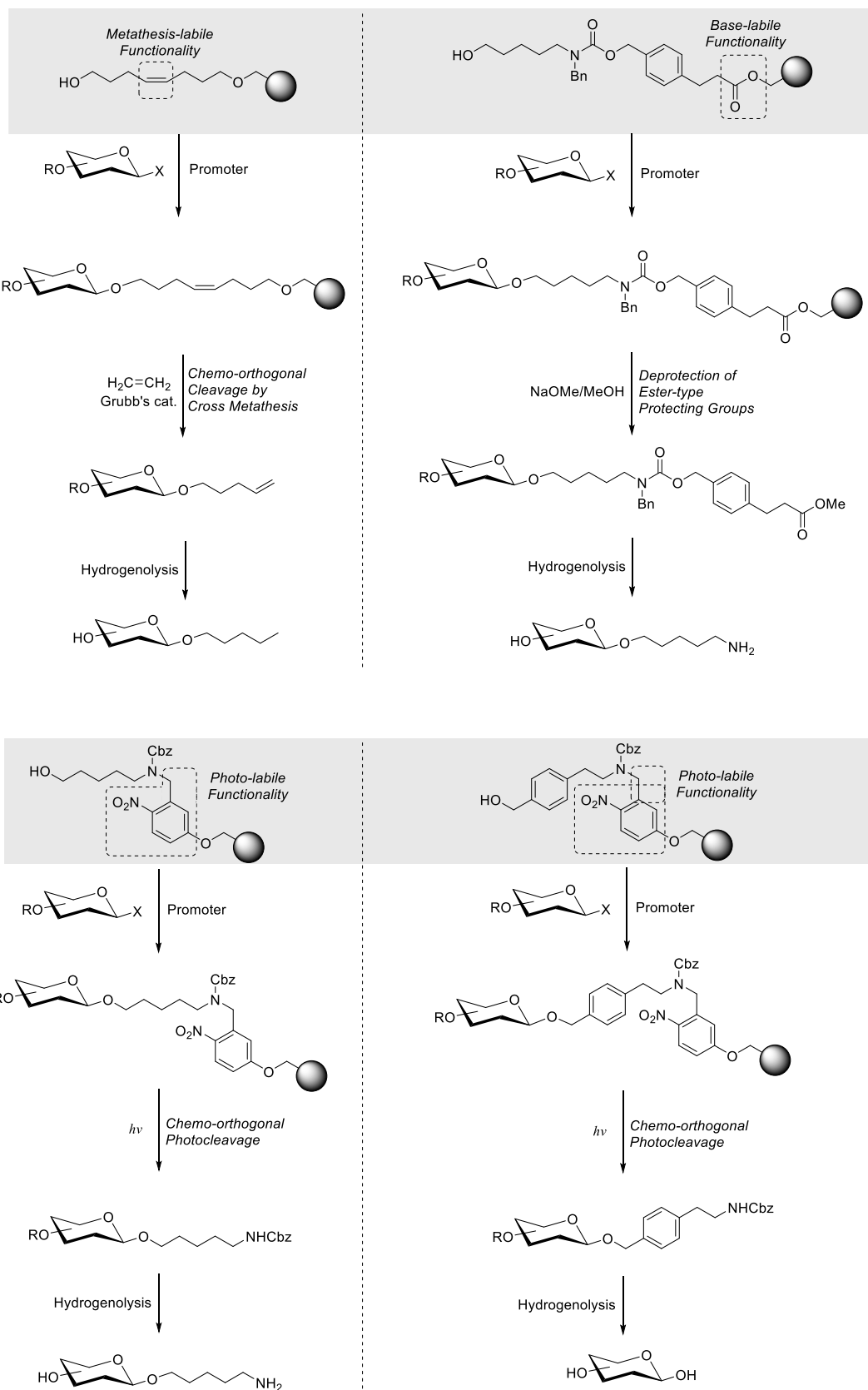
There are several types of linkers that can be used in automated glycan assembly: metathesis labile linker;⁹⁹ base labile linker;¹⁰⁰ and photo labile linkers^{91, 101} (Scheme 14).⁹⁸

Metathesis labile linkers were used for the synthesis of a broad range of structures.^{95, 97, 99, 103-105} The advantages of these linkers are orthogonal cleavage conditions to many common AGA synthesis conditions and the possibility to get the oligosaccharide coupled to alkyl moiety that can be used as a glycosylation donor. The major disadvantage is that the linker is not stable in the presence of electrophiles, therefore it will react with NIS/TfOH, is the promotor for thioglycoside glycosylations.

Base-labile linkers are stable in the broad range of glycosylation conditions and can be used with most known glycosylation donors.^{100, 106} Another advantage of this linker is the possibility to obtain conjugation-ready oligosaccharides. Free amino-group of the linker can be used for immobilization of oligosaccharide on the surface (that enables applications in glycan arrays)¹⁰⁷ or for a coupling to a protein (forming glycoconjugates that can be used, for example, in vaccine development).¹⁰⁸⁻¹¹¹ The major disadvantage are the harsh cleavage conditions. This linker cannot be used for the synthesis of compounds that are not stable under strongly basic conditions (for example, sulfated oligosaccharides).

Another type of linker that is used for AGA are photo cleavable linkers.⁹¹ These linkers were used mostly in recent years for the synthesis of large variety of glycans.^{91-94, 98, 112-116} One of the major advantages of these linkers, compared to base- or metathesis labile ones, is the possibility for orthogonal cleavage in mild conditions. The most commonly used photo cleavable linker also allows the synthesis of conjugation-ready oligosaccharides. Recently, a traceless photo cleavable linker has also been developed that allows the synthesis of oligosaccharides with free reducing ends.¹⁰¹

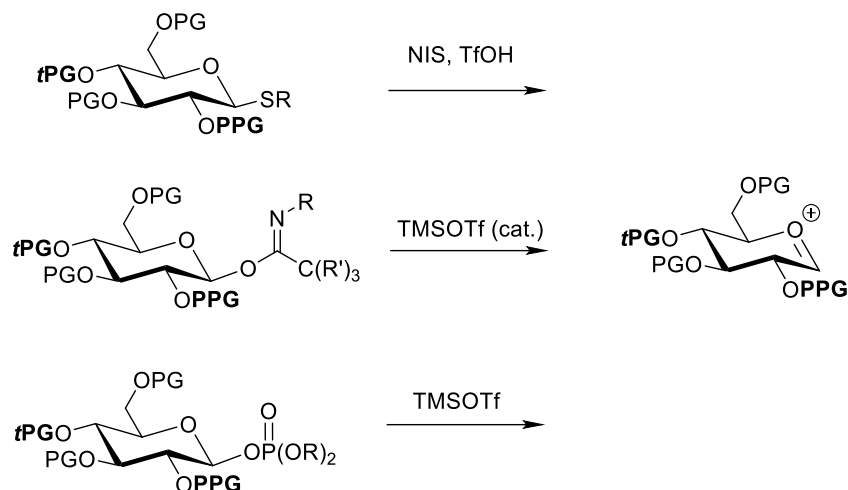
The major difficulty with them is achieving high efficiency in the photo cleavage process. For this pursuit, a continuous flow reactor is used in the Seeberger laboratory.



Scheme 13 Linkers used in AGA. Modified from ref. 98

1.3.5.3 Building blocks for AGA

Three types of glycosyl-donors have been used in AGA: glycosyl thioglycosides, glycosyl trichloroimidates, and phosphates. There are several aspects that determine the building block choice for a synthesis: 1) reactivity; 2) stability under synthesis conditions; 3) selectivity of glycosylation; 4) solubility.



Scheme 14. Types of glycosylation donors used in AGA and promoters for their activation.

For the activation of the three glycosylation donors, different conditions are required. The reagents used for the activation of the above glycosylation donors are well-established (Scheme 15). But the exact conditions (reaction temperature and time) vary from building block to building block. Many factors determine the reactivity of glycosylation donor. The reactivity of the respective the glycosylating agent is determined predominantly by the stability of the carbocation that is formed during glycosylation process. In this regard, electron donating protecting groups, like benzyl ethers, increase reactivity, whereas electron withdrawing protecting groups, such as -OAc, -OBz, -OLev, decrease the reactivity of building blocks.

Another important aspect is the stereoselectivity of the glycosylation reaction. In most cases, building blocks contain participating group in the C-2 position of a building block to achieve anti-selectivity of glycosylation. Recently, remote participating groups were successfully used for the synthesis of several biologically important oligosaccharides containing multiple cis-glycosidic linkages.¹¹⁷ The usage of solvent effect⁶¹ for controlling glycosylation stereoselectivity may be difficult to apply in the solid-phase synthesis conditions, as Merrifield resin does not swell well in acetonitrile which might lead to low reaction efficiency.

One more important property of the building blocks is their solubility. Most of the glycosylation reactions in AGA are performed in a DCM/Dioxane mixture or pure DCM. As glycosylation efficiency depends on the concentration of the building block, it is important that glycosylation donors are soluble to some degree in DCM or the DCM/Dioxane mixture.

1.4 Aim of the thesis

The overall goal of this work is to contribute to the development of rapid and modular approach that would enable the access to an oligosaccharide library for structural investigations. Even though carbohydrates are a widespread type of biomolecules, the lack of homogeneous oligo- and polysaccharides in a lot of cases hinders structural and biological investigations of these molecules.

The first objective of this work is to optimize all the steps of automated glycan assembly (AGA). In order to develop standardized conditions that can be applied for the various building blocks, the analysis and optimization of all the steps of AGA has to be performed. The possibility to improve the efficiency of the synthesis (increase the yield, reduce reaction time, decrease the amount of building blocks and solvents used) has to be investigated.

Standardized conditions will make it possible to synthesize a collection of natural and unnatural oligo- and polysaccharides, structures of which can be afterwards studied using molecular dynamics.

Another objective of this dissertation is the development of synthetic strategies for homogeneous fully-protected glycosaminoglycans (GAGs). These molecules attract a lot of interest because their biological importance (they play a role in cell-cell adhesion, cell differentiation and proliferation), but the investigations and medical application of these compounds is complicated by their heterogeneity. Synthesis of homogeneous GAGs is challenging: these sulfated molecules are not stable in both acidic and basic media and, therefore, require mild synthetic conditions. Hence it is importance to develop new approaches to access GAGs.

Monosaccharide building blocks required for the synthesis of dermatan and chondroitin sulfate oligosaccharides have to be prepared. Dermatan sulfate oligosaccharides have to be assembled in solution phase in order to test potential synthetic strategies. Then, automated solid-phase synthesis of dermatan sulfate oligosaccharides has to be performed.

2 Automated Solid-Phase Oligosaccharide Synthesis Optimization

2.1 Introduction

N. Kottari *et. al.* recently made a major achievement in AGA, having synthesized a 50-mer mannoside, the longest oligosaccharide synthesized via automated synthesis¹¹² (the previous longest sugar was a 30-mer, synthesized by O. Calin *et. al.* in 2012)¹¹⁸. His work illuminated several important issues:

1) The yield of automated solid-phase synthesis of mannoside trimer is 56%, while the yield of 50-mer is 5%. Figure 2 shows that the yield of the synthesis decreases very drastically for the first few saccharide units and then decreases at a slower, gradual rate until the 50-mer. This pattern means that the chain elongation step during automated solid-phase synthesis proceeds with quite high yield (average yield of one elongation cycle is 95%), while the major loss of yield occurs either during the first glycosylation or the photocleavage.

2) The time required for one chain elongation in AGA is relatively high, when compared to peptide synthesis. One elongation cycle takes approximately 180 minutes such that the synthesis of hexamer takes approximately 18 hours and the synthesis of a 50-mer takes approximately ten days.

3) The amount of building block used for automated synthesis is relatively high. For the synthesis of 0.4 mg of fully unprotected 50-mer 2.74 g of building block is needed.

4) The quantity of solvents used during the synthesis is high (see Table 1).

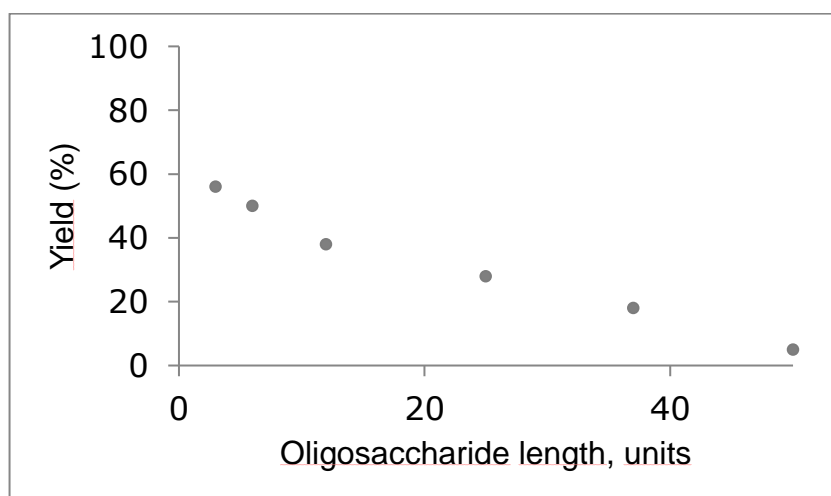


Figure 7. The dependence of synthesis yield on oligosaccharide length

Table 1. Amount of solvent used for the synthesis of a 50-mer.

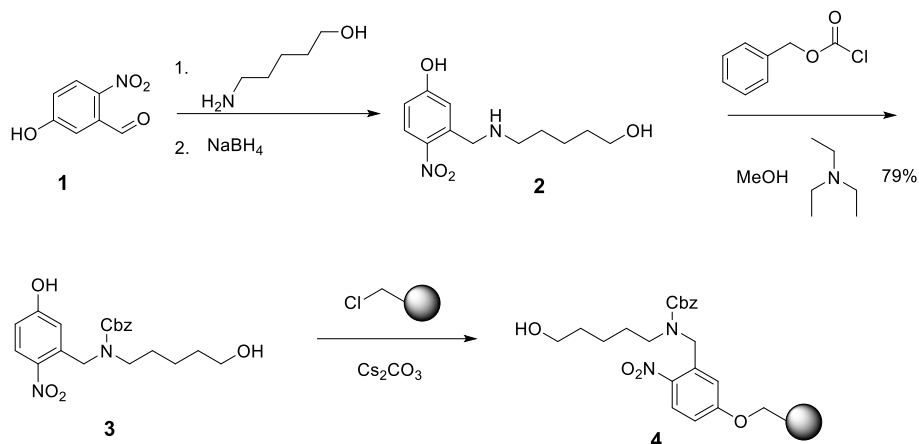
Solvent	Amount, L
DCM	2.5
DMF	1.5
Dioxane	0.1
DCE	0.12
THF	0.30

The aim of the following optimization is to understand these four issues and to develop a faster elongation cycle that uses less building blocks and solvents. To optimize automated solid-phase synthesis, every step was analyzed in detail.

2.2 Photo cleavable Linker and Solid Support

2.2.1 Existing synthesis of photo cleavable linker and resin preparation

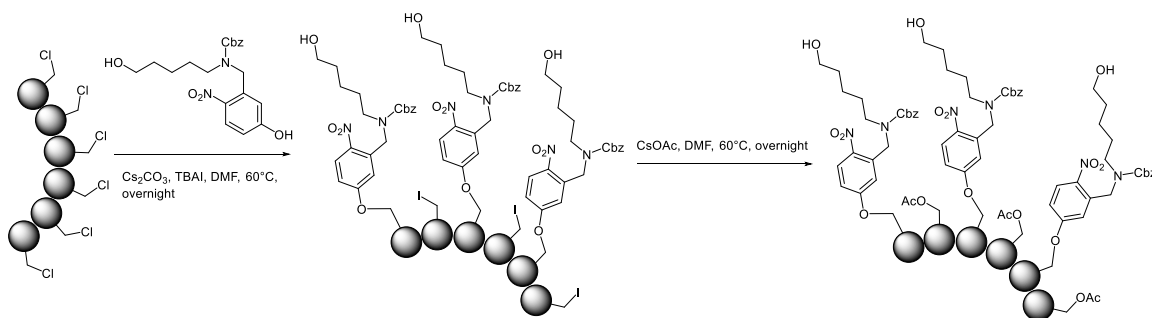
For AGA, Merrifield resin modified with a photo cleavable linker is frequently used. This resin is prepared by a method previously developed in Seeberger group (Scheme 9).⁹¹ In the first step, 5-hydroxy-2-nitrobenzaldehyde (**1**) forms an imine with 5-aminopentanol, then this imine is reduced using sodium borohydride to complete the reductive amination reaction. Then, the product is treated with CbzCl, to protect the resultant secondary amine, and after purification the prepared linker is loaded on Merrifield resin.



Scheme 15. Synthesis of photo cleavable linker.

2.2.2 Investigation of resin loading and photo cleavage

The first step of automated solid-phase synthesis is the functionalization of the Merrifield resin with the photocleavable linker. The process is shown in Scheme 10.



Scheme 16. Modification of the Merrifield resin with the photo cleavable linker.

The process of resin functionalization was developed in the Seeberger laboratory.⁹¹ In the first step, photo cleavable linker, Cs_2CO_3 (base) and TBAI (promotor) are added to Merrifield resin swollen in DMF. Then, the reaction mixture is left rotating on the rotorvap at 60°C overnight.

The resin is subsequently washed with various solvents (THF/water (1/1), THF, DMF, MeOH, DCM, and MeOH) and is swollen again in DMF. Then, the resin is treated with CsOAc at 60°C overnight to acetylate all potential active electrophilic sites on the resin.

There are several methods to determine the resin loading developed in our laboratory:

- 1) determination of the number of free hydroxyl-groups on the surface of the resin;
- 2) gravimetric quantification of monosaccharide after photo cleavage;
- 3) determination of Fmoc-groups on the resin after the first glycosylation.

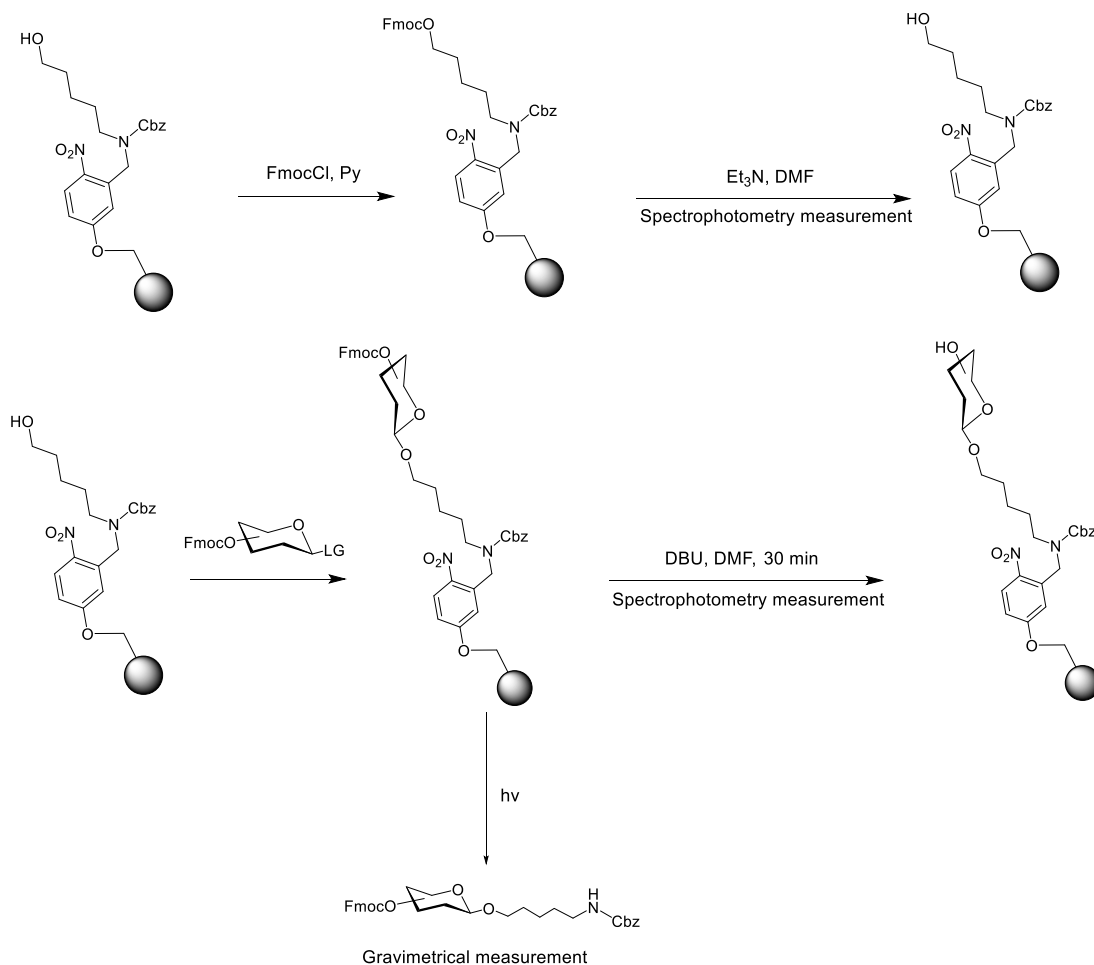
The methods are described in more detail below.

1) In the first method, Merrifield resin modified by the linker is treated with an excess of FmocCl in pyridine in order to protect all of the free hydroxyl groups on the resin. The subsequent treatment of the resin with triethylamine makes it possible to remove all the Fmoc-protecting groups and by spectrophotometry, quantify the loading of the resin. The resulting quantification represents the number of hydroxyl groups on the surface of the solid-support before performing glycosylation reactions.

2) The second method utilizes glycosylation of the resin with an excess of the building block (most commonly mannose). Subsequent to photo cleavage the mass of the product is measured.

3) The third method uses the following procedure: Merrifield resin is glycosylated with an excess of the building block containing Fmoc-protecting group. The resin is subsequently treated with DBU (1,8-diazabicycloundec-7-ene) and the amount of Fmoc-derivative released is measured by spectrophotometry. This method is similar to one that is widely used in peptide solid-phase synthesis.¹¹⁹

To understand which of these three methods should be applied for the resin loading quantification further investigations were performed.



Scheme 17. Methods of loading determination

The resin loading determination results differed significantly between methods. For example, for one of the resin batches, the resin loading was determined as follows for the three methods: 1) 0.36 mmol/g, 2) 0.18 mmol/g, 3) 0.25 mmol/g.

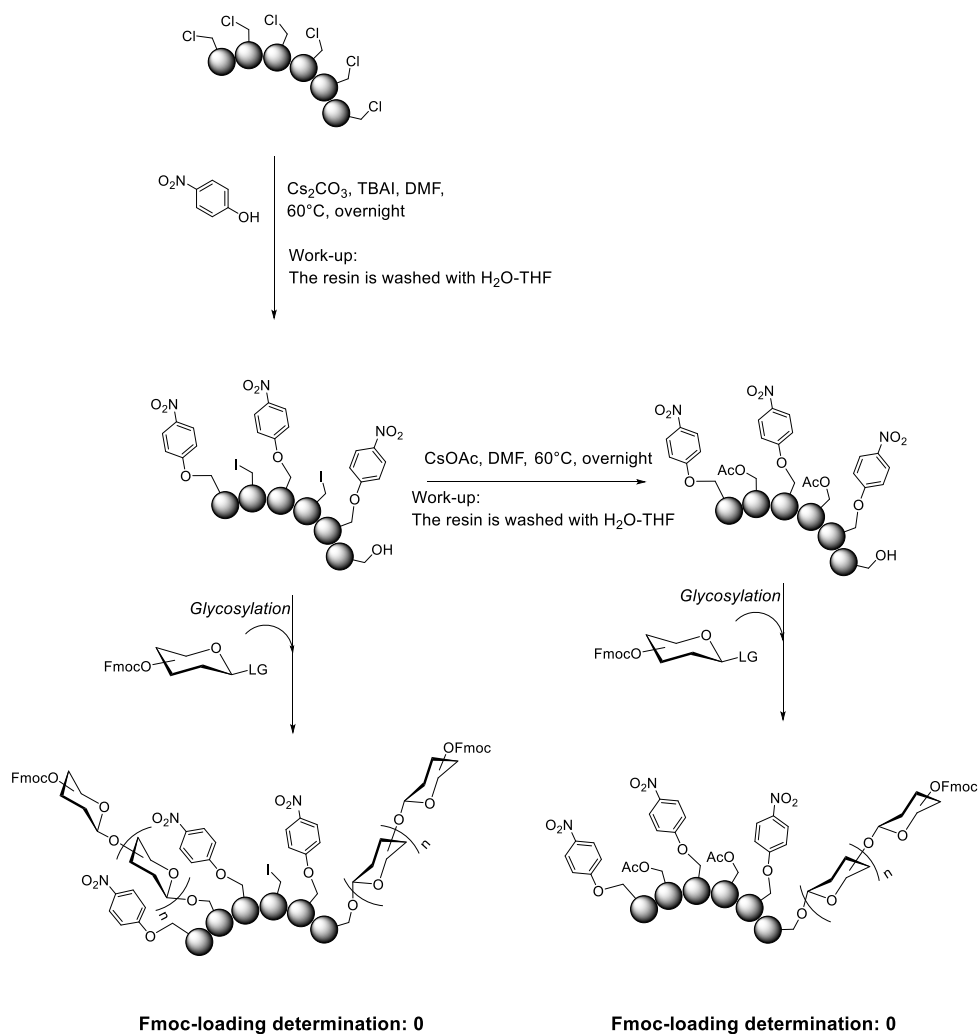
Several explanations for the differences in resin loading determination results are possible. The likely reason why the first method gives higher results than the subsequent methods is the fact that not all hydroxyl-groups of the linker on the surface are available for the glycosylation reaction. Therefore, this method shows the amount of linker that is attached to the surface of the resin.

The difference in the second and the third method of loading determination is likely because the monosaccharide does not get completely cleaved from the resin. The failing to cleave completely could be due to two factors. The first potential reason is that some oligosaccharide molecules are coupled directly to the Merrifield resin, without the linker in between. That would make the cleavage of these molecules from the resin impossible. The

second potential reason is that the photo cleavage itself doesn't proceed effectively. Both of these hypotheses had to be tested.

In the first hypothesis, oligosaccharide molecules could be directly coupled to the surface of the resin. This could be possible when some reactive nucleophilic centers are still present on the surface of the resin. One potential nucleophilic center could be hydroxyl groups, that could be then glycosylated. How then could hydroxyl groups potentially be on the surface of the resin? During the resin functionalization process the active electrophile (with a C-I bond) are formed. One of the steps of resin functionalization is washing of the resin with the THF-water mixture (1:1). As long as there is excess base in the system, in the water-containing mixture would form OH^- anions that can nucleophilically attack the C-I bond, forming hydroxyl groups directly on the surface of the resin. Similar processes can also happen during the resin capping step. In that step, an excess of cesium acetate is used and the resin is washed with the THF-water mixture (1:1). The partial hydrolysis of cesium acetate in water-containing media can also lead to the formation of hydroxide anion and cause the formation of hydroxyl groups on the surface of the resin.

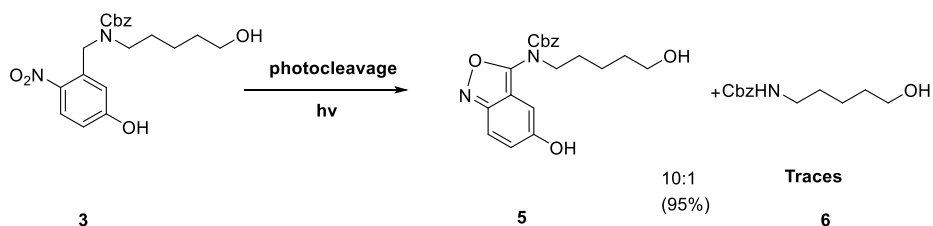
In order to test these hypotheses, the following experiments have been carried out (Scheme 12). Merrifield resin was functionalized with para-nitrophenol in the same conditions as is normally done for photo cleavable linker. In this case, if it is possible to couple a monosaccharide donor to the surface of the resin, it means that the presence of hydroxyl groups directly on the surface of the resin is proved. To test whether the glycosylation reaction does proceed, Fmoc-quantification of the resin after glycosylation can be performed. In this experiment it was determined that the resin does not have monosaccharide molecules attached to it, meaning that hydroxyl groups are not forming on it during resin functionalization.



Scheme 18. Testing the efficiency of resin functionalization.

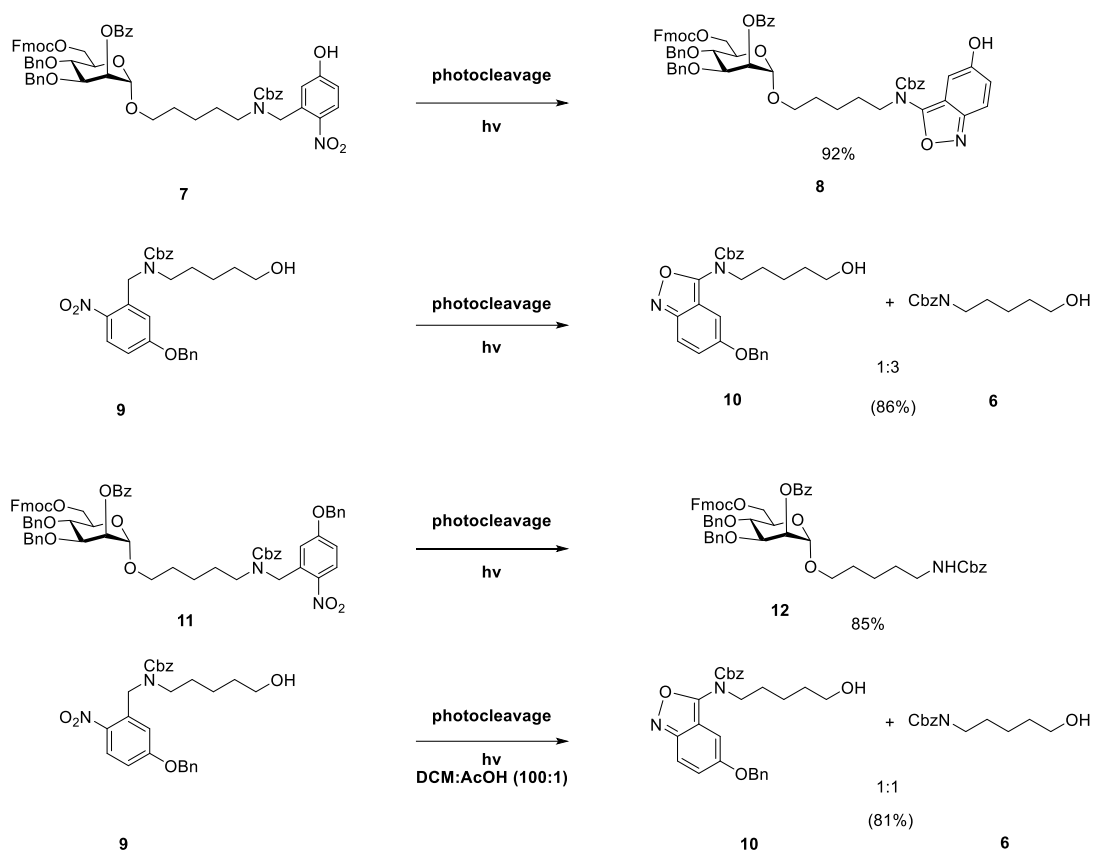
These results indicate that the difference in loading determination may originate from inefficiencies associated with photo cleavage process.

The first step of analyzing the photo cleavage reaction, was an investigation of how the photo cleavable linker behaves under the reaction conditions. I found that mainly product **6** was formed (Scheme 14). The photocleavage of the linker itself might, however, differ from the photocleavage process of the linker coupled to Merrifield resin.



Scheme 19. Photo cleavage of the standard photo cleavable linker.

To mimic the conditions of the photo cleavage on the resin, several molecules were prepared and their reactivities studied. Surprisingly, it was found that the photo cleavable linker undergoes a rearrangement to give unusual product. Increasing acidity of the reaction resulted in increasing amount of rearrangement product.



Scheme 20. The reactivity of different photo cleavable linker derivatives.

Based on this information, studies of the photo cleavage of resin, modified with the photo cleavable linker and monosaccharide were performed. Resin with a loading of 0.25 mmol/g was subjected to photo cleavage conditions at different pH. Different numbers of injections in the photo reactor represents different reaction times (each injection is 10 min). Afterwards, the measurement of residual resin loading was performed (Table 2).

Table 2. The influence of acidity on the photo cleavage reaction.

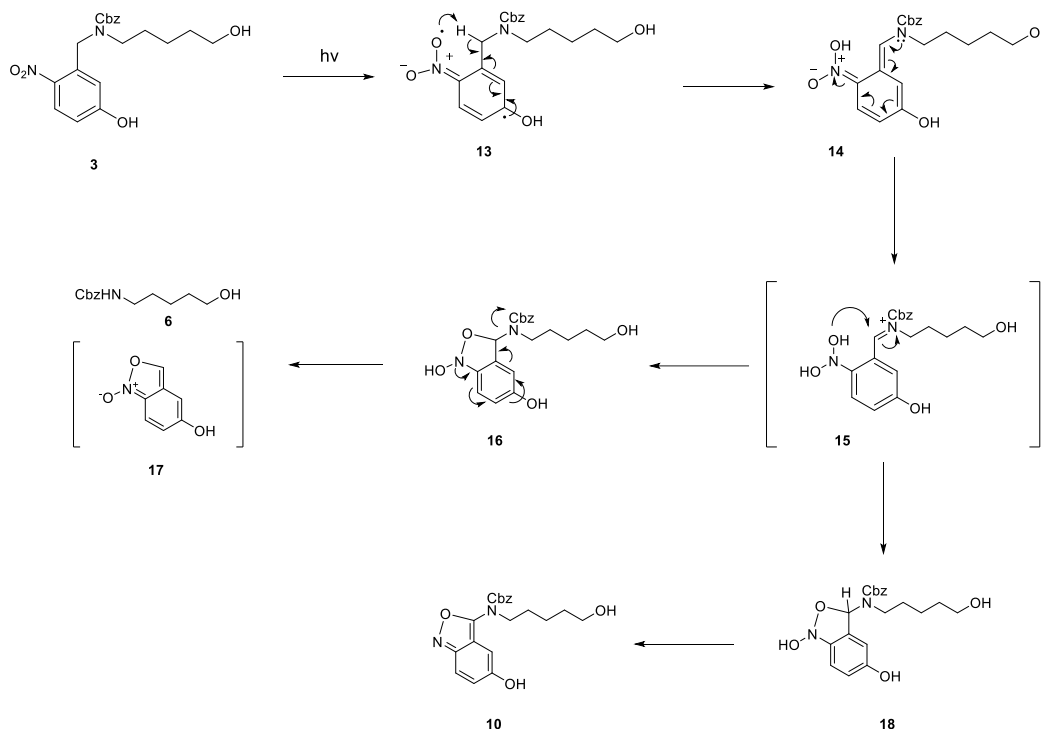
Entry	Cleavage conditions	Residual resin loading	Estimated yield (%)
1	DCM (1 injection)	0.14	44
2	DCM (2 injections)	0.12	52
3	DCM/lutidine (1%) (2 injections)	0.18	28
4	DCM/lutidine (0.05%) (2 injections)	0.13	48
5	DCM (washed with NaHCO ₃) (1 injection)	0.10	60
6	DCM (washed with NaHCO ₃) (2 injections)	0.07	72
7	DCM (pH=2) (2 injections)	0.21	16

The standard conditions of photo cleavage (Table 2, entries 1 and 2) result in 44-52% yield, depending on the number of injections. Since acidic conditions promote linker rearrangement, experiments with catalytic amounts of the strong base lutidine were carried out. However, the yield of these reactions was even lower than in case of standard photo cleavage conditions. One of the reasons for this outcome could be that lutidine can absorb light energy, act as a scavenger and inhibit the photo cleavage reaction. When the reaction was performed in DCM washed with a saturated solution of NaHCO₃. It was possible to obtain 60-72% of the oligosaccharide from the resin. Performing the reaction in DCM in

strongly acidic media results in very low yield (only 16%) of photo cleavage. These results prove that the photo cleavage process is strongly pH-dependent.

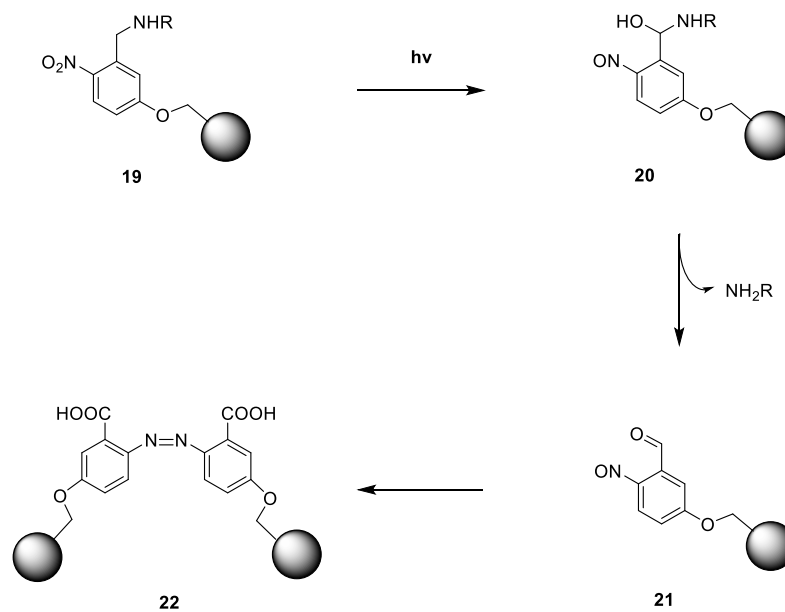
To improve the outcome of the photo cleavage reaction, the mechanism behind byproduct formation during photo cleavage should be understood. In the literature, several similar processes are described.¹²⁰⁻¹²¹

During the first possible mechanism a reactive intermediate is formed first which can undergo two different conversions (see Scheme 16).¹²⁰



Scheme 21. One possible mechanism of the photo cleavage process.

The other possible process that can explain the decrease in yield of photo cleavage (Scheme 17). In this case, nitroso-aldehyde as a reactive intermediate is formed. This molecule is not stable in acidic media and can undergo a disproportionation reaction, giving a diazo-compound. This diazo-compound stays on the resin and can absorb light, thereby preventing further photo cleavage reactions (Scheme 11).¹²¹



Scheme 11. Formation of diazo-compounds during photocleavage.

Both mechanisms involve the abstraction of the hydrogen atom from the CHNHR-group. Therefore, introduction of a methyl-group to this position should avoid formation of these byproducts, improving the overall yield of photo cleavage reaction.

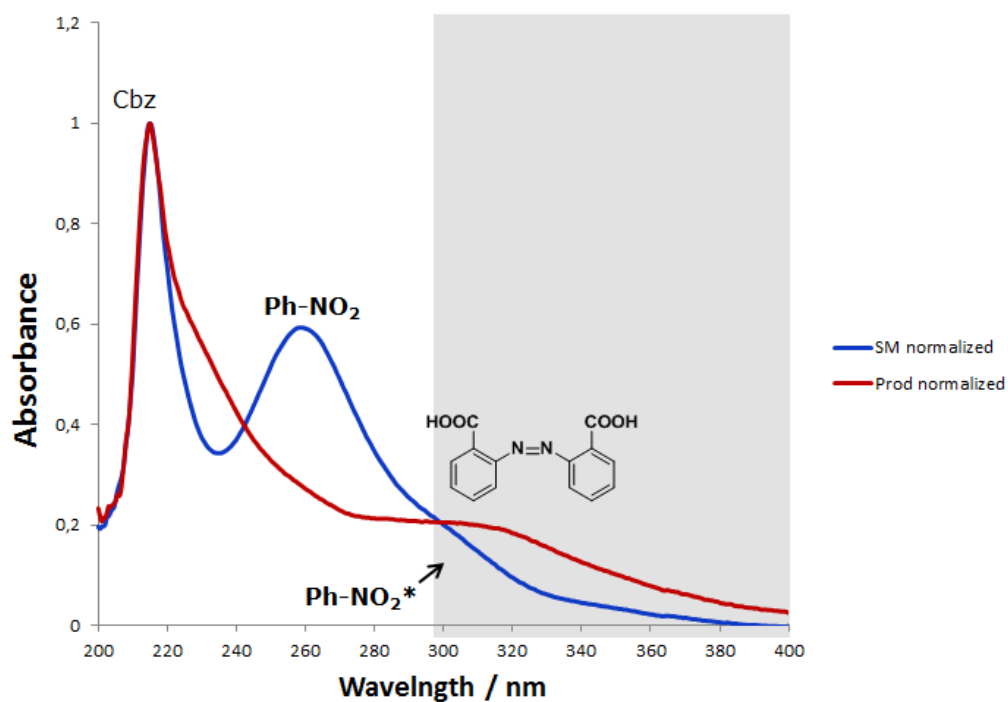
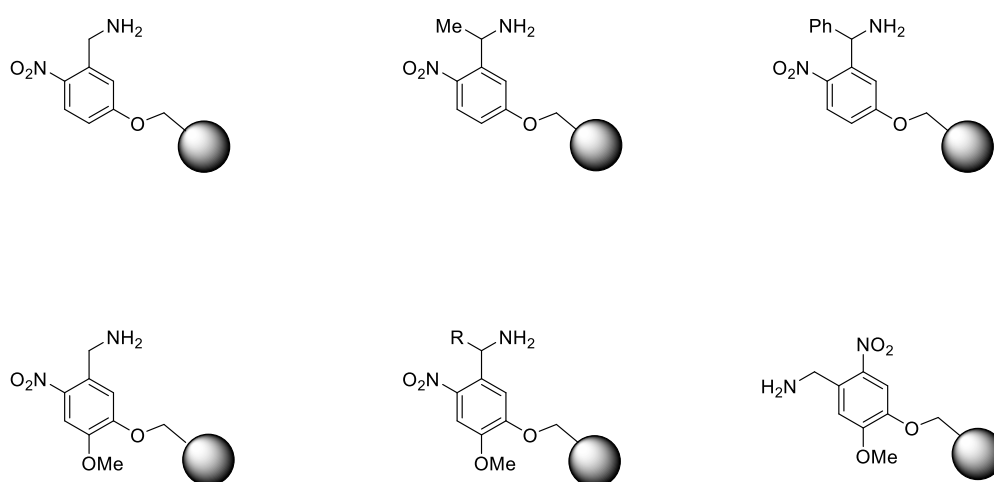


Figure 3. Absorbance spectra of nitrobenzene and diazo compounds

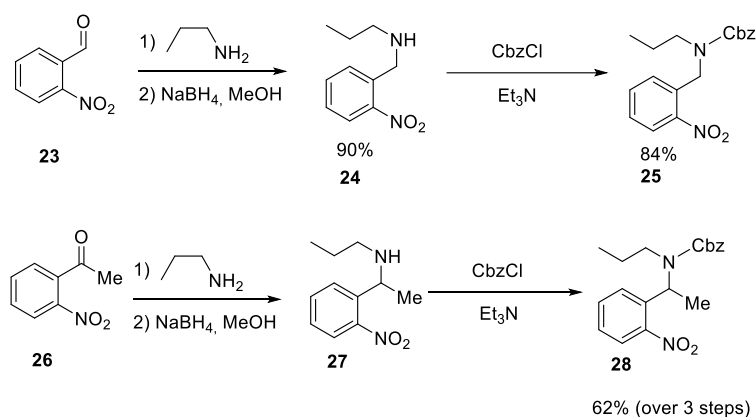
2.2.3 The development of a new photo cleavable linker

Several photo cleavable linkers (see Scheme 12) were chosen as potential linkers for AGA. Similar linkers have been used in oligonucleotide synthesis. Some of them have either Me- or Ph-groups instead of hydrogen that might help in avoiding the a forementioned side products. Apart from this, some of the molecules carry MeO-groups on the phenyl ring. Electron donating effects of this group help to stabilize radicals that are formed during photocleavage.¹²²



Scheme 22. Structures of potential functionalized resins that can be used for photo cleavage.

Before the synthesis of a photo cleavable linker that can be attached to the surface of the resin, model studies of reactivity were performed. To perform these experiments, two model compounds were synthesized (see the Scheme 13)



Scheme 23. Synthesis of model compounds for investigation of the photocleavage reaction.

Compounds **25** and **28** were subjected to the photocleavage process at different pH (Figure 4 and 5). Photocleavage of the compounds gives the mixture of nitroso-aldehyde and amine. Notably the amount of aldehyde present in the mixture decreases with increasing acidity of the reaction media. It can be explained by the fact that acidic conditions promote disproportionation of nitroso-aldehyde.

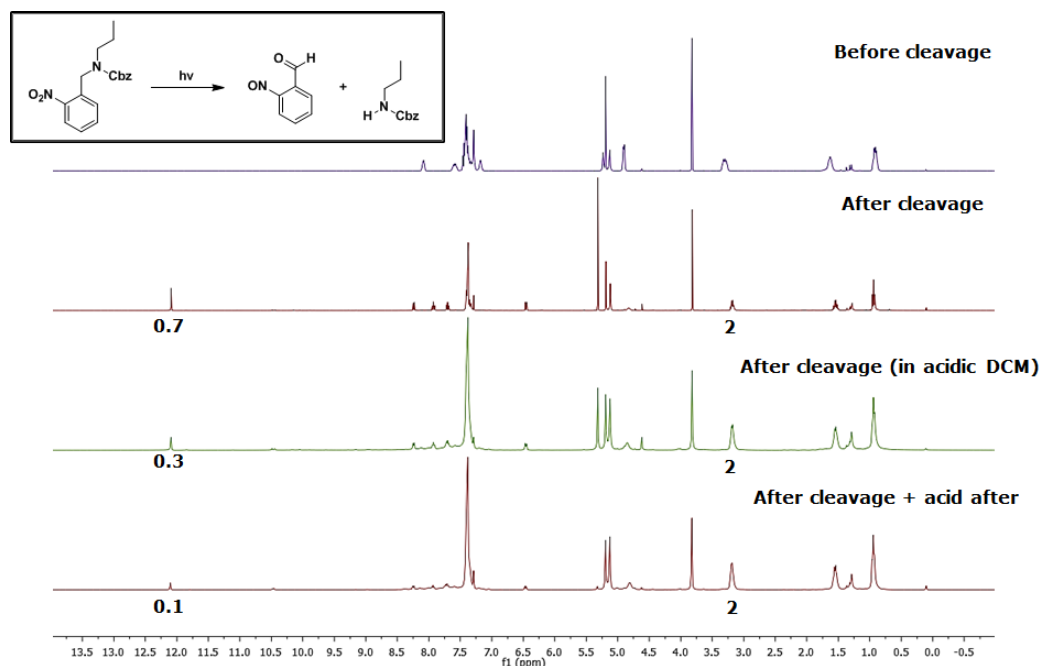


Figure 4. Investigation of the reactivity of model compound.

In case of compound **19** another reaction pattern is observed, as a mixture of two compounds is obtained (Figure 5). Since disproportionation of the ketone is not possible, this compound is a good model for the development of the new linker for automated solid-phase synthesis.

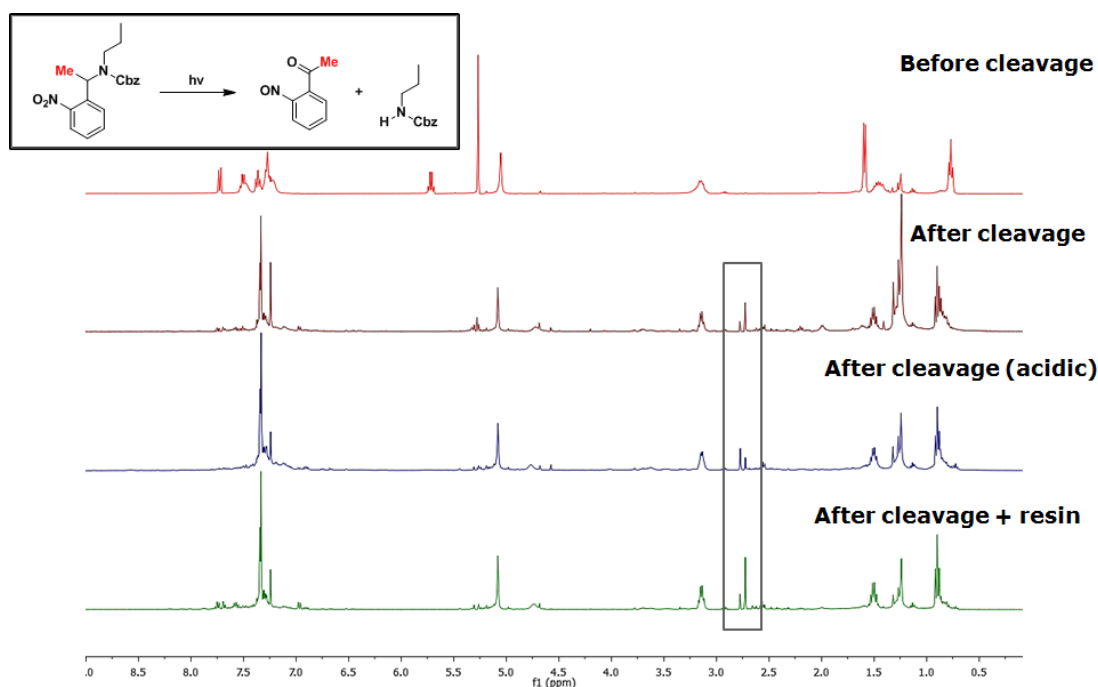
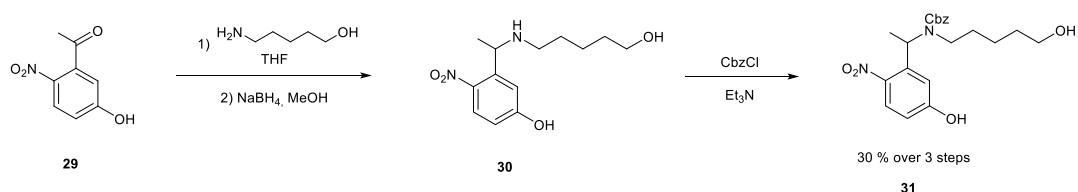
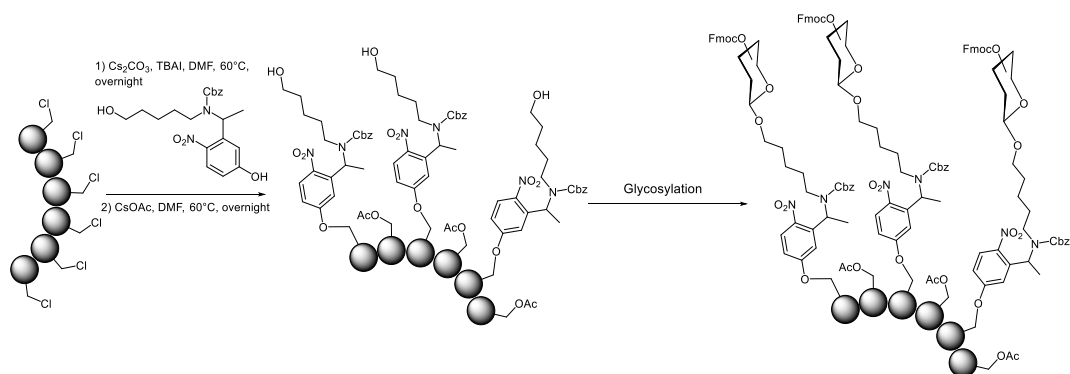


Figure 5. Investigation of the reactivity of model compound.

At the next step, the new photo cleavable linker was synthesized (Scheme 14). This compound was attached to Merrifield resin using the standard conditions and the loading determination measurements for this resin were performed (using method 3). The loading was determined to be 0.29 mmol/g, which is comparable to the loading of the original linker.



Scheme 24. Synthesis of new photocleavable linker.

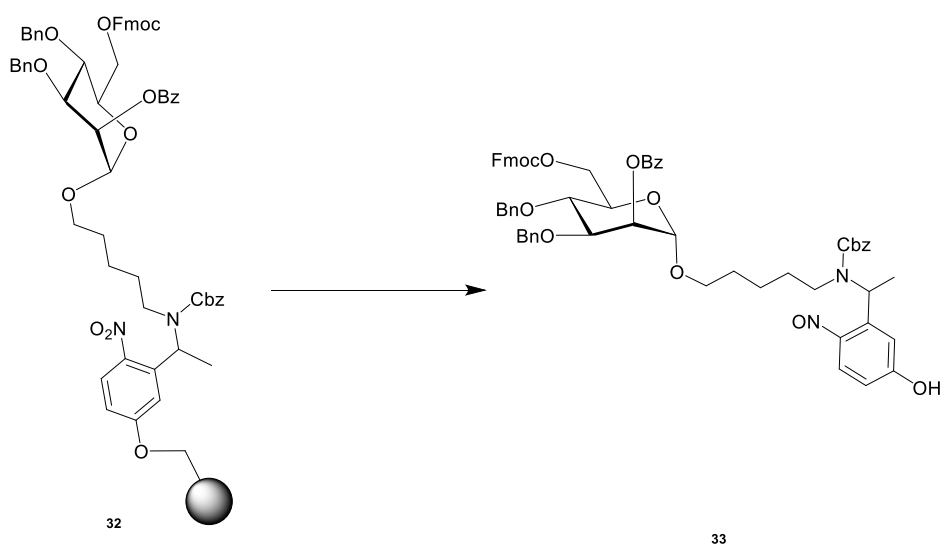


Scheme 25. Functionalization of the resin with the new linker.

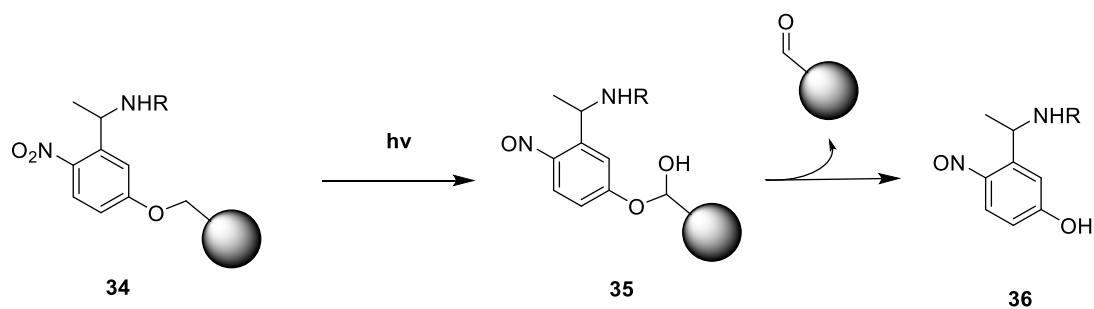
The resin modified with the new linker was glycosylated (Scheme 20), to test the cleavage of the new linker. Surprisingly, it releases a molecule with a phenyl ring and the

nitroso-group in its structure (Scheme 21). The residual loading of the resin was determined to be 0.15 mmol/g, meaning that the yield of photocleavage was 50%.

In order to gain a better understanding of the photocleavage process, the photocleavage of the new linker itself was performed. The linker itself does not undergo any reaction even after several injections. One probable explanation for this result could be different stability of the radicals that are formed during photocleavage process. For the new linker, proton abstraction from the CH₂ group of Merrifield resin leads to the formation of a more stable radical, in comparison to the tertiary radical, $\bullet\text{C}(\text{Me})\text{NCbzR}$ (Scheme 22).



Scheme 26. Photocleavage of the resin functionalized with the new photocleavable linker.

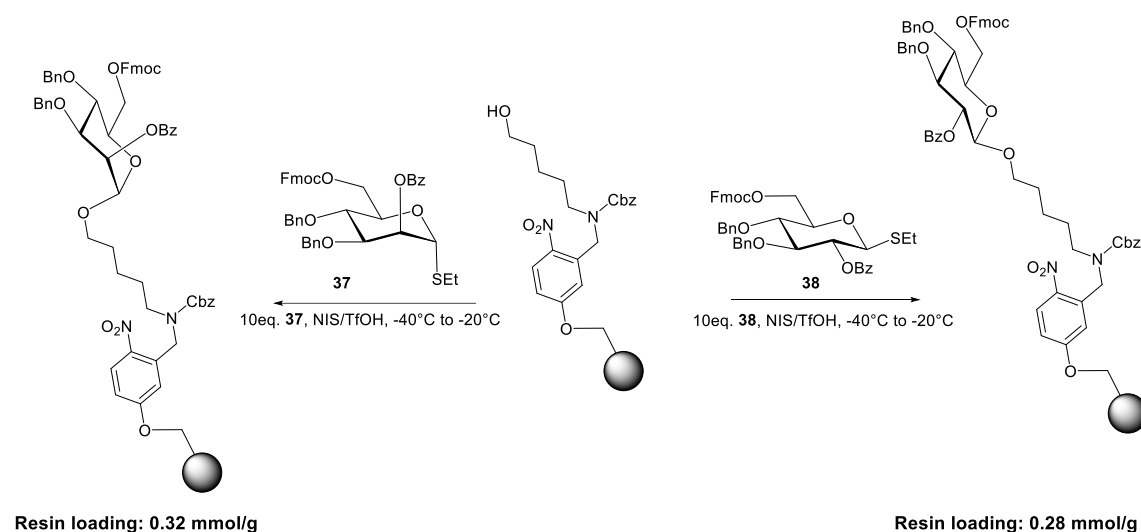


Scheme 27. Possible explanation for the unexpected result with the new photocleavable linker.

Considering these results, the further investigations are required to find a linker and photo cleavage procedure that would improve the yield.

2.3 Resin loading determination using different building blocks

A very important issue in automated solid-phase synthesis is the determination of resin loading. As discussed above, three methods of resin loading determination can be used: 1) the method based on the determination of the number of free hydroxyl-groups on the surface of the resin; 2) gravimetric quantification of the amount of monosaccharide after photo cleavage; 3) the method that is based on the determination of Fmoc-groups on the resin after the first glycosylation. Method 3 proved most suitable since it provides the information about the number of reactive sides on the surface of the resin that are accessible for glycosylation.



Scheme 28. Resin loading determination using two different types of building blocks.

There is one very important aspect about this loading determination method: generally, mannose building block is used to determine resin loading. However, when different monosaccharides are used for the first glycosylation the result might be different. In order to investigate this aspect, the following experiment has been performed: Merrifield resin functionalized with linker was glycosylated using two building blocks **37** and **38**, and the loading was measured (Scheme 23). No significant difference between loadings obtained was observed.

2.4 Optimization of automated solid-phase synthesis

In order to accelerate automated solid-phase synthesis, improve yields and reduce the amount of reagents and solvents used, the stepwise optimization of the synthesis was conducted. Several steps are part of the overall elongation cycle: acidic wash, glycosylation,

deprotection. Initially I analyzed how much time it takes to perform each step of the synthetic cycle (Table 3).

Table 3. Time required for different steps in standard AGA

Cycle	Time, min
Acidic wash	30
Glycosylation	70
Deprotection	60
Total time	160

2.4.1 Acidic wash optimization

The initial step of each elongation cycle in AGA is the acidic wash. During acidic wash any base that might have been left on the resin from the previous steps (generally, after deprotection step that is done in highly basic conditions) is neutralized. As long as the following glycosylation step acid is performed under acidic conditions it is important to make sure that no traces of base left on the resin.

The acidic wash includes several steps (Table 4): the reaction vessel with resin is cooled down to -30°C , TMSOTf solution in DCM is delivered and left bubbling for 2 min. Then, the resin is washed with DCM. Overall, it takes 25 minutes to perform the whole process of acidic wash.

The slowest step of the process is cooling the reaction vessel to -30°C . The acidic wash procedure should be performed at low temperature to ensure that the compound on the surface of the resin is not affected by highly acidic media. The solution that is used for the acidic wash (TMSOTf in DCM) was also used as an activator solution for phosphate glycosylation donors in AGA⁹⁰ and is generally applied at temperatures from -40°C to -20°C . In this regard, the temperature for acidic wash was chosen to be -20°C that helped to reduce the time for this cycle by 4 minutes.

Table 4. Optimization of acidic wash cycle.

Step	Standard Cycle	Optimized Cycle
Chiller to (-30°C)	1140	
Wash lines	120	120
Chiller to (-20°C)		900
TMSOTf Delivery	120	120
Wash lines	60	60
Bubbling with TMSOTf	120	120
Wash with DCM	30	30
Total time (s)	1470	1230
Total time (min)	24.5	20.5

2.4.2 Glycosylation cycle

The glycosylation cycle is the most important step of automated solid-phase synthesis of oligosaccharides and it is important to optimize the conditions of performing it. Generally, it is necessary to optimize the reaction conditions, such as glycosylation temperature, reaction time as well as the amount of building block used, for each building block: different monosaccharides have different reactivity and glycosylation conditions may vary from one glycosylating agent to another. But there are several aspects that are common for most of the building blocks and that have to be optimized:

1) The standard glycosylation cycle includes several steps. First, the reaction vessel is cooled down to the temperature T1 that is by 20°C lower than the actual reaction temperature T2. At the temperature T1 the building block solution as well as the activator solution are added to the resin. Then, the temperature is set to increase gradually to T2. The reason for pre-cooling of the reaction mixture is the fact that glycosylation reaction is

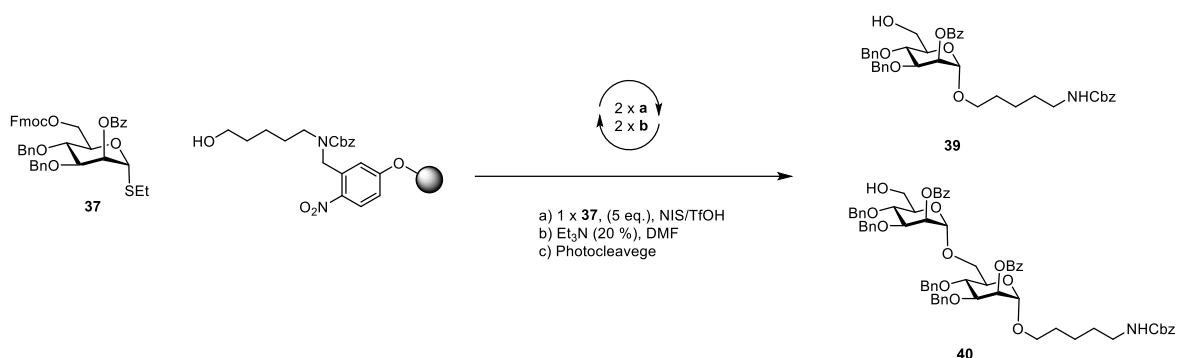
exothermic and the addition of reagents results in local overheating of the reaction mixture. This might lead to the formation of byproducts. The pre-cooling process, however, takes substantial time that slows down the overall synthesis.

2) The amount of building blocks used for one glycosylation step is quite high, as overall 10 eq. of building block are used for one elongation step.

3) One elongation step involves two glycosylation cycles. This leads to long time of elongation not only because of overall long reaction time, but also because of the time between glycosylation cycles when the temperature is brought down to T1 again.

4) The number of washing steps is excessive and results in long time and high DCM usage per elongation cycle.

In order to optimize glycosylation cycle, the glycosylation reaction of the mannose building block **37** was used as a model process. It was shown by N. Kottari *et. al.* that this building block is highly reactive and allows for good separation of deletion sequences.¹¹²



Scheme 29. Synthesis of mannoside dimer used as a model reaction for glycosylation cycle optimization.

Initially, I investigated the optimal temperature for performing glycosylation reaction for building block **37**. Therefore, the model process (shown on Scheme 23) was performed at different conditions (Table 5).

The glycosylation was most efficient at T1=-20°C and T2=0°C as at these conditions a single glycosylation using 5.0 eq. of building block **37** gives very good results: the ratio of monosaccharide: disaccharide is 7:93. In order to achieve the full conversion during glycosylation process, the number of equivalents of building blocks was increased. It was found that 6.5 equivalents for one elongation cycle is enough to avoid deletion sequences formation.

Table 5. Optimization of glycosylation conditions

T (°C)	Glyc. / min	mono : di (30 : 31)
-40 to -20	70	10 : 90
-20	10	28:72
-20	20	17:83
-20	30	15:85
-20 to 0	20	7:93

The necessity of performing the washing procedures was analyzed. There are several washing steps that are crucial in the glycosylation cycle: it is important to wash away all the activator solution from the resin and it can be done with the subsequent washing of the reaction mixture with dioxane and then with DCM (twice). The washing with dioxane is necessary for the reason that NIS that is used as an activator in the glycosylation reaction is poorly soluble in DCM, but has good solubility in dioxane. As the following test show this washing steps were sufficient to achieve good glycosylation results.

Overall, as a result of the optimization of the glycosylation step, several improvements have been achieved:

- 1) The glycosylation cycle time was substantially reduced.
- 2) One glycosylation cycle is enough to achieve full conversion using 6.5 eq. of building block **37**.
- 3) The amount of building block and solvents used was significantly reduced.

The overview of the glycosylation cycle optimization and solvent usage is shown in Table 6 and Table 7 respectively.

Even though the described glycosylation cycle was optimized using mannose building block **37**, it can be also applied for different monosaccharides (as shown in Chapter 3). It can be also modified for the glycosylation donors with low reactivity (the number of equivalents that are used can be increased, two cycles of glycosylation can be performed, reaction time during each of the glycosylations can be increased).

Table 6. Optimization of glycosylation cycle

	Standard Cycle (s)	Optimized Cycle (s)
Chiller to (T1)	From prev.	From prev.
Wash lines	70	70
Delivery of BB	90	90
Push back BB	60	60
Wash Activator line	270	
Prime Activator line	60	
Wait for T1		
Delivery of activator	210	210
Push back activator	120	120
Bubble at T1	300	300
Wait for T2	120	
Bubble at T2	1800	300
Chiller to T3 (Fmoc)		(25°C)
Wash with Dioxane	90	90
Wash with DCM (x6)	180	50 (25 x 2)
Wait for 25°C	480	
Wash BB lines	150	
Wash with DCM (x6)	180	
Total time (s)	4180	1290
Total time (min)	70.0	21.5

Table 7. Total amount of solvents used in the glycosylation cycle

Solvent	Standard Cycle	Optimized Cycle
DCM	28 mL	4 mL
Dioxane	2 mL	2 mL

2.4.3 Deprotection cycle

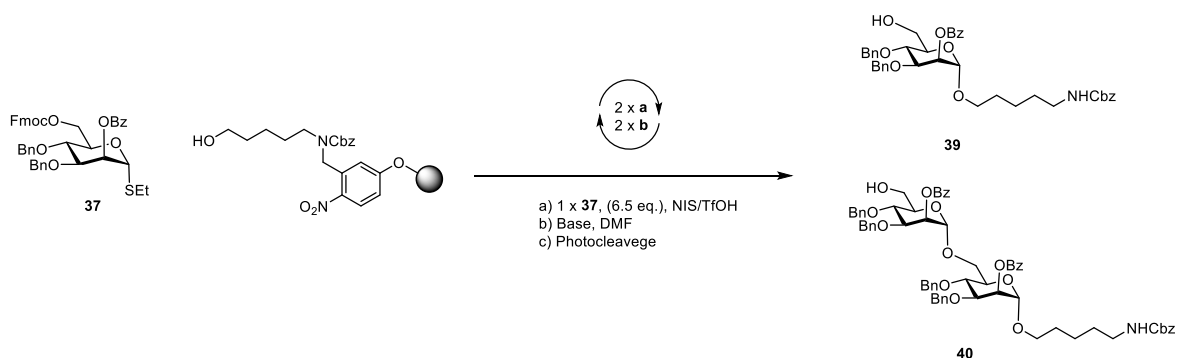
In AGA, several methods of Fmoc-deprotection cycles have been used. The most common cycle utilizes excess of a 20% solution of Et₃N in DMF. This method allows for effective removal of Fmoc-protecting group, but requires a lot of time: as it takes almost one hour to perform the whole cycle. In order to accelerate the process, the cycle has to be optimized.

There are several important considerations that have to be kept in mind concerning the optimization of the deprotection step:

- 1) The conditions used for the reaction should not affect protecting groups that are generally used for the AGA (OBz, OLev, etc.), as some of the protecting groups can be labile in highly basic conditions.
- 2) The procedure should be fast and, ideally, should not require a large amount of solvents used.

Several aspects of Fmoc-deprotection process have to be discussed: solvent and base that is used for the reaction, as well as reaction temperature and time.

Most of the reported methods of Fmoc-deprotection utilize strong base in the solution of DMF or DCM. Considering the fact that glycosylation cycle is performed mainly in DCM or DCM/dioxane mixture, it is desirable, that Fmoc-deprotection cycle is also performed in DCM (in this case it will be not necessary to perform the additional washing of resin because of the change of the solvent). It was however shown in Seeberger group that the Fmoc-deprotection reaction is slower in DCM than in DMF and might take up to four hours depending on the carbohydrate, so the usage of DCM as a solvent for the deprotection reaction in automation is not efficient.



Scheme 30. Synthesis of mannoside dimer as a model reaction for the deprotection cycle optimization.

Table 8. Optimization of the Fmoc-deprotection cycle

Base (solution in DMF)	Reaction time (min)	mono : di (30 : 31)
Et ₃ N (20%)	15 (x2)	0 : 100
Et ₃ N (20%)	15	15 : 85
Et ₃ N (50%)	15	10 : 90
Piperidine (20%)	15	0 : 100
Piperidine (20%)	10	0 : 100
Piperidine (20%)	5	0 : 100

Mindful of these considerations, several reaction conditions for deprotection were selected (see Table 8). The synthesis of mannose dimer with an optimized glycosylation cycle was used as a model process (Scheme 25). The best conditions for Fmoc-group deprotection in AGA are a piperidine solution in DMF. The reaction is completed within 5 minutes and only one cycle is necessary to achieve full conversion.

Washing procedures that were used during the cycle have been also analyzed. There are several washing steps that are indispensable for performing this cycle: in the beginning of the cycle the resin has to be washed three times with DMF (because all the previous steps were done in DCM); after the deprotection reaction, washing with DMF is required to remove any traces of base that are left on the resin; at the end of the cycle the resin should be washed with DCM, because the next step, generally the glycosylation, is performed in DCM. All the other washing procedures were found to be not necessary and were removed from the cycle. It was possible to reduce the time required for the deprotection cycle from 55 min to 22 min and significantly reduce the amount of solvents used (Tables 9 and 10).

Table 9. Optimization of Fmoc-deprotection cycle

	Standard Cycle	Optimized Cycle
Wash DMF	30x3	30x3
Delivery of DMF	5	
Wash dep. lines	270	
Prime dep. lines	60	

DMF to waste	150	150
Dep 1	750	0
Dep 2	750	0
Dep 3	750	750
Wash with DMF	60	60
Wash dep. lines	150	150
Wash with DCM	15	0
Wash with DMF x3	30x3	0
Wash with THF x3	30x3	0
Wash with DCM	30x3	30x2
Total time (s)	3320	1300
Total time (min)	55	22

Table 10. Total amount of solvents used in the deprotection cycle

Solvent	Standard Cycle	Optimized Cycle
DCM	14 mL	10 mL
DMF	20 mL	14 mL
THF	6 mL	0

2.5 Conclusions and perspectives

The described experiments made it possible to improve several aspects of automated solid-phase synthesis of oligosaccharides:

- 1) The overall cycle time has been significantly reduced: in the optimized version one elongation cycle takes one hour (in comparison with previous standard cycle – three hours).
- 2) The amount of building block used for one elongation cycle has been notably reduced: it is required 6.5 equivalents of building block **37** per elongation cycle to ensure the full conversion (previously – 10 equivalents).

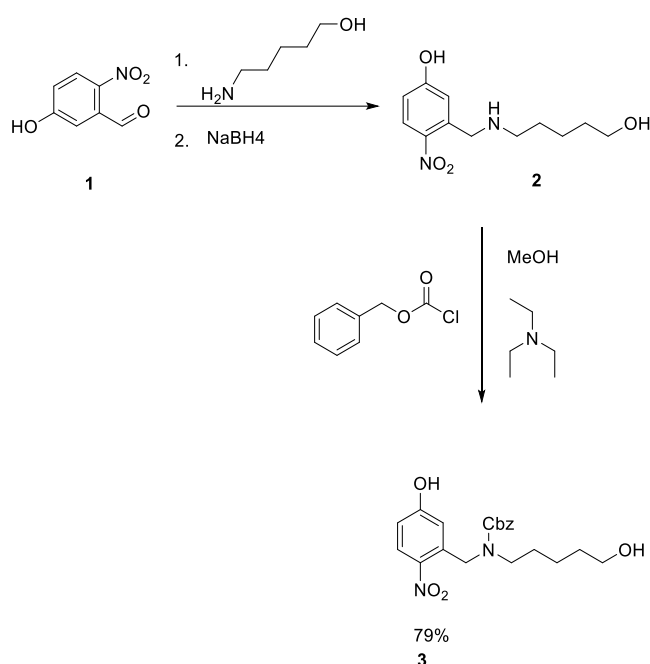
3) Total amount of solvents used was lowered.

The next step is testing of the optimized conditions on various building blocks and application of the new cycles to the synthesis of a library of compounds.

2.6 Experimental part

2.6.1 Synthesis of photo cleavable linkers and their derivatives

Synthesis of compound 3

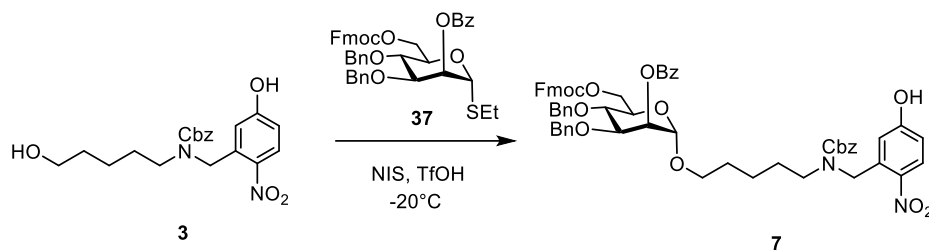


5-Hydroxy-2-nitrobenzaldehyde **1** (0.5 g, 3.0 mmol) and 5-aminopentanol (0.31 g, 3.0 mmol) were stirred in anhydrous methanol (10 mL) at room temperature for 2.5 h under argon atmosphere. Then, the reaction mixture was cooled to 0°C and NaBH₄ (0.12 g, 3.0 mmol) was added a portionwise and allowed to warm to room temperature. After 1h, excess NaBH₄ was quenched by the addition of acetone (15 mL) and the solvents were evaporated to furnish the secondary amine **2**. Secondary amine **2** was re-dissolved and stirred in MeOH (80 mL) followed by the addition of triethylamine (1.25 mL, 8.9 mmol) and Cbz-Cl (1.68 mL, 7.48 mmol) at room temperature. After 1 h, K₂CO₃ (2.0 g) was added to the reaction mixture and stirred for an hour. The reaction mixture was then filtered through celite and the solvents were evaporated to dryness. The crude product was dissolved in DCM and washed with 0.1 M HCl and water. The organic layer was dried over MgSO₄, filtered, concentrated and subjected to

flash chromatography (Silica/ EtOAc:Hexane) to obtain photo-cleavable linker **3** in 85% yield (0.98 g)⁹¹.

Analytical data for linker **3**: ¹H NMR (400 MHz, CDCl₃) δ (ppm) 8.19 - 8.07 (m, 1H), 7.38 - 7.24 (m, 5H), 6.85 - 6.71 (m, 2H), 5.17 - 5.05 (m, 2H), 4.91 (s, 2H), 3.63 - 3.60 (m, 2H), 3.38 - 3.35 (m), 1.57 - 1.41 (m, 6H); ¹³C NMR (101 MHz, Chloroform-*d*) δ (ppm) 162.7, 162.1, 157.1, 157.1, 139.6, 137.5, 135.7, 128.8, 128.8, 128.4, 128.3, 128.2, 128.2, 128.2, 128.2, 128.1, 128.0, 127.9, 127.4, 114.8, 114.8, 114.6, 113.8, 113.8, 113.0, 67.6, 62.2, 49.9, 49.9, 49.8, 49.6, 48.8, 48.7, 48.46 48.4, 48.4, 31.8, 28.1, 27.6, 22.8. Analytical data in accordance with previously reported data.⁹¹

Synthesis of compound **7**

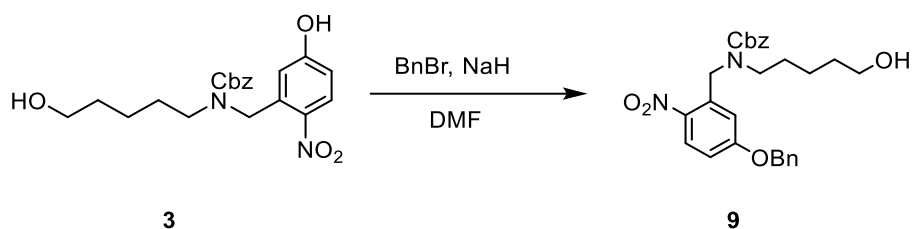


To a solution of building block **37** (120 mg, 0.16 mmol) and linker **3** (191 mg, 0.493 mmol) in anhydrous DCM (10 mL) molecular sieves (4 Å, powder) were added. The mixture was stirred for 10 minutes before NIS (55 mg, 0.25 mmol) was added. After stirring for 20 minutes the reaction mixture was cooled down to -20°C before TfOH (0.015 mL, 0.16 mmol) was added dropwise to the reaction mixture. The reaction mixture was stirred for 20 minutes and allowed to warm to room temperature. The reaction was successively quenched by saturated NaHCO₃ solution (15 mL) and saturated Na₂S₂O₃ solution. The organic layer was washed with brine (3x 15 mL), dried over Na₂SO₄ and concentrated in vacuum. The crude product was purified by column chromatography (silica gel, hexane – EtOAc, 1:3 to 1:1), giving product **7** (145 mg, 0.137 mmol, 84%) as yellow syrup.

Analytical data for compound **6**: ¹H NMR (400 MHz, CDCl₃) δ 8.19 – 8.05 (m, 3H), 7.78 (d, J = 7.5 Hz, 2H), 7.62 – 7.58 (m, 2H), 7.53 (t, J = 7.6 Hz, 1H), 7.40 (q, J = 7.7 Hz, 4H), 7.38 – 7.24 (m, 17H), 6.85 – 6.71 (m, 2H), 5.71 (s, 1H), 5.42 (s, 1H), 5.17 – 5.05 (m, 2H), 4.94 – 4.89 (m, 3H), 4.80 – 4.75 (m, 1H), 4.61 – 4.58 (m, 2H), 4.47 (s, 2H), 4.39 (d, J = 7.7 Hz, 2H), 4.35 – 4.23 (m, 2H), 4.07 – 3.94 (m, 2H), 3.39 - 3.35 (m, 2H), 2.67 – 2.62 (m, 2H), 1.57 – 1.48 (m, 4H), 1.47 – 1.40 (m, 2H), 1.32 – 1.25 (m, 3H). ¹³C NMR (101 MHz,

Chloroform-*d*) δ 165.65, 162.72, 162.08, 157.12, 156.82, 139.62, 138.10, 137.56, 137.51, 135.65, 133.26, 129.42, 129.12, 128.76, 128.35, 128.15, 128.01, 127.95, 127.92, 127.76, 127.68, 114.78, 114.72, 114.61, 113.82, 113.02, 82.45, 78.42, 75.12, 74.04, 72.20, 71.51, 70.89, 67.64, 62.20, 61.94, 49.91, 48.75, 48.72, 48.65, 48.46, 31.82, 28.14, 27.65, 25.56, 22.82, 14.83. MS (ESI) m/z calcd for $C_{62}H_{60}N_2O_{14}$ $[M+Na]^+$ 1080.5. Found 1080.7.

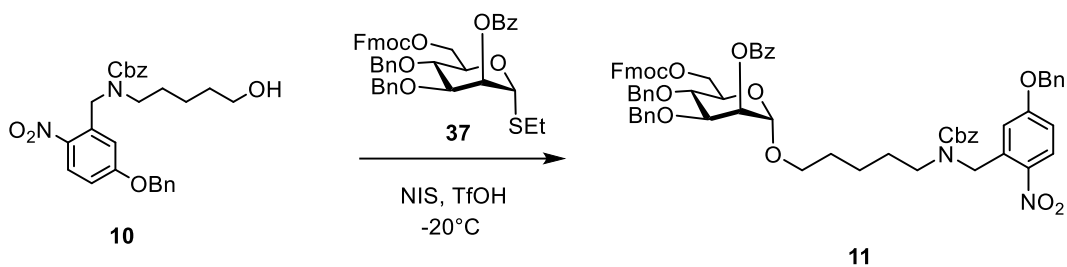
Synthesis of benzyl (5-(benzyloxy)-2-nitrobenzyl)(5-hydroxypentyl)carbamate **9**



The solution of the compound **3** (320 mg, 0.82 mmol) and benzyl bromide (0.14 mL, 1.1 mmol) in 10 mL DMF was cooled down to 0°C before NaH (40 mg, 1.1 mmol) was added dropwise. The reaction mixture was allowed to warm up to RT and was stirred for three hours before being quenched by saturated solution of NH_4Cl . The reaction mixture was diluted with EtOAc and washed with brine. Volatiles were removed under vacuum, the crude product was purified by column chromatography (silica gel, hexane – EtOAc, 1:4 to 1:1), giving product **9** (315 mg, 0.66 mmol, 80%) as yellow syrup.

Analytical data for compound **10**: 1H NMR (400 MHz, $CDCl_3$) δ 8.13 (d, $J = 9.1$ Hz, 1H), 7.42 – 7.29 (m, 7H), 7.28 – 7.11 (m, 3H), 6.90 (d, $J = 9.1$ Hz, 1H), 6.74 (d, $J = 32.3$ Hz, 1H), 5.22 (d, $J = 35.9$ Hz, 1H), 5.04 (d, $J = 17.0$ Hz, 2H), 4.89 (d, $J = 24.3$ Hz, 3H), 3.56 (dt, $J = 19.5, 6.5$ Hz, 3H), 3.18 (dt, $J = 20.8, 7.5$ Hz, 3H), 1.64 – 1.45 (m, 4H), 1.37 – 1.29 (m, 2H). ^{13}C NMR (101 MHz, Chloroform-*d*) δ 153.25, 135.99, 130.48, 128.53, 127.26, 117.09, 97.04, 69.18, 67.33, 65.47, 48.59, 41.28, 31.99, 26.81, 23.05, 21.78. MS (ESI) m/z calcd for $C_{27}H_{30}N_2O_6$ $[M+Na]^+$ 500.5. Found 500.9.

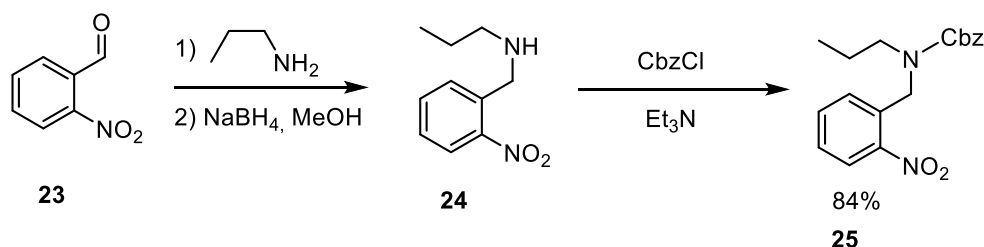
Synthesis of compound **11**



To a solution of building block **37** (180 mg, 0.24 mmol) and linker **10** (360 mg, 0.75 mmol) in anhydrous DCM (15 mL) molecular sieves (4 Å, powder) were added. The mixture was stirred for 10 minutes before NIS (83 mg, 0.37 mmol) was added. After stirring for 20 minutes the reaction mixture was cooled down to -20°C before TfOH (0.023 mL, 0.24 mmol) was added dropwise to the reaction mixture. The reaction mixture was stirred for 20 minutes and allowed to warm to room temperature. The reaction was successively quenched by saturated NaHCO_3 solution (15 mL) and saturated $\text{Na}_2\text{S}_2\text{O}_3$ solution. The organic layer was washed with brine (3x 15 mL), dried over Na_2SO_4 and concentrated in vacuum. The crude product was purified by column chromatography (silica gel, hexane – EtOAc, 1:3 to 1:1), giving product **11** (198 mg, 0.173 mmol, 72%) as yellow syrup.

Analytical data for compound **12**: $^1\text{H NMR}$ (400 MHz, Chloroform-*d*) δ 8.17 (d, $J = 9.1$ Hz, 1H), 8.10 (d, $J = 7.7$ Hz, 2H), 7.60 (t, $J = 7.4$ Hz, 1H), 7.48 (t, $J = 7.7$ Hz, 2H), 7.45 – 7.29 (m, 11H), 7.29 – 7.15 (m, 6H), 6.93 (d, $J = 9.2$ Hz, 1H), 6.79 (d, $J = 32.8$ Hz, 1H), 5.61 (s, 1H), 5.25 (d, $J = 16.7$ Hz, 1H), 5.07 (d, $J = 22.4$ Hz, 2H), 4.93 (dd, $J = 16.0, 5.3$ Hz, 5H), 4.81 (d, $J = 11.4$ Hz, 1H), 4.68 (d, $J = 10.9$ Hz, 1H), 4.60 (d, $J = 11.3$ Hz, 1H), 4.18 – 4.07 (m, 2H), 3.98 (t, $J = 9.6$ Hz, 1H), 3.94 – 3.79 (m, 2H), 3.79 – 3.59 (m, 2H), 3.41 (dq, $J = 14.6, 8.1, 7.4$ Hz, 1H), 3.22 (dt, $J = 16.7, 7.7$ Hz, 2H), 1.60 (dp, $J = 15.3, 7.6$ Hz, 4H), 1.35 (dq, $J = 14.6, 6.6$ Hz, 2H). MS (ESI) m/z calcd for $\text{C}_{69}\text{H}_{66}\text{N}_2\text{O}_{14}$ $[\text{M}+\text{Na}]^+$ 1170.2. Found 1169.9.

Synthesis of benzyl (2-nitrobenzyl)(propyl)carbamate **16**



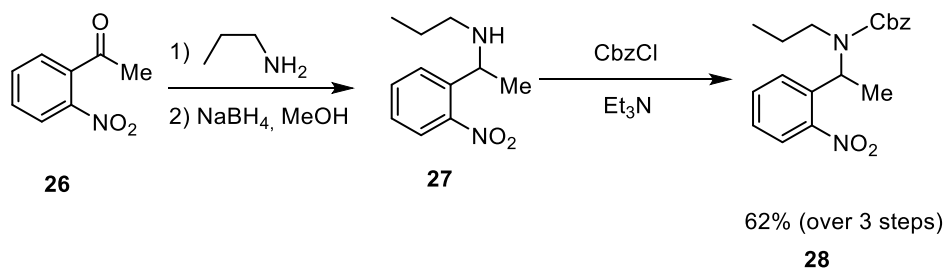
Starting material **23** (1 g, 6.6 mmol) and propylamine (0.60 mL, 7.3 mmol) were dissolved in 10 mL anhydrous THF. The reaction was stirred for two hours at RT. The reaction mixture was concentrated in vacuum and dissolved in anhydrous MeOH (10 mL).

Then, the reaction mixture was cooled down to 0°C and NaBH₄ (249 mg, 6.6 mmol) was added portionwise. The reaction was stirred for two hours before being quenched by acetone. All volatile products were removed under vacuum. The crude product was subjected to the next step without purification.

Crude product was dissolved in anhydrous MeOH and CbzCl (1.1 mL, 7.9 mmol) was added. Triethylamine (1.9 mL, 13 mmol) was added and the reaction mixture was stirred for four hours at RT. Afterwards all the volatile products were removed under vacuum, the solid material was dissolved in DCM, washed by HCl (twice), NaHCO₃ (twice), dried over MgSO₄ and concentrated under vacuum. Purification by column chromatography gave 1.82 g (3.8 mmol, 84% yield) of compound **25**.

Analytical data for compound **25**: ¹H NMR (400 MHz, Chloroform-*d*) δ 8.09 – 7.99 (m, 1H), 7.54 (p, *J* = 7.8 Hz, 1H), 7.43 – 7.27 (m, 6H), 7.14 (s, 1H), 5.17 (d, *J* = 15.9 Hz, 2H), 5.08 (s, 1H), 4.92 – 4.79 (m, 2H), 3.26 (p, *J* = 7.5 Hz, 2H), 1.58 (q, *J* = 7.9 Hz, 2H), 0.87 (dt, *J* = 14.0, 7.5 Hz, 3H). MS (ESI) *m/z* calcd for C₁₈H₂₀N₂O₄ [M+Na]⁺ 351.1. Found 351.4.

Synthesis of benzyl (1-(2-nitrophenyl)ethyl)(propyl)carbamate 19

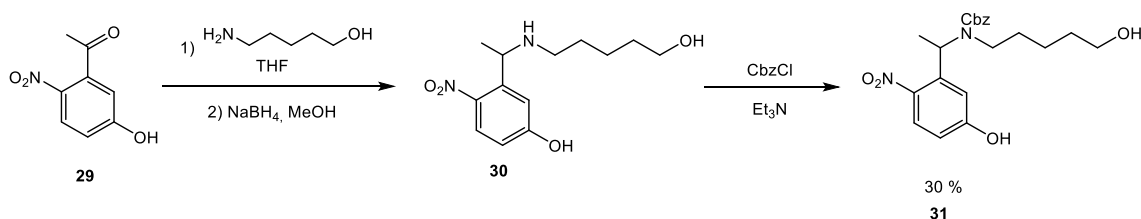


Starting material **26** (1 g, 6.1 mmol) and propylamine (0.55 mL, 6.7 mmol) were dissolved in 10 mL anhydrous THF. The reaction was stirred for two hours at RT. The reaction mixture was concentrated in vacuum and dissolved in anhydrous MeOH (10 mL). Then, the reaction mixture was cooled down to 0°C and NaBH₄ (230 mg, 6.1 mmol) was added portionwise. The reaction was stirred for two hours before being quenched by acetone. All the volatile products were removed under vacuum. The crude product was subjected to the next step without purification.

Crude product was dissolved in anhydrous MeOH and CbzCl (1.02 mL, 7.2 mmol) was added. Triethylamine (1.7 mL, 12 mmol) was added and the reaction mixture was stirred for four hours at RT. Afterwards all the volatile products were removed under vacuum, the solid material was dissolved in DCM, washed by HCl (twice), NaHCO₃ (twice), dried over MgSO₄ and concentrated under vacuum. Purification by column chromatography gave 1.29 g (3.8 mmol, 62% yield) of compound **28**.

Analytical data for compound **28**: ^1H NMR (400 MHz, Chloroform-*d*) δ 7.73 (dd, $J = 8.1, 1.3$ Hz, 1H), 7.50 (q, $J = 7.8$ Hz, 2H), 7.36 (td, $J = 7.7, 7.2, 3.4$ Hz, 1H), 7.33 – 7.16 (m, 5H), 5.72 (q, $J = 7.0$ Hz, 1H), 5.05 (s, 2H), 3.29 – 3.06 (m, 2H), 1.59 (d, $J = 7.1$ Hz, 3H), 1.55 – 1.36 (m, 2H), 0.77 (t, $J = 7.4$ Hz, 3H). MS (ESI) m/z calcd for $\text{C}_{19}\text{H}_{22}\text{N}_2\text{O}_4$ $[\text{M}+\text{Na}]^+$ 365.3. Found 365.5.

Synthesis of benzyl (1-(5-hydroxy-2-nitrophenyl)ethyl)(5-hydroxypentyl)carbamate **25**

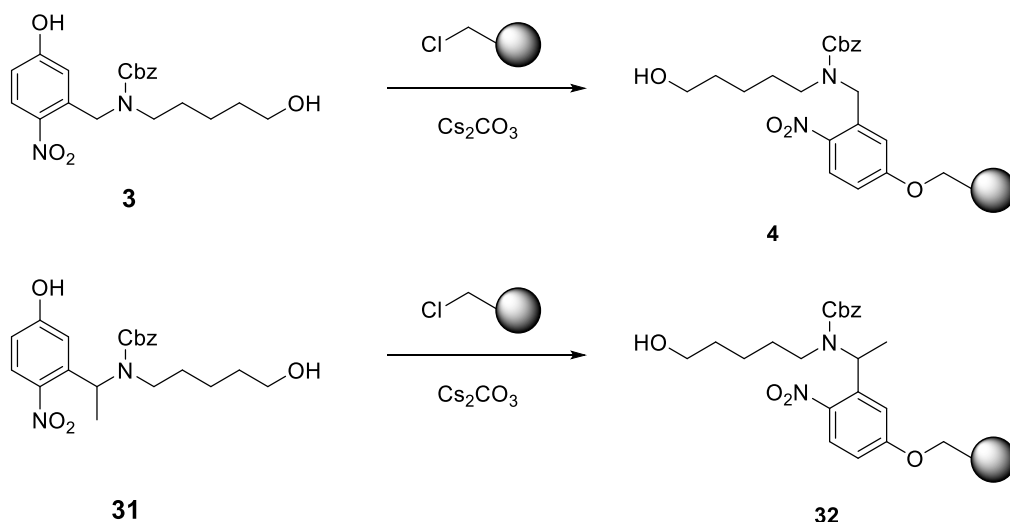


Starting material (500 mg, 2.8 mmol) and propylamine (0.25 mL, 3.1 mmol) were dissolved in 10 mL anhydrous THF. The reaction was stirred overnight at RT. The reaction mixture was concentrated in vacuum and dissolved in anhydrous MeOH (10 mL). Then the reaction mixture was cooled down to 0°C and NaBH₄ (106 mg, 2.8 mmol) was added portionwise. The reaction was stirred for two hours before being quenched by acetone. All the volatile products were removed under vacuum. The crude product was subjected to the next step without purification.

Crude product was dissolved in anhydrous MeOH and CbzCl (0.50 mL, 3.5 mmol) was added. Triethylamine (0.85 mL, 6.0 mmol) was added and the reaction mixture was stirred for four hours at RT. Afterwards all the volatile products were removed under vacuum, the solid material was dissolved in DCM, washed by HCl (twice), NaHCO₃ (twice), dried over MgSO₄ and concentrated under vacuum. Purification by column chromatography gave 0.340 g (3.8 mmol, 30% yield) of compound **25**.

Analytical data for compound **25**: ^1H NMR (400 MHz, Chloroform-*d*) δ 8.07 (d, $J = 9.1$ Hz, 1H), 7.70 (dd, $J = 8.0, 1.5$ Hz, 1H), 7.55 – 7.49 (m, 2H), 7.41 – 7.34 (m, 1H), 7.32 – 7.10 (m, 4H), 5.70 (q, $J = 7.0$ Hz, 1H), 5.08 (s, 2H), 3.27 – 3.06 (m, 2H), 1.56 (d, $J = 7.1$ Hz, 3H), 1.53 – 1.34 (m, 2H), 0.80 (t, $J = 7.3$ Hz, 3H). MS (ESI) m/z calcd for $\text{C}_{21}\text{H}_{26}\text{N}_2\text{O}_6$ $[\text{M}+\text{Na}]^+$ 425.4. Found 452.1.

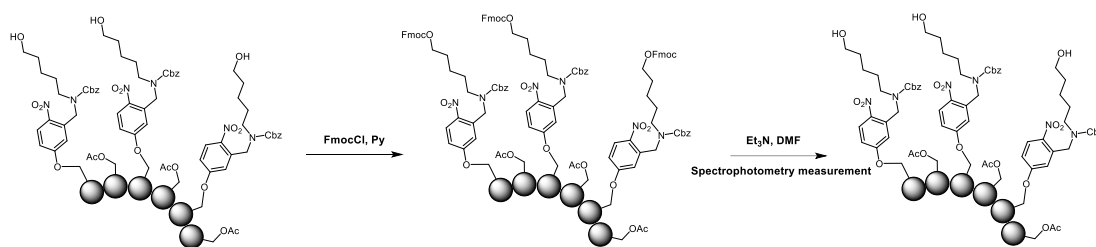
Resin functionalization and resin loading determination



Resin functionalization. Merrifield resin (0.50 mmol/g, 8.0 g, 4.0 mmol, 1.0 eq.) and linker **3** or **31** (6.21 g, 16 mmol, 4.0 eq.) were taken up in a minimal amount of anhydrous DMF (~4 mL DMF/g resin) to completely swell the resin and solubilize the linker. The suspension was then degassed by placing the flask under high vacuum for a couple of minutes, followed by refilling the evacuated flask with Argon. After repeating this degassing procedure two more times, Cs₂CO₃ (5.21 g, 16 mmol, 4.0 eq.) and TBAI (1.48 g, 4.0 mmol, 1.0 eq.) were added to the flask and the entire suspension rotated on a rotovap at 60 °C and atmospheric pressure overnight. The next morning, water was added to the resin to dissolve all solids and the resin was subsequently washed with THF/water (1/1), THF, DMF, MeOH, DCM, MeOH, and finally DCM (six times each) to remove the yellow color. The resin was transferred again to a round bottom flask, swollen in a minimal amount of DMF (4 mL DMF/g resin) and the flask degassed as above. Afterwards, CsOAc (1.54 g, 8.0 mmol) was added and the entire suspension rotated on a rotovap at 60 °C and atmospheric pressure overnight. The next morning, the resin was washed with THF/water (1/1), THF, DMF, MeOH, DCM, MeOH, and finally DCM (six times each) to remove the yellow color. It was then dried under high vacuum overnight and stored in the dark.

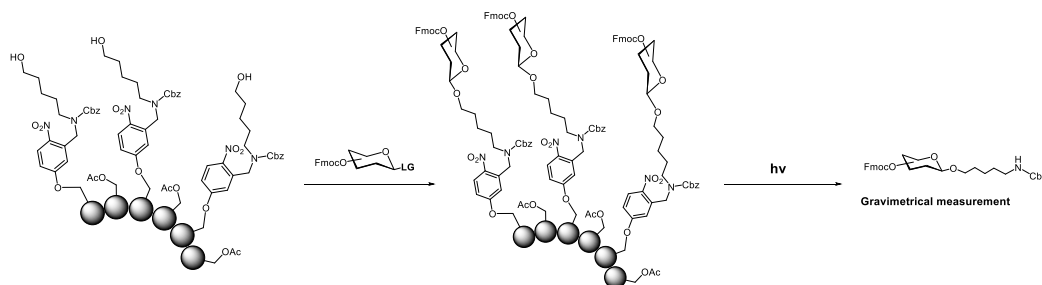
Resin loading determination methods.

Method 1.



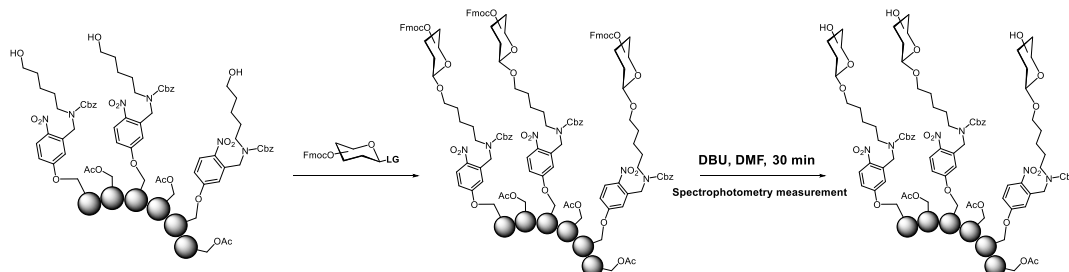
An aliquot of the resin (20-30 mg) is swollen in DCM (1 mL) for 1 hour. To this suspension was subsequently added FmocCl (100 mg) and pyridine (100 μ L) and shaken overnight at room temperature. The next morning, the resin was drained and washed with MeOH and DCM (six alternating washes). A solution of 20% triethylamine in DMF (6 mL) was then added to the resin and shaken at RT for 4 hours. After draining the resin, a 100 μ L aliquot of the solution was taken and diluted to 10 mL using 20% triethylamine in DMF and the absorbance at 301 nm ($\epsilon = 7800$ L/mol*cm) measured.

Method 2.



An aliquot of the resin (40 mg) is subjected to the glycosylation cycle (Module C) with 10 equiv. of building block **37** followed by the photo cleavage, HPLC purification and measurement of the mass of the resulting compound.

Method 3.



An aliquot of the resin (40 mg) is subjected to the glycosylation cycle (Module C) with 10 equiv. of building block **37** followed by DBU promoted Fmoc-cleavage and determination of dibenzofulvene production by measuring its UV absorbance.

2.6.2 Photo cleavage of linkers and functionalized resin

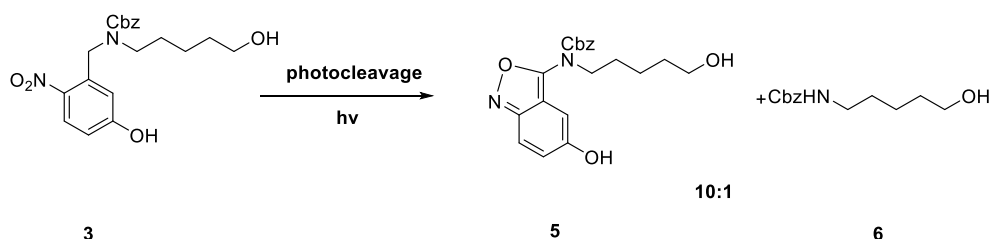
2.6.2.1 General procedure for photo cleavage of the resin

The resin is suspended in 20 mL of DCM is pumped through the Vaportec E-Series UV-150 photo reactor Flow Chemistry System at a flow rate of 0.8 mL/min. After passing the resulting solution through the filter, all the volatiles are removed under vacuum and the crude products are subjected to purification.

2.6.2.2 General procedure for photo cleavage of the compounds:

The solution of the compound in DCM is pumped through the Vaportec E-Series UV-150 photo reactor Flow Chemistry System at a flow rate of 0.8 mL/min. The resulting solution was concentrated under vacuum and the crude mixture was analyzed by NMR.

Photo cleavage of benzyl (5-hydroxy-2-nitrobenzyl)(5-hydroxypentyl)carbamate **3**

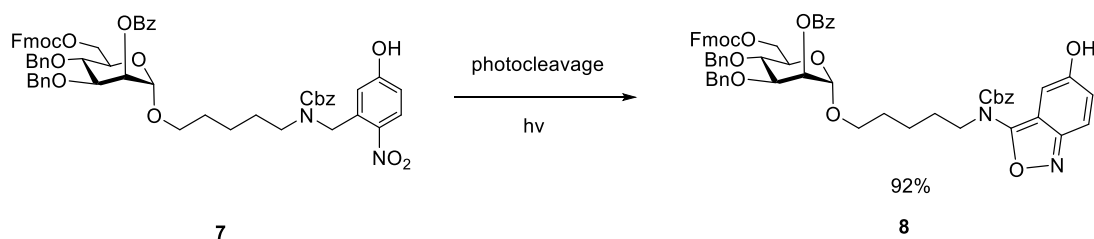


Linker **3** (25 mg, 0.071 mmol) was dissolved in 20 mL of anhydrous DCM and the solution was subjected to the photo cleavage procedure as described above.

Analytical data for rearrangement product **5**: $^1\text{H NMR}$ (400 MHz, CDCl_3) δ 7.40 – 7.24 (m, 6H), 6.99 (dt, $J = 9.6, 2.0$ Hz, 1H), 6.38 (s, 1H), 5.19 (s, 2H), 3.83 (t, $J = 7.0$ Hz, 2H), 3.58 (t, $J = 6.2$ Hz, 2H), 1.68 – 1.56 (m, 2H), 1.56 – 1.47 (m, 2H), 1.43 – 1.32 (m, 2H). MS (ESI) m/z calcd for $\text{C}_{20}\text{H}_{22}\text{N}_2\text{O}_5$ $[\text{M}+\text{Na}]^+$ 393.4. Found 393.7.

Analytical data for linker **6**: $^1\text{H NMR}$ (400 MHz, CDCl_3) δ 7.38 – 7.22 (m, 5H), 5.09 (s, 2H), 3.63 (t, $J = 6.5$ Hz, 2H), 3.23 – 3.15 (m, 2H), 1.68 – 1.49 (m, 4H), 1.44 – 1.36 (m, 2H). Analytical data in accordance with previously reported data.¹²³

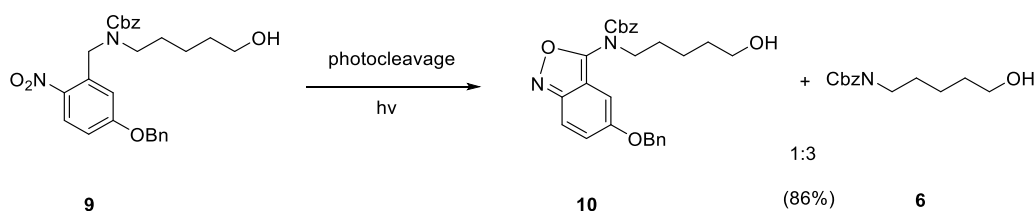
Photo cleavage of compound **8**



Linker **7** (26 mg, 0.025 mmol) was dissolved in 20 mL anhydrous DCM and the solution was subjected to the photo cleavage procedure as described above.

Analytical data for compound **8**: $^1\text{H NMR}$ (400 MHz, CDCl_3) δ 8.10 (d, $J = 7.8$ Hz, 2H), 7.74 (d, $J = 7.6$ Hz, 2H), 7.61 (dd, $J = 13.5, 7.8$ Hz, 2H), 7.56 – 7.52 (m, 1H), 7.43 – 7.24 (m, 22H), 6.99 (dt, $J = 9.6, 2.0$ Hz, 1H), 6.38 (s, 1H), 5.73 (s, 1H), 5.44 (s, 1H), 5.19 (s, 2H), 4.92 (d, $J = 11.0$ Hz, 1H), 4.83 – 4.75 (m, 1H), 4.65 – 4.52 (m, 2H), 4.47 (s, 2H), 4.41 (d, $J = 7.8$ Hz, 2H), 4.38 – 4.23 (m, 2H), 4.07 – 3.94 (m, 2H), 3.81 (t, $J = 7.1$ Hz, 2H), 3.56 (t, $J = 6.2$ Hz, 2H), 1.69 – 1.58 (m, 2H), 1.57 – 1.47 (m, 2H), 1.41 – 1.32 (m, 2H). MS (ESI) m/z calcd for $\text{C}_{62}\text{H}_{58}\text{N}_2\text{O}_{13}$ $[\text{M}+\text{Na}]^+$ 1062.1. Found 1062.3.

Photo cleavage of benzyl (5-(benzyloxy)-2-nitrobenzyl)(5-hydroxypentyl)carbamate **10**

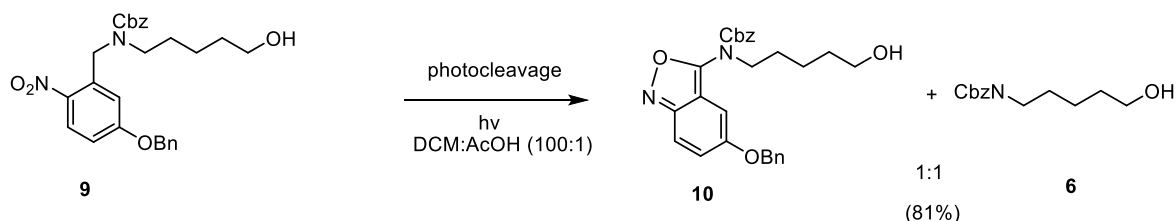


Linker **9** (25 mg, 0.055 mmol) was dissolved in 20 mL anhydrous DCM and the solution was subjected to the photo cleavage procedure as described above.

Analytical data for rearrangement product **10**: $^1\text{H NMR}$ (400 MHz, CDCl_3) δ 7.40 – 7.24 (m, 11H), 7.02 – 6.98 (m, 1H), 6.35 (s, 1H), 5.21 (s, 2H), 5.21 (s, 2H), 5.05 (s, 2H), 3.88 (t, $J = 6.8$ Hz, 2H), 3.56 – 3.50 (m, 2H), 1.66 – 1.53 (m, 2H), 1.52 – 1.46 (m, 2H), 1.44 – 1.33 (m, 2H). MS (ESI) m/z calcd for $\text{C}_{27}\text{H}_{28}\text{N}_2\text{O}_5$ $[\text{M}+\text{Na}]^+$ 483.5. Found 483.2.

Analytical data for the linker **6**: $^1\text{H NMR}$ (400 MHz, CDCl_3) δ 7.38-7.27 (m, 5H), 5.09 (s, 2H), 4.82 (s, 1H), 3.63 (t, 2H, $J = 6.5$ Hz), 3.20 (q, 2H, $J = 6.5$ Hz), 1.62 (s, 1H), 1.61-1.53 (m, 6H). Analytical data in accordance with previously reported data.¹²³

Photo cleavage of benzyl (5-(benzyloxy)-2-nitrobenzyl)(5-hydroxypentyl)carbamate **9 in acidic media**

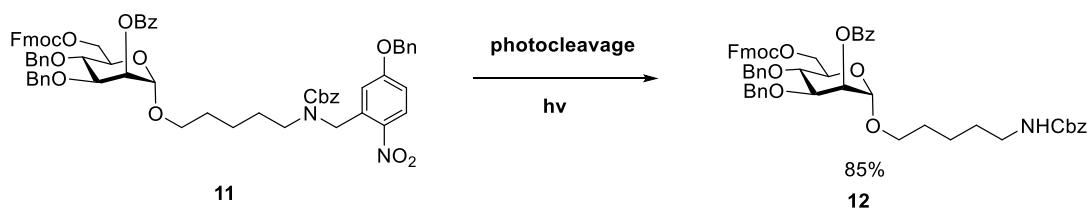


Compound **9** (25 mg, 0.055 mmol) was dissolved in 20 mL the mixture of DCM: AcOH (100:1) and the solution was subjected to the photo cleavage procedure as described above.

Analytical data for rearrangement product **10**: $^1\text{H NMR}$ (400 MHz, CDCl_3) δ 7.40 – 7.24 (m, 11H), 7.02 – 6.98 (m, 1H), 6.35 (s, 1H), 5.21 (s, 2H), 5.21 (s, 2H), 5.05 (s, 2H), 3.88 (t, $J = 6.8$ Hz, 2H), 3.56 – 3.50 (m, 2H), 1.66 – 1.53 (m, 2H), 1.52 – 1.46 (m, 2H), 1.44 – 1.33 (m, 2H). MS (ESI) m/z calcd for $\text{C}_{27}\text{H}_{28}\text{N}_2\text{O}_5$ $[\text{M}+\text{Na}]^+$ 483.5. Found 483.2.

Analytical data for the linker **6**: $^1\text{H NMR}$ (400 MHz, CDCl_3) δ 7.38-7.27 (m, 5H), 5.09 (s, 2H), 4.82 (s, 1H), 3.63 (t, 2H, $J = 6.5$ Hz), 3.20 (q, 2H, $J = 6.5$ Hz), 1.62 (s, 1H), 1.61-1.53 (m, 6H). Analytical data in accordance with previously reported data.¹²³

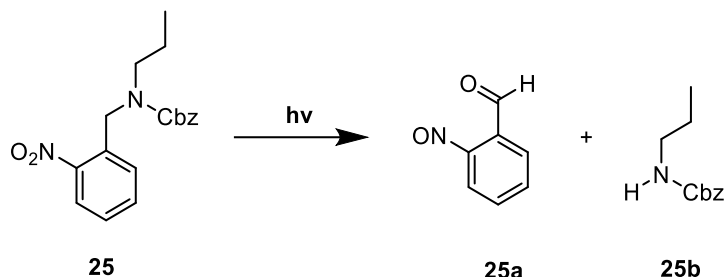
Photo cleavage of compound **12**



Compound **11** (26 mg, 0.025 mmol) was dissolved in 20 mL anhydrous DCM and the solution was subjected to the photo cleavage procedure as described above.

Analytical data for compound **12**: $^1\text{H NMR}$ (400 MHz, CDCl_3) δ 8.12 (d, $J = 7.7$ Hz, 2H), 7.73 (d, $J = 7.6$ Hz, 2H), 7.60 (dd, $J = 13.3, 7.7$ Hz, 2H), 7.55 (t, $J = 7.7$ Hz, 1H), 7.41 (q, $J = 7.7$ Hz, 4H), 7.38-7.23 (m, 17H), 5.73 (s, 1H), 5.42 (s, 1H), 4.92 (d, $J = 11.4$ Hz, 1H), 4.82 – 4.75 (m, 2H), 4.62 (dd, $J = 21.3, 11.1$ Hz, 2H), 4.49 (s, 2H), 4.39 (d, $J = 7.7$ Hz, 2H), 4.35 – 4.21 (m, 2H), 4.07 – 3.96 (m, 2H), 3.62 (t, 2H, $J = 6.2$ Hz), 3.22 – 3.16 (m, 2H), 1.64 – 1.56 (m, 2H), 1.55 – 1.44 (m, 2H), 1.42 – 1.33 (m, 2H). MS (ESI) m/z calcd for $\text{C}_{55}\text{H}_{55}\text{NO}_{11}$ $[\text{M}+\text{Na}]^+$ 929.0. Found 929.2.

Photo cleavage of benzyl (2-nitrobenzyl)(propyl)carbamate 16

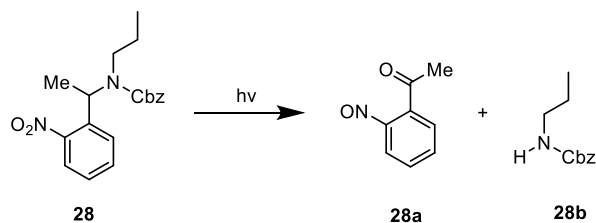


Compound **25** (25 mg, 0.076 mmol) was dissolved in 20 mL anhydrous DCM and the solution was subjected to the photo cleavage procedure as described above.

Analytical data for the aldehyde **25a**: $^1\text{H NMR}$ (400 MHz, CDCl_3) δ 12.03 (s, 1H), 8.19 (d, $J = 7.7$ Hz, 1H), 7.88 (t, $J = 7.6$ Hz, 1H), 7.69 – 7.62 (m, 1H), 7.27 – 7.22 (m, 1H).

Analytical data for the linker **25b**: $^1\text{H NMR}$ (400 MHz, CDCl_3) δ 7.38–7.32 (m, 5H), 5.09 (s, 2H), 4.78 (s, 1H), 3.20–3.10 (m, 2H), 1.57–1.44 (m, 2H), 0.92 (t, $J = 7.5$ Hz, 3H). Analytical data in accordance with previously reported data.¹²⁴

Photo cleavage of benzyl (1-(2-nitrophenyl)ethyl)(propyl)carbamate 19



Compound **28** (25 mg, 0.076 mmol) was dissolved in 20 mL anhydrous DCM and the solution was subjected to the photo cleavage procedure as described above.

Analytical data for the ketone **28a**: $^1\text{H NMR}$ (400 MHz, CDCl_3) δ 8.22 – 8.16 (m, 1H), 7.90 – 7.84 (m, 1H), 7.72 – 7.67 (m, 1H), 7.27 – 7.22 (m, 1H), 2.73 (s, 3H).

Analytical data for the linker **28b**: $^1\text{H NMR}$ (400 MHz, CDCl_3) δ 7.38–7.32 (m, 5H), 5.09 (s, 2H), 4.78 (s, 1H), 3.20–3.10 (m, 2H), 1.57–1.44 (m, 2H), 0.92 (t, $J = 7.5$ Hz, 3H). Analytical data in accordance with previously reported data.¹²⁴

2.6.3 Automated glycan assembly

2.6.3.1 General materials and methods

All solvents used were HPLC-grade. The solvents used for the building block, activator, TMSOTf and capping solutions were taken from an anhydrous solvent system (jcmeyer-solvent systems). The building blocks were co-evaporated three times with chloroform and dried for 1 h on high vacuum before use. Activator, deprotection, acidic wash and building block solutions were freshly prepared and kept under argon during the automation run. All yields of products obtained by AGA were calculated on the basis of resin loading.

2.6.3.2 Preparation of stock solutions

- **Building Blocks:** between 0.062 and 0.080 mmol of the building block **28** was dissolved in 1 mL of DCM.
- **Activator solution:** 1.35 g of NIS was dissolved in 40 mL of a 2:1 mixture of anhydrous DCM and anhydrous dioxane. Then triflic acid (55 μ L) was added. The solution is kept at 0°C for the duration of the automation run.
- **Fmoc deprotection solution 1:** A solution of 20% Et₃N in DMF (v/v) was prepared.
- **Fmoc deprotection solution 2:** A solution of 20% piperidine in DMF (v/v) was prepared.
- **TMSOTf Solution:** TMSOTf (0.45 mL) was added to DCM (40 mL).

2.6.3.3 Optimized modules for automated synthesis

Module A: Resin Preparation for Synthesis (20 min)

All automated syntheses were performed on 0.0125 mmol scale. Resin was placed in the reaction vessel and swollen in DCM for 20 min at room temperature prior to synthesis. During this time, all reagent lines needed for the synthesis were washed and primed. Before the first glycosylation, the resin was washed with the DMF, THF, and DCM (three times each with 2 mL for 25 s).

Module B: Acidic Wash with TMSOTf Solution (20 min)

The resin was swollen in 2 mL DCM and the temperature of the reaction vessel was adjusted to -20 °C. Upon reaching the low temperature, TMSOTf solution (1 mL) was added

drop wise to the reaction vessel. After bubbling for 3 min, the acidic solution was drained and the resin was washed with 2 mL DCM for 25 s.

Action	Cycles	Solution	Amount	T (°C)	Incubation time
Cooling	-	-	-	-20	(15 min)*
Deliver	1	DCM	2 mL	-20	-
Deliver	1	TMSOTf solution	1 mL	-20	3 min
Wash	1	DCM	2 mL	-20	25 s

*Time required to reach the desired temperature.

Module C: Thioglycoside Glycosylation (35 min)

The building block solution (0.08 mmol of BB in 1 mL DCM per glycosylation) was delivered to the reaction vessel. After the set temperature was reached, the reaction was started by drop wise addition of the activator solution (1.0 mL, excess). The glycosylation conditions are building block dependent (we report the most common set of conditions). After completion of the reaction, the solution is drained and the resin was washed with DCM, DCM:dioxane (1:2, 3 mL for 20 s) and DCM (two times, each with 2 mL for 25 s). The temperature of the reaction vessel is increased to 25 °C for the next module.

Action	Cycles	Solution	Amount	T (°C)	Incubation time
Cooling	-	-	-	-20	-
Deliver	1	BB solution	1 mL	-20	-
Deliver	1	Activator solution	1 mL	-20	-
Reaction time	1			-20 to 0	5 min 20 min
Wash	1	DCM	2 mL	0	5 s
Wash	1	DCM : Dioxane (1:2)	2 mL	0	20 s
Heating	-	-	-	25	-
Wash	2	DCM	2 mL	> 0	25 s

Module D: Fmoc Deprotection (14 min)

The resin was washed with DMF (three times with 2 mL for 25 s) and the temperature of the reaction vessel was adjusted to 25 °C. Fmoc deprotection solution (2 mL) was delivered into the reaction vessel. After 5 min, the reaction solution was drained and the resin washed

with DMF (three times with 3 mL for 25 s) and DCM (five times each with 2 mL for 25 s). The temperature of the reaction vessel is decreased to -20 °C for the next module.

Action	Cycles	Solution	Amount	T (°C)	Incubation time
Heating	-	-	-	25	(5 min)
Wash	3	DMF	2 mL	25	25 s
Deliver	1	Fmoc depr. solution	2 mL	25	5 min
Wash	1	DMF	2 mL		
Cooling	-	-	-	-20	-
Wash	3	DMF	2 mL	< 25	25 s
Wash	5	DCM	2 mL	< 25	25 s

2.6.3.4 Post-synthesizer manipulations

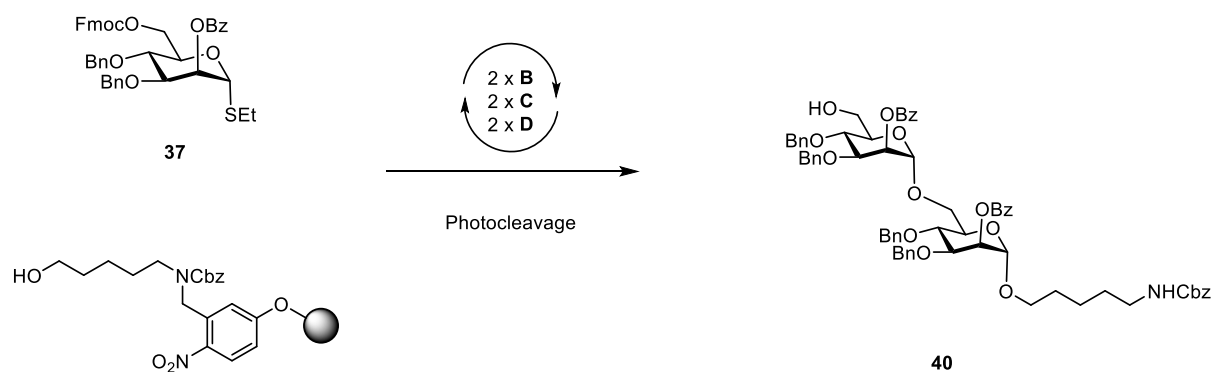
Cleavage from Solid Support

After automated synthesis, the oligosaccharides were cleaved from the solid support using a continuous-flow photoreactor as described previously.⁹¹

Purification

Solvent is evaporated *in vacuo* and the crude products were analyzed and purified using analytical and preparative HPLC (Agilent 1200 Series spectrometer).

Synthesis of dimer 31



	Module	Conditions
	A: Resin Preparation for Synthesis	
2	B: Acidic Wash with TMSOTf Solution	BB 37, 10 eq (-20° for 5 min, 0° for 20 min)
	C: Thioglycoside Glycosylation	
	D: Fmoc Deprotection	

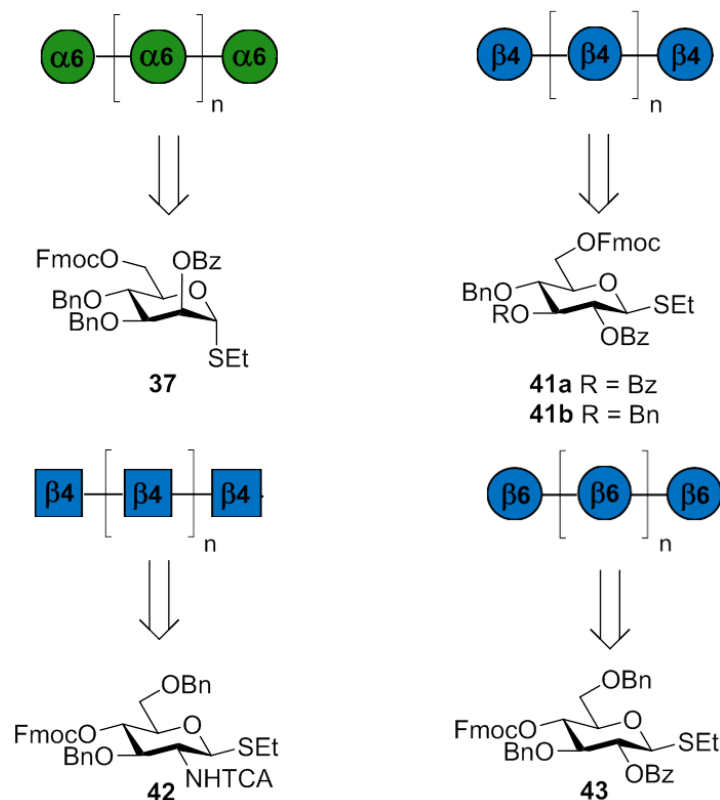
Cleavage from the solid support as described in *Post-synthesizer manipulation* followed by purification using preparative HPLC afforded compound **31** (9.2 mg, 62%)

Analytical data for **40**: ^1H NMR (400 MHz, Chloroform-*d*) δ 8.10 (dd, $J = 19.2, 7.5$ Hz, 4H), 7.59 (t, $J = 7.6$ Hz, 1H), 7.52 – 7.44 (m, 5H), 7.36 – 7.09 (m, 25H), 5.73 (s, 1H), 5.63 (s, 1H), 5.09 (s, 3H), 4.92 – 4.86 (m, 3H), 4.83 (d, $J = 11.4$ Hz, 1H), 4.74 (d, $J = 11.7$ Hz, 1H), 4.63 (d, $J = 10.9$ Hz, 1H), 4.57 (d, $J = 11.0$ Hz, 1H), 4.52 – 4.45 (m, 2H), 4.09 (d, $J = 8.6$ Hz, 2H), 4.01 – 3.92 (m, 2H), 3.87 (d, $J = 8.7$ Hz, 2H), 3.76 (q, $J = 10.5, 10.0$ Hz, 4H), 3.67 (d, $J = 8.9$ Hz, 1H), 3.43 (q, $J = 7.4$ Hz, 1H), 3.18 (q, $J = 7.0$ Hz, 2H), 1.56 (dt, $J = 32.2, 7.5$ Hz, 4H), 1.38 (q, $J = 7.9$ Hz, 2H); ^{13}C NMR (100 MHz, CDCl₃) δ 165.82, 165.52, 156.40, 138.28, 138.23, 137.90, 137.69, 133.26, 129.94, 129.89, 129.84, 129.80, 128.56, 128.48, 128.34, 128.30, 128.13, 128.08, 128.01, 127.94, 127.76, 127.68, 127.65, 127.61, 97.83, 78.54, 77.87, 75.18, 74.26, 73.85, 72.14, 71.62, 71.31, 70.57, 69.03, 68.78, 67.81, 66.56, 66.22, 61.96, 40.95, 29.76, 29.02, 23.42.

3 Synthesis of oligosaccharides for structural investigations

Carbohydrates are the most abundant type of organic materials.¹ However, relatively little is known about the correlation between the molecular structure and macroscopic properties of polysaccharides. Establishing this correlation requires chemically well-defined oligosaccharides.

Carbohydrates can be accessed from natural sources or via enzymatic and/or chemical synthesis. A large variety of carbohydrates (like glycosaminoglycans,¹⁹⁻²⁴ plant carbohydrates,²⁵ capsular polysaccharides²⁶⁻²⁸ etc.) can be extracted from natural sources, but these results in heterogeneous samples making structural investigations very challenging. Enzymatic synthesis, on contrary, permits the synthesis of homogeneous oligosaccharides,^{32, 125-126} But the scope of molecules that could be accessed by this approach is limited by the number of available enzymes and substrates. This limitation could be overcome by solution-phase synthesis of oligosaccharides.¹²⁷⁻¹²⁸ The main difficulty here is the fact that this method relies on multiple protecting group manipulations and often requires many synthetic steps. Hence, solution-phase synthesis often does not allow for the rapid access to the desired compounds.

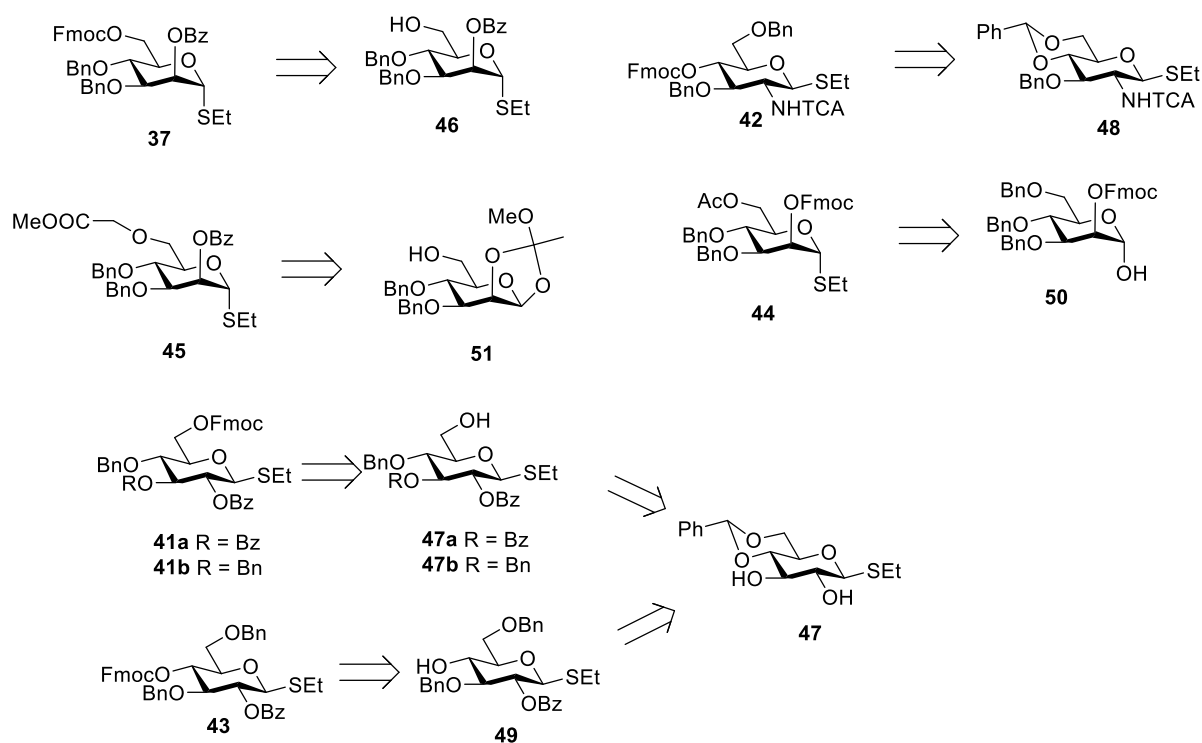


Scheme 31. Retrosynthetic analysis of natural and unnatural oligosaccharides.

Automated glycan assembly can enable the preparation of well-defined oligo- and polysaccharides. In order to shed light on the correlation between polymer composition, three-dimensional structure and macroscopic properties of carbohydrates, several natural (cellulose and chitin) and unnatural oligosaccharides (1→6 mannosides and 1→6 glucosides) were chosen as synthetic targets (Scheme 31).

3.1 Synthesis of building blocks

For the synthesis of the oligosaccharide collection building blocks **37**, **41-45** were used (Scheme 32). Benzyl ethers served as non-participating permanent protecting groups for alcohols while benzoyl or acetyl esters as well as trichloroacetyl (TCA) were used as permanent participating protecting groups ensuring selective trans-glycoside formation. The fluorenylmethyloxycarbonyl (Fmoc) temporary protecting group is removed following each elongation cycle.

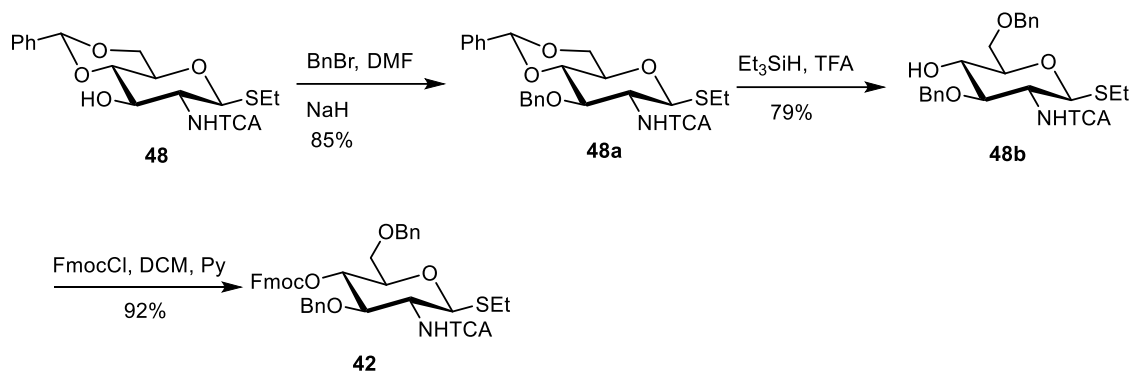


Scheme 32. Retrosynthetic analysis of the building blocks

Mannose BB **37** was synthesized from commercially available precursor **46** via an established protocol.¹¹² Glucose BBs **41a,b**ⁱ were obtained from precursors **47a,b** respectively, that were obtained from the compound **47** using the described procedures.¹²⁹⁻¹³⁰

ⁱBuilding blocks **41a,b** were provided by Dr. Delbianco

Glucosamine BB **42** was synthesized from commercially available precursor **48** via an established protocol (Scheme 33).¹³¹ Glucose BB **43**ⁱⁱ was obtained from **47** using a described methodology.¹³¹ Mannose BB **44**ⁱⁱⁱ used for 1→2 linkages was synthesized from compound **50**. Building block **45**^{iv} for the synthesis of oligosaccharides with carboxylic group functionalities was synthesized from precursor **51** using a described synthetic route.¹¹²



Scheme 33. Synthesis of glucosamine building block.

3.2 Synthesis of an oligosaccharide library

Automated glycan assembly was performed for thioglycoside building blocks **37**, **41** – **45** using optimized conditions. Glycosylation cycles were performed using 6.5 equiv. of BBs (5.0 equiv. for BB **41b** because of its high reactivity) in the presence of NIS/TfOH at -20°C (5 min) – 0°C (20 min). The removal of Fmoc protecting group was performed using 20% piperidine in DMF and a TMSOTf (63mM in DCM) solution was used for acidic wash prior to the next glycosylation.

Mannose BB **37** for the synthesis of 6-mer **52a**, 12-mer **52b** and 20-mer of mannose **52c** (Scheme 34, Table 11). In all the cases, it was possible to achieve a high yield of the synthesis and access the desired oligosaccharides in less than one day.

Table 11. AGA of mannose oligosaccharides

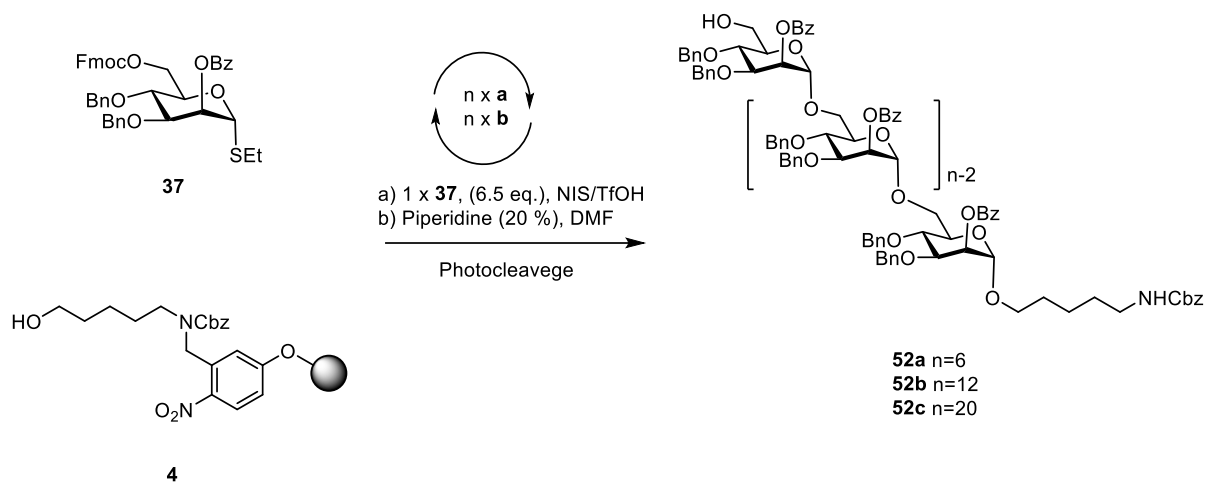
Oligosaccharide	Synthesis (h)	Yield, %
6-mer, 52a	7	51
12-mer, 52b	14	29
20-mer, 52c	23	19

ⁱⁱBuilding block **43** was synthesized by Mr. Yu

ⁱⁱⁱBuilding block **44** was provided by Mr. Pardo

^{iv}Building block **45** was provided by Dr. Kottari

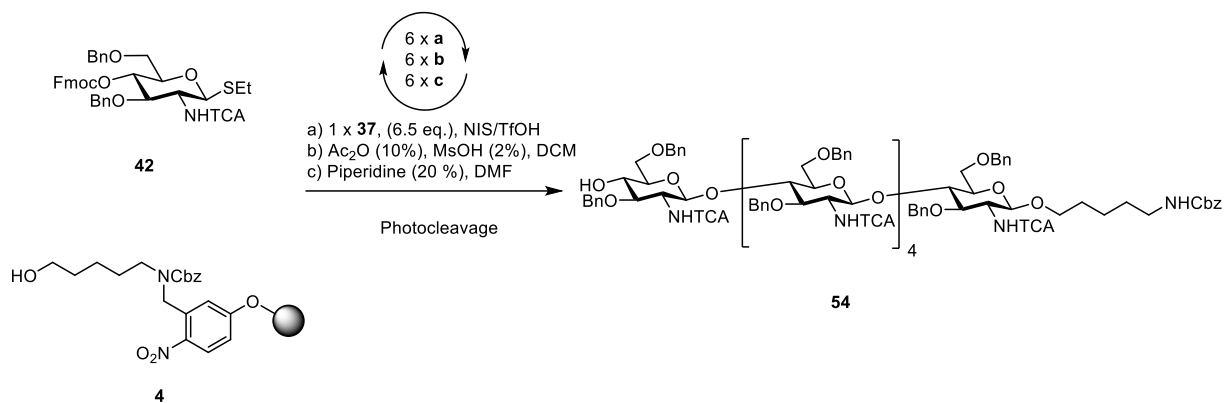
Assembly of 1→6 glucosides was initially performed using building block **41b**. This building block exhibits a very high reactivity and gives excellent results in automated synthesis. However, the global deprotection of oligosaccharides obtained from BB **41b** was hindered by insolubility of oligosaccharides formed. Glucose BB **41a** is less reactive (it contains an additional electron withdrawing protecting group OBz, instead of the OBn in building block **41b**), but it helped to overcome the solubility issues during the global deprotection step and made it possible to synthesize glucose oligosaccharides **53a** and **53b**.



Scheme 34. Scheme of oligosaccharide synthesis for compounds **52a-c**

Glucosamine building block **42** has lower reactivity as a glycosidic donor, therefore a capping step was performed. A capping step is used to block the unreacted hydroxyl groups after each glycosylation preventing any unreacted chains from growing to form internal deletion sequences. Recently, a new capping procedure utilizing Ac₂O (10%) and methanesulfonic acid (2%) in DCM was developed in Seeberger group.¹³² This procedure was implemented in the synthesis of chitin and cellulose oligomers. (Scheme 35). Analogous method was used for the synthesis of 1→4 hexaglucoide **55** from building block **43**.^v

^v Compound 55 was synthesized by Mr. Yu



Scheme 35. Scheme of AGA for chitin hexasaccharide **54** (with capping).

Oligosaccharides **52** - **55** were purified using HPLC and subjected to the deprotection procedure (methanolysis and hydrogenation).^{vi} As a result, target oligosaccharides **d-52** – **d-55** were obtained. Interestingly, the glucose oligosaccharides were obtained in much lower yields (2% for **d-53b**), in comparison to the other synthesized compounds. The reason for this is insolubility of these oligosaccharides in most solvents.

One of the major advantages of automated synthesis technology is its modularity: it allows introduction of modifications at any position in the sequence of the desired oligosaccharide. This advantage was utilized in the synthesis of heteropolymers **56** – **59**. In an attempt to disrupt the 3D structure of glucose oligomers, mixed oligomers containing one mannose unit **56a,b** were prepared. It was found that the introduction of a mannose unit was indeed beneficial. The more soluble 12-mer (**56b**) containing one mannoside unit in position 7 was isolated in 20% yield.

The introduction of different linkages was also explored where building block **50** was used for the installation of the (1→2) linkage (**58**). Using building blocks **37** and **45** oligosaccharides **59a** and **59b**, bearing a carboxylic acid group allowing for further block-coupling, were synthesized.

^{vi} Global deprotection of oligosaccharides was performed by Dr. Delbianco

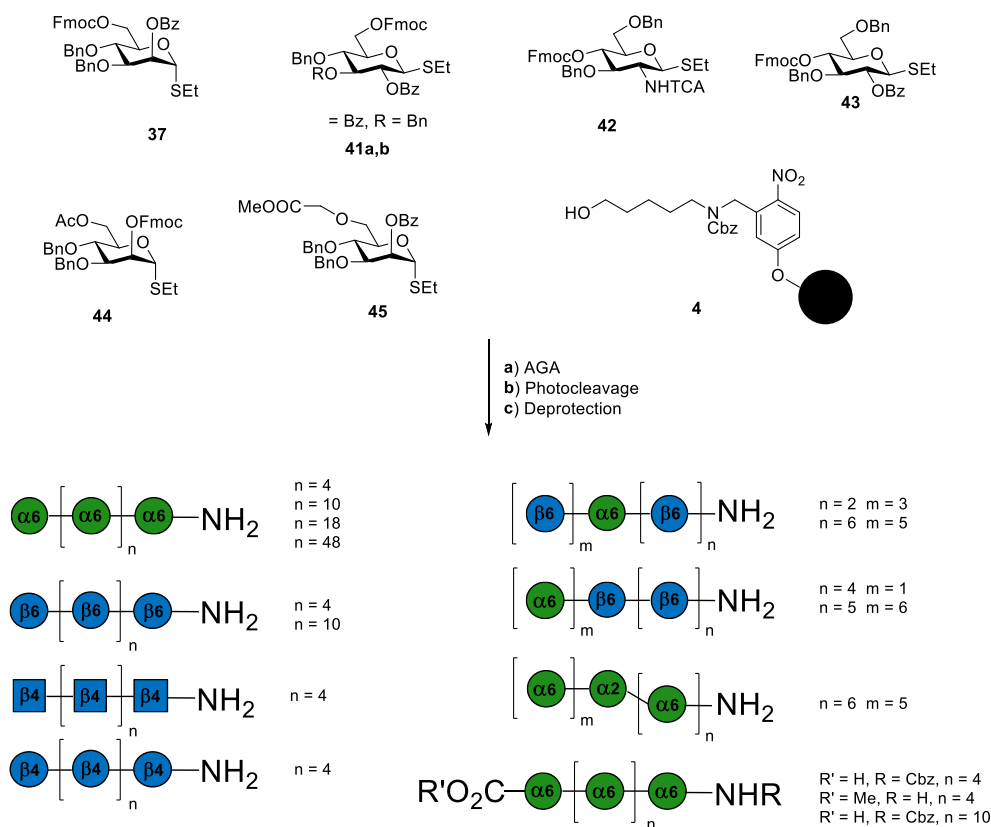


Figure 8. Overview of the oligosaccharides prepared by AGA.

3.3 AGA of a mannose 50-mer

The longest oligosaccharide synthesized via AGA was a mannose 50-mer.¹¹² However, the synthesis of this compound was performed within 10 days and the poly-mannoside was obtained only in 5% yield.¹¹² In order to improve this result, the applicability of the optimized AGA conditions for the synthesis of mannoside 50-mer was investigated.

The optimized elongation cycle, including the new capping procedure was used for the synthesis of 50-mer **60**. Several advantages of the newly developed synthetic procedure, in comparison to previously reported,¹¹² can be pointed out. First of all, the overall synthesis was much faster: 80 hours in comparison with 250 hours reported before. The yield improvement was also significant: 22% instead of 5%. That means that the average yield of the elongation cycle is 98% and making AGA comparable to oligopeptide or oligonucleotide synthesis. Also, the usage of solvents has been reduced drastically (Table 12). Optimization helped to reduce the amount of waste generated during AGA and therefore made the overall process greener.

Table 12. Amount of solvents used for the synthesis of 50-mer.

Solvent Usage	Previous cycle, L	Optimized cycle, L
DCM	2.5	1.2
DMF	1.5	0.7
Dioxane	0.1	0.1
DCE	0.12	0.06
THF	0.30	0

In addition to the mannose 50-mer (**60**), mannose 49-mer both uncapped (**60a**) and acetylated (**60b**) were prepared. For acetylation of the 49-mer the conditions, analogous to the capping procedure were utilized (Ac₂O (10%) and methanesulfonic acid (2%) in DCM).^{vii} These three compounds were used for the evaluation of the HPLC resolution power in the separation of long polysaccharides. Uncapped 50-mer **60**, that represents the desired final product of AGA, and the potential deletion sequence, the uncapped 49-mer **60a** are eluted with virtually the same retention time, while capped 49-mer **60b** is eluted more than one minute before either of the other two compounds and can be readily separated from the final product (Figure 9). This finding demonstrates that capping not only improves the yield, but also generates more readily separable side-products, even when polysaccharides are prepared.

^{vii} Acetylation of 49-mer was performed by Mr. Yu

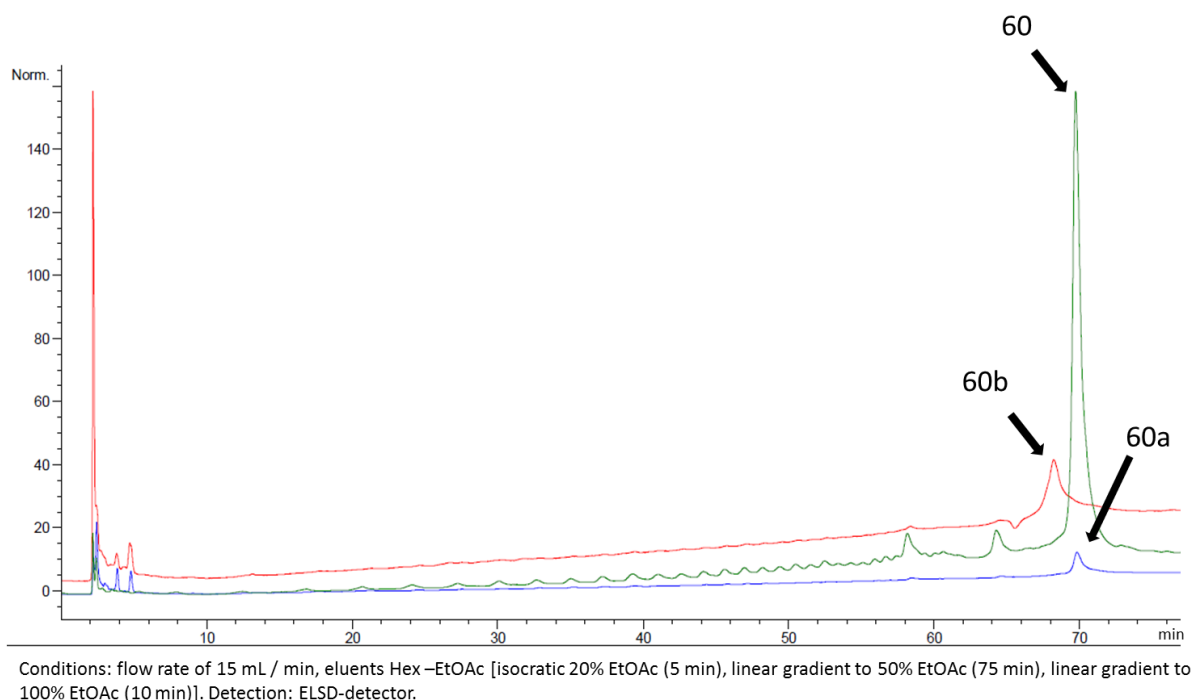


Figure 9. HPLC trace of the crude 50-mer **60** compared with the potential deletion sequence **60a** and uncapped 49-mer **60b**.

3.4 Molecular dynamics investigations^{viii}

With this collection of oligo- and polysaccharides in hand, we began to investigate the 3D structure of such materials in order to correlate glycan sequence with macroscopic properties. Ideally, we would be able to understand how modifications such as the insertion of a different monosaccharide affect the overall molecular geometry.

Long molecular dynamics (MD) simulations (between 500 ns and 5.5 μ s) using the AMBER12 package¹³³ with ff12SB,¹³³ GAFF,¹³⁴ and GLYCAM06j¹³⁵ force fields provided conformational and dynamic information and revealed significant structural differences between the different polymers (Figure 10). The geometries of different hexamers were compared by analyzing different parameters, including the radius of gyration (RoG), the RMSD values (root-mean square deviation of atomic positions), the distances between the non-reducing end moiety with all other residues, the torsion angles around the glycosidic linkages (Figure 11), and the shape of the six-membered rings. The RoG describes the overall extension of the molecule and is defined as the root mean square distance of the collection of atoms from their common center of gravity.

^{viii} All molecular dynamics simulation were performed by Prof. Dr. Jiménez-Barbero and Dr. Poveda

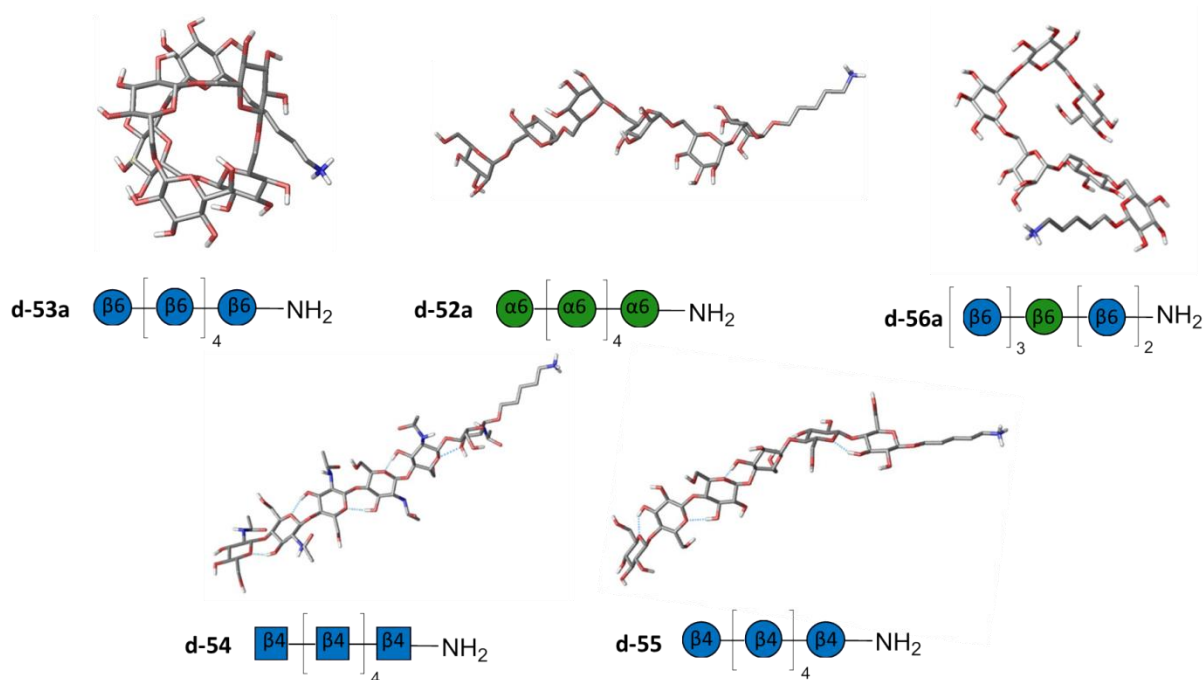


Figure 10. The global minima conformations of oligosaccharides obtained by molecular dynamics simulations.

In particular, the major conformer of the β 1,6-Glc hexasaccharide **d-53a** adopts a helical structure with an internal cavity (Figure 10, **d-53a**). The cavity resembles a crown ether, with the oxygens presenting the same spatial orientation while the non-polar faces of the Glc rings point the opposite direction. The exo-anomeric Φ value (ca. 42°)¹³⁶ is kept throughout the simulation, while Ψ varies from to 80° to 180° . Analysis of the Cremer-Pople parameters¹³⁷ showed some chair-to-chair interconversions where the 4C_1 chair always dominates (85 - 96%), while alternative boats and skew boat conformers are observed for less than 1.5% of all pyranose rings. The populations of the alternative 1C_4 conformers reach 12-15% for the glucose residues 2 and 5.¹³⁸ The relatively small RoG (ca. 5.6 Å) and the distance between both ends, that rarely extended beyond 20 Å, indicate that the molecule adopts bent or rolled compact shapes most of the time.

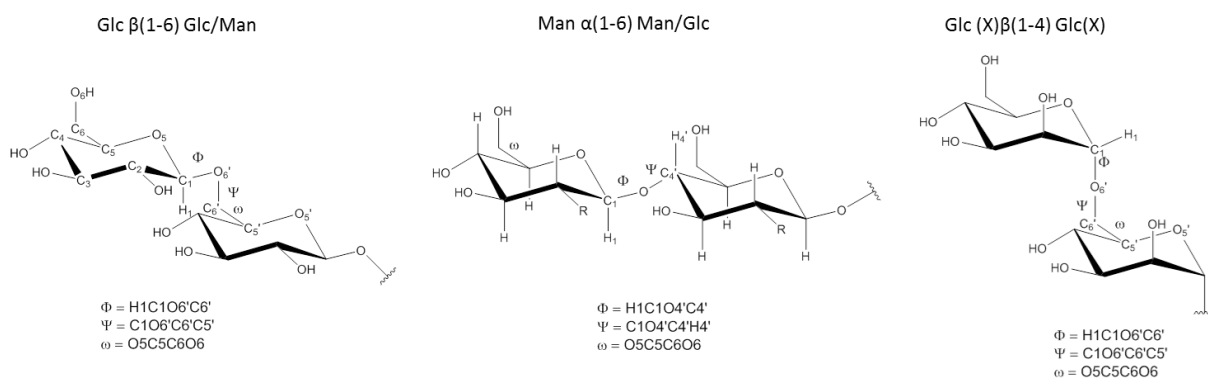


Figure 11. Definition of the torsion angles for every type of linkage

The MD simulations suggest a significantly more rigid structure for the α 1,6 hexamannoside (Figure 10, **d-52a**) The calculated mean RoG for this molecule is now significantly larger (7.5 Å), albeit with values ranging from 5 to 9 Å and a maximum between 8-9 Å. Most of the time the molecule adopts extended shapes (RoG closer to 9 Å) but bent conformations are also observed for a period of time. The distance between both ends usually remained between 20-25 Å. For the major conformer, the hydroxyl groups on the periphery of the chain are available to interact with polar groups. Chair-to-chair interconversions are rare (< 1%) as the 4C_1 chair is always favored from both stereoelectronic and steric perspectives.

The insertion of mannose in position 3 of the β 1,6-Glc hexamer (**d-56a**) indeed distorts the chain and results in a less defined helical structure (Figure 10, **d-56a**). A larger RoG than for the β 1,6-Glc hexasaccharide **d-53a** is predicted. In this particular case, there is not any clear preference for a given shape. A single chain of cellulose, represented by the β 1,4 hexaglucoside **d-55** adopts a twisted ribbon-like structure with no cavity where the C3 hydroxyl of one residue hydrogen bonds with the O5 of the preceding moiety.¹³⁹ The C2 and C6 hydroxyl groups that are not engaged in the intramolecular hydrogen bonds are oriented outside the major axis of the ribbon, ready to interact with other polar donors.¹³⁹ The β 1,4-Glc hexamer (**d-55**) displays the largest RoG (>9 Å), and the highest mean distances between the two remote ends (>25 Å).

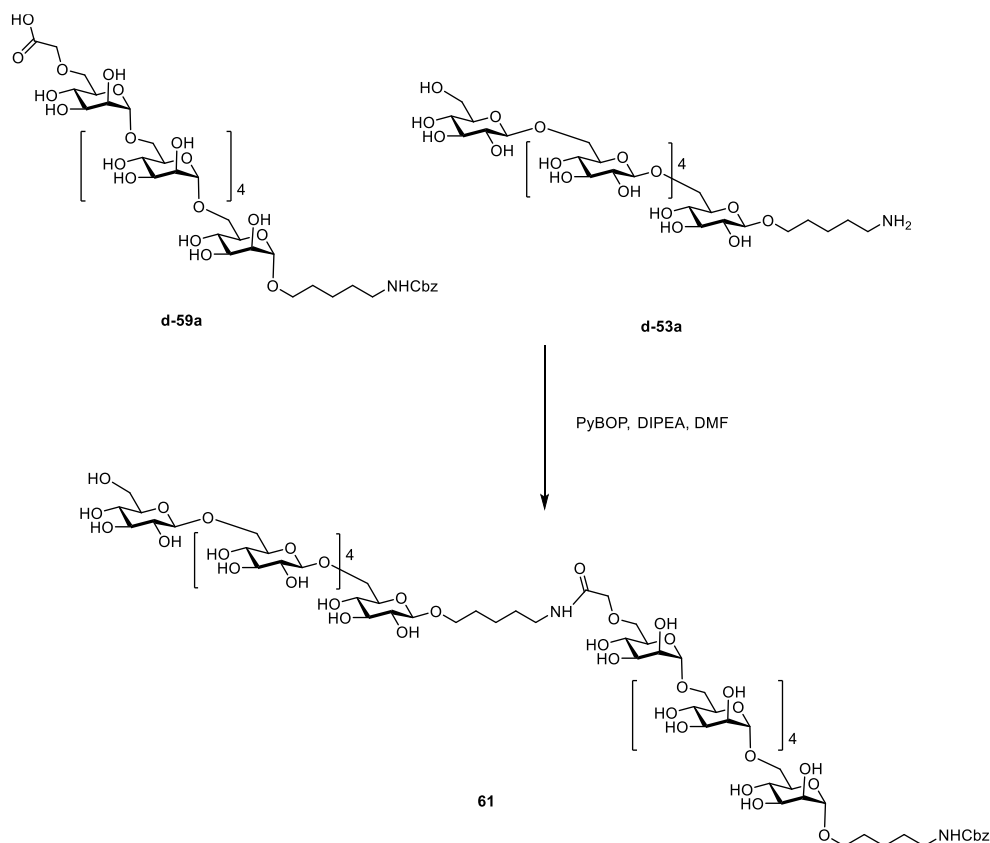
Chitin **d-54**, where the C2-hydroxyl groups present in cellulose are replaced by C2-*N*-acetyls adopts a structure similar to that of cellulose. The chair-to-chair interconversions of the six-membered rings are even smaller than those for the cellulose hexamer as the bulkier C2 NHAc substituents prevent the transitions to this geometry. The molecule adopts a helix-like structure with no internal cavity. The acetamide moieties, like the C6 hydroxyls, adorn the periphery of the main axis, displaying the NH and CO hydrogen bond donor and acceptors. The methyl groups can be engaged in van der Waals interactions with other partners.¹⁴⁰

3.5 Toward tailor-made carbohydrate-based materials^{ix}

Oligomers of different conformation are ideal “bricks” to create novel carbohydrate-based synthetic materials. To combine these “bricks”, connection points at either side of the

^{ix} Block-coupling was performed by Dr. Delbianco

oligomer are required. The reducing terminus of all synthetic oligomers prepared by AGA carries a unique primary amine group. Placement of a BB containing a C6 carboxymethyl group (**45**) during the last cycle of the assembly resulted in carbohydrate oligomers where an amine and a carboxylic acid can be exploited for conjugation (**d-59a,b**).



Scheme 36. An example of block-coupling procedure

Three block couplings based on PyBOP/DIPEA mediated amide bond formation were explored (Scheme 36). After simply connecting oligo-mannose blocks, oligo-mannose and oligo-glucose blocks of different geometries and solubility were combined. All the coupling products were isolated in high yields and easily purified using RP-HPLC.

3.6 Conclusions and perspectives

Automated glycan assembly enables the preparation of well-defined oligo- and polysaccharides resembling natural as well as unnatural structures. It has been shown that the optimized glycosylation cycle can be used for various thioglycoside building blocks (mannose, glucose, glucosamine) and for different types of glycosidic linkages (1→2, 1→4, 1→6). Long homopolymers (as 50-mers) as well as heteropolymers can be also obtained.

The structure of the synthesized hexasaccharides was investigated using molecular dynamics. It was found that mannosides (1→6), glucosides (1→4 and 1→6) and glucosaminosides (1→4) present different geometries and flexibility that can lead to differences in the macroscopic properties of polysaccharides (for example, solubility). AGA modularity allowed for specific modifications, permitting the fine tuning of the polymer shape and conformation. Oligomers of different conformation are ideal “bricks” to create novel carbohydrate-based synthetic materials.

Optimized AGA procedures can be applied for the synthesis of a larger collection of oligo- and polysaccharides. The synthesized glycans can be used for further structural investigations.

3.7 Experimental part

3.7.1 Automated glycan assembly

3.7.1.1 General materials and methods

All solvents used were HPLC-grade. The solvents used for the building block, activator, TMSOTf and capping solutions were taken from an anhydrous solvent system (jcmeyer-solvent systems). The building blocks were co-evaporated three times with chloroform and dried for 1 h on high vacuum before use. Activator, deprotection, acidic wash and building block solutions were freshly prepared and kept under argon during the automation run. All yields of products obtained by AGA were calculated on the basis of resin loading.

3.7.1.2 Preparation of stock solutions

- **Building Blocks:** between 0.062 and 0.080 mmol of the building block **28** was dissolved in 1 mL of DCM.
- **Activator solution:** 1.35 g of NIS was dissolved in 40 mL of a 2:1 mixture of anhydrous DCM and anhydrous dioxane. Then triflic acid (55 μ L) was added. The solution is kept at 0°C for the duration of the automation run.
- **Fmoc deprotection solution 1:** A solution of 20% Et₃N in DMF (v/v) was prepared.

- **Fmoc deprotection solution 2:** A solution of 20% piperidine in DMF (v/v) was prepared.
- **TMSOTf Solution:** TMSOTf (0.45 mL) was added to DCM (40 mL).

3.7.1.3 *Optimized modules for automated synthesis*

Module A: Resin Preparation for Synthesis (20 min)

All automated syntheses were performed on 0.0125 mmol scale. Resin was placed in the reaction vessel and swollen in DCM for 20 min at room temperature prior to synthesis. During this time, all reagent lines needed for the synthesis were washed and primed. Before the first glycosylation, the resin was washed with the DMF, THF, and DCM (three times each with 2 mL for 25 s).

Module B: Acidic Wash with TMSOTf Solution (20 min)

The resin was swollen in 2 mL DCM and the temperature of the reaction vessel was adjusted to -20 °C. Upon reaching the low temperature, TMSOTf solution (1 mL) was added drop wise to the reaction vessel. After bubbling for 3 min, the acidic solution was drained and the resin was washed with 2 mL DCM for 25 s.

Action	Cycles	Solution	Amount	T (°C)	Incubation time
Cooling	-	-	-	-20	(15 min)
Deliver	1	DCM	2 mL	-20	-
Deliver	1	TMSOTf solution	1 mL	-20	3 min
Wash	1	DCM	2 mL	-20	25 s

Module C: Thioglycoside Glycosylation (35 min)

The building block solution (0.08 mmol of BB in 1 mL of DCM per glycosylation) was delivered to the reaction vessel. After the set temperature was reached, the reaction was started by drop wise addition of the activator solution (1.0 mL, excess). The glycosylation conditions are building block dependent (we report the most common set of conditions). After completion of the reaction, the solution is drained and the resin was washed with DCM, DCM:dioxane (1:2, 3 mL for 20 s) and DCM (two times, each with 2 mL for 25 s). The temperature of the reaction vessel is increased to 25 °C for the next module.

Action	Cycles	Solution	Amount	T (°C)	Incubation time
Cooling	-	-	-	-20	-

Deliver	1	BB solution	1 mL	-20	-
Deliver	1	Activator solution	1 mL	-20	-
Reaction time	1			-20 to 0	5 min 20 min
Wash	1	DCM	2 mL	0	5 s
Wash	1	DCM : Dioxane (1:2)	2 mL	0	20 s
Heating	-	-	-	25	-
Wash	2	DCM	2 mL	> 0	25 s

Module D: Fmoc Deprotection (14 min)

The resin was washed with DMF (three times with 2 mL for 25 s) and the temperature of the reaction vessel was adjusted to 25 °C. 2 mL of Fmoc deprotection solution was delivered into the reaction vessel. After 5 min, the reaction solution was drained and the resin washed with DMF (three times with 3 mL for 25 s) and DCM (five times each with 2 mL for 25 s). The temperature of the reaction vessel is decreased to -20 °C for the next module.

Action	Cycles	Solution	Amount	T (°C)	Incubation time
Heating	-	-	-	25	(5 min)
Wash	3	DMF	2 mL	25	25 s
Deliver	1	Fmoc depr. solution	2 mL	25	5 min
Wash	1	DMF	2 mL		
Cooling	-	-	-	-20	-
Wash	3	DMF	2 mL	< 25	25 s
Wash	5	DCM	2 mL	< 25	25 s

3.7.1.4 Post-synthesizer manipulations

Cleavage from Solid Support

After automated synthesis, the oligosaccharides were cleaved from the solid support using a continuous-flow photoreactor as described previously.⁹¹

Purification

Solvent is evaporated *in vacuo* and the crude products were analyzed and purified using analytical and preparative HPLC (Agilent 1200 Series spectrometer).

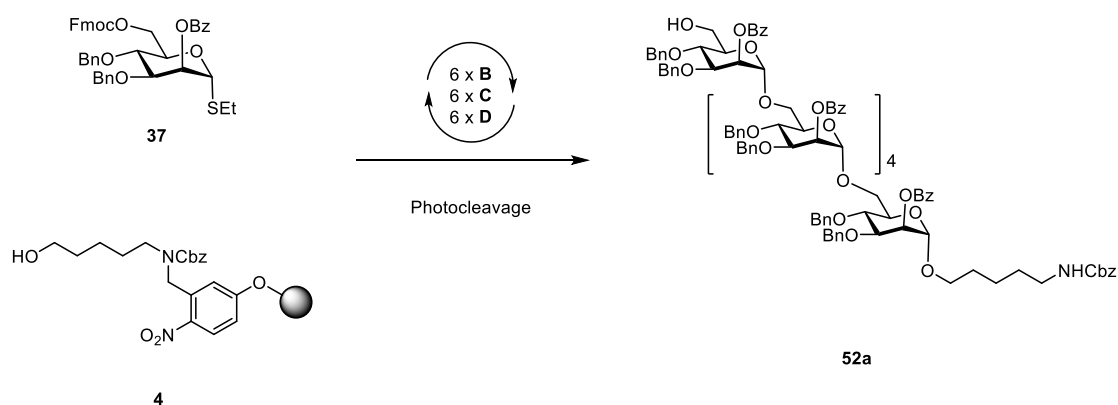
Module E: Capping (30 min)

The resin was washed with DMF (two times with 2 mL for 25 s) and the temperature of the reaction vessel was adjusted to 25 °C. 2 mL of Pyridine solution (10% in DMF) was delivered into the reaction vessel. After 1 min, the reaction solution was drained and the resin washed with DCM (three times with 3 mL for 25 s). 4 mL of capping solution was delivered into the reaction vessel. After 20 min, the reaction solution was drained and the resin washed with DCM (three times with 3 mL for 25 s).

Action	Cycles	Solution	Amount	T (°C)	Incubation time
Heating	-	-	-	25	(5 min)
Wash	2	DMF	2 mL	25	25 s
Deliver	1	10% Pyridine in DMF	2 mL	25	1 min
Wash	3	DCM	2 mL	25	25 s
Deliver	1	Capping Solution	4 mL	25	20 min
Wash	3	DCM	2 mL	25	25 s

3.7.2 Synthesis of homopolymers

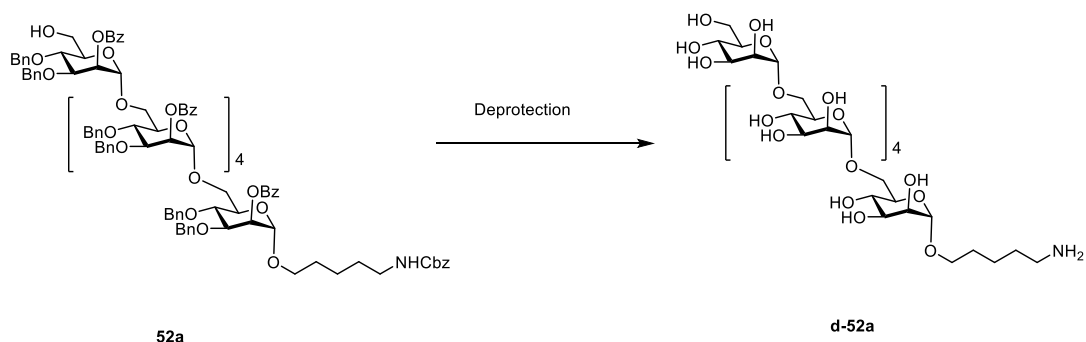
Synthesis of $\alpha(1-6)$ hexamannoside, 52a



Module	Conditions
A: Resin Preparation for Synthesis	
B: Acidic Wash with TMSOTf Solution	
6 { C: Thioglycoside Glycosylation	BB 37, 6.5 eq (-20° for 5 min, 0° for 20 min)

Cleavage from the solid support as described in *Post-synthesizer manipulation* followed by purification using preparative HPLC afforded compound **52a** (21.3 mg, 58%).

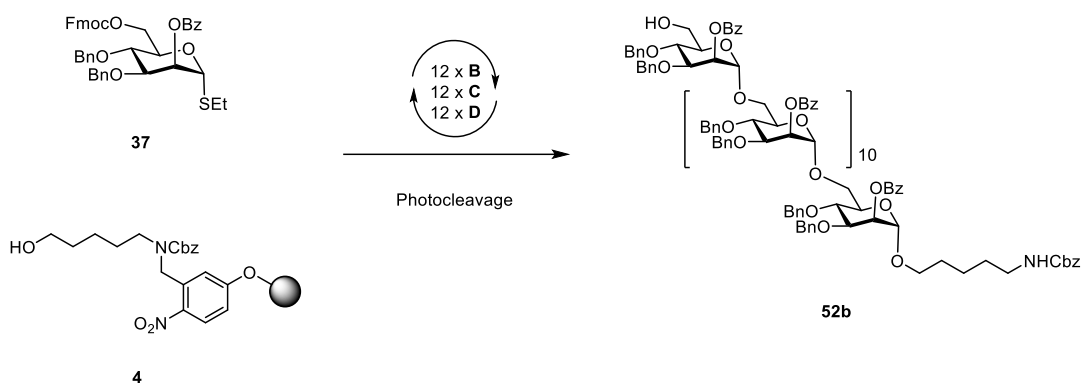
Analytical data for **52a**: ^1H NMR (400 MHz, Chloroform-*d*) δ 8.24 – 8.13 (m, $J = 10\text{H}$), 8.11 (d, $J = 7.7\text{ Hz}$, 2H), 7.62 (t, $J = 7.5\text{ Hz}$, 2H), 7.59 – 7.47 (m, 18H), 7.39 – 7.30 (m, 7H), 7.30 – 7.23 (m, 18H), 7.23 – 7.07 (m, 38H), 5.88 – 5.82 (m, 3H), 5.80 (s, 1H), 5.66 (s, 1H), 5.14 (s, 1H), 5.12 – 5.04 (m, 5H), 4.92 (d, $J = 11.7\text{ Hz}$, 4H), 4.86 – 4.79 (m, 7H), 4.75 (d, $J = 11.4\text{ Hz}$, 2H), 4.61 (dd, $J = 15.6, 11.0\text{ Hz}$, 3H), 4.52 (d, $J = 3.6\text{ Hz}$, 1H), 4.50 – 4.40 (m, 6H), 4.40 – 4.34 (m, 3H), 4.12 (dt, $J = 9.0, 4.1\text{ Hz}$, 2H), 4.09 – 3.93 (m, 10H), 3.92 – 3.88 (m, 3H), 3.85 – 3.75 (m, 6H), 3.74 – 3.59 (m, 9H), 3.55 (t, $J = 9.8\text{ Hz}$, 3H), 3.50 – 3.37 (m, 4H), 3.20 (q, $J = 6.9\text{ Hz}$, 2H), 1.65 – 1.56 (m, 2H), 1.56 – 1.45 (m, 2H), 1.43 – 1.32 (m, 2H); ^{13}C NMR (101 MHz, Chloroform-*d*) δ 165.87, 165.63, 165.55, 165.43, 156.40, 138.53, 138.47, 138.31, 138.26, 137.94, 137.63, 137.57, 137.54, 136.67, 133.34, 133.30, 129.98, 129.93, 129.88, 128.67, 128.60, 128.51, 128.37, 128.33, 128.24, 128.19, 128.16, 128.07, 128.03, 127.72, 127.68, 127.65, 127.43, 127.38, 127.33, 127.24, 127.14, 127.11, 98.47, 98.41, 98.14, 97.89, 77.68, 77.26, 75.20, 75.11, 75.05, 75.02, 74.19, 73.90, 73.80, 73.74, 73.68, 72.10, 71.65, 71.42, 71.32, 71.20, 70.99, 70.91, 70.73, 69.05, 68.54, 68.42, 68.36, 67.79, 66.57, 66.09, 65.81, 65.72, 65.43, 61.83, 40.97, 29.79, 29.05, 23.45; m/z (HRMS+) 2937.160 $[\text{M} + \text{Na}]^+$ ($\text{C}_{175}\text{H}_{175}\text{NO}_{39}\text{Na}$ requires 2937.163).



Deprotection of **52a** (18.0 mg, 6.2 μ mol) as reported in Section 3.5 (Module F and G) followed by purification using preparative HPLC afforded compound **d-52a** (5.8 mg, 88%).

Analytical data for **d-52a**: ^1H NMR (400 MHz, Deuterium Oxide) δ 4.80 (d, $J = 1.8$ Hz, 1H), 4.80 – 4.77 (m, 4H), 4.75 (d, $J = 1.7$ Hz, 1H), 3.90 – 3.86 (m, 5H), 3.86 – 3.79 (m, 6H), 3.77 (d, $J = 1.7$ Hz, 2H), 3.76 – 3.68 (m, 11H), 3.68 – 3.60 (m, 10H), 3.60 – 3.57 (m, 2H), 3.55 (d, $J = 9.3$ Hz, 1H), 3.46 (dt, $J = 9.9, 6.1$ Hz, 1H), 2.93 – 2.85 (m, 2H), 1.63 – 1.50 (m, 4H), 1.35 (hept, $J = 6.8$ Hz, 2H). ^{13}C NMR (176 MHz, Deuterium Oxide) δ 99.89, 99.42, 99.32, 99.29, 72.72, 70.92, 70.84, 70.80, 70.77, 70.72, 70.69, 70.55, 70.07, 69.99, 69.94, 67.63, 66.75, 66.61, 66.57, 65.62, 65.58, 65.53, 61.32, 60.94, 39.38, 30.65, 28.04, 27.99, 26.57, 26.46, 22.54, 22.03; m/z (HRMS+) 1076.425 $[\text{M} + \text{H}]^+$ ($\text{C}_{41}\text{H}_{74}\text{NO}_{31}$ requires 1076.424).

Synthesis of $\alpha(1-6)$ dodecamannoside, **52b**

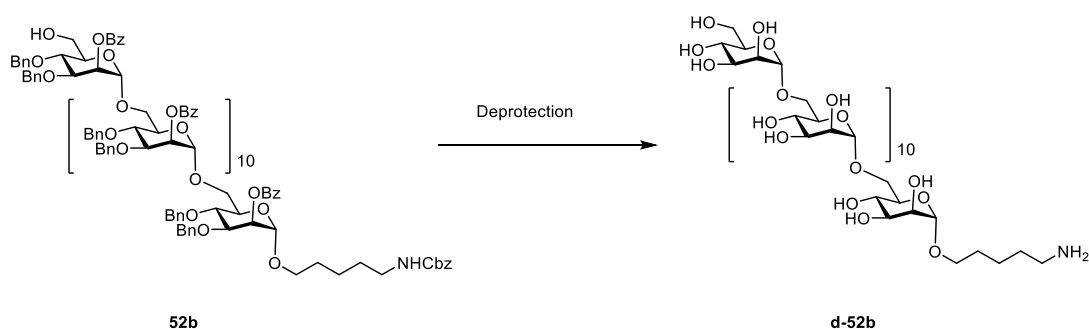


	Module	Conditions
	A: Resin Preparation for Synthesis	
12	B: Acidic Wash with TMSOTf Solution	
	C: Thioglycoside Glycosylation	BB 37 , 6.5 eq (-20° for 5 min, 0° for 20 min)
	D: Fmoc Deprotection	

Cleavage from the solid support as described in *Post-synthesizer manipulation* followed by purification using preparative HPLC afforded compound **52b** (26.5 mg, 38%).

Analytical data for **52b**: ^1H NMR (600 MHz, Chloroform-*d*) δ 8.19 – 8.11 (m, 19H), 8.10 (d, $J = 7.3$ Hz, 2H), 8.07 (d, $J = 7.8$ Hz, 2H), 7.57 (t, $J = 7.5$ Hz, 2H), 7.53 – 7.42 (m, 35H), 7.35 – 7.25 (m, 11H), 7.25 – 7.20 (m, 12H), 7.20 – 7.13 (m, 55H), 7.13 – 7.09 (m, 24H), 7.09 – 7.02 (m, 23H), 5.85 – 5.80 (m, 8H), 5.80 – 5.77 (m, 2H), 5.76 (s, 1H), 5.61 (d, $J = 3.0$ Hz, 1H), 5.09 (s, 1H), 5.07 – 5.01 (m, 11H), 4.90 – 4.83 (m, 12H), 4.83 – 4.81 (m, 2H), 4.81 – 4.73 (m, 10H) 4.71 (d, $J = 11.3$ Hz, 2H), 4.58 (d, $J = 11.1$ Hz, 2H), 4.54 (d, $J = 11.0$ Hz, 2H), 4.48 – 4.43 (m, 3H), 4.40 (d, $J = 10.9$ Hz, 10H), 4.36 – 4.30 (m, 8H), 4.07 (td, $J = 8.2, 7.5, 3.0$ Hz, 2H), 4.04 – 3.99 (m, 8H), 3.98 – 3.92 (m, 12H), 3.92 – 3.86 (m, 3H), 3.86 – 3.80 (m, 3H), 3.80 – 3.75 (m, 4H), 3.75 – 3.67 (m, 10H), 3.67 – 3.61 (m, 4H), 3.61 – 3.37 (m, 9H), 3.54 – 3.47 (m, 2H), 3.18 – 3.12 (m, 2H), 1.61 – 1.52 (m, 2H), 1.52 – 1.44 (m, 2H), 1.38 – 1.30 (m, 2H); ^{13}C NMR (151 MHz, Chloroform-*d*) δ 165.81, 165.58, 165.48, 165.37, 156.34, 138.50, 138.44, 138.40, 138.27, 138.22, 137.91, 137.62, 137.54, 137.51, 137.48, 136.66, 133.27, 133.22, 129.97, 129.92, 129.87, 129.82, 128.61, 128.53, 128.45, 128.33, 128.30, 128.26, 128.22, 128.18, 128.10, 128.00, 127.97, 127.74, 127.64, 127.59, 127.38,

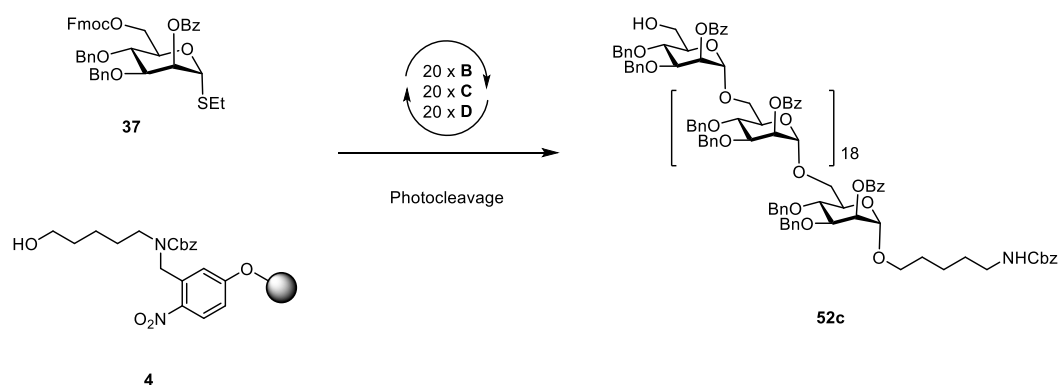
127.33, 127.31, 127.26, 127.20, 127.07, 127.04, 127.00, 126.82, 98.51, 98.46, 98.37, 98.13, 98.09, 97.84, 78.56, 78.27, 78.17, 77.66, 77.25, 77.20, 77.04, 76.99, 76.83, 76.78, 75.14, 75.06, 75.01, 74.96, 74.18, 73.88, 73.77, 73.69, 73.53, 73.49, 72.07, 71.61, 71.38, 71.30, 71.26, 71.16, 70.96, 70.87, 70.71, 69.04, 68.54, 68.42, 68.34, 68.14, 67.74, 66.51, 66.08, 65.77, 65.70, 65.52, 65.41, 61.81, 40.92, 29.74, 29.01, 23.40; m/z (HRMS⁺) 2817.099 [M + H + K]²⁺ (C₃₃₇H₃₃₂NO₇₅K requires 2817.096).



Deprotection of **52b** (22.2 mg, 4.0 μ mol) as reported in Section 3.5 (Module F and G) followed by purification using preparative HPLC afforded the compound **d-52b** (6.3 mg, 77%).

Analytical data for **d-52b**: ¹H NMR (700 MHz, Deuterium Oxide) δ 4.84 (d, $J = 1.5$ Hz, 1H), 4.83 (d, $J = 1.7$ Hz, 10H), 4.79 (d, $J = 1.7$ Hz, 1H), 3.93 – 3.90 (m, 10H), 3.90 – 3.84 (m, 12H), 3.82 (dd, $J = 12.2, 2.1$ Hz, 1H), 3.80 – 3.74 (m, 20H), 3.74 – 3.68 (m, 14H), 3.68 – 3.62 (m, 14H), 3.58 (t, $J = 9.7$ Hz, 2H), 3.49 (dt, $J = 10.0, 6.1$ Hz, 1H), 2.93 (t, $J = 7.7$ Hz, 2H), 1.65 – 1.56 (m, 4H), 1.38 (dh, $J = 29.2, 7.3$ Hz, 2H); ¹³C NMR (176 MHz, Deuterium Oxide) δ 99.90, 99.35, 72.72, 70.84, 70.70, 70.55, 69.99, 67.63, 66.76, 66.60, 65.52, 60.94, 39.37, 28.03, 26.57, 22.53; m/z (HRMS⁺) 2048.735 [M + H]⁺ (C₇₇H₁₃₄NO₆₁ requires 2048.741).

Synthesis of $\alpha(1-6)$ icosamannoside, **52c**

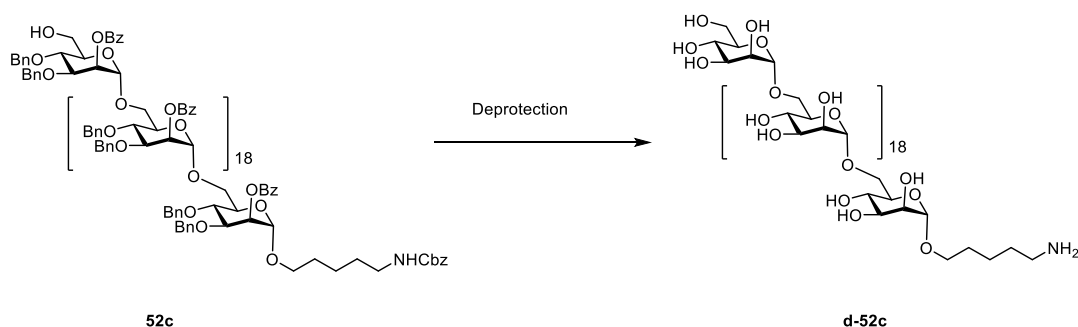


Module	Conditions
A: Resin Preparation for Synthesis	
B: Acidic Wash with TMSOTf Solution	
C: Thioglycoside Glycosylation	BB 37 , 6.5 eq (-20° for 5 min, 0° for 20 min)
D: Fmoc Deprotection	

Cleavage from the solid support as described in *Post-synthesizer manipulation* followed by purification using preparative HPLC afforded compound **52c** (38 mg, 33%).

Analytical data for **52c**: ^1H NMR (600 MHz, Chloroform-*d*) δ 8.22 – 8.20 (m, 2H), 8.20 – 8.12 (m, 32H), 8.12 – 8.09 (m, 3H), 8.08 – 8.04 (m, 5H), 8.01 – 7.97 (m, 4H), 7.60 – 7.55 (m, 4H), 7.55 – 7.41 (m, 56H), 7.39 – 7.26 (m, 26H), 7.26 – 7.20 (m, 24H), 7.20 – 7.09 (m, 109H), 7.09 – 7.00 (m, 40H), 5.86 – 5.81 (m, 12H), 5.81 – 5.77 (m, 3H), 5.76 (t, $J = 2.4$ Hz, 1H), 5.65 (d, $J = 8.2$ Hz, 2H), 5.63 – 5.60 (m, 6H), 5.51 (t, $J = 9.6$ Hz, 2H), 5.47 (d, $J = 5.5$ Hz, 1H), 5.35 – 5.29 (m, 2H), 5.20 – 5.13 (m, 3H), 5.11 – 5.04 (m, 6H), 5.03 (s, 6H), 4.90 – 4.84 (m, 14H), 4.81 – 4.76 (m, 14H), 4.71 (d, $J = 11.5$ Hz, 3H), 4.68 – 4.64 (m, 2H), 4.64 – 4.58 (m, 7H), 4.58 – 4.53 (m, 4H), 4.49 – 4.43 (m, 5H), 4.43 – 4.37 (m, 14H), 4.37 – 4.26 (m, 17H), 4.21 (td, $J = 12.6, 4.7$ Hz, 5H), 4.18 – 4.13 (m, 2H), 4.13 – 4.05 (m, 7H), 4.05 – 3.91 (m, 30H), 3.91 – 3.87 (m, 3H), 3.86 – 3.80 (m, 5H), 3.80 – 3.63 (m, 24H), 3.62 – 3.51 (m, 15H), 3.41 (t, $J = 9.7$ Hz, 14H), 3.17 – 3.13 (m, 2H), 1.60 – 1.52 (m, 2H), 1.49 (p, $J = 7.5$ Hz, 2H), 1.37 – 1.31 (m, 2H); ^{13}C NMR (151 MHz, Chloroform-*d*) δ 170.77, 170.74, 170.66, 170.63, 169.56, 169.32, 169.27, 169.26, 169.25, 169.07, 168.98, 168.75, 165.83, 165.50, 165.39, 138.44, 138.26, 138.21, 137.90, 137.61, 137.52, 137.46, 136.64, 133.64, 133.61,

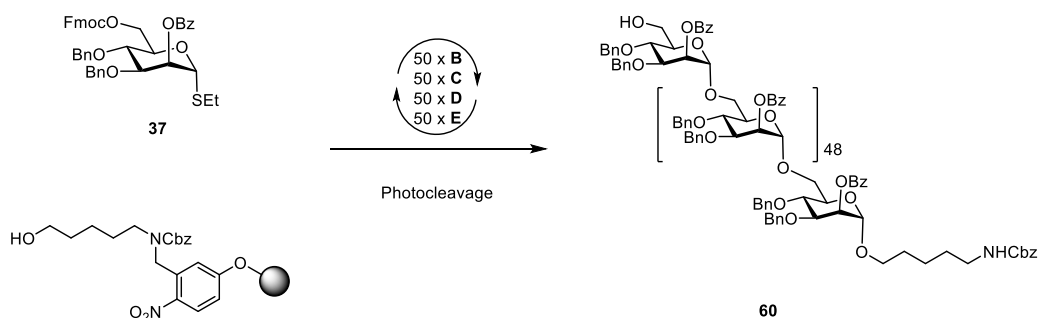
133.30, 133.24, 129.96, 129.88, 129.83, 128.62, 128.48, 128.46, 128.43, 128.34, 128.31, 128.27, 128.19, 128.10, 128.02, 127.98, 127.95, 127.82, 127.78, 127.66, 127.60, 127.48, 127.39, 127.33, 127.26, 127.20, 127.05, 126.97, 99.30, 98.50, 98.37, 98.21, 98.12, 97.84, 91.97, 91.74, 91.56, 89.49, 89.24, 82.87, 80.82, 79.95, 78.57, 78.47, 78.16, 77.81, 77.65, 77.22, 77.01, 76.80, 75.15, 74.96, 74.76, 74.18, 73.87, 73.67, 73.46, 73.35, 73.19, 72.99, 72.89, 72.80, 72.15, 72.07, 71.76, 71.61, 71.51, 71.26, 71.16, 70.85, 70.70, 70.31, 70.25, 70.15, 70.03, 69.27, 69.10, 69.01, 68.53, 68.34, 67.74, 67.66, 66.52, 66.07, 65.68, 65.40, 63.07, 61.77, 61.46, 40.93, 29.74, 29.01, 23.41, 20.87, 20.75, 20.73, 20.69, 20.59, 20.50; m/z (MALDI-TOF) 9201.212 [M + Na]⁺ (C₅₅₃H₅₃₉N₁O₁₂₄Na requires 9199.579).



Deprotection of **52c** (15.1 mg, 1.6 μ mol) as reported in Section 3.5 (Module F and G) followed by purification using preparative HPLC afforded compound **d-52c** (3.1 mg, 57%).

Analytical data for **d-52c**: ¹H NMR (700 MHz, Deuterium Oxide) δ 4.83 (d, J = 1.6 Hz, 19H), 4.79 (d, J = 1.6 Hz, 1H), 3.94 – 3.90 (m, 18H), 3.87 (m, 20H), 3.82 (dd, J = 12.2, 2.1 Hz, 2H), 3.77 (m, 36H), 3.70 (m, 20H), 3.68 – 3.62 (m, 23H), 3.59 (d, J = 9.7 Hz, 1H), 3.58 – 3.55 (m, 1H), 3.52 – 3.46 (m, 1H), 2.95 – 2.89 (m, 2H), 1.65 – 1.56 (m, 4H), 1.38 (dh, J = 28.4, 7.3 Hz, 2H). ¹³C NMR (176 MHz, Deuterium Oxide) δ 171.02, 99.90, 99.35, 70.84, 70.70, 69.98, 66.60, 65.51, 60.94; m/z (HRMS⁺) 1673.588 [M + 2H]²⁺ (C₁₂₅H₂₁₅NO₁₀₁ requires 1673.587).

Synthesis of 50-mer mannose (1-6), **60**

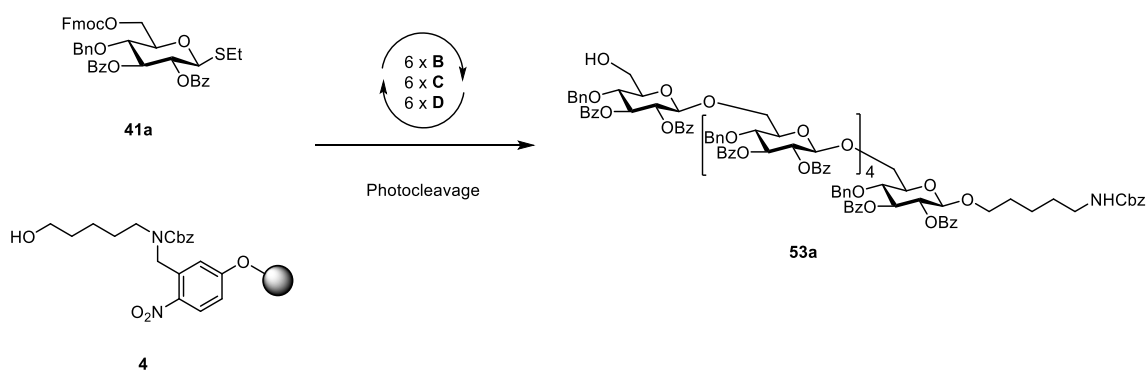


	Module	Conditions
	A: Resin Preparation for Synthesis	
	B: Acidic Wash with TMSOTf Solution	
50	C: Thioglycoside Glycosylation	BB 37, 6.5 eq (-20° for 5 min, 0° for 20 min)
	E: Capping	
	D: Fmoc Deprotection	

Cleavage from the solid support as described in *Post-synthesizer manipulation* followed by purification using preparative HPLC afforded compound **60** (64 mg, 22%).

Analytical data for **37**: ¹H NMR (700 MHz, Chloroform-*d*) δ 8.21 – 8.17 (m, 100H), 7.54 – 7.48 (m, 125H), 7.25 – 7.06 (m, 530), 5.87 – 5.84 (m, 50H), 5.06 (s, 50H), 4.89 (d, *J* = 11.5 Hz, 50H), 4.80 (d, *J* = 10.9 Hz, 50H), 4.44 (d, *J* = 10.9 Hz, 50H), 4.36 (t, *J* = 11.2 Hz, 50H), 4.04 (dd, *J* = 9.3, 3.1 Hz, 50H), 3.99 (t, *J* = 9.5 Hz, 50H), 3.75 (d, *J* = 10.6 Hz, 50H), 3.60 (d, *J* = 9.7 Hz, 50H), 3.45 (d, *J* = 11.1 Hz, 50H), 3.15 – 3.13 (m, 2H), 1.58 – 1.52 (m, 2H), 1.49 (m, 2H), 1.35 – 1.31 (m, 2H). ¹³C NMR (176 MHz, CDCl₃) δ 165.54, 138.53, 138.48, 137.51, 133.31, 130.01, 129.86, 128.65, 128.49, 128.36, 128.34, 128.14, 128.01, 127.68, 127.64, 127.37, 127.30, 127.24, 127.09, 127.01, 98.55, 78.20, 77.21, 77.02, 76.84, 75.18, 75.00, 73.71, 71.30, 70.90, 68.39, 65.73, 29.72.

Synthesis of 6-mer glucose(1-6), 53a



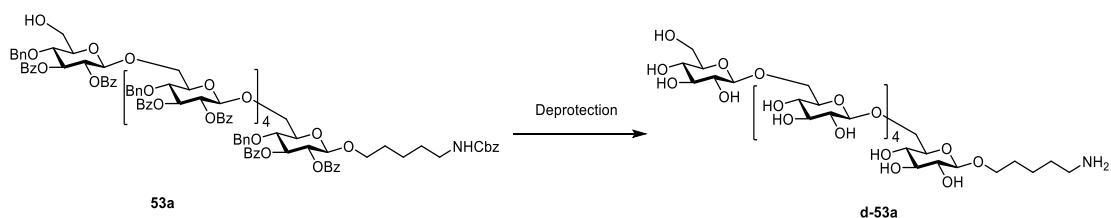
	Module	Conditions
	A: Resin Preparation for Synthesis	
	B: Acidic Wash with TMSOTf Solution	
6	C: Thioglycoside Glycosylation	BB 41a, 6.5 eq (-20° for 5 min, 0° for 20

min)

D: Fmoc Deprotection

Cleavage from the solid support as described in *Post-synthesizer manipulation* followed by purification using preparative HPLC afforded **53a** (17.2 mg, 45%).

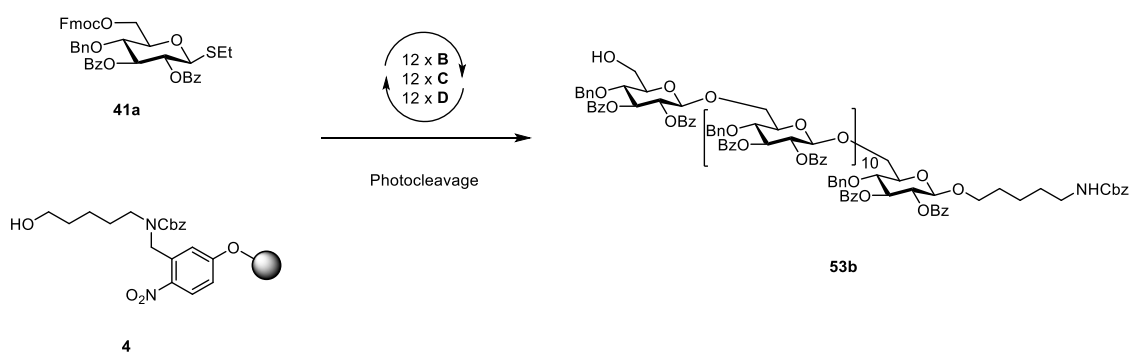
Analytical data for **53a**: ^1H NMR (600 MHz, Chloroform-*d*) δ 8.29 – 8.22 (m, 6H), 8.20 (d, $J = 7.7$ Hz, 2H), 8.14 – 8.08 (m, 4H), 8.07 (d, $J = 7.9$ Hz, 2H), 8.03 (d, $J = 8.0$ Hz, 1H), 8.01 – 7.92 (m, 6H), 7.90 – 7.86 (m, 2H), 7.53 – 7.43 (m, 4H), 7.42 – 7.20 (m, 22H), 7.20 – 6.99 (m, 21H), 6.99 – 6.94 (m, 2H), 6.93 – 6.85 (m, 5H), 6.85 – 6.73 (m, 4H), 6.73 – 6.64 (m, 5H), 6.61 (t, $J = 7.4$ Hz, 1H), 6.53 (t, $J = 7.5$ Hz, 2H), 6.50 – 6.44 (m, 4H), 6.41 (t, $J = 7.5$ Hz, 2H), 6.02 (t, $J = 9.6$ Hz, 2H), 5.95 (td, $J = 9.6, 7.1$ Hz, 2H), 5.89 – 5.78 (m, 4H), 5.72 – 5.60 (m, 3H), 5.53 – 5.43 (m, 3H), 5.31 (d, $J = 8.0$ Hz, 1H), 5.27 (d, $J = 8.1$ Hz, 1H), 5.11 (t, $J = 10.5$ Hz, 1H), 5.07 – 4.95 (m, 3H), 4.95 – 4.88 (m, 1H), 4.78 (br, 1H), 4.69 – 4.60 (m, 4H), 4.42 – 4.22 (m, 11H), 4.22 – 4.12 (m, 4H), 4.09 – 3.92 (m, 7H), 3.85 – 3.72 (m, 3H), 3.71 – 3.65 (m, 2H), 3.63 (d, $J = 9.6$ Hz, 1H), 3.59 – 3.53 (m, 2H), 3.51 (t, $J = 9.5$ Hz, 1H), 3.28 – 3.24 (m, 1H), 3.21 (dd, $J = 13.4, 2.6$ Hz, 1H), 2.93 (dq, $J = 12.5, 6.3$ Hz, 2H), 1.68 – 1.59 (m, 2H), 1.47 – 1.35 (m, 2H), 1.34 – 1.27 (m, 2H); ^{13}C NMR (151 MHz, Chloroform-*d*) δ 165.74, 165.58, 164.95, 164.83, 164.51, 164.30, 156.35, 138.02, 137.52, 137.30, 136.77, 136.49, 133.04, 132.81, 132.69, 132.51, 132.41, 132.25, 130.45, 130.20, 129.97, 129.92, 129.78, 129.67, 129.58, 128.96, 128.91, 128.87, 128.47, 128.36, 128.32, 128.24, 128.18, 128.15, 128.09, 128.04, 127.93, 127.86, 127.82, 127.66, 127.55, 127.40, 104.29, 103.75, 103.14, 102.55, 101.84, 100.38, 79.75, 79.36, 78.76, 78.57, 76.25, 76.15, 75.86, 75.75, 75.64, 75.29, 75.16, 75.07, 74.04, 73.61, 73.38, 73.03, 72.89, 72.65, 72.54, 72.39, 69.80, 66.17, 61.73, 41.05, 29.10, 28.70, 23.10; m/z (HRMS+) 3021.043 $[\text{M} + \text{Na}]^+$ ($\text{C}_{175}\text{H}_{163}\text{NO}_{45}\text{Na}$ requires 3021.039).



Deprotection of **37** (7.0 mg, 2.3 μmol) as reported in Section 3.5 (Module F and G) followed by purification using preparative HPLC afforded the **d-53a** (1.4 mg, 56%).

Analytical data for **37d**: ^1H NMR (600 MHz, Deuterium Oxide) δ 4.42 – 4.35 (m, 5H), 4.33 (d, J = 8.0 Hz, 1H), 4.08 (ddd, J = 11.7, 6.7, 2.1 Hz, 5H), 3.83 – 3.66 (m, 7H), 3.62 – 3.52 (m, 2H), 3.52 – 3.44 (m, 6H), 3.35 (dq, J = 14.0, 10.4, 9.7 Hz, 11H), 3.26 (t, J = 9.4 Hz, 1H), 3.18 (t, J = 8.4 Hz, 5H), 3.13 (t, J = 8.5 Hz, 1H), 2.87 (t, J = 7.5 Hz, 2H), 1.54 (dq, J = 14.1, 7.3, 6.8 Hz, 4H), 1.32 (t, J = 7.8 Hz, 2H); ^{13}C NMR (151 MHz, Deuterium Oxide) δ 102.93, 102.90, 102.82, 102.14, 75.84, 75.65, 75.59, 75.50, 74.82, 73.00, 72.96, 70.11, 69.54, 69.38, 68.71, 68.53, 60.64, 39.29, 28.11, 26.34, 22.02; m/z (HRMS+) 1076.427 [$M + \text{H}$] $^+$ ($\text{C}_{41}\text{H}_{74}\text{NO}_{31}$ requires 1076.424).

Synthesis of 12-mer glucose (1-6), **53b**

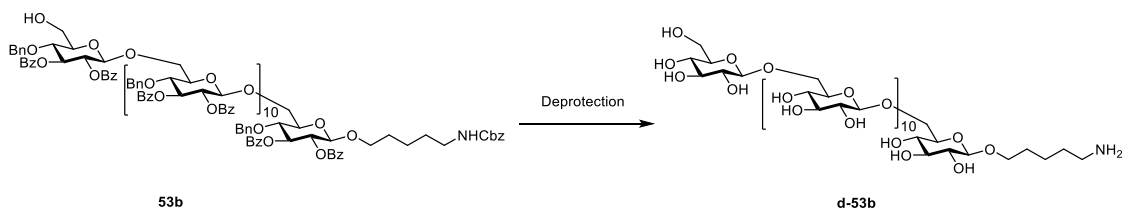


	Module	Conditions
	A: Resin Preparation for Synthesis	
	B: Acidic Wash with TMSOTf Solution	
12	C: Thioglycoside Glycosylation	BB 41b , 6.5 eq (-20° for 5 min, 0° for 20 min)
	D: Fmoc Deprotection	

Cleavage from the solid support as described in *Post-synthesizer manipulation* followed by purification using preparative HPLC afforded **53b**.

Analytical data for **53b**: ^1H NMR (700 MHz, Chloroform- d) δ 8.49 – 8.27 (m, 26H), 8.27 – 8.19 (m, 13H), 8.14 (d, J = 8.0 Hz, 2H), 8.09 – 7.96 (m, 6H), 7.60 (t, J = 7.4 Hz, 1H), 7.51 (tq, J = 13.5, 7.1, 6.4 Hz, 11H), 7.46 – 7.29 (m, 35H), 7.28 – 7.12 (m, 18H), 7.08 (dq, J = 16.0, 7.6 Hz, 12H), 7.02 (d, J = 6.9 Hz, 2H), 6.94 (dt, J = 22.2, 8.7 Hz, 9H), 6.88 (t, J = 7.7 Hz, 2H), 6.80 (dt, J = 24.1, 7.7 Hz, 2H), 6.76 – 6.61 (m, 18H), 6.54 (ddd, J = 29.4, 18.7, 7.7

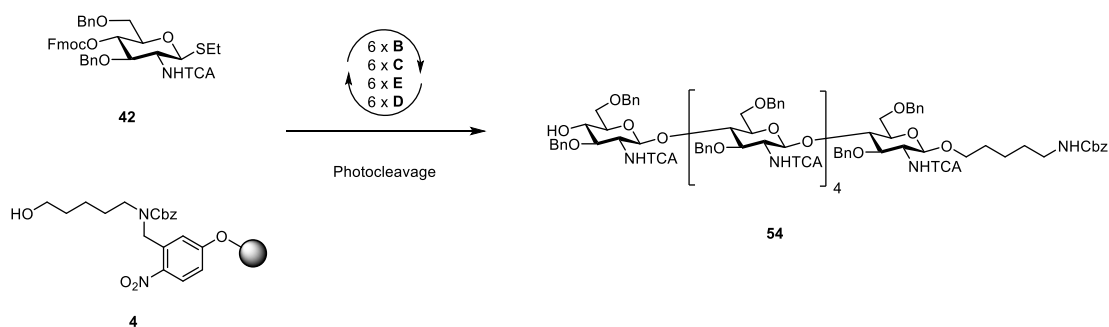
Hz, 25H), 6.39 (q, $J = 7.7$ Hz, 4H), 6.20 – 5.79 (m, 22H), 5.75 (t, $J = 8.6$ Hz, 1H), 5.69 (dt, $J = 17.6, 8.2$ Hz, 3H), 5.62 (d, $J = 7.9$ Hz, 1H), 5.58 (t, $J = 9.0$ Hz, 1H), 5.47 (d, $J = 8.0$ Hz, 1H), 5.43 (t, $J = 8.9$ Hz, 2H), 5.39 (dd, $J = 8.1, 5.0$ Hz, 2H), 5.35 (d, $J = 7.9$ Hz, 1H), 5.31 (d, $J = 8.3$ Hz, 2H), 5.28 (d, $J = 7.7$ Hz, 1H), 5.25 – 4.94 (m, 8H), 4.90 – 4.84 (m, 2H), 4.76 – 4.67 (m, 4H), 4.67 – 4.60 (m, 1H), 4.54 (d, $J = 8.7$ Hz, 1H), 4.53 – 4.30 (m, 10H), 4.28 (d, $J = 8.8$ Hz, 1H), 4.26 – 3.91 (m, 23H), 3.88 (dd, $J = 12.4, 6.4$ Hz, 3H), 3.76 – 3.66 (m, 4H), 3.67 – 3.53 (m, 5H), 3.53 – 3.39 (m, 6H), 3.36 (t, $J = 7.9$ Hz, 3H), 3.28 (dt, $J = 22.4, 8.4$ Hz, 3H), 3.18 (d, $J = 13.4$ Hz, 1H), 3.04 – 2.92 (m, 2H), 1.68 – 1.59 (m, 2H), 1.47 – 1.35 (m, 2H), 1.34 – 1.27 (m, 2H); ^{13}C NMR (151 MHz, Chloroform- d) δ 165.74, 165.54, 165.42, 165.14, 164.20, 138.12, 137.56, 137.21, 136.39, 133.02, 132.78, 132.52, 132.19, 130.52, 130.27, 130.10, 129.80, 129.60, 129.46, 129.31, 129.06, 128.92, 128.86, 128.37, 128.25, 128.17, 128.13, 128.06, 127.83, 127.78, 127.61, 127.53, 127.46, 104.20, 103.26, 102.75, 101.96, 100.41, 79.71, 78.77, 76.01, 75.70, 75.41, 75.16, 75.02, 73.51, 73.41, 72.64, 72.45, 72.15, 69.81, 66.17, 61.74, 41.10, 29.67, 28.72, 23.16; m/z (HRMS+) 2900.971 [$\text{M} + \text{H} + \text{K}$] $^{2+}$ ($\text{C}_{337}\text{H}_{308}\text{NO}_{87}\text{K}$ requires 2900.972).



Deprotection of **53b** (5.2 mg, 0.9 μmol) as reported in Section 3.5 (Module F and G) followed by purification using preparative HPLC afforded the **d-53b** (0.3 mg, 16%).

Analytical data for **d-53b**: ^1H NMR (600 MHz, Deuterium Oxide) δ 4.38 (t, $J = 8.5$ Hz, 11H), 4.33 (d, $J = 8.0$ Hz, 1H), 4.09 (d, $J = 11.2$ Hz, 11H), 3.78 (d, $J = 11.8$ Hz, 2H), 3.72 (dd, $J = 11.9, 6.0$ Hz, 12H), 3.52 – 3.45 (m, 14H), 3.41 (dd, $J = 11.8, 6.5$ Hz, 3H), 3.35 (p, $J = 9.3$ Hz, 20H), 3.27 (d, $J = 9.5$ Hz, 1H), 3.19 (t, $J = 8.4$ Hz, 10H), 3.13 (t, $J = 8.4$ Hz, 1H), 2.87 (t, $J = 7.6$ Hz, 2H), 1.61 – 1.43 (m, 4H), 1.33 (d, $J = 7.8$ Hz, 2H); m/z (HRMS+) 2048.739 [$\text{M} + \text{H}$] $^+$ ($\text{C}_{77}\text{H}_{134}\text{NO}_{61}$ requires 2048.741).

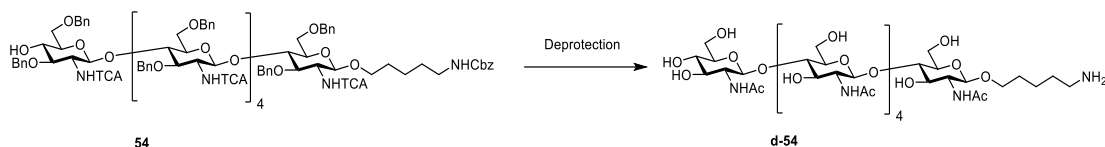
Synthesis of 6-mer glucosamine (1-4), **54**



Module	Conditions
A: Resin Preparation for Synthesis	
B: Acidic Wash with TMSOTf Solution	
6 {	C: Thioglycoside Glycosylation
	E: Capping
	D: Fmoc Deprotection
BB 42 , 6.5 eq (-20° for 5 min, 0° for 20 min)	

Cleavage from the solid support as described in *Post-synthesizer manipulation* followed by purification using preparative HPLC afforded **54** (11.5 mg, 45%).

Analytical data for **54** (1-4): ¹H NMR (600 MHz, Chloroform-d) δ 7.36 – 7.25 (m, 35H), 7.24 – 7.15 (m, 30H), 6.20 (d, J = 8.5 Hz, 2H), 6.10 (d, J = 9.0 Hz, 1H), 6.06 – 6.00 (m, 1H), 5.06 (s, 2H), 5.00 (dd, J = 11.8, 5.4 Hz, 2H), 4.95 (d, J = 11.5 Hz, 1H), 4.82 (d, J = 11.1 Hz, 1H), 4.78 (d, J = 11.4 Hz, 1H), 4.77 – 4.66 (m, 4H), 4.61 – 4.55 (m, 2H), 4.54 – 4.45 (m, 5H), 4.43 – 4.38 (m, 3H), 4.38 – 4.31 (m, 5H), 4.24 (d, J = 8.2 Hz, 1H), 4.20 (dd, J = 14.4, 8.3 Hz, 2H), 4.14 – 4.03 (m, 4H), 4.02 – 3.92 (m, 5H), 3.92 – 3.86 (m, 2H), 3.85 – 3.75 (m, 5H), 3.74 – 3.61 (m, 6H), 3.60 – 3.52 (m, 5H), 3.52 – 3.47 (m, 3H), 3.47– 3.37 (m, 5H), 3.32 (dd, J = 9.7, 6.6 Hz, 1H), 3.31 – 3.23 (m, 2H), 3.23 – 3.18 (m, 1H), 3.16 – 2.98 (m, 6H), 1.68 – 1.59 (m, 2H), 1.47 – 1.35 (m, 2H), 1.34 – 1.27 (m, 2H). ¹³C NMR (151 MHz, cdcl₃) δ 161.59, 156.34, 138.60, 138.34, 137.96, 137.61, 137.51, 137.33, 137.21, 136.61, 128.97, 128.92, 128.85, 128.70, 128.52, 128.47, 128.29, 128.23, 128.07, 128.03, 127.94, 127.88, 127.73, 127.68, 127.58, 127.51, 127.41, 127.31, 99.59, 99.43, 98.98, 92.58, 92.58, 92.49, 80.05, 79.16, 79.06, 78.92, 78.77, 77.99, 77.19, 76.98, 76.77, 75.88, 75.67, 74.94, 74.59, 74.32, 74.20, 74.11, 74.04, 73.77, 73.59, 73.49, 73.38, 72.51, 71.27, 69.53, 68.14, 67.85, 66.54, 57.10, 56.88, 40.89, 31.90, 29.67, 29.53, 28.92, 23.18, 22.66; m/z (HRMS⁺) 3170.578 [M + Na]⁺ (C₁₄₅H₁₅₁Cl₁₈N₇O₃₃Na requires 3170.464)

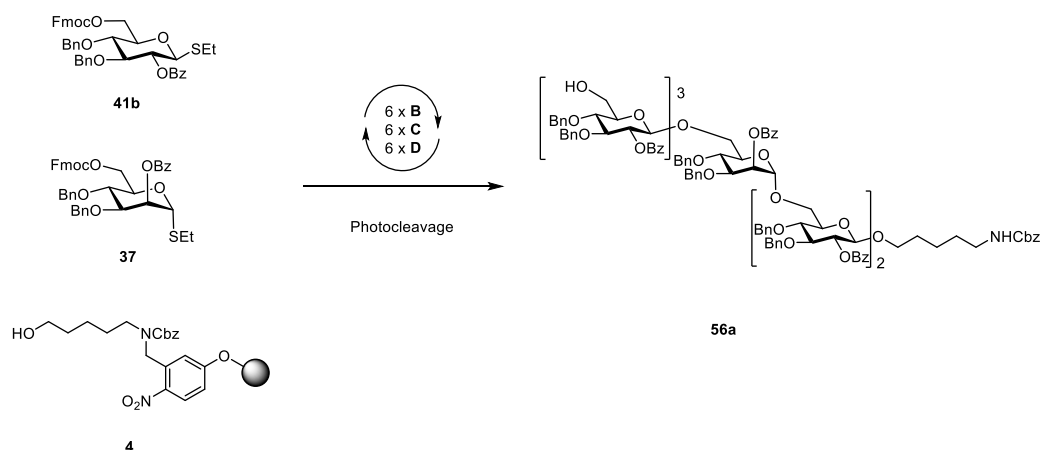


Deprotection of **54** (9.0 mg, 2.9 μmol) as reported in Section 3.5 (Module F and G) followed by purification using preparative HPLC afforded the **d-54** (1.8 mg, 48 %).

Analytical data for **d-54**: ^1H NMR (600 MHz, Deuterium Oxide) δ 4.46 – 4.40 (m, 5H), 4.35 (d, $J = 7.6$ Hz, 1H), 3.80 – 3.76 (m, 3H), 3.76 – 3.66 (m, 5H), 3.66 – 3.47 (m, 19H), 3.47 – 3.38 (m, 7H), 3.38 – 3.30 (m, 4H), 2.84 (t, $J = 7.7$ Hz, 2H), 1.97 – 1.88 (m, 18H), 1.53 (p, $J = 7.7$ Hz, 2H), 1.50 – 1.42 (m, 2H), 1.26 (d, $J = 9.0$ Hz, 2H). ^{13}C NMR (151 MHz, Deuterium Oxide) δ 174.51, 101.16, 78.84, 74.45, 71.97, 70.03, 60.45, 59.85, 54.96, 39.26, 27.98, 26.29, 22.03; m/z (HRMS $^+$) 1322.584 [$\text{M} + \text{H}$] $^+$ ($\text{C}_{53}\text{H}_{92}\text{N}_7\text{O}_{31}$ requires 1322.583).

3.7.3 Synthesis of heteropolymers

Synthesis of 6-mer **56a**

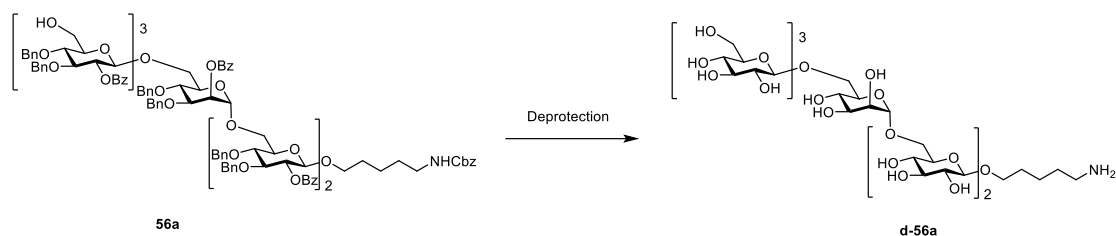


	Module	Conditions
	A: Resin Preparation for Synthesis	
2	B: Acidic Wash with TMSOTf Solution	
	C: Thioglycoside Glycosylation	BB 41b , 6.5 eq (-20° for 5 min, 0° for 20 min)
	D: Fmoc Deprotection	
	B: Acidic Wash with TMSOTf Solution	
	C: Thioglycoside Glycosylation	BB 37 , 6.5 eq (-20° for 5 min, 0° for 20 min)
	D: Fmoc Deprotection	

-
- 3 } **B:** Acidic Wash with TMSOTf Solution
C: Thioglycoside Glycosylation **BB 41b**, 6.5 eq (-20° for 5 min, 0° for 20 min)
D: Fmoc Deprotection
-

Cleavage from the solid support as described in *Post-synthesizer manipulation* followed by purification using preparative HPLC afforded **56a** (15.6 mg, 43%).

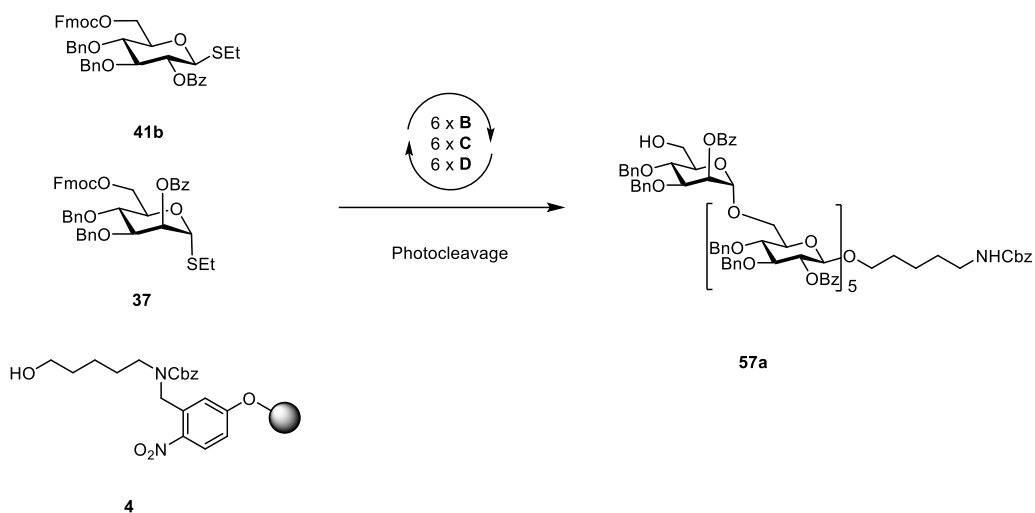
Analytical data for **56a**: ^1H NMR (400 MHz, Chloroform-*d*) δ 8.31 – 8.21 (m, 2H), 8.03 – 7.93 (m, 7H), 7.89 – 7.82 (m, 4H), 7.69 – 7.59 (m, 3H), 7.57 – 7.02 (m, 75H), 6.97 (dd, $J = 7.2, 2.2$ Hz, 2H), 6.86 (dd, $J = 7.3, 2.3$ Hz, 2H), 5.65 – 5.58 (m, 1H), 5.45 – 5.23 (m, 4H), 5.18 – 5.04 (m, 3H), 4.85 (d, $J = 10.8$ Hz, 2H), 4.80 – 4.23 (m, 31H), 4.18 – 4.09 (m, 2H), 4.05 – 3.85 (m, 5H), 3.85 – 3.26 (m, 20H), 3.08 (s, 1H), 2.89 – 2.74 (m, 2H), 2.44 (s, 1H), 1.28 – 1.15 (m, 4H), 1.09 – 0.95 (m, 2H); ^{13}C NMR (101 MHz, Chloroform-*d*) δ 164.98, 156.26, 138.61, 137.97, 137.82, 136.76, 133.04, 130.40, 129.95, 129.67, 128.79, 128.49, 128.39, 128.24, 128.15, 128.09, 128.02, 127.96, 127.83, 127.75, 127.56, 127.16, 101.87, 100.90, 98.05, 83.03, 82.53, 82.11, 75.65, 75.15, 74.80, 74.47, 74.05, 73.66, 70.98, 70.67, 69.07, 68.38, 66.45, 65.92, 61.55, 40.80, 29.34, 28.76, 23.08; m/z (HRMS $^+$) 2937.180 [$\text{M} + \text{Na}$] $^+$ ($\text{C}_{175}\text{H}_{175}\text{NO}_{39}\text{Na}$ requires 2937.163).



Deprotection of **56a** (12.2 mg, 4.1 μmol) as reported in Section 3.5 (Module F and G) followed by purification using preparative HPLC afforded the compound **d-56a** (2.5 mg, 55%).

Analytical data for **d-56a**: ^1H NMR (600 MHz, Deuterium Oxide) δ 4.76 (d, $J = 1.7$ Hz, 1H), 4.39 (dt, $J = 9.0, 7.3$ Hz, 4H), 4.33 (d, $J = 8.1$ Hz, 1H), 4.11 – 4.02 (m, 4H), 3.87 – 3.43 (m, 19H), 3.40 – 3.31 (m, 9H), 3.31 – 3.23 (m, 1H), 3.23 – 3.16 (m, 4H), 3.13 (dd, $J = 9.1, 8.0$ Hz, 1H), 2.85 (t, $J = 7.5$ Hz, 2H), 1.54 (h, $J = 7.5, 7.1$ Hz, 4H), 1.32 (p, $J = 7.7, 7.3$ Hz, 2H); ^{13}C NMR (151 MHz, Deuterium Oxide) δ 102.90, 102.81, 102.61, 102.16, 99.55, 75.84, 75.59, 74.88, 73.01, 69.80, 69.42, 66.24, 60.66, 39.35, 28.15, 26.58, 22.06; m/z (HRMS $^+$) 1076.420 [$\text{M} + \text{H}$] $^+$ ($\text{C}_{41}\text{H}_{74}\text{NO}_{31}$ requires 1076.424).

Synthesis of 6-mer **57a**

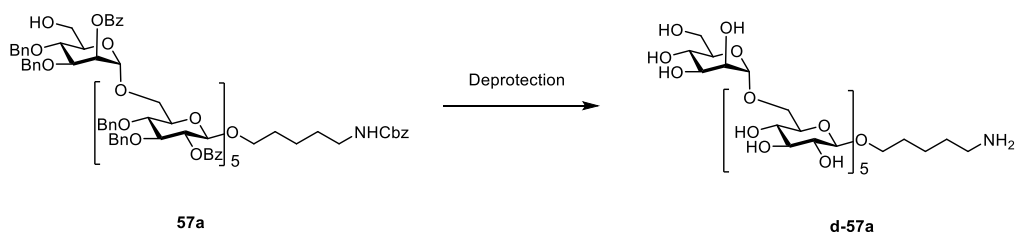


	Module	Conditions
	A: Resin Preparation for Synthesis	
5	B: Acidic Wash with TMSOTf Solution	
	C: Thioglycoside Glycosylation	BB 41b , 6.5 eq (-20° for 5 min, 0° for 20 min)
	D: Fmoc Deprotection	
	B: Acidic Wash with TMSOTf Solution	
	C: Thioglycoside Glycosylation	BB 37 , 6.5 eq (-20° for 5 min, 0° for 20 min)
	D: Fmoc Deprotection	

Cleavage from the solid support as described in *Post-synthesizer manipulation* followed by purification using preparative HPLC afforded **57a** (16.8 mg, 47%).

Analytical data for **57a**: ^1H NMR (600 MHz, Chloroform-*d*) δ 8.11 – 7.85 (m, 14H), 7.59 – 6.87 (m, 81H), 5.66 (s, 1H), 5.40 (t, $J = 8.7$ Hz, 1H), 5.25 (dq, $J = 18.1, 8.5$ Hz, 3H), 5.15 (t, $J = 8.7$ Hz, 1H), 5.05 (s, 3H), 4.89 (d, $J = 11.2$ Hz, 1H), 4.79 (d, $J = 11.3$ Hz, 1H), 4.74 – 4.17 (m, 29H), 4.10 – 3.89 (m, 4H), 3.89 – 3.31 (m, 25H), 3.18 (d, $J = 8.8$ Hz, 1H), 2.80 (q, $J = 6.8$ Hz, 2H), 1.33 – 1.11 (m, 4H), 1.03 (dq, $J = 29.5, 7.4, 7.0$ Hz, 2H); ^{13}C NMR (101 MHz, Chloroform-*d*) δ 165.38, 165.11, 164.95, 164.88, 156.24, 138.40, 137.93, 137.83, 137.78, 137.67, 136.80, 133.22, 133.10, 133.02, 132.92, 130.00, 129.92, 129.84, 129.69, 129.64, 128.51, 128.44, 128.40, 128.35, 128.28, 128.25, 128.23, 128.10, 128.07, 128.01, 127.95, 127.92, 127.88, 127.80, 127.76, 127.70, 127.67, 127.60, 127.54, 127.43, 127.37, 101.64, 101.27, 101.10, 100.98, 100.77, 98.08, 83.03, 82.87, 82.51, 78.19, 78.05, 77.69,

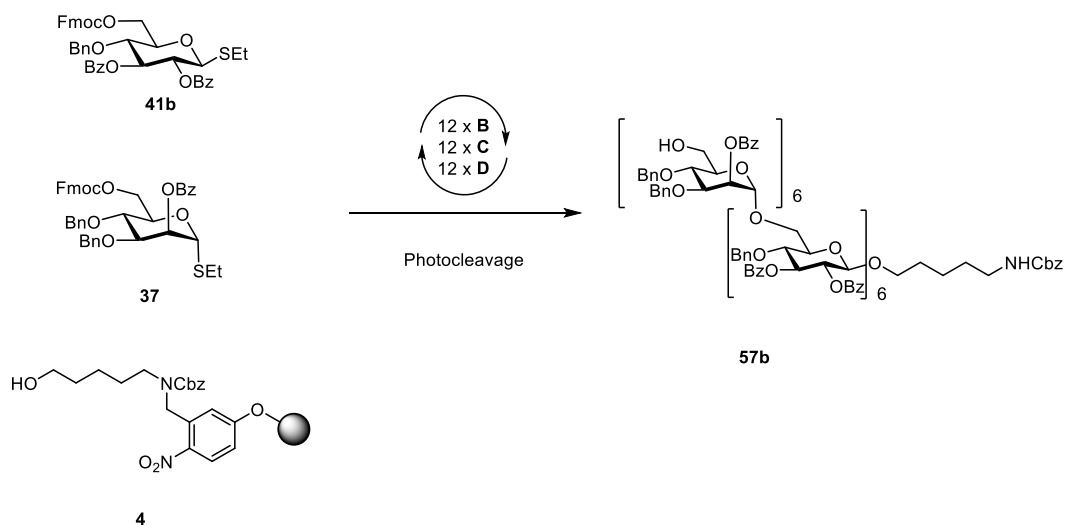
75.10, 74.81, 74.67, 74.41, 74.27, 73.87, 73.61, 72.26, 71.22, 69.08, 68.71, 68.59, 68.05, 66.37, 66.00, 61.84, 40.80, 29.27, 28.68, 23.07; m/z (HRMS+) 2937.180 $[M + Na]^+$ ($C_{175}H_{175}NO_{39}Na$ requires 2937.163).



Deprotection of **57a** (15.1 mg, 5.2 μmol) as reported in Section 3.5 (Module F and G) followed by purification using preparative HPLC afforded the compound **d-57a** (2.8 mg, 51%).

Analytical data for **d-57a**: ^1H NMR (600 MHz, Deuterium Oxide) δ 4.76 (d, $J = 1.7$ Hz, 1H), 4.39 (dt, $J = 7.6, 3.6$ Hz, 4H), 4.33 (d, $J = 8.0$ Hz, 1H), 4.12 – 4.02 (m, 4H), 3.85 (dd, $J = 3.5, 1.7$ Hz, 1H), 3.83 – 3.60 (m, 10H), 3.58 – 3.43 (m, 8H), 3.34 (td, $J = 9.2, 3.4$ Hz, 10H), 3.18 (t, $J = 8.5$ Hz, 4H), 3.13 (t, $J = 8.5$ Hz, 1H), 2.87 (t, $J = 7.6$ Hz, 2H), 1.54 (dq, $J = 14.1, 7.3, 6.8$ Hz, 4H), 1.33 (q, $J = 7.9$ Hz, 2H); ^{13}C NMR (151 MHz, Deuterium Oxide) δ 102.93, 102.90, 102.83, 102.14, 99.44, 75.65, 75.50, 74.82, 72.95, 70.50, 70.11, 69.82, 69.37, 68.69, 66.58, 65.34, 64.98, 64.55, 60.79, 39.29, 28.11, 26.34, 22.02; m/z (HRMS+) 1076.429 $[M + H]^+$ ($C_{41}H_{74}NO_{31}$ requires 1076.424).

Synthesis of 12-mer **57b**

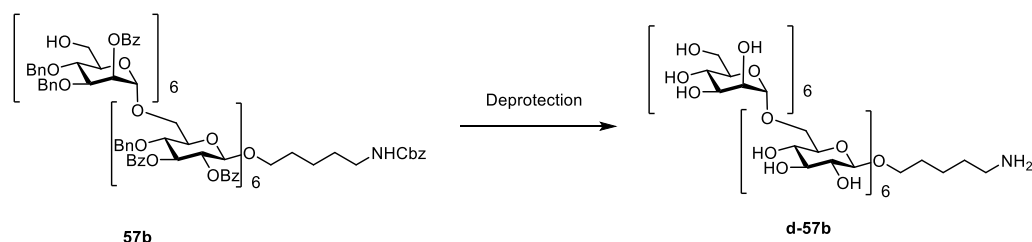


	Module	Conditions
	A: Resin Preparation for Synthesis	
6	B: Acidic Wash with TMSOTf Solution	
	C: Thioglycoside Glycosylation	BB 41b, 6.5 eq (-20° for 5 min, 0° for 20 min)
	D: Fmoc Deprotection	
	B: Acidic Wash with TMSOTf Solution	
6	C: Thioglycoside Glycosylation	BB 37, 6.5 eq (-20° for 5 min, 0° for 20 min)
	D: Fmoc Deprotection	

Cleavage from the solid support as described in *Post-synthesizer manipulation* followed by purification using preparative HPLC afforded **57b** (28.8 mg, 41%).

Analytical data for **57b**: ¹H NMR (700 MHz, Chloroform-*d*) δ 8.29 (td, *J* = 6.7, 1.7 Hz, 6H), 8.26 – 8.24 (m, 2H), 8.24 – 8.21 (m, 2H), 8.21 – 8.18 (m, 6H), 8.18 – 8.13 (m, 7H), 8.13 – 8.08 (m, 2H), 8.02 – 7.99 (m, 2H), 7.99 – 7.94 (m, 4H), 7.94 – 7.92 (m, 2H), 7.90 (d, *J* = 7.8 Hz, 2H), 7.63 – 7.59 (m, 1H), 7.58 – 7.54 (m, 4H), 7.54 – 7.38 (m, 12H), 7.46 – 7.38 (m, 3H), 7.38 – 7.24 (m, 33H), 7.24 – 7.02 (m, 57H), 7.02 – 6.90 (m, 9H), 6.89 – 6.86 (m, 2H), 6.86 – 6.82 (m, 1H), 6.75 (t, *J* = 7.7 Hz, 3H), 6.73 – 6.71 (m, 2H), 6.70 – 6.65 (m, 3H), 6.59 (t, *J* = 7.5 Hz, 2H), 6.56 – 6.52 (m, 4H), 6.49 (dt, *J* = 15.2, 7.5 Hz, 3H), 6.08 (dt, *J* = 18.8, 9.6 Hz, 2H), 6.00 (t, *J* = 9.2 Hz, 2H), 5.97 – 5.90 (m, 2H), 5.90 – 5.77 (m, 8H), 5.74 – 5.61 (m, 4H), 5.58 (d, *J* = 8.1 Hz, 1H), 5.56 – 5.49 (m, 2H), 5.33 (dd, *J* = 13.1, 8.0 Hz, 2H), 5.16 (d, *J* = 1.7 Hz, 1H), 5.09 – 5.00 (m, 7H), 4.97 (d, *J* = 1.8 Hz, 1H), 4.94 – 4.86 (m, 6H), 4.86 – 4.77 (m, 7H), 4.76 – 4.70 (m, 2H), 4.70 – 4.65 (m, 2H), 4.62 (d, *J* = 11.1 Hz, 1H), 4.59 (d, *J* = 8.0 Hz, 1H), 4.54 – 4.50 (m, 2H), 4.50 – 4.37 (m, 11H), 4.37 – 4.27 (m, 9H), 4.27 – 3.82 (m, 25H), 3.79 – 3.63 (m, 12H), 3.56 (dtt, *J* = 12.8, 6.8, 3.2 Hz, 8H), 3.49 (dd, *J* = 11.4, 3.4 Hz, 1H), 3.45 (dd, *J* = 11.7, 1.7 Hz, 1H), 3.43 – 3.37 (m, 2H), 3.32 – 3.24 (m, 2H), 3.03 – 2.87 (m, 2H), 1.75 – 1.63 (m, 2H), 1.50 – 1.39 (m, 2H), 1.34 (dd, *J* = 14.1, 7.4 Hz, 2H), ¹³C NMR (176 MHz, CDCl₃) δ 165.86, 165.80, 165.78, 165.74, 165.70, 165.67, 165.57, 165.53, 165.50, 165.47, 165.42, 165.39, 165.30, 165.02, 164.85, 164.81, 164.35, 156.40, 138.90, 138.68, 138.63, 138.55, 138.49, 138.32, 138.18, 137.95, 137.89, 137.69, 137.58, 137.55, 137.52, 137.48, 137.44, 137.41, 137.05, 136.88, 136.57, 133.29, 133.25, 133.05, 132.96, 132.86, 132.80, 132.65, 132.50, 132.40, 132.26, 130.46, 130.30, 130.28, 130.20, 130.14, 130.06, 130.04, 130.01, 129.99, 129.96, 129.91, 129.88, 129.86, 129.84, 129.81, 129.79, 129.75, 129.72, 129.70, 129.66, 129.63, 129.60, 129.52, 128.99, 128.87, 128.81, 128.75,

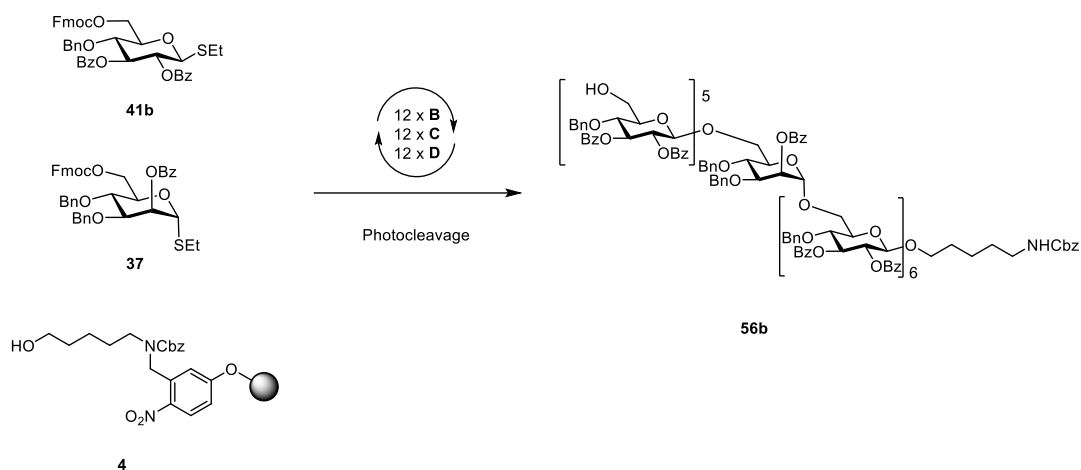
128.65, 128.59, 128.50, 128.46, 128.43, 128.41, 128.38, 128.37, 128.33, 128.29, 128.25, 128.23, 128.21, 128.18, 128.13, 128.08, 128.07, 128.05, 128.01, 127.99, 127.96, 127.94, 127.88, 127.85, 127.81, 127.78, 127.69, 127.65, 127.62, 127.60, 127.55, 127.50, 127.41, 127.36, 127.34, 127.20, 127.15, 127.10, 127.05, 126.96, 126.92, 126.87, 104.08, 103.66, 103.34, 102.59, 101.86, 100.44, 98.64, 98.55, 98.52, 98.20, 97.69, 79.86, 79.41, 79.35, 78.99, 78.80, 78.70, 78.29, 78.20, 78.19, 78.15, 77.70, 76.32, 76.25, 75.92, 75.75, 75.38, 75.18, 75.12, 75.10, 75.05, 74.99, 74.96, 74.93, 74.89, 74.85, 74.10, 73.91, 73.80, 73.73, 73.68, 73.66, 73.61, 73.47, 73.11, 73.06, 73.02, 72.76, 72.53, 72.45, 72.36, 72.11, 71.62, 71.33, 71.26, 71.23, 71.20, 71.17, 70.95, 70.89, 70.82, 70.79, 69.86, 68.57, 68.46, 68.37, 68.32, 68.25, 66.32, 66.18, 66.11, 65.80, 65.65, 65.42, 61.85, 41.10, 29.12, 28.77, 23.14; m/z (HRMS⁺) 2862.556 [M + 2Na]²⁺ (C₃₃₇H₃₁₉NO₈₁Na₂ requires 2862.538).



Deprotection of **57b** (19.2 mg, 3.4 μmol) as reported in Section 3.5 (Module F and G) followed by purification using preparative HPLC afforded the **d-57b** (3.5 mg, 52%).

Analytical data for **d-57b**: ¹H NMR (700 MHz, Deuterium Oxide) δ 4.86 – 4.80 (m, 6H), 4.45 (td, $J = 6.9, 3.6$ Hz, 5H), 4.40 (d, $J = 8.0$ Hz, 1H), 4.18 – 4.11 (m, 6H), 3.92 (pd, $J = 4.7, 3.8, 1.8$ Hz, 6H), 3.86 (dt, $J = 9.5, 3.4$ Hz, 6H), 3.82 (dd, $J = 12.2, 2.1$ Hz, 1H), 3.77 (dtd, $J = 17.1, 8.7, 8.2, 4.4$ Hz, 14H), 3.73 – 3.68 (m, 7H), 3.65 (dddd, $J = 18.2, 8.5, 6.9, 3.9$ Hz, 6H), 3.59 (d, $J = 9.8$ Hz, 1H), 3.58 – 3.51 (m, 7H), 3.45 – 3.36 (m, 13H), 3.25 (td, $J = 8.6, 7.9, 2.2$ Hz, 6H), 3.19 (t, $J = 8.6$ Hz, 1H), 2.94 (t, $J = 7.6$ Hz, 2H), 1.61 (dt, $J = 16.0, 7.8$ Hz, 4H), 1.39 (p, $J = 7.7$ Hz, 2H); ¹³C NMR (176 MHz, Deuterium Oxide) δ 103.01, 102.91, 102.23, 99.54, 99.41, 99.28, 75.90, 75.74, 75.59, 75.01, 74.90, 73.91, 73.04, 72.72, 70.84, 70.78, 70.70, 70.55, 70.19, 69.99, 69.47, 68.80, 68.66, 66.76, 66.61, 65.62, 65.52, 65.24, 60.94, 39.37, 28.19, 26.42, 22.10; m/z (HRMS⁺) 2048.743 [M + H]⁺ (C₇₇H₁₃₄NO₆₁ requires 2048.741).

Synthesis of 12-mer 56b

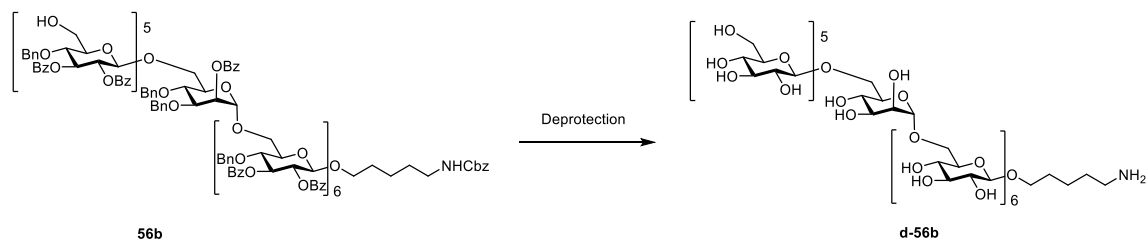


	Module	Conditions
	A: Resin Preparation for Synthesis	
6	B: Acidic Wash with TMSOTf Solution	
	C: Thioglycoside Glycosylation	BB 41b , 6.5 eq (-20° for 5 min, 0° for 20 min)
	D: Fmoc Deprotection	
	B: Acidic Wash with TMSOTf Solution	
5	C: Thioglycoside Glycosylation	BB 37 , 6.5 eq (-20° for 5 min, 0° for 20 min)
	D: Fmoc Deprotection	
	B: Acidic Wash with TMSOTf Solution	
	C: Thioglycoside Glycosylation	BB 41b , 6.5 eq (-20° for 5 min, 0° for 20 min)
	D: Fmoc Deprotection	

Cleavage from the solid support as described in *Post-synthesizer manipulation* followed by purification using preparative HPLC afforded **56b** (21 mg, 29%).

Analytical data for **56b**: ^1H NMR (600 MHz, Chloroform-*d*) δ 8.35 – 8.26 (m, 2H), 8.21 (dd, $J = 19.2, 7.7$ Hz, 12H), 8.17 – 7.95 (m, 28H), 7.96 – 7.82 (m, 7H), 7.74 (q, $J = 10.0, 9.6$ Hz, 9H), 7.57 (q, $J = 5.0$ Hz, 2H), 7.55 – 7.27 (m, 39H), 7.22 – 6.34 (m, 86H), 6.16 – 6.00 (m, 4H), 6.00 – 5.73 (m, 10H), 5.73 – 5.15 (m, 16H), 5.01 (d, $J = 9.0$ Hz, 8H), 4.90 (t, $J = 10.3$ Hz, 3H), 4.84 – 4.43 (m, 16H), 4.43 – 3.42 (m, 49H), 3.39 – 3.18 (m, 6H), 2.91 (br, 4H), 1.64 – 1.59 (m, 2H), 1.46 – 1.34 (m, 2H), 1.33 – 1.26 (m, 2H); ^{13}C NMR (151 MHz, Chloroform-*d*) δ 166.14, 165.83, 165.74, 165.66, 165.49, 165.47, 165.44, 165.12, 165.05, 164.86, 164.60, 164.56, 164.45, 138.94, 138.64, 138.13, 138.00, 137.90, 137.55, 137.50, 137.46, 137.30, 136.93, 136.88, 136.58, 136.55, 133.03, 132.73, 132.35, 132.17, 131.67,

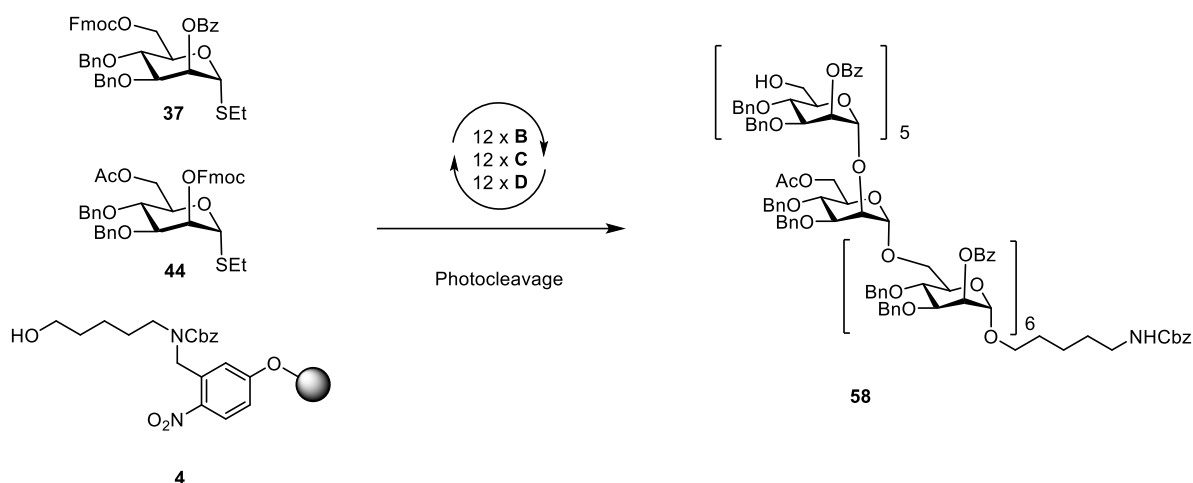
130.51, 130.39, 130.19, 130.14, 130.06, 130.00, 129.92, 129.89, 129.85, 129.80, 129.79, 129.74, 129.66, 129.57, 129.53, 129.07, 128.80, 128.76, 128.64, 128.58, 128.51, 128.37, 128.34, 128.30, 128.22, 128.19, 128.17, 128.14, 128.12, 128.02, 127.99, 127.96, 127.92, 127.88, 127.84, 127.80, 127.75, 127.73, 127.67, 127.61, 127.60, 127.57, 127.40, 127.31, 126.95, 126.79, 126.58, 104.83, 103.62, 102.40, 102.15, 101.73, 100.42, 79.20, 79.14, 79.06, 78.36, 76.27, 76.13, 75.97, 75.81, 75.66, 75.53, 75.36, 75.18, 75.13, 74.98, 74.77, 74.13, 73.74, 73.65, 73.31, 73.19, 73.02, 72.91, 72.77, 72.47, 72.28, 72.05, 71.36, 69.78, 66.14, 46.38, 41.04, 29.68, 28.73, 23.10; m/z (HRMS⁺) 2875.012 [M + 2H]²⁺ (C₃₃₇H₃₁₁NO₈₆ requires 2875.004).



Deprotection of **56b** (11.0 mg, 1.9 μmol) as reported in Section 3.5 (Module F and G) followed by purification using preparative HPLC afforded the compound **d-56b** (2.7 mg, 68%).

Analytical data for **d-56b**: ¹H NMR (600 MHz, Deuterium Oxide) δ 4.77 (d, $J = 1.7$ Hz, 1H), 4.44 – 4.37 (m, 10H), 4.34 (d, $J = 8.0$ Hz, 1H), 4.08 (td, $J = 11.4, 7.7$ Hz, 11H), 3.91 – 3.64 (m, 16H), 3.63 – 3.53 (m, 2H), 3.49 (q, $J = 7.1$ Hz, 11H), 3.41 – 3.30 (m, 22H), 3.27 (q, $J = 10.4, 9.5$ Hz, 1H), 3.20 (ddt, $J = 10.5, 8.5, 3.5$ Hz, 10H), 3.13 (t, $J = 8.5$ Hz, 1H), 2.88 (t, $J = 7.6$ Hz, 2H), 1.55 (dt, $J = 14.8, 7.5$ Hz, 4H), 1.32 (p, $J = 7.8$ Hz, 2H); ¹³C NMR (151 MHz, Deuterium Oxide) δ 102.99, 102.94, 102.90, 102.82, 102.61, 102.15, 99.54, 75.84, 75.80, 75.66, 75.59, 75.51, 75.40, 74.86, 74.82, 73.88, 73.01, 72.97, 71.60, 70.42, 70.12, 69.55, 69.39, 69.28, 68.72, 68.41, 66.27, 65.32, 60.66, 39.30, 28.12, 26.35, 22.03; m/z (HRMS⁺) 2048.738 [M + H]⁺ (C₇₇H₁₃₄NO₆₁ requires 2048.741).

Synthesis of 12-mer 58

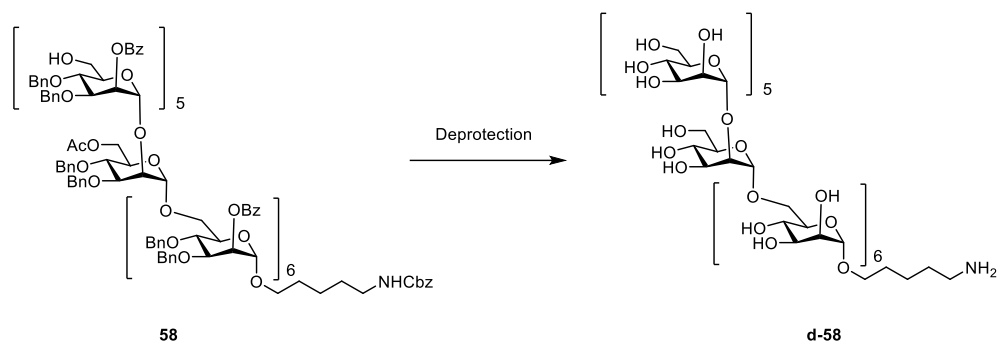


	Module	Conditions
	A: Resin Preparation for Synthesis	
6	B: Acidic Wash with TMSOTf Solution	
	C: Thioglycoside Glycosylation	BB 37 , 6.5 eq (-20° for 5 min, 0° for 20 min)
	D: Fmoc Deprotection	
	B: Acidic Wash with TMSOTf Solution	
5	C: Thioglycoside Glycosylation	BB 44 , 6.5 eq (-20° for 5 min, 0° for 20 min)
	D: Fmoc Deprotection	
	B: Acidic Wash with TMSOTf Solution	
	C: Thioglycoside Glycosylation	BB 37 , 6.5 eq (-20° for 5 min, 0° for 20 min)
	D: Fmoc Deprotection	

Cleavage from the solid support as described in *Post-synthesizer manipulation* followed by purification using preparative HPLC afforded **58** (25.5 mg, 37%).

Analytical data for **58**: ^1H NMR (600 MHz, Chloroform-*d*) δ 8.19 – 8.02 (m, 28H), 7.57 (t, $J = 7.4$ Hz, 1H), 7.53 – 7.39 (m, 34H), 7.39 – 6.94 (m, 117H), 5.87 – 5.72 (m, 10H), 5.61 (t, $J = 2.4$ Hz, 1H), 5.17 (d, $J = 1.8$ Hz, 1H), 5.12 – 4.97 (m, 11H), 4.96 – 4.65 (m, 29H), 4.62 – 4.26 (m, 27H), 4.12 – 3.33 (m, 57H), 3.16 (q, $J = 7.0$ Hz, 2H), 1.71 (s, 3H), 1.58 (tt, $J = 14.1, 7.0$ Hz, 2H), 1.52 – 1.43 (m, 2H), 1.34 (dt, $J = 8.9, 3.5$ Hz, 2H); ^{13}C NMR (151 MHz, Chloroform-*d*) δ 170.61, 165.82, 165.58, 165.53, 165.50, 165.47, 165.43, 165.41, 165.37, 138.52, 138.50, 138.46, 138.44, 138.42, 138.40, 138.34, 138.28, 138.22, 137.97, 137.92, 137.69, 137.63, 137.61, 137.58, 137.54, 137.51, 137.47, 137.44, 137.33, 133.25, 133.21, 130.04, 130.00, 129.97, 129.92, 129.87, 129.84, 129.82, 129.81, 129.73, 128.61, 128.59,

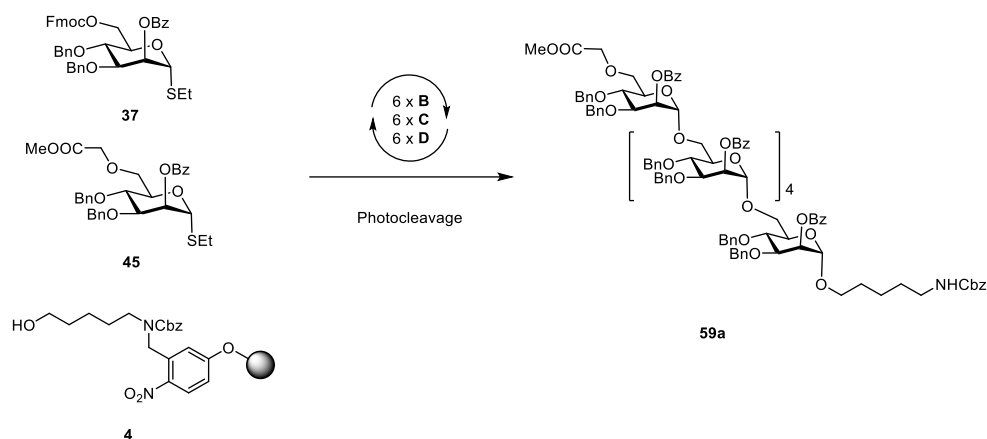
128.54, 128.48, 128.45, 128.41, 128.35, 128.34, 128.31, 128.29, 128.27, 128.26, 128.22, 128.19, 128.14, 128.12, 128.10, 128.07, 128.05, 128.01, 127.99, 127.97, 127.75, 127.66, 127.64, 127.60, 127.58, 127.39, 127.32, 127.29, 127.27, 127.23, 127.18, 127.15, 127.06, 127.03, 127.01, 126.95, 99.59, 98.77, 98.50, 98.45, 98.40, 98.14, 98.10, 97.85, 79.49, 78.56, 78.35, 78.26, 78.20, 78.17, 78.14, 78.10, 78.05, 77.65, 75.30, 75.14, 75.10, 75.05, 75.02, 74.95, 74.92, 74.78, 74.18, 73.88, 73.84, 73.78, 73.68, 73.15, 72.06, 71.69, 71.61, 71.43, 71.38, 71.29, 71.26, 71.22, 71.16, 71.13, 71.04, 70.99, 70.93, 70.90, 70.84, 70.71, 69.98, 69.05, 68.76, 68.55, 68.52, 68.43, 68.36, 68.30, 67.74, 66.51, 66.42, 66.30, 66.07, 65.76, 65.68, 65.62, 65.36, 64.34, 62.72, 61.80, 40.93, 29.75, 29.01, 23.41, 20.60; m/z (HRMS+) 2789.100 [M + 2Na]²⁺ (C₃₃₂H₃₂₉NO₇₅Na₂ requires 2789.093).



Deprotection of **58** (17.5 mg, 2.5 μ mol) as reported in Section 3.5 (Module F and G) followed by purification using preparative HPLC afforded the compound **d-58** (3.4 mg, 64%).

Analytical data for **d-58**: ¹H NMR (600 MHz, Deuterium Oxide) δ 4.97 – 4.93 (m, 1H), 4.90 (d, J = 1.7 Hz, 1H), 4.77 (qd, J = 6.1, 5.7, 1.4 Hz, 9H), 4.72 (d, J = 1.6 Hz, 1H), 3.94 (dd, J = 3.5, 1.7 Hz, 1H), 3.91 – 3.75 (m, 30H), 3.75 – 3.48 (m, 42H), 3.43 (dt, J = 9.9, 6.1 Hz, 1H), 2.87 (t, J = 7.7 Hz, 2H), 1.55 (dp, J = 21.6, 7.5 Hz, 4H), 1.32 (dq, J = 15.2, 7.4, 6.9 Hz, 2H); ¹³C NMR (151 MHz, Deuterium Oxide) δ 102.11, 99.82, 99.23, 97.92, 78.79, 72.78, 72.78, 72.65, 70.99, 70.85, 70.76, 70.61, 70.47, 70.40, 70.14, 69.91, 67.55, 66.68, 66.52, 65.83, 65.45, 60.87, 39.30, 27.97, 26.50, 22.47; m/z (HRMS+) 2048.742 [M + H]⁺ (C₇₇H₁₃₄NO₆₁ requires 2048.741).

Synthesis of 6-mer mannose (1-6) for block coupling 59a

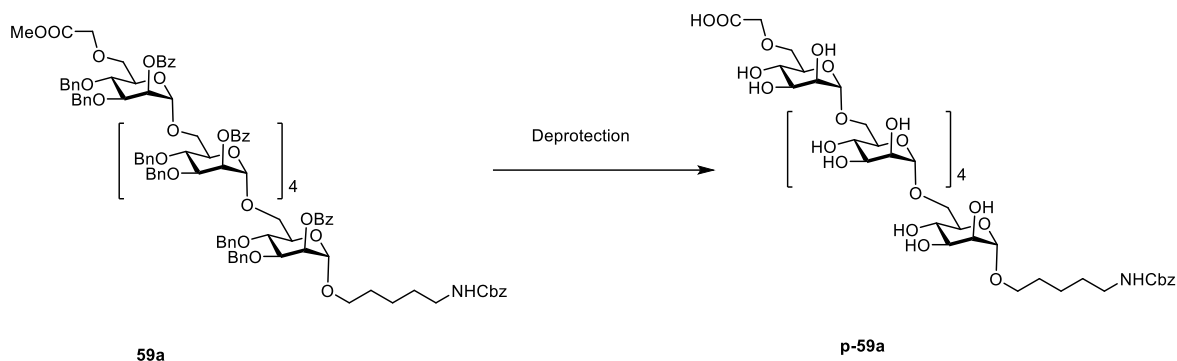


	Module	Conditions
	A: Resin Preparation for Synthesis	
5	B: Acidic Wash with TMSOTf Solution	
	C: Thioglycoside Glycosylation	BB 37 , 6.5 eq (-20° for 5 min, 0° for 20 min)
	D: Fmoc Deprotection	
	B: Acidic Wash with TMSOTf Solution	
	C: Thioglycoside Glycosylation	BB 45 , 6.5 eq (-20° for 5 min, 0° for 20 min)
	D: Fmoc Deprotection	

Cleavage from the solid support as described in *Post-synthesizer manipulation* followed by purification using preparative HPLC afforded **59a** (23.5 mg, 63%).

Analytical data for **59a**: ^1H NMR (600 MHz, Chloroform-*d*) δ 8.16 – 8.08 (m, 12H), 7.59 – 7.53 (m, 1H), 7.51 – 7.41 (m, 18H), 7.33 – 7.01 (m, 64H), 5.83 – 5.74 (m, 5H), 5.61 (dd, $J = 3.3, 1.8$ Hz, 1H), 5.10 – 4.99 (m, 7H), 4.89 – 4.83 (m, 6H), 4.81 (dd, $J = 11.3, 2.6$ Hz, 3H), 4.77 (d, $J = 11.0$ Hz, 4H), 4.70 (d, $J = 11.4$ Hz, 1H), 4.63 (d, $J = 11.1$ Hz, 1H), 4.54 (d, $J = 11.0$ Hz, 1H), 4.45 (dd, $J = 11.1, 4.8$ Hz, 2H), 4.43 – 4.38 (m, 5H), 4.37 (d, $J = 11.5$ Hz, 1H), 4.35 – 4.29 (m, 2H), 4.18 (d, $J = 16.4$ Hz, 1H), 4.06 (ddd, $J = 9.5, 6.3, 3.3$ Hz, 2H), 4.03 – 3.92 (m, 12H), 3.89 – 3.68 (m, 9H), 3.67 (s, 3H), 3.66 – 3.53 (m, 5H), 3.51 – 3.41 (m, 3H), 3.39 (d, $J = 9.2$ Hz, 1H), 3.14 (t, $J = 7.3$ Hz, 2H), 1.57 – 1.45 (m, 4H), 1.38 – 1.28 (m, 2H); ^{13}C NMR (151 MHz, Chloroform-*d*) δ 170.56, 165.81, 165.57, 165.49, 156.33, 138.55, 138.50, 138.47, 138.41, 138.22, 137.90, 137.61, 137.59, 137.55, 137.53, 137.51, 136.64, 133.25, 133.11, 130.00, 129.96, 129.91, 129.82, 129.79, 128.60, 128.53, 128.45, 128.39, 128.31, 128.29, 128.26, 128.24, 128.22, 128.18, 128.15, 128.13, 128.11, 128.09, 128.07, 128.00, 127.87, 127.64, 127.59, 127.53, 127.42, 127.38, 127.30, 127.22, 127.20, 127.16,

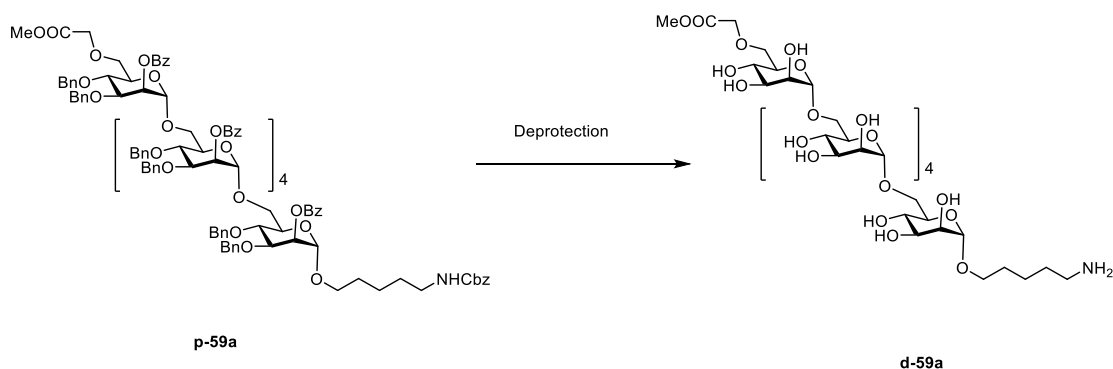
127.10, 127.08, 98.44, 98.37, 98.22, 98.10, 97.84, 78.56, 78.27, 78.22, 78.18, 78.13, 77.70, 75.14, 75.01, 74.97, 74.17, 73.88, 73.79, 73.71, 73.67, 71.86, 71.60, 71.38, 71.30, 71.26, 71.13, 70.94, 70.71, 69.95, 69.04, 68.82, 68.54, 68.46, 68.41, 68.35, 67.74, 66.51, 66.07, 65.78, 65.72, 65.66, 65.61, 51.63, 40.92, 29.74, 29.00, 23.40; m/z (HRMS⁺) 3009.184 [M + Na]⁺ (C₁₇₈H₁₇₉NO₄₁Na requires 3009.185).



Deprotection of **59a** (17.3 mg, 5.7 μ mol) as reported is Section 3.5 (Module F and G and H) followed by purification using preparative HPLC afforded the compound **p-59a** (4.3 mg, 57%).

Analytical data for **p-59a**: ¹H NMR (400 MHz, Deuterium Oxide) δ 7.28 – 7.10 (m, 5H), 4.90 (s, 2H), 4.67 (t, $J = 3.7$ Hz, 6H), 3.91 (s, 2H), 3.79 – 3.68 (m, 12H), 3.68 – 3.42 (m, 25H), 3.36 – 3.28 (m, 1H), 2.92 (d t, $J = 7.6$ Hz, 2H, 2H), 1.44 – 1.35 (m, 2H), 1.29 (q, $J = 7.1$ Hz, 2H), 1.19 – 1.10 (m, 2H); ¹³C NMR (101 MHz, Deuterium Oxide) δ 128.62, 128.16, 127.43, 99.72, 99.23, 99.15, 71.08, 70.74, 70.67, 70.50, 70.24, 69.93, 69.79, 69.67, 67.66, 66.59, 66.39, 65.29, 40.12, 28.40, 27.96, 22.52; m/z (HRMS⁺)1268.476 [M + H]⁺ (C₅₁H₈₂NO₃₅ requires 1268.466).

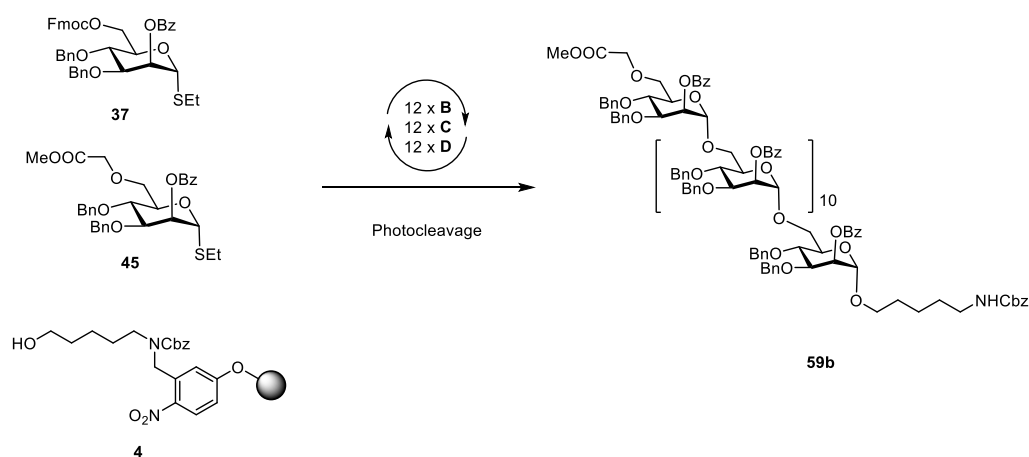
Synthesis of 6-mer mannose (1-6) for block coupling 48d2



Deprotection of **p-59a** (20.1 mg, 7.0 μmol) as reported in Section 3.5 (Module F and G) followed by purification using preparative HPLC afforded the **d-59a** (3.7 mg, 46%).

Analytical data for **d-59a**: ^1H NMR (400 MHz, Deuterium Oxide) δ 4.81 – 4.73 (m, 6H), 4.16 (s, 2H), 3.90 – 3.77 (m, 12H), 3.75 – 3.51 (m, 25H), 3.65 (s, 3H), 3.44 (dt, $J = 9.8, 6.0$ Hz, 1H), 2.87 (t, $J = 7.6$ Hz, 2H), 1.54 (dq, $J = 9.5, 7.4, 6.8$ Hz, 4H), 1.41 – 1.23 (m, 2H); ^{13}C NMR (101 MHz, Deuterium Oxide) δ 172.84, 99.82, 99.22, 70.67, 70.57, 69.87, 67.89, 67.53, 66.47, 65.38, 52.32, 39.26, 27.95, 26.49, 22.46; m/z (HRMS+) 1148.447 $[\text{M} + \text{H}]^+$ ($\text{C}_{44}\text{H}_{78}\text{NO}_{33}$ requires 1148.445).

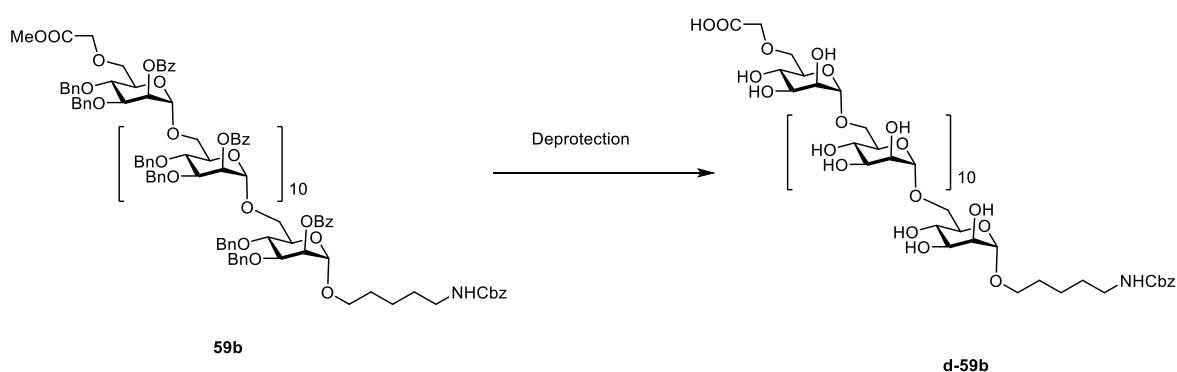
Synthesis of 12-mer mannose (1-6) for block coupling 59b



	Module	Conditions
	A: Resin Preparation for Synthesis	
11	B: Acidic Wash with TMSOTf Solution	
	C: Thioglycoside Glycosylation	BB 37 , 6.5 eq (-20° for 5 min, 0° for 20 min)
	D: Fmoc Deprotection	
	B: Acidic Wash with TMSOTf Solution	
	C: Thioglycoside Glycosylation	BB 45 , 6.5 eq (-20° for 5 min, 0° for 20 min)
	D: Fmoc Deprotection	

Cleavage from the solid support as described in *Post-synthesizer manipulation* followed by purification using preparative HPLC afforded compound **59b** (20.7 mg, 56%).

Analytical data for **59b**: ^1H NMR (700 MHz, Chloroform-*d*) δ 8.22 – 8.11 (m, 25H), 7.60 (t, $J = 7.5$ Hz, 1H), 7.56 – 7.46 (m, 38H), 7.37 – 7.30 (m, 7H), 7.26 (ddd, $J = 8.0, 6.4, 4.5$ Hz, 9H), 7.24 – 7.05 (m, 105H), 5.89 – 5.77 (m, 11H), 5.69 – 5.60 (m, 1H), 5.10 (td, $J = 13.9, 12.5, 1.7$ Hz, 5H), 5.08 – 5.04 (m, 8H), 4.90 (td, $J = 10.9, 4.3$ Hz, 12H), 4.87 – 4.83 (m, 3H), 4.81 (dt, $J = 10.9, 3.6$ Hz, 11H), 4.75 (d, $J = 11.4$ Hz, 1H), 4.68 (d, $J = 11.0$ Hz, 1H), 4.58 (d, $J = 11.0$ Hz, 1H), 4.49 (dd, $J = 11.1, 4.7$ Hz, 2H), 4.47 – 4.41 (m, 12H), 4.39 (s, 1H), 4.36 (dd, $J = 11.9, 4.8$ Hz, 8H), 4.22 (d, $J = 16.4$ Hz, 1H), 4.12 – 4.07 (m, 3H), 4.07 – 4.02 (m, 12H), 3.99 – 3.92 (m, 10H), 3.95 – 3.83 (m, 4H), 3.83 – 3.73 (m, 11H), 3.71 (s, 3H), 3.68 – 3.56 (m, 10H), 3.55 – 3.41 (m, 10H), 3.22 – 3.14 (m, 2H), 1.61 – 1.48 (m, 4H), 1.44 – 1.32 (m, 2H); ^{13}C NMR (151 MHz, Chloroform-*d*) δ 170.58, 165.85, 165.62, 165.52, 156.37, 138.60, 138.56, 138.54, 138.53, 138.49, 138.45, 138.27, 137.96, 137.67, 137.64, 137.61, 137.58, 137.56, 137.54, 136.71, 133.30, 133.27, 133.24, 133.14, 130.03, 129.97, 129.86, 129.83, 128.64, 128.62, 128.56, 128.50, 128.48, 128.42, 128.35, 128.32, 128.28, 128.25, 128.21, 128.18, 128.14, 128.10, 128.08, 128.06, 128.04, 128.02, 127.91, 127.77, 127.67, 127.63, 127.56, 127.46, 127.42, 127.36, 127.34, 127.32, 127.30, 127.28, 127.25, 127.20, 127.12, 127.08, 127.05, 98.56, 98.51, 98.42, 98.28, 98.14, 97.88, 78.60, 78.31, 78.25, 78.23, 78.20, 77.75, 75.17, 75.05, 75.01, 74.23, 73.93, 73.83, 73.77, 73.75, 73.71, 71.92, 71.65, 71.42, 71.34, 71.30, 71.18, 71.01, 70.98, 70.93, 70.76, 70.63, 70.01, 69.10, 68.87, 68.60, 68.52, 68.48, 68.44, 68.40, 67.78, 66.54, 66.13, 65.83, 65.75, 65.70, 65.65, 64.36, 60.39, 51.65, 40.96, 29.78, 29.04, 23.44; m/z (HRMS+) 2851.641 $[\text{M} + \text{K} + \text{H}]^{2+}$ ($\text{C}_{340}\text{H}_{336}\text{NO}_{77}\text{K}$ requires 2851.602).



Deprotection of **59b** (10.3 mg, 1.8 μmol) as reported in Section 3.5 (Module F and G and H) followed by purification using preparative HPLC afforded the **d-59b** (1.4 mg, 35%).

Analytical data for **d-59b**: ^1H NMR (600 MHz, Deuterium Oxide) δ 7.32 – 7.18 (m, 5H), 4.98 (s, 2H), 4.80 – 4.69 (m, 12H), 3.91 – 3.75 (m, 26H), 3.75 – 3.49 (m, 49H), 3.46 –

3.36 (m, 1H), 2.99 (t, $J = 6.7$ Hz, 2H), 1.54 – 1.41 (m, 2H), 1.37 (t, $J = 7.2$ Hz, 2H), 1.28 – 1.17 (m, 2H); ^{13}C NMR (151 MHz, Deuterium Oxide) δ 128.72, 99.27, 71.24, 70.77, 70.62, 70.31, 69.91, 66.52, 65.43; m/z (HRMS+) 2240.788 $[\text{M} + \text{H}]^+$ ($\text{C}_{87}\text{H}_{142}\text{NO}_{65}$ requires 2240.783).

4 Synthesis of Glycosaminoglycans

4.1 Introduction

Glycosaminoglycans (GAGs) are involved in many fundamental biological processes, such as cell recognition, cell proliferation and differentiation.¹⁴¹⁻¹⁴⁴ They are linear polymers comprised of disaccharide repeating units consisting of a hexuronic acid (generally, glucuronic or iduronic) linked to hexosamine (galactosamine or glucosamine).¹⁴¹ Depending on the nature of disaccharide repeating units, GAGs are classified into several major types: keratan sulfate, chondroitin sulfate, dermatan sulfate, hyaluronic acid and heparan sulfate (Figure 11).

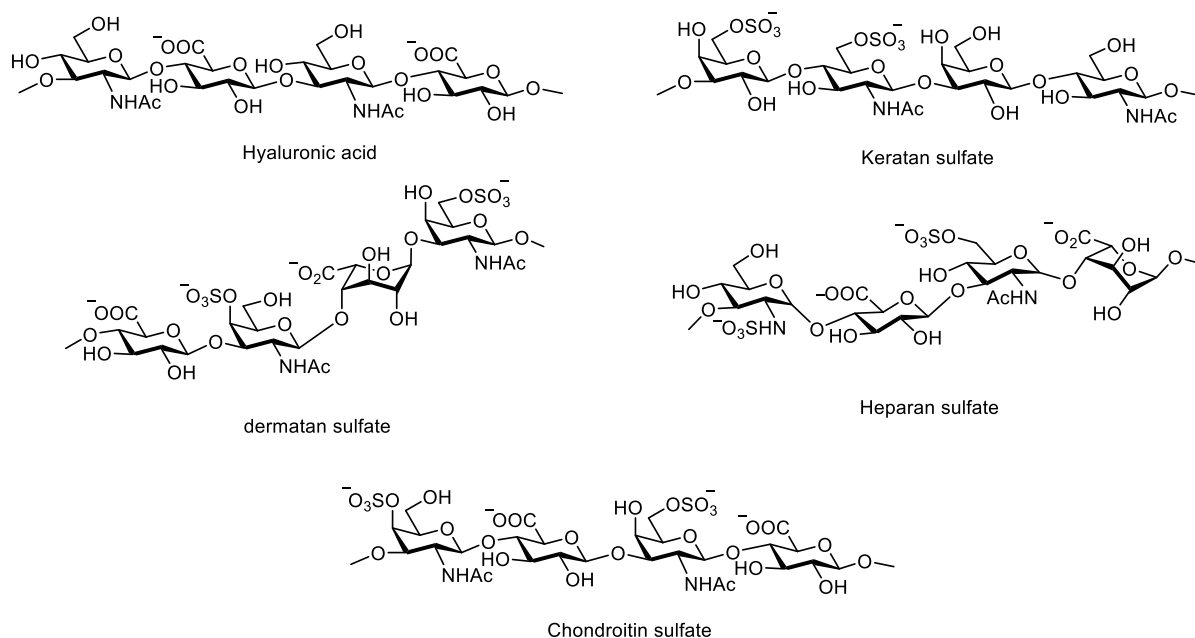


Figure 12. Types of glycosaminoglycans¹⁴¹

Heterogeneity in GAGs results from various possible degrees of O-sulfation and, in some cases, from the presence of two types of hexuronic acid residues. This microheterogeneity complicates biological studies of these polysaccharides and causes difficulties in their applications in biology and medicine.¹⁴⁵ In order to investigate the mode of action of GAGs and determine the structural fragments that are responsible for the interactions with biological targets, homogeneous oligosaccharide fragments of GAGs are required.

Several approaches to synthesize GAG oligosaccharides have been described. Chemoenzymatic synthesis enables an access to heparin, chondroitin and dermatan sulfate, as well as sulfated hyaluron.¹⁴⁶ But the number of possible repeating units that can be synthesized using this method is limited by the types of available enzymes.

To date, many methods of solution phase synthesis of GAG oligosaccharides have been reported. But most of these methods rely on many manual operations and do not allow for rapid access the desired compounds. Recently, automated glycan assembly was employed for the synthesis of dermatan, chondroitin and keratan sulfate repeating units.^{91, 131, 147} However, most of the methods access only fully-protected oligosaccharides: the global deprotection of them remains challenging. The main challenge is the fact that sulfated molecules are not stable in highly acidic and basic media, requiring very mild conditions for their synthesis. Therefore, new synthetic strategies that would enable the access to fully-deprotected GAG-oligosaccharide have to be developed.

Dermatan and chondroitin sulfate repeating units are an interesting target for automated glycan assembly. AGA modularity makes it possible to synthesize large collections of oligosaccharides. Several chondroitin and dermatan sulfate repeating units have been chosen as a synthetic target (Figure 13).

4.2 Synthetic Strategies to Access GAGs

In order to access different repeating units comprising dermatan and chondroitin sulfates, several building blocks been designed (Figure 13): two galactosamine BBs **62a** and **62b**, two iduronic BBs **63** and **64**, and one glucuronic acid BB **65**. Benzyl ethers (Bn) serve as permanent protecting groups. Levulinic ester protecting groups will be selectively cleaved before sulfation of the corresponding hydroxides. The fluorenylmethyloxycarbonyl (Fmoc) temporary protecting groups will be removed following elongation cycle during automated synthesis.

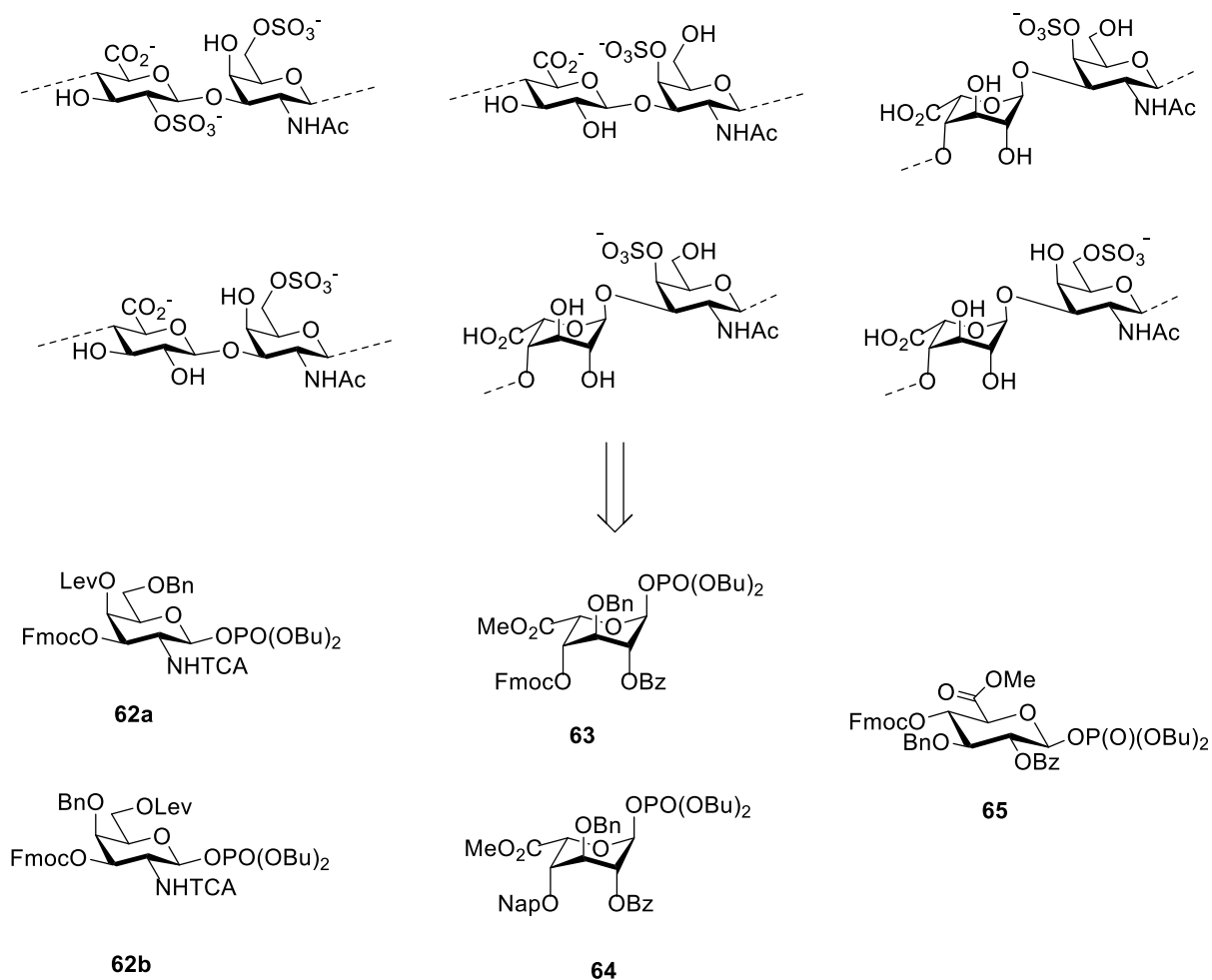
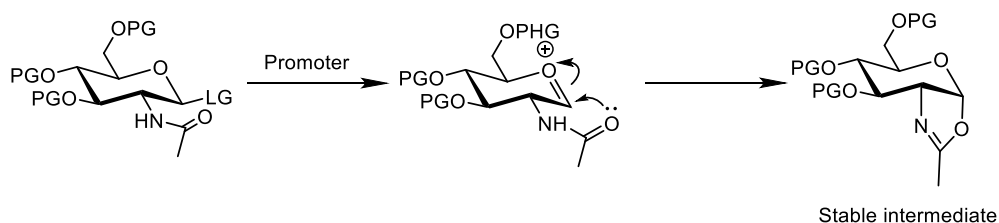


Figure 13. Building blocks required for the synthesis of dermatan and chondroitin sulfate repeating units.

For C-2 position of galactosamine BBs acetyl-protecting group would be a desirable option, because it will minimize protecting-group manipulations. But it has been previously shown, that for *N*-acetylaminosugars oxocarbenium ion undergoes rearrangement (Scheme 37) leading to stable oxazoline intermediate.¹⁴⁸ In order to avoid oxazoline formation, the trichloroacetyl (TCA) protecting group should be used.

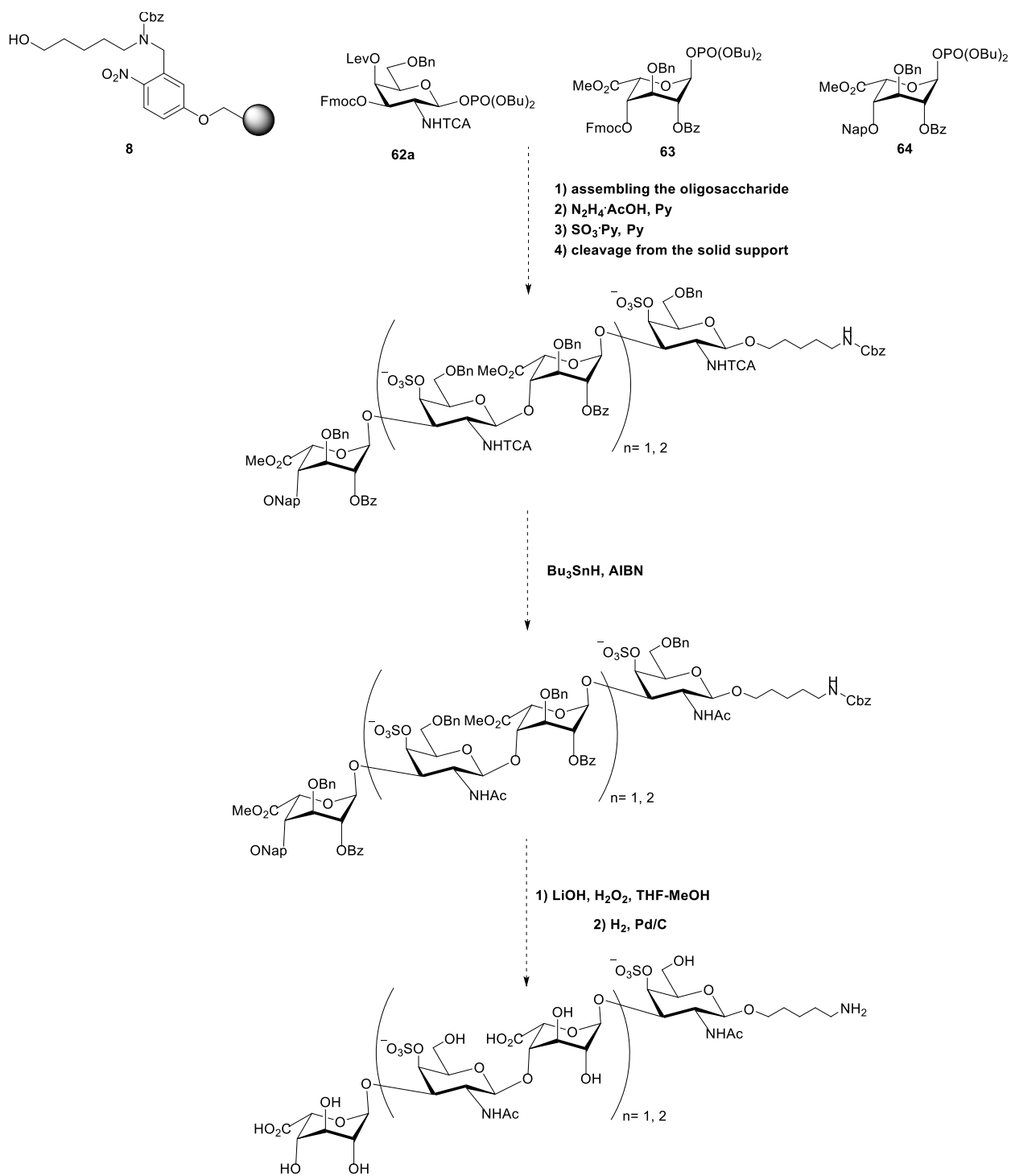


Scheme 37. Rearrangement of oxocarbenium ion to oxazoline for aminosugars.

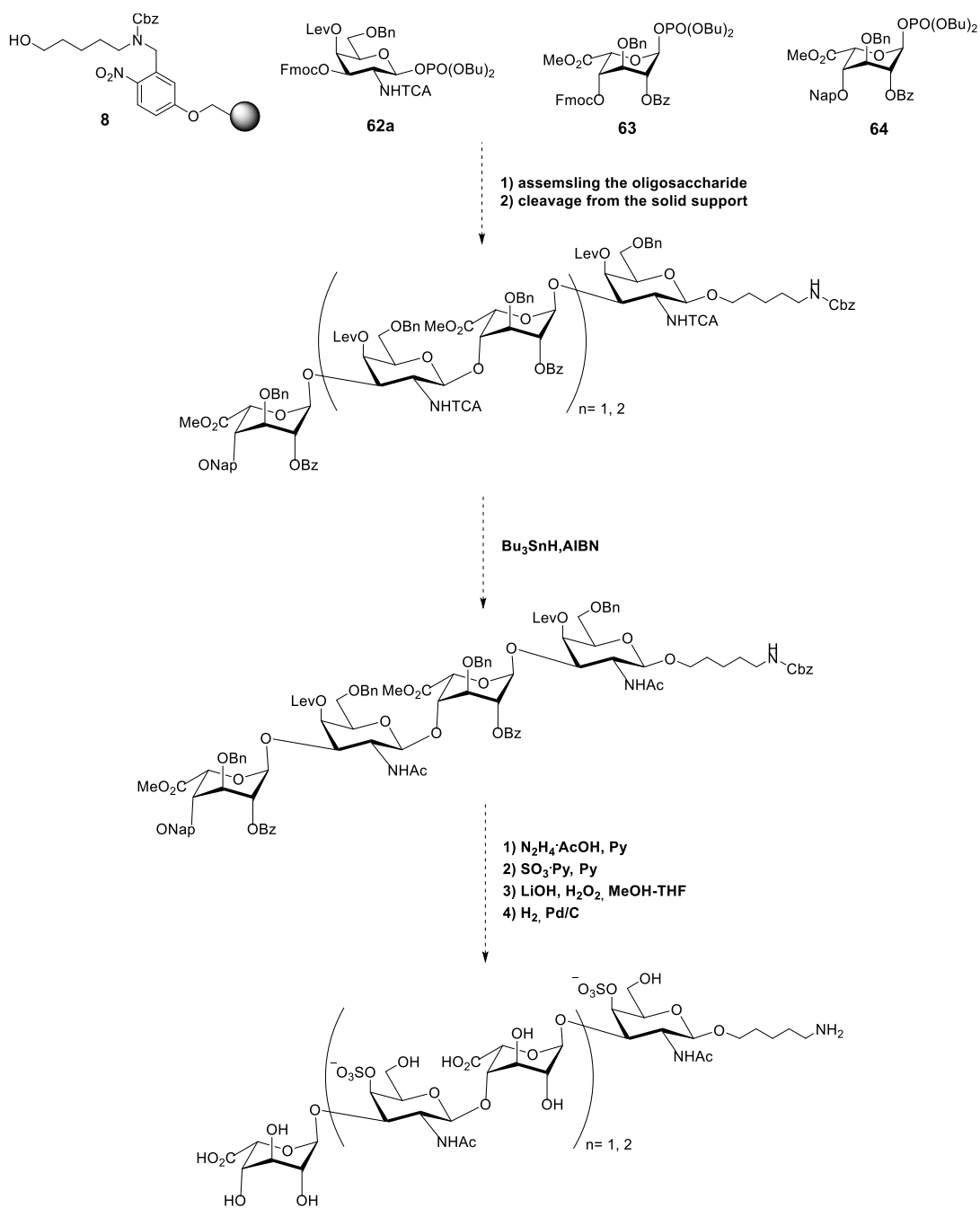
Iduronic acid building blocks have benzoyl ester as a neighboring participating group that ensures selective trans-glycoside formation. BB **64** will be the last to install in oligosaccharide chain, therefore its C-4 hydroxyl group should be protected in order to avoid the sulfation of this position. The protecting group has to be stable in the conditions of deprotection of levulinic and benzoyl esters and should be easily cleaved in hydrogenolysis process. Therefore, naphthyl ether was chosen as the protecting group for this position.

Two potential strategies for GAGs synthesis were considered (Scheme 38 and 39). The key synthetic step in both of them is radical reduction of trichloroacetyl protecting group by tributyltin hydride (Bu_3SnH) in the presence of azobisisobutyronitrile (AIBN). In the strategy I (Scheme 38) a sulfated glycan is assembled via AGA, and then subjected to reduction by Bu_3SnH and further global deprotection. The advantage of this strategy is the possibility to perform most of the synthetic steps in a glycan synthesizer.

Strategy II (Scheme 39) implies the assembly of a fully-protected oligosaccharide via AGA and further reduction of trichloroacetyl protecting groups by Bu_3SnH . Then, deprotection and sulfation steps could lead to target oligosaccharides, while all the reactions of sulfated compounds are performed in mild conditions.



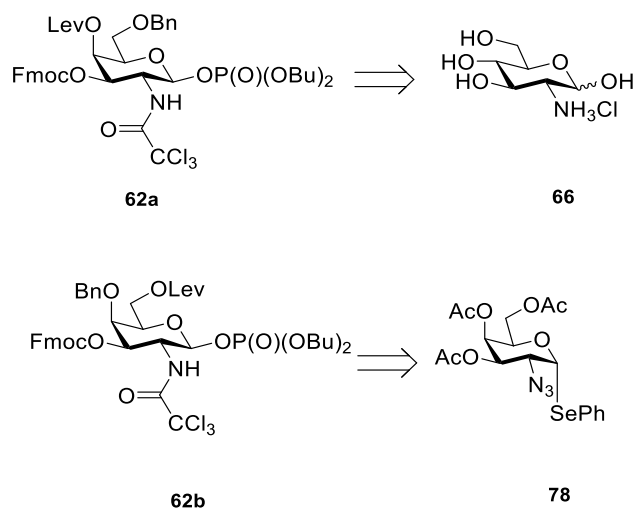
Scheme 38. Strategy I for the synthesis of dermatan sulfate.



Scheme 39. Strategy II for the synthesis of dermatan sulfate.

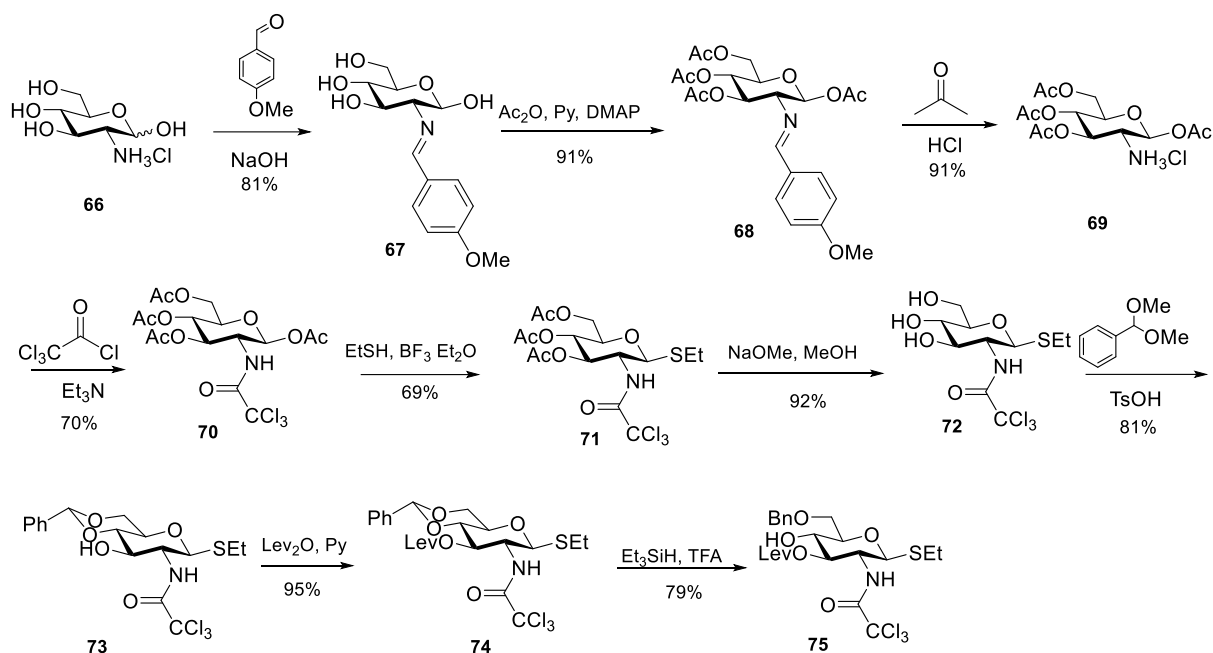
4.3 Synthesis of Building Blocks

4.3.1 Synthesis of galactosamine building blocks



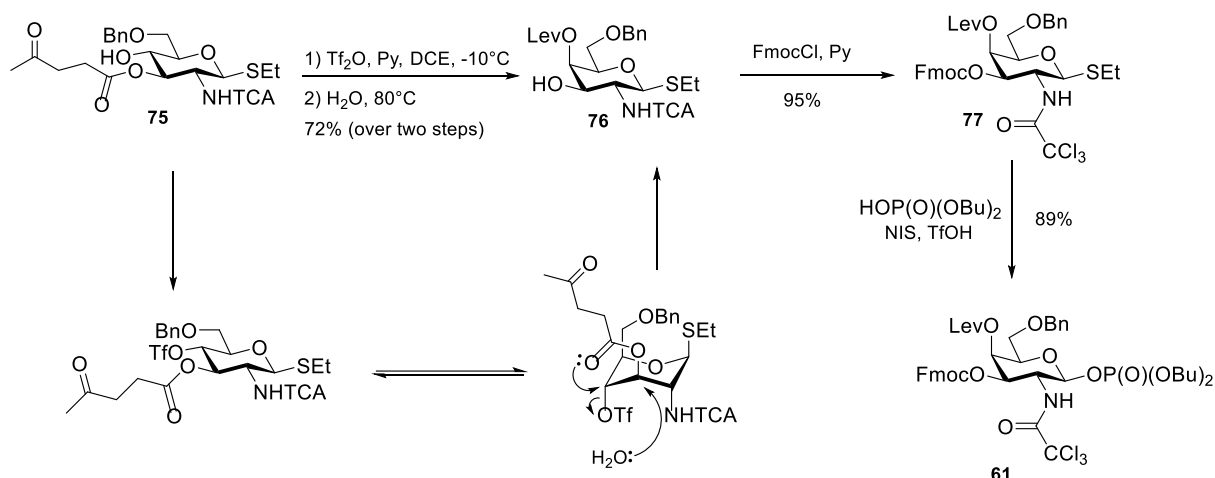
Scheme 40. Galactosamine BBs: retrosynthetic analysis.

Galactosamine building (**62a**) block was synthesized from glucosamine (Scheme 40) via an established protocol.¹⁴⁷ First, glucosamine **66** was coupled with *p*-methoxybenzaldehyde giving compound **67**. Then, after acetylation of all the hydroxyl groups and hydrolysis of the imine, the compound was subjected to acetylation by trichloroacetyl chloride, resulting in compound **70**. The reaction with ethylthiol produces compound **71**, basic hydrolysis of acetic groups results in compound **72**. Then, **72** reacted with benzaldehyde dimethyl acetal giving compound **73**. Interaction of **73** with levulinic acid anhydride enables to install levulinic ester protecting group on the position C3 of glucosamine. The further reduction of compound **74** by $\text{Et}_3\text{SiH/TFA}$ selectively yields compound **75**.



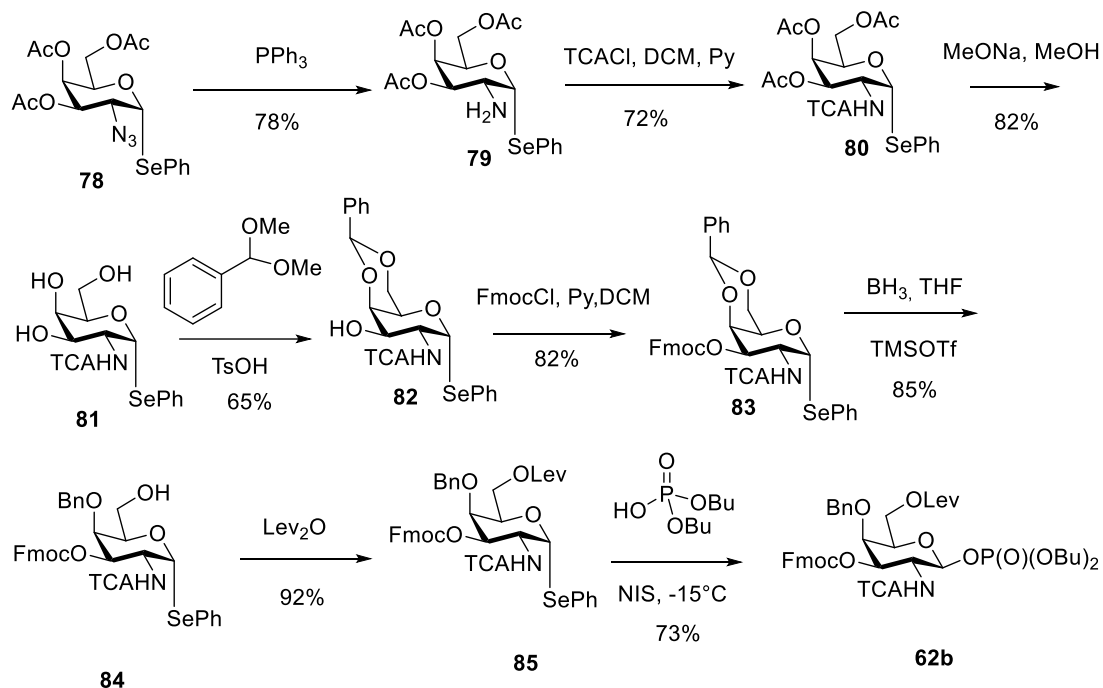
Scheme 41. Synthesis of glucosamine derivative **75**

The key step in the synthesis of galactosamine derivatives from glucosamine is the reaction of levulinic ester migration of from position C3 to C4, accompanied by the inversion of configuration of the C4 center. In this reaction compound **75** is firstly treated by $\text{Tf}_2\text{O}/\text{Py}$, giving the corresponding triflate. Treatment of **75** with water under conditions this triflate undergoes the reaction analogous to intramolecular nucleophilic substitution, resulting in galactosamine derivative **76**. In order to place a Fmoc-protecting group on the position C3, compound **76** was treated by FmocCl/Py . The further reaction with $(\text{HO})\text{P}(\text{O})(\text{OBu})_2$ results in building block **62a** in excellent yield.



Scheme 42. Synthesis of galactosamine BB **62a** from **75**. Mechanism of C-4 inversion.

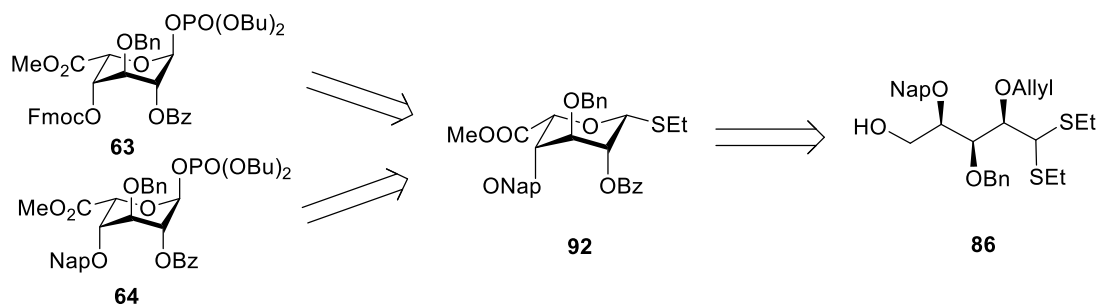
The other galactosamine building block **62b** was synthesized via a described protocol from galactose derivative **78**.⁹¹ Azide **78** was reduced by PPh₃, resulting in galactosamine derivative **79**, that was then treated by trichloroacetyl chloride giving **80**. Subsequent removal of acetyl protecting groups and reaction with benzaldehyde dimethyl acetal yielded **81**. Installation of a Fmoc-protecting group, selective opening of the benzylidene ring, followed by treatment with levulinic acid anhydride gave **85**, that was reacted with (HO)P(O)(OBu)₂ to give final building block **62**.



Scheme 43. Synthesis of galactosamine building block **62b**

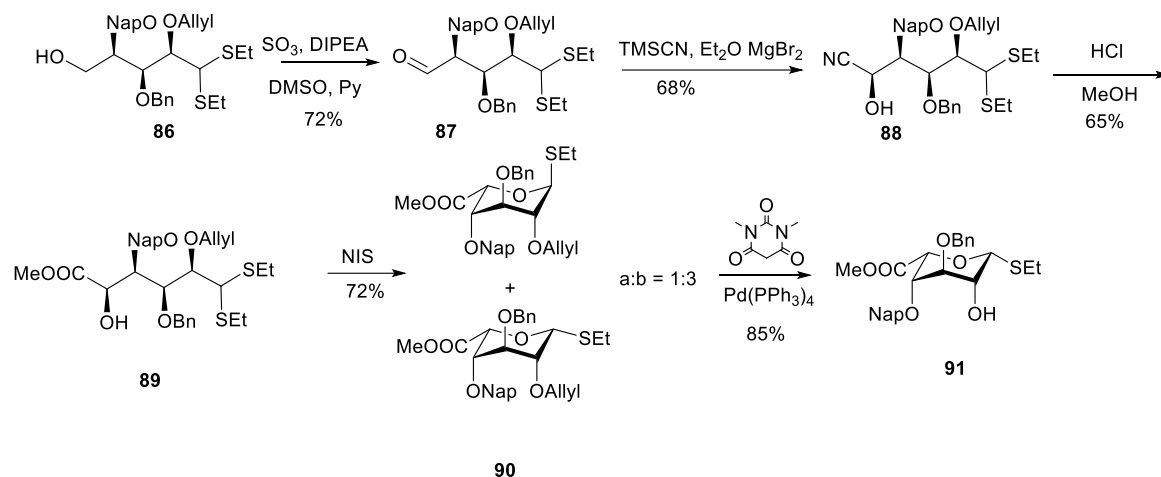
4.3.2 Synthesis of iduronic acid building blocks

The building blocks **63** and **64** could be synthesized from the protected D-xylose (**17**) (scheme 4).

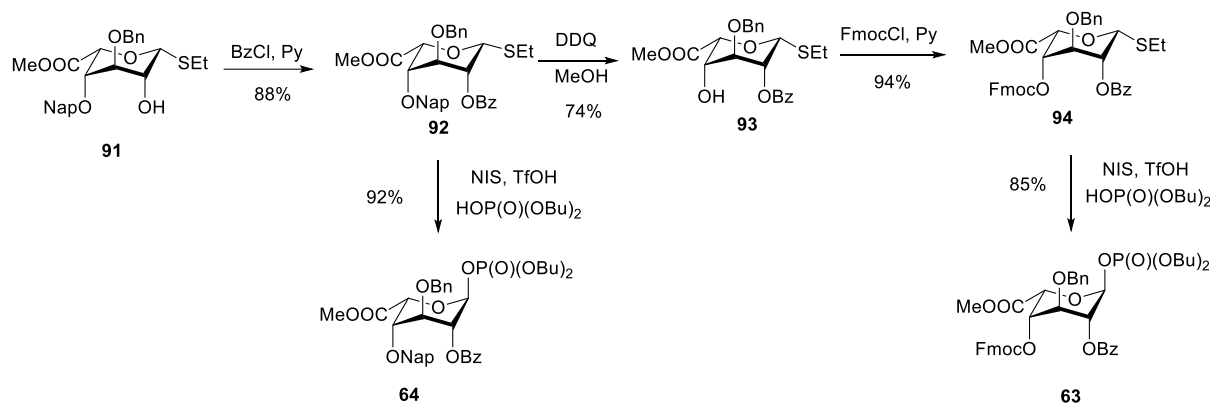


Scheme 44. Retrosynthetic analysis of iduronic acid building blocks

Compound **86^x** is oxidized, using Parikh-Doering oxidation conditions¹⁴⁹, giving aldehyde **87**. Further chelate-control diastereoselective cyanation of compound **87** results in compound **88** with a moderate yield. In this reaction, MgBr₂ is used as a chelating activator that furnishes only one diastereomer of **88**. Nitrile **88** was then treated by MeOH and anhydrous HCl that was generated directly in the reaction mixture from methanol and acetyl chloride. As a result of this reaction, ester **89** was obtained. The reaction of this compound with NIS results in the mixture of **90a** and **90b**.



Scheme 45. Synthesis of iduronic acid building blocks.



Scheme 46. Synthesis of iduronic acid building blocks

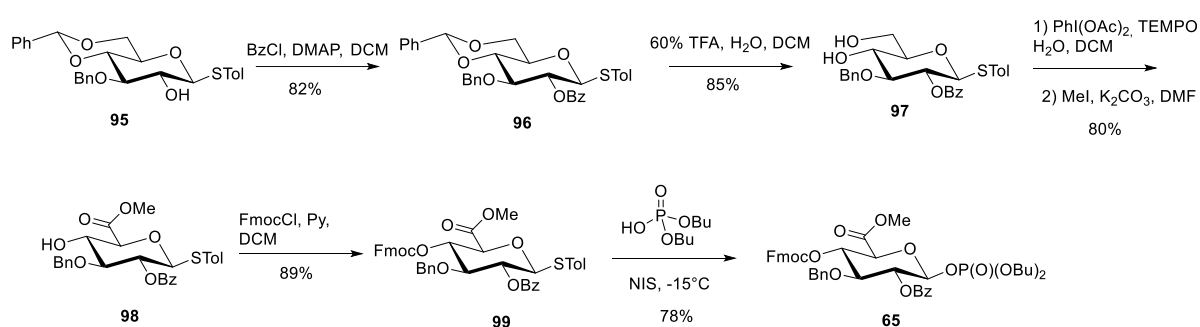
The reaction of **90** with a barbituric acid derivative and Pd(PPh₃)₄ enables the cleavage of the allyl group, and the subsequent treatment by BzCl/Py results in the placement of benzoyl protecting group on C2 position of iduronic acid, giving compound **92**. The reaction of this compound with (HO)P(O)(OBu)₂ furnishes building block **64** in good yield. Treatment of **92** with DDQ enables the selective deprotection of the naphtyl protecting group, giving

^x Compound **86** was provided by Dr. Kandasamy

compound **93**. The further reaction of **93** with FmocCl/Py and subsequent treatment with dibutyl phosphate gives building block **63** in good yield.

4.3.3 Synthesis of glucuronic acid building block

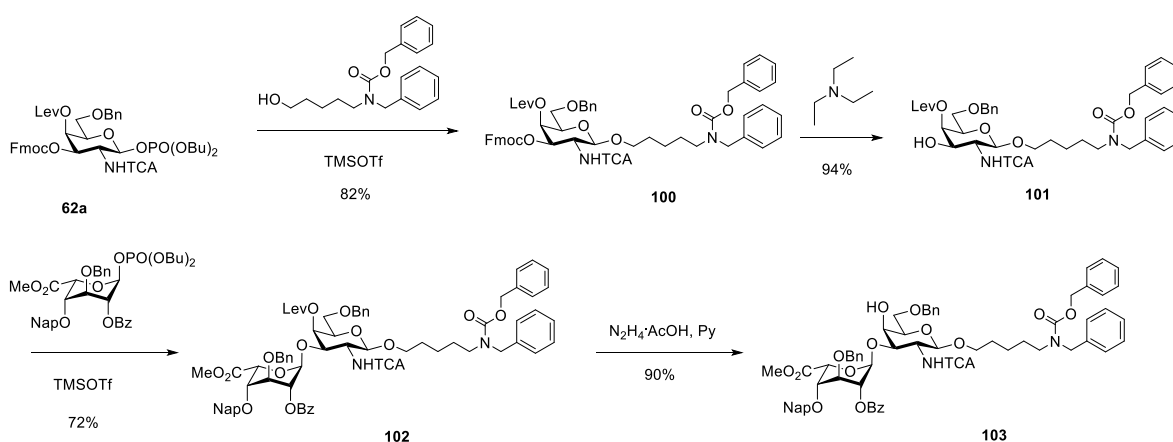
Glucuronic acid building block was synthesized from compound xx^{xi} using procedure, analogous to the one previously described.⁹¹ Benzoylation of C-2 hydroxide of compound **95**, followed by removing the benzylidene protecting group resulted in **97**. TEMPO-mediated oxidation of the C6 hydroxide and esterification of the resulting carboxylic acid gave **98**. Compound **98** was treated by FmocCl giving **99**, the reaction of which with dibutyl phosphate gave phosphate glycoside **65**.



Scheme 47. Synthesis of glucuronic acid building block **65**

4.4 Testing synthetic strategies to access dermatan sulfate

With the necessary building blocks in hand, testing of the synthetic strategies were tested. Initially, disaccharide **103** was synthesized in solution-phase (Scheme 48).

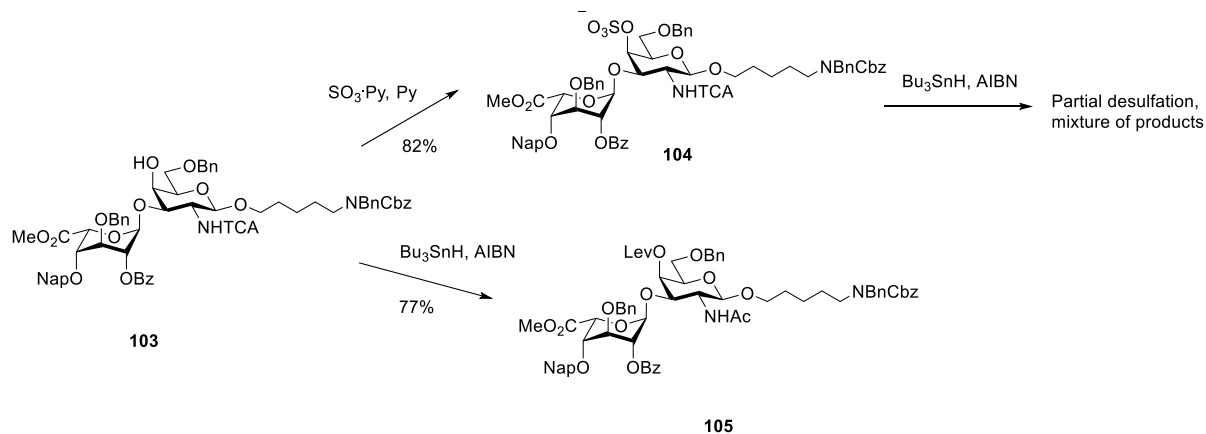


Scheme 48. Synthesis of disaccharide **103**

^{xi} Compound **95** was provided by Dr. Liang

In order to test the potential applicability Strategy I, disaccharide **103** was first sulfated by sulfur trioxide pyridine complex, giving compound **104**. Then, it was subjected to reduction by Bu_3SnH . This reaction led to the mixture of products: partial desulfation was observed. This means that sulfated oligosaccharides are not stable under radical conditions and this synthetic strategy cannot be applied for the synthesis of sulfated glycosaminoglycans.

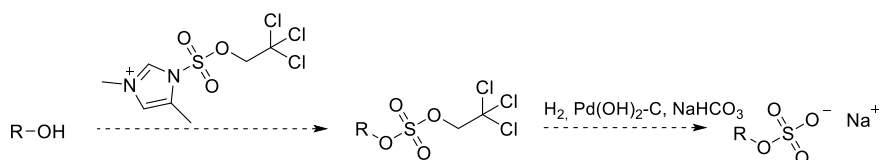
These findings led me to the investigation of synthetic strategy II. In this case, the reduction selectivity had to be tested. For this purpose, disaccharide **103** was subjected to reduction by Bu_3SnH that led selectively to formation of disaccharide **105**. Levulinic ester protecting group of this oligosaccharide can be further removed and this disaccharide can be sulfated. The global deprotection of the resulting molecule will not lead to the formation of HCl in the reaction mixture and, therefore, sulfate groups should stay intact.



Scheme 49. Investigation of synthetic strategies on dermatan sulfate disaccharide

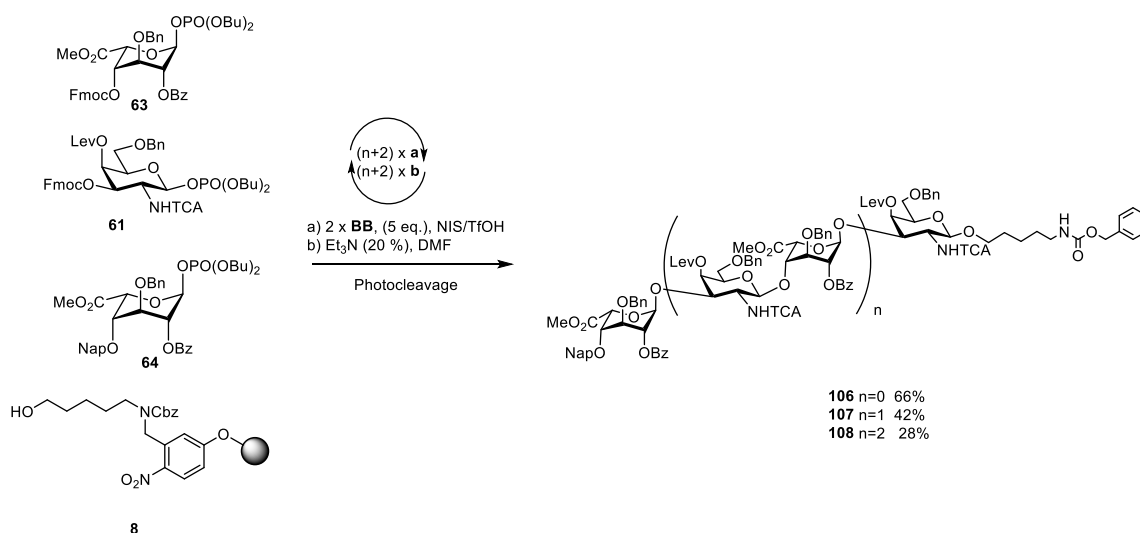
Strategy II, though, is not the best way for the synthesis of sulfated GAGs via AGA. In this strategy, sulfation has to take place after the reduction of the trichloroacetyl-protecting group. As long as this reaction requires very aggressive reagents (Bu_3SnH), it is not advisable to perform this step in the automated synthesizer. Also, the photocleavable linker may not be stable in the presence of active radicals, generated during the reduction reaction. All these considerations lead to the fact that most of the synthetic steps in this strategy have to be performed in via solution-phase synthesis.

Another potential strategy that can be explored is the usage 2,2,2-trichloroethyl sulfate for sulfation (Scheme 50).¹⁵⁰ In this case, the sulfate group is “protected” and therefore is more stable during the synthetic manipulations. Although, the conditions for sulfation in an automated synthesizer have to be firstly explored.



Scheme 50. Potential sulfation method

4.5 Automated synthesis of dermatan sulfate oligosaccharides



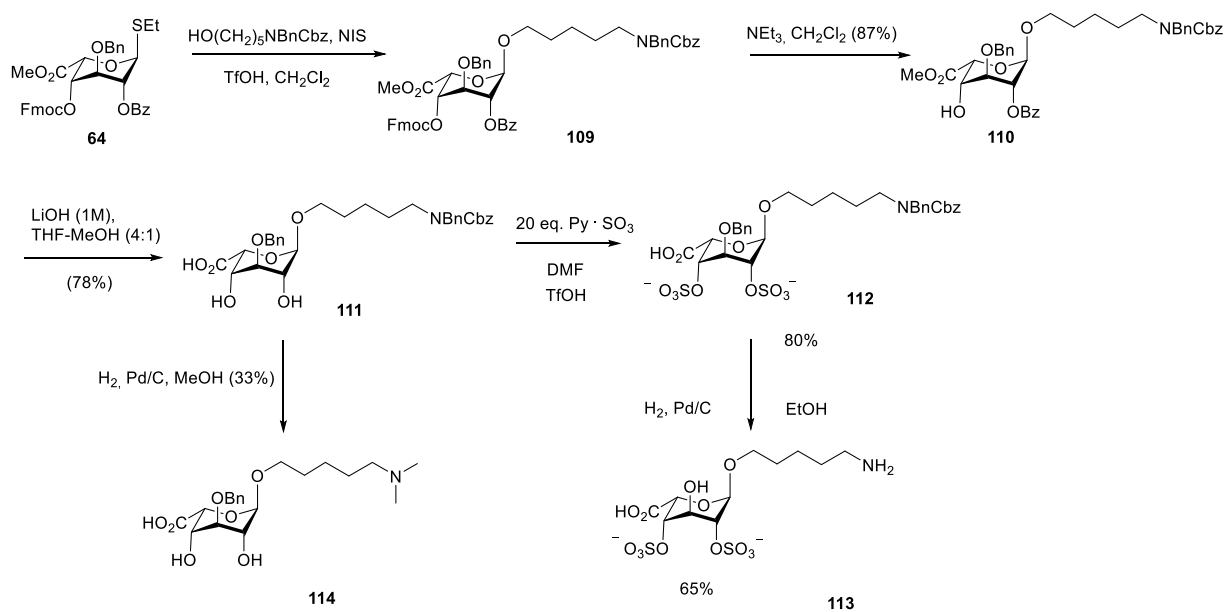
Scheme 51. AGA of dermatan sulfate oligosaccharides

Building blocks **61a**, **63** and **64** were utilized for the assembly of dermatan sulfate oligosaccharides via AGA (Scheme 51). TMSOTf solution (0.125 mM in DCM) was used as an activator and Et₃N (20% in DMF) was used for Fmoc-protecting group removal. Galactosamine and iduronic acid building blocks were assembled alternately, and building block **64** was installed at the end of the chain. Because of low reactivity of the iduronic acid building blocks, two glycosylation cycles (each one using 5 eq. of building block) were used for one elongation reaction. As a result, di-, tetra- and hexasaccharide of dermatan sulfate were obtained. These oligosaccharides can be used for further investigation of deprotection strategies.

4.6 Synthesis of disulfated iduronic acid

Identification of glycosaminoglycan sequences that determine the affinity to specific chemokines is a critical step for strategies to interfere with chemokine-mediated leukocyte trafficking. Disulfated iduronic acid derivative **113** was synthesized as a part of a heparin-like glycan library for investigation of the chemokine CCL20 binding profile.¹⁵¹

The synthesis of compound **113** was performed from iduronic acid building block **64** (Scheme 52). Building block **64** was coupled to C-5 linker, followed by Fmoc-deprotection. Further basic hydrolysis led to compound **111**, that was sulfated to give derivative **112**, before global deprotection resulted in target compound **113**. Non-sulfated iduronic acid derivative (**114**) was synthesized as a control compound.



Scheme 52. Synthesis of iduronic acid derivatives

Interestingly, the data from surface plasmon resonance (SPR) showed that CCL20 binds to immobilized Di-S-IdoA in the micromolar range ($K_D=2.9 \times 10^{-6}\text{M}$).^{xii} In Cultured F2 cells, that are known to express endogenous heparin sulfate, Di-S-IdoA also interfered with the CCL20–heparin sulfate interactions in a dose-dependent manner. These results suggest that Di-S-IdoA is an effective as a functional inhibitor of CCL20 chemokine activity. To study the specificity of Di-S-IdoA, the inhibitory effect of Di-S-IdoA on the bindings between the various proteins and endothelial cells was assayed. It is known that CCL21, IL-8, L-selectin and complement component 5a (C5a) are involved both in the binding to heparin/heparan sulfate in vitro and in the asthma pathogenesis. The result showed that Di-S-IdoA did not block the attachment of CCL21 to mouse endothelial F2 cells, whereas heparin efficiently blocked. Di-S-IdoA significantly blocked the binding of L-selectin to F2 cells. However, Di-S-IdoA showed even higher inhibitory effect than heparin in IL-8 binding. In

^{xii} All the biological studies were performed by the group of Prof. Minoru Fukuda

this experimental model, C5a did not show any bindings to F2 cells. Those results indicate Di-S-IdoA has unique binding preferences distinct from heparin.

4.7 Conclusions and perspectives

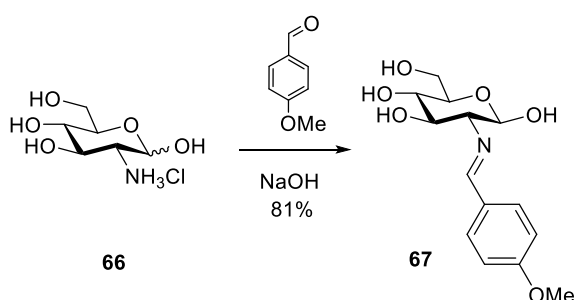
Building blocks required for the synthesis of chondroitin and dermatan sulfate oligosaccharides were prepared. Synthetic strategies for dermatan sulfate oligosaccharides were investigated. It was found that sulfated dermatan sulfate oligosaccharides are not stable in radical conditions. Several dermatan sulfate oligosaccharides were assembled via automated solid-phase synthesis.

The synthesis of disulfated iduronic acid that is a potential inhibitor of heparin sulfate-CCL20 interaction was optimized. Non-sulfated iduronic acid analogue was synthesized. In order to enable the access to fully-deprotected sulfated GAG oligosaccharides, new sulfation methods in automated synthesis have to be explored. Further biological investigations of disulfated iduronic acid have to be performed.

4.8 Experimental Part

4.8.1 Synthesis of galactosamine building blocks

Synthesis of 2-p-Methoxybenzylidenamino-D-glucopyranose 67

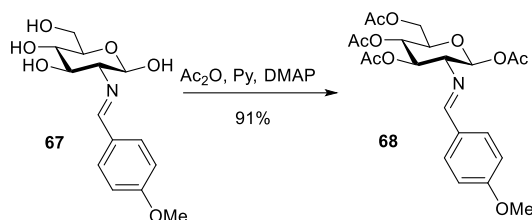


D-Glucosamine hydrochloride (50.0 g, 0.232 mol) was dissolved in 240 mL of 1 M aqueous sodium hydroxide, forming a colorless solution. Anisaldehyde (28.5 mL, 0.235 mol) was added using a syringe while stirring the mixture intensely, and a turbid solution formed. After several minutes of agitation, a white precipitate was formed. The system was kept in an ice bath for one hour to ensure complete precipitation. The solid was then collected by

filtration and washed with water (2 × 200 mL) and a 1:1 mixture of methanol and ether (2 × 200 mL).

Analytical data for **67** ¹H NMR (400 MHz, DMSO-d₆): δ = 8.09 (s, 1H), 7.67 (d, J = 9.6 Hz, 2H), 6.96 (d, J = 9.6 Hz, 2H), 6.53 (d, J = 6.8 Hz, 2H), 4.93 (d, J = 5.3 Hz, 1H), 4.82 (d, J = 5.6 Hz, 1H), 4.67 (t, J = 9.6 Hz, 1H), 4.55 (t, J = 9.6 Hz, 1H), 3.79 (s, 3H), 3.67-3.85 (m, 1H), 3.35-3.50 (m, 2H), 3.17-3.23 (m, 1H), 3.09-3.16 (m, 1H), 2.77 (t, J = Hz, 1H).

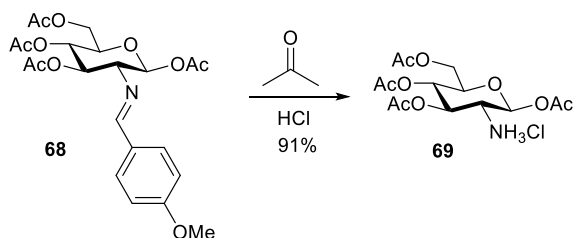
Synthesis of 2-*p*-Methoxybenzylidenamino-*D*-glucopyranose **68**



To the imide **67** (0.73 g) under cooling conditions (ice bath) acetic anhydride (2.84 mL), 5.2 mL of pyridine and 10 mg of DMAP were added. After 30 minutes, all the starting material was dissolved and the transparent solution formed. The mixture was stirred at 0 °C for 90 minutes in total. Then, the mixture was allowed to warm up to room temperature and stirred overnight. Then, the reaction mixture was poured out in the 25 mL of ice. The white precipitate formed. The precipitate was washed by water (4x10 mL), then by Et₂O (4x10 mL). The product was dried under vacuum.

Analytical data for **68** ¹H NMR (400 MHz, cdcl₃) δ 8.15 (s, 1H), 7.66 (d, J = 8.6 Hz, 2H), 7.24 (d, J = 19.8 Hz, 1H), 6.92 (d, J = 8.7 Hz, 2H), 5.96 (t, J = 14.1 Hz, 1H), 5.43 (t, J = 9.6 Hz, 1H), 5.14 (t, J = 9.8 Hz, 1H), 4.38 (dd, J = 12.4, 4.5 Hz, 1H), 4.13 (dd, J = 12.4, 1.9 Hz, 1H), 3.97 (ddd, J = 10.0, 4.4, 1.9 Hz, 1H), 3.82 (d, J = 19.8 Hz, 3H), 3.51 – 3.39 (m, 1H), 2.10 (s, 3H), 2.03 (d, J = 5.7 Hz, 5H), 1.88 (s, 3H).

Synthesis of 2-*p*-Methoxybenzylidenamino-*D*-glucopyranose **69**

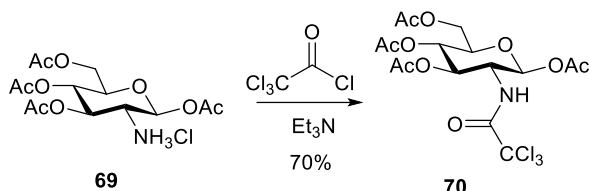


Compound **68** (9.7 g) was dissolved in refluxing acetone (50 mL). To the resulting solution, 4.9 mL 5N HCl was added dropwise. White precipitate was formed. The mixture

was cooled to the room temperature, the precipitate was filtered and washed with acetone (25 mL) and Et₂O (2x50 mL) giving compound **69**.

Analytical data for **69** ¹H NMR (400 MHz, dmsO) δ 8.65 (s, 3H), 5.86 (s, 1H), 5.32 (s, 1H), 4.92 (s, 1H), 4.16 (s, 1H), 4.04 (s, 1H), 3.96 (s, 1H), 3.55 (s, 1H), 2.15 (s, 3H), 2.01 (t, *J* = 3.9 Hz, 3H), 1.98 (s, 3H), 1.96 (d, *J* = 0.6 Hz, 3H).

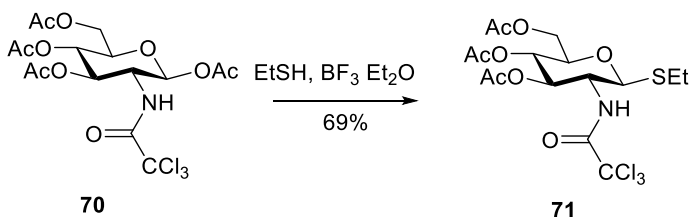
Synthesis of 2-*p*-Methoxybenzylidenamino-*D*-glucopyranose **70**



Compound **69** was dispersed in 50 mL of DCM, the mixture was cooled down to 0°C. Triethylamine (4.2 mL) and trichloroacetyl chloride (2.2 mL) was added to the mixture. The mixture was stirred for 2 hours. Then, the resulting solution was washed by water (3x25 mL), NaHCO₃ (3x25 mL), dried over Na₂SO₄ and concentrated in vacuum. The resulting solid was washed by hexane, giving the product.

Analytical data for **70** ¹H NMR (400 MHz, cdcl₃) δ 6.96 (s, 1H), 5.79 (s, 1H), 5.31 (s, 1H), 5.18 (s, 1H), 4.30 (dd, *J* = 5.4, 3.0 Hz, 1H), 4.27 (s, 1H), 4.16 (s, 1H), 3.87 (d, *J* = 2.1 Hz, 1H), 2.12 (d, *J* = 0.8 Hz, 3H), 2.11 (s, 3H), 2.07 (d, *J* = 0.8 Hz, 3H), 2.05 (s, 3H).

Synthesis of 2-*p*-Methoxybenzylidenamino-*D*-glucopyranose **71**

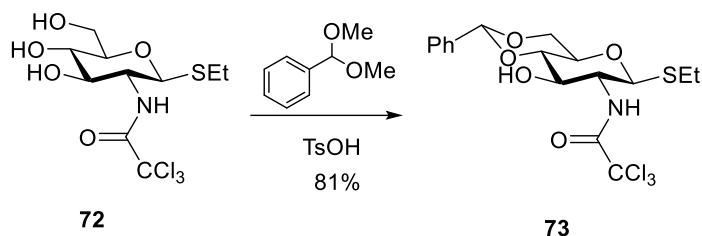


Compound **70** (15.4 g) was dissolved in DCM (Volume: 35 mL). To the resulting solution ethanethiol (2.31 mL) was added. The mixture was cooled to 0°C. Then BF₃·OEt₂ (1.12 mL) was added dropwise. The mixture was stirred at this temperature for 30 minutes. Then it was allowed to warm up to r.t. The mixture was left stirring overnight. Then the mixture was diluted by DCM to the volume of 70 mL, washed by NaHCO₃ (2x30mL), then by brine (2x30mL) and dried over Na₂SO₄. Volatile components were removed under the vacuum. Crude product was washed by hexane. Yield - 10.8 g (69%).

Analytical data for **71** ¹H NMR (400 MHz, cdcl₃) δ 6.75 (d, *J* = 9.2 Hz, 1H), 5.27 (q, *J* = 9.9 Hz, 1H), 5.13 (dd, *J* = 19.8, 10.1 Hz, 1H), 4.65 (t, *J* = 10.1 Hz, 1H), 4.26 (dd, *J* = 12.4,

5.0 Hz, 1H), 4.15 (dd, $J = 12.6, 2.4$ Hz, 1H), 4.09 (d, $J = 10.0$ Hz, 1H), 3.73 (ddd, $J = 10.0, 5.0, 2.1$ Hz, 1H), 2.81 – 2.66 (m, 2H), 2.11 – 2.07 (m, 3H), 2.05 (t, $J = 2.6$ Hz, 3H), 2.03 (d, $J = 0.5$ Hz, 3H), 1.60 (s, 1H), 1.32 – 1.23 (m, 3H).

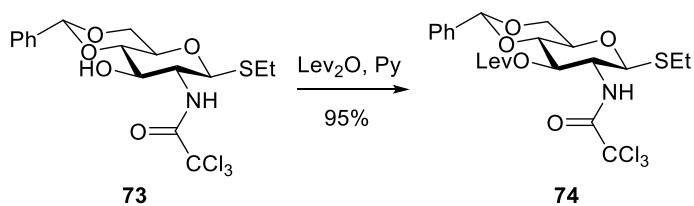
Synthesis of Ethyl 4,6-O-benzyliden-2-deoxy-2-N-trichloroacetamido-thio- β -D-glucopyranoside 73



Starting material was coevaporated with toluene, then was dried overnight under vacuum. Then, 1.3 g of it was dissolved in 17 mL of MeCN. Benzaldehyde dimethyl acetal (1.1 mL) was added. Then, 61 mg of TsOH was added. The mixture was stirred at r.t. for 24 hours (control of the reaction by MS). The mixture was neutralized by triethylamine (0.1 mL). After it, volatile products were removed under vacuum. The crude product was dissolved in DCM (20 mL), washed with brine (2x10 mL), dried over Na_2SO_4 . The volatiles were removed under the vacuum. Yield - 1.3g (81%)

Analytical data for **73** ^1H NMR (400 MHz, cdCl_3) δ 7.53 – 7.43 (m, 2H), 7.38 (dd, $J = 4.7, 2.4$ Hz, 2H), 6.88 (d, $J = 7.8$ Hz, 1H), 5.56 (s, 1H), 4.96 (dd, $J = 10.4, 2.2$ Hz, 1H), 4.41 – 4.31 (m, 1H), 4.24 (t, $J = 8.1$ Hz, 1H), 3.78 (dd, $J = 17.9, 9.6$ Hz, 1H), 3.73 – 3.65 (m, 1H), 3.62 – 3.50 (m, 2H), 2.80 – 2.68 (m, 2H), 1.57 (s, 2H), 1.29 (td, $J = 7.4, 2.5$ Hz, 3H).

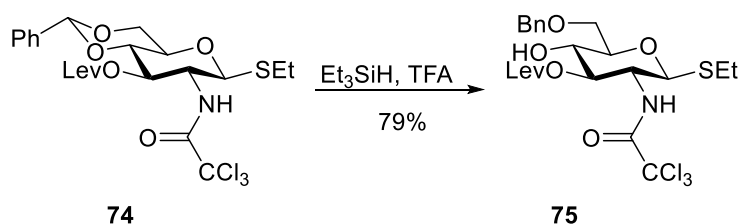
Synthesis of 4,6-O-benzyliden-3-O-levulinoyl-2-deoxy-2-N-trichloroacetamido-thio- β -D-glucopyranoside 74



Thioglycoside (8.0 g, 21.7 mmol) and levulinic anhydride (Lev_2O , 6.3 g, 29.6 mmol) were stirred in a mixture of dichloromethane (DCM) and pyridine (100 mL, 1:1) at room temperature and the progress was monitored by TLC. After completion (~ 18 h), the reaction mixture was diluted with DCM and washed with 0.1M HCl, saturated NaHCO_3 and brine. The organic layer was then dried over MgSO_4 , concentrated and subjected to flash column chromatography to obtain Lev-protected thioglycoside in 91% yield (8.84 g).

Analytical data for **74** ^1H NMR (400 MHz, cdCl_3) δ 7.48 (d, $J = 2.3$ Hz, 1H), 7.47 – 7.42 (m, 2H), 7.37 – 7.28 (m, 3H), 5.51 (dd, $J = 15.5, 5.7$ Hz, 1H), 5.49 (s, 1H), 4.54 (d, $J = 10.4$ Hz, 1H), 4.12 (dt, $J = 7.1, 6.2$ Hz, 1H), 4.00 (dd, $J = 10.0, 4.7$ Hz, 1H), 3.68 (t, $J = 9.4$ Hz, 1H), 3.62 (t, $J = 10.0$ Hz, 1H), 3.57 – 3.50 (m, 1H), 2.76 – 2.68 (m, 2H), 2.64 – 2.49 (m, 4H), 2.12 (s, 3H), 1.18 (t, $J = 7.4$ Hz, 3H).

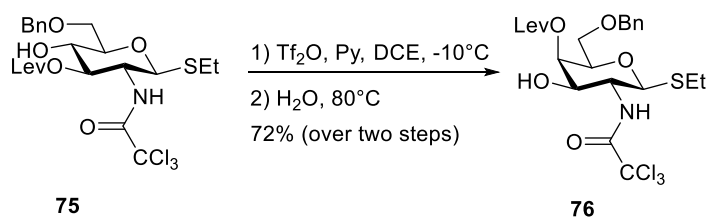
Synthesis of ethyl 6-O-benzyl-3-O-levulinoyl-2-deoxy-2-N-trichloroacetamido-thio- β -D-glucopyranoside 75



Thioglycoside **74** (8 g, 14.4 mmol), triethylsilane (9.21 mL, 57.7 mmol), and hot gun-dried 4 Å molecular sieves (powdered, 2.5 g) were stirred in anhydrous DCM (25 mL) for 30 minutes at room temperature and cooled down to 0°C. Trifluoroacetic acid (4.4 mL, 57.7 mL) was added dropwise and the reaction mixture was allowed to warm to room temperature. After complete conversion of the starting material the reaction mixture was neutralized with Et_3N and diluted with DCM. Molecular sieves were filtered off and the filtrate was washed with H_2O , saturated NaHCO_3 and brine. The organic layer was then dried over MgSO_4 , concentrated and subjected to flash column chromatography (Silica, Hexane/ EtOAc) to obtain thioglycoside **75** in 77% yield (6.2 g). The analytical data was in agreement with the literature data.

Analytical data for **75** ^1H NMR (400 MHz, cdCl_3) δ 7.00 – 6.95 (m, 1H), 5.22 (dd, $J = 10.4, 9.0$ Hz, 1H), 4.61 – 4.52 (m, 3H), 4.04 (td, $J = 10.3, 9.5$ Hz, 1H), 3.81 – 3.74 (m, 3H), 3.63 (dt, $J = 9.5, 4.3$ Hz, 1H), 3.31 (s, 1H), 2.79 – 2.64 (m, 4H), 2.62 – 2.52 (m, 1H), 2.52 – 2.43 (m, 1H), 2.15 (s, 3H), 1.24 (t, $J = 7.4$ Hz, 3H).

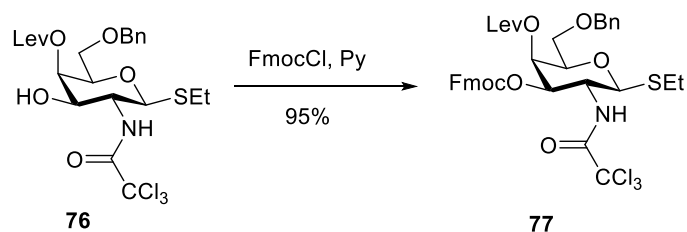
Synthesis of ethyl 6-O-benzyl-4-O-levulinoyl-2-deoxy-2-N-trichloroacetamido-thio- β -D-galactopyranoside 76



Thioglycoside **75** (5 g, 9.0 mmol) was stirred in a mixture of DCE and pyridine (30 mL, 10:1) at -15°C. Tf₂O (9.9 mL, 1M solution in DCM) was added dropwise to the reaction mixture and the progress was monitored by TLC. After complete conversion of the starting material, H₂O (4 mL) was added and the mixture was stirred at ~80°C for 5h. The reaction mixture was then cooled down to room temperature, diluted with DCM, and washed with 0.1M HCl, saturated NaHCO₃ and brine. The organic layer was dried over MgSO₄, concentrated and subjected to flash column chromatography to obtain title compound in 78% yield (3.9 g).

Analytical data for **76** ¹H NMR (400 MHz, cdcl₃) δ 7.32 (dt, *J* = 3.1, 1.5 Hz, 1H), 7.30 (d, *J* = 1.9 Hz, 2H), 7.28 (dd, *J* = 2.8, 1.3 Hz, 1H), 7.27 – 7.24 (m, 1H), 6.89 (d, *J* = 8.1 Hz, 1H), 5.46 (d, *J* = 2.7 Hz, 1H), 4.80 – 4.72 (m, 1H), 4.48 (q, *J* = 11.7 Hz, 2H), 4.10 – 4.03 (m, 1H), 3.84 (ddd, *J* = 12.7, 10.1, 7.8 Hz, 2H), 3.58 (dd, *J* = 9.8, 6.0 Hz, 1H), 3.50 (dd, *J* = 9.8, 6.5 Hz, 1H), 2.82 – 2.75 (m, 2H), 2.75 – 2.68 (m, 2H), 2.64 (ddd, *J* = 13.5, 8.3, 4.3 Hz, 1H), 2.60 – 2.53 (m, 2H), 2.18 (s, 3H), 1.26 (dd, *J* = 9.3, 5.6 Hz, 3H).

Synthesis of ethyl 6-O-benzyl-3-O-fluorenylmethoxycarbonyl-4-O-levulinoyl-2-deoxy-2-N-trichloroacetamido-thio-β-D-galactopyranoside 77

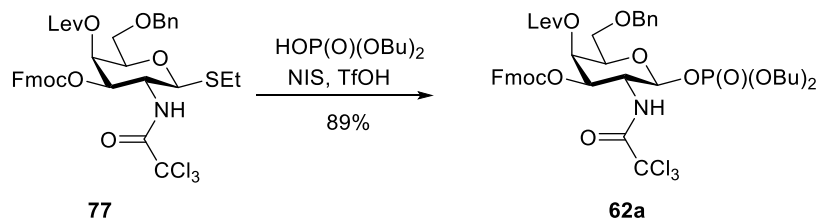


Thioglycoside **76** (3.9 g, 7.0 mmol) and FmocCl (3.6 g, 14.0 mmol) were stirred in DCM at 0°C and pyridine (2.5 mL) was added dropwise. After stirring for 4h at room temperature, the reaction mixture was concentrated and co-evaporated with toluene (twice) and subjected to S-5 flash column chromatography using Hexane/EtOAc to afford Fmoc-protected thioglycoside **77** in 93% yield (5.1 g).

Analytical data for **77** ¹H NMR (400 MHz, cdcl₃) δ 7.73 (d, *J* = 7.6 Hz, 2H), 7.55 (dd, *J* = 10.2, 3.6 Hz, 2H), 7.42 – 7.34 (m, 2H), 7.34 – 7.31 (m, 1H), 7.31 – 7.29 (m, 3H), 7.29 – 7.27 (m, 1H), 7.26 (dd, *J* = 4.2, 3.4 Hz, 1H), 6.78 (d, *J* = 8.7 Hz, 1H), 5.67 (d, *J* = 3.1 Hz, 1H), 5.19 (dd, *J* = 10.8, 3.3 Hz, 1H), 4.88 – 4.81 (m, 1H), 4.48 (d, *J* = 5.0 Hz, 2H), 4.43 (dd, *J* = 10.0, 6.8 Hz, 1H), 4.30 – 4.24 (m, 1H), 4.23 (d, *J* = 7.0 Hz, 1H), 4.21 – 4.12 (m, 1H), 3.95 –

3.87 (m, 1H), 3.61 (dt, $J = 10.2, 5.1$ Hz, 1H), 3.52 (dd, $J = 9.6, 6.9$ Hz, 1H), 2.82 – 2.58 (m, 6H), 2.13 (d, $J = 3.1$ Hz, 3H), 1.27 (t, $J = 7.4$ Hz, 3H).

Synthesis of di-*O*-butyl 6-*O*-benzyl-3-*O*-fluorenylmethoxycarbonyl-4-*O*-levulinoyl-2-deoxy-2-*N*-trichloroacetamido-thio- β -*D*-galactopyranosylphosphate 62a

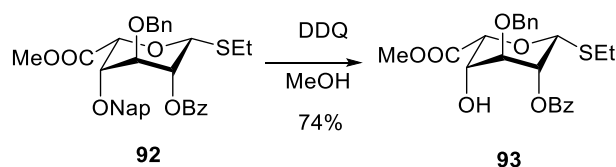


Fmoc-protected thioglycoside (5.0 g, 6.5 mmol), dibutyl hydrogen phosphate (6.5 mL, 32.7 mmol) and hot gun-dried 4 Å molecular sieves (3.0 g, powdered) were stirred in anhydrous DCM (15 mL) at room temperature. After for 30 minutes, N-iodosuccinimide (NIS, 1.76 g, 7.8 mmol) was added to the reaction mixture at once and cooled immediately to -5°C . After 3 minutes, a catalytic amount of TfOH (0.1 mL) was added and stirred for 1h at the same temperature. After complete conversion of the starting material the reaction mixture was neutralized with pyridine and diluted with DCM. Molecular sieves were filtered off and the filtrate was washed with saturated $\text{Na}_2\text{S}_2\text{O}_3$, NaHCO_3 and brine. The organic phase was dried over MgSO_4 , concentrated and subjected for flash column chromatography (Silica; Hexane/EtOAc), to obtain phosphoglycoside **62a** in 93% yield, 5.56 g.

Analytical data for **62a** ^1H NMR (400 MHz, cdCl_3) δ 7.74 (d, $J = 7.5$ Hz, 2H), 7.55 (dd, $J = 6.8, 5.9$ Hz, 2H), 7.38 (dd, $J = 10.7, 4.3$ Hz, 2H), 7.34 – 7.31 (m, 1H), 7.31 – 7.29 (m, 3H), 7.28 – 7.25 (m, 2H), 7.00 (d, $J = 9.1$ Hz, 1H), 5.81 (dt, $J = 14.1, 7.0$ Hz, 1H), 5.70 (d, $J = 3.0$ Hz, 1H), 5.17 (dd, $J = 11.3, 3.1$ Hz, 1H), 4.63 (ddt, $J = 12.1, 9.1, 3.1$ Hz, 1H), 4.48 (s, 2H), 4.46 – 4.42 (m, 1H), 4.42 – 4.37 (m, 1H), 4.27 (t, $J = 4.8$ Hz, 1H), 4.23 (dd, $J = 12.1, 5.4$ Hz, 1H), 4.10 – 3.98 (m, 4H), 3.56 (ddd, $J = 19.5, 9.7, 6.3$ Hz, 2H), 2.88 – 2.59 (m, 5H), 2.14 (s, 3H), 1.63 – 1.53 (m, 4H), 1.39 – 1.28 (m, 4H), 0.88 (td, $J = 7.4, 1.7$ Hz, 5H).

4.8.2 Synthesis of iduronic acid building blocks

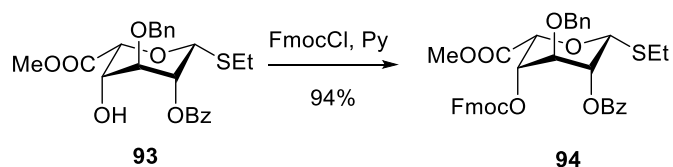
Synthesis of methyl(ethyl 2-*O*-benzoyl-3-*O*-benzyl-1-thio- α -*L*-idopyranosyl)urate 93



Thioglycoside **92** (5.5 g, 9.37 mmol) was stirred in a mixture of dichloromethane (DCM) and methanol (50 mL, 4:1) at room temperature and 2,3-dichloro-5,6-dicyano-1,4-benzoquinone (DDQ) (4.26 g, 18.75 mmol) was added at once and the progress was monitored by TLC. After completion (~ 8 h), the reaction mixture was diluted with DCM and washed with saturated NaHCO₃, and brine. The organic layer was then dried over MgSO₄, concentrated and subjected to flash column chromatography (Silica, Hexane/EtOAc) to obtain thioglycoside **93** in 88% yield (3.7 g).

Analytical data for **93**: ¹H NMR (400 MHz, cdcl₃) δ 8.15 – 8.08 (m, 2H), 7.75 – 7.61 (m, 2H), 7.49 – 7.38 (m, 4H), 7.34 – 7.25 (m, 2H), 5.43 (d, *J* = 2.2 Hz, 1H), 5.35 – 5.28 (m, 1H), 5.19 – 5.16 (m, 1H), 4.34 – 4.24 (m, 2H), 4.13 (dd, *J* = 14.2, 7.1 Hz, 1H), 4.04 – 3.99 (m, 1H), 3.77 (s, 3H), 2.82 – 2.64 (m, 2H), 1.38 – 1.29 (m, 3H).

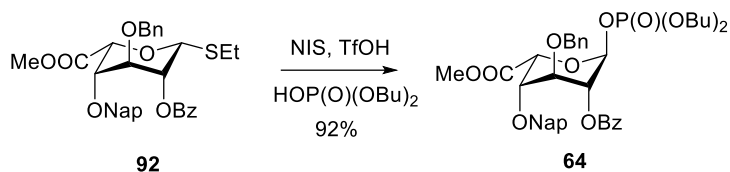
Synthesis of methyl(ethyl 2-O-benzoyl-3-O-benzyl-4-O-fluorenylmethoxycarbonyl-1-thio- α -L-idopyranosyl)urate **94**



Thioglycoside **93** (3.7 g, 8.30 mmol) and FmocCl (4.29 g, 16.6 mmol) were stirred in DCM (50 mL) at 0°C and pyridine (4 mL) was added dropwise. After stirring for 4h at room temperature, the reaction mixture was concentrated, co-evaporated with toluene (twice) and subjected to column chromatography (Silica, Hexane/EtOAc) to afford thioglycoside **94** in 94% yield (5.2 g).

Analytical data for **94**: ¹H NMR (400 MHz, cdcl₃) δ 8.16 – 8.11 (m, 2H), 7.74 (dd, *J* = 7.6, 0.7 Hz, 2H), 7.58 (dt, *J* = 7.7, 3.9 Hz, 1H), 7.46 – 7.43 (m, 2H), 7.43 – 7.38 (m, 3H), 7.38 – 7.34 (m, 3H), 7.34 – 7.30 (m, 1H), 7.28 (dt, *J* = 3.9, 1.5 Hz, 2H), 7.26 (dd, *J* = 3.5, 0.7 Hz, 1H), 7.22 – 7.17 (m, 1H), 5.59 (s, 1H), 5.39 (d, *J* = 2.0 Hz, 1H), 5.31 (dt, *J* = 2.5, 1.1 Hz, 1H), 5.18 – 5.14 (m, 1H), 4.85 (d, *J* = 11.8 Hz, 1H), 4.75 – 4.70 (m, 1H), 4.36 – 4.28 (m, 1H), 4.22 (dd, *J* = 10.3, 7.3 Hz, 1H), 4.09 (dd, *J* = 14.5, 6.9 Hz, 1H), 4.00 (td, *J* = 2.9, 1.1 Hz, 1H), 3.79 (s, 3H), 2.80 – 2.62 (m, 2H), 1.35 – 1.28 (m, 3H).

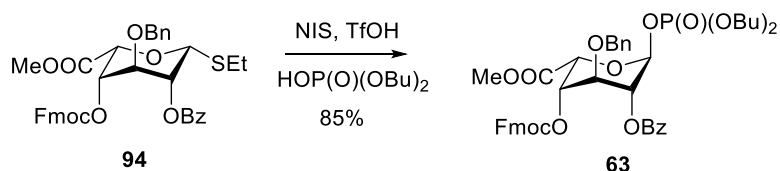
Synthesis of methyl 2-O-benzoyl-3-O-benzyl-4-O-fluorenylmethoxycarbonyl-1-di-O-butylphosphatidyl- α -L-idopyranosyluronate **64**



Thioglycoside **92** (4.32 g, 7.82 mmol), dibutyl hydrogen phosphate (7.03 mL, 35.5 mmol), and hot gun-dried 4 Å molecular sieves (powdered, 3.2 g) were stirred in anhydrous DCM (15 mL) at room temperature. After 30 minutes, NIS (2.1 g, 9.36 mmol) was added to the reaction mixture at once and immediately cooled to -5°C. After 3 minutes, a catalytic amount of TfOH (0.1 mL) was added to the reaction and stirred for 1h at the same temperature and monitored by TLC. After complete conversion of the starting material the reaction mixture was neutralized with pyridine and diluted with DCM. Molecular sieves were filtered off and the filtrate was washed with saturated Na₂S₂O₃, NaHCO₃, and brine. The organic phase was dried over MgSO₄, concentrated and subjected for column chromatography (Silica; Hexane/Ethyl acetate) to obtain phosphoglycoside **64** in 92% yield (4.88 g).

Analytical data for **64**: ¹H NMR (400 MHz, cdcl₃) δ 8.15 – 8.09 (m, 2H), 7.74 (d, *J* = 7.6 Hz, 2H), 7.56 (d, *J* = 7.5 Hz, 1H), 7.50 – 7.44 (m, 1H), 7.43 – 7.39 (m, 3H), 7.38 (s, 2H), 7.36 – 7.30 (m, 4H), 7.28 (dd, *J* = 9.8, 2.3 Hz, 2H), 7.19 (td, *J* = 7.5, 1.0 Hz, 1H), 5.95 (d, *J* = 6.8 Hz, 1H), 5.33 (d, *J* = 1.1 Hz, 1H), 5.25 – 5.19 (m, 1H), 5.16 (d, *J* = 1.9 Hz, 1H), 4.86 (d, *J* = 11.6 Hz, 1H), 4.77 (d, *J* = 11.6 Hz, 1H), 4.31 (dd, *J* = 10.3, 8.0 Hz, 1H), 4.22 – 4.14 (m, 1H), 4.13 – 3.99 (m, 6H), 3.81 (d, *J* = 5.5 Hz, 3H), 1.68 – 1.56 (m, 4H), 1.44 – 1.29 (m, 4H), 0.89 (tt, *J* = 4.8, 3.9 Hz, 6H).

Synthesis of methyl 2-O-benzoyl-3-O-benzyl-4-O-(2-naphthyl)methyl-1-di-O-butylphosphatidyl- α -L-idopyranosyluronate **63**



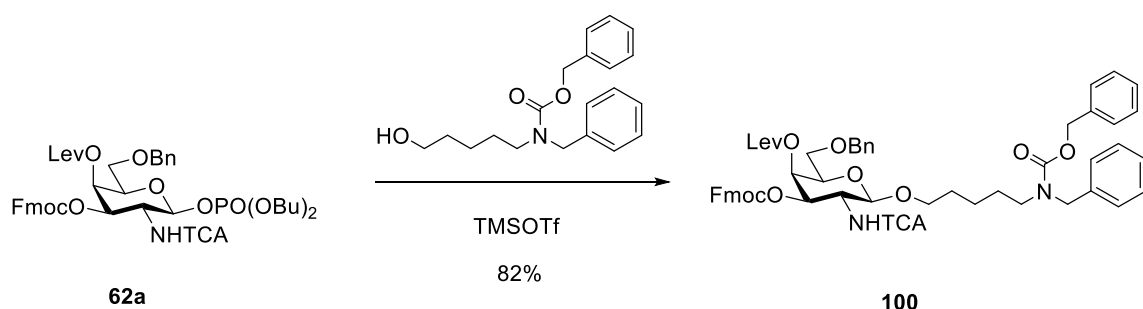
Thioglycoside **94** (5.30 g, 8.44 mmol), dibutyl hydrogen phosphate (8.38 mL, 42.3 mmol), and hot gun-dried 4 Å molecular sieves (powdered, 3.5 g) were stirred in anhydrous DCM (15 mL) at room temperature. After 30 minutes, NIS (2.27 g, 10.1 mmol) was added to the reaction mixture at once and immediately cooled to -5°C. After 3 minutes, a catalytic

amount of TfOH (0.1 mL) was added to the reaction and stirred for 1h at the same temperature and monitored by TLC. After complete conversion of the starting material the reaction mixture was neutralized with pyridine and diluted with DCM. Molecular sieves were filtered off and the filtrate was washed with saturated Na₂S₂O₃, NaHCO₃, and brine. The organic phase was dried over MgSO₄, concentrated and subjected for column chromatography (Silica; Hexane/Ethyl acetate) to obtain phosphoglycoside **63**. Yield 85% (5.45 g).

Analytical data for **63**: ¹H NMR (400 MHz, cdcl₃) δ 7.98 – 7.93 (m, 2H), 7.79 – 7.74 (m, 1H), 7.67 – 7.62 (m, 2H), 7.51 (s, 1H), 7.44 (dt, *J* = 5.6, 2.0 Hz, 2H), 7.42 – 7.39 (m, 1H), 7.31 (dd, *J* = 3.5, 2.3 Hz, 1H), 7.29 – 7.23 (m, 2H), 7.22 – 7.14 (m, 3H), 5.94 (d, *J* = 6.8 Hz, 1H), 5.28 (t, *J* = 2.8 Hz, 1H), 5.00 (d, *J* = 2.1 Hz, 1H), 4.79 (d, *J* = 11.7 Hz, 1H), 4.62 (d, *J* = 11.8 Hz, 1H), 4.60 – 4.50 (m, 2H), 4.09 – 4.02 (m, 2H), 4.02 – 3.94 (m, 4H), 3.74 (s, 3H), 1.63 – 1.51 (m, 4H), 1.40 – 1.23 (m, 4H), 0.88 (t, *J* = 5.8 Hz, 3H), 0.85 (t, *J* = 5.8 Hz, 3H).

4.8.3 Synthetic strategies for dermatan sulfate

Synthesis of compound 110

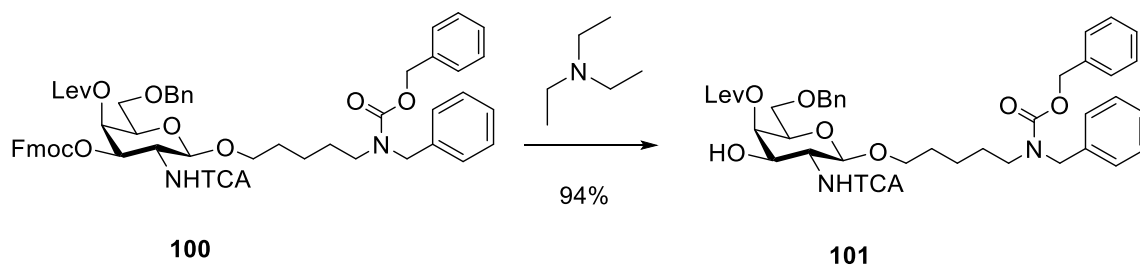


Phosphate **62a** (1.35 g, 1.8 mmol) and linker (0.66 g, 2.0 mmol) were dissolved in anhydrous DCM (15 mL) the solution was cooled to -10°C before TMSOTf (0.36 mL, 2.0 mmol) was added to the reaction mixture. The reaction mixture was allowed to warm up to 0°C. After stirring for 1 hour, the reaction mixture was neutralized with pyridine and diluted with DCM, washed with saturated NaHCO₃, and brine. The organic phase was dried over MgSO₄, concentrated and subjected for column chromatography (Silica; Hexane/Ethyl acetate) to obtain compound **100** (1.49 g, 82% yield).

Analytical data for **100**: ¹H NMR (400 MHz, cdcl₃) 7.73 (d, *J* = 7.4 Hz, 2H), 7.58 – 7.53 (m, 4H), 7.41 – 7.24 (m, 12H), 7.03 (d, *J* = 8.9 Hz, 1H), 5.36 (d, *J* = 3.1 Hz, 1H), 5.12 (s, 2H), 4.90 – 4.79 (m, 4H), 4.50 (d, *J* = 5.2 Hz, 2H), 4.43 – 4.39 (m, 1H), 4.31 – 4.27 (m, 1H),

4.25 (d, $J = 7.2$ Hz, 1H), 4.18 – 4.10 (m, 1H), 3.93 – 3.87 (m, 1H), 3.70 – 3.62 (m, 1H), 3.55 – 3.51 (m, 1H), 2.84 – 2.63 (m, 6H), 2.15 – 2.10 (m, 3H), 1.29 (t, $J = 7.2$ Hz, 3H).

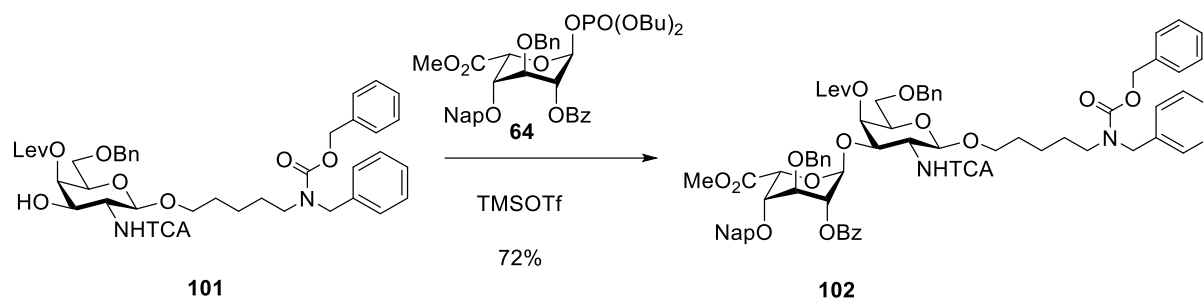
Synthesis of compound 101



Compound **100** (1.49 g, 1.63 mmol) was dissolved in anhydrous DCM (20 mL) the solution was cooled to 0°C before NEt₃ (1.1 mL, 8.2 mmol) was added to the reaction mixture. The reaction mixture was warmed up to room temperature. After stirring for 4 hours, the reaction mixture was washed with 1M HCl and brine. The organic phase was dried over MgSO₄, concentrated and subjected for column chromatography (Silica; Hexane/Ethyl acetate) to give **101**. Yield 94% (1.05 g).

Analytical data for **101**: ¹H NMR (400 MHz, cdcl₃) ¹H NMR (400 MHz, cdcl₃) 7.55 – 7.50 (m, 2H), 7.43 – 7.26 (m, 8H), 7.06 (d, $J = 9.1$ Hz, 1H), 5.34 (d, $J = 3.2$ Hz, 1H), 5.10 (s, 2H), 4.93 – 4.80 (m, 4H), 4.55 (d, $J = 5.4$ Hz, 2H), 4.41 – 4.38 (m, 1H), 4.30 – 4.24 (m, 2H), 4.16 – 4.10 (m, 1H), 3.95 – 3.88 (m, 1H), 3.71 – 3.65 (m, 1H), 3.56 – 3.53 (m, 1H), 2.88 – 2.66 (m, 6H), 2.17 – 2.10 (m, 3H), 1.33 – 1.26 (m, 3H).

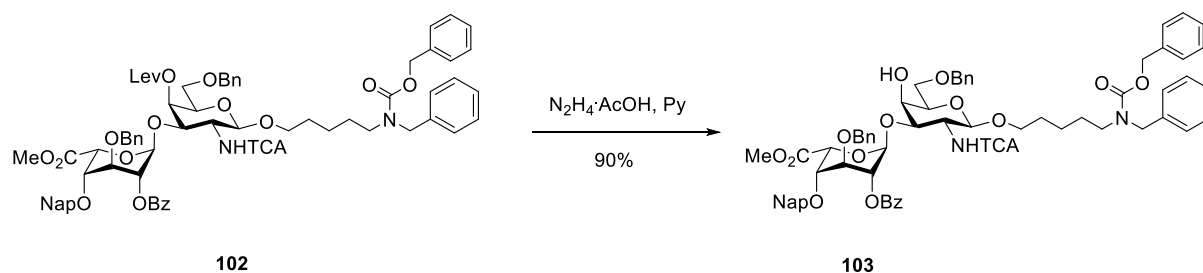
Synthesis of compound 102



Compound **101** (1.05 g, 1.54 mmol) and building block **64** (1.10 mg, 1.62 mmol) were dissolved in anhydrous DCM (30 mL) the solution was cooled to -10°C before TMSOTf (0.32 mL) was added to the reaction mixture. After stirring for 1 hour, the reaction mixture was neutralized with pyridine and diluted with DCM, washed with saturated NaHCO_3 , and brine. The organic phase was dried over MgSO_4 , concentrated and subjected for column chromatography (Silica; Hexane/Ethyl acetate) to obtain **102**. Yield 72% (1.30 g).

Analytical data for **102**: ^1H NMR (400 MHz, cdCl_3) 8.12 – 8.06 (m, 2H), 7.78 – 7.70 (m, 2H), 7.57 (d, $J = 7.8$ Hz, 1H), 7.52 – 7.43 (m, 3H), 7.41 – 7.22 (m, 19H), 7.17 – 7.10 (m, 2H), 5.97 (d, $J = 6.6$ Hz, 1H), 5.38 (d, $J = 3.0$ Hz, 1H), 5.31 (d, $J = 1.3$ Hz, 1H), 5.28 – 5.22 (m, 1H), 5.12 (d, $J = 1.7$ Hz, 1H), 5.02 (s, 2H), 4.96 – 4.84 (m, 5H), 4.75 (d, $J = 11.0$ Hz, 1H), 4.58 (d, $J = 5.6$ Hz, 2H), 4.43 – 4.39 (m, 1H), 4.33 – 4.25 (m, 3H), 4.22 – 4.10 (m, 2H), 4.10 – 3.97 (m, 2H), 3.97 – 3.90 (m, 1H), 3.83 (s, 3H), 3.73 – 3.68 (m, 1H), 3.55 – 3.52 (m, 1H), 2.88 – 2.70 (m, 6H), 2.15 – 2.10 (m, 3H), 1.35 – 1.25 (m, 3H).

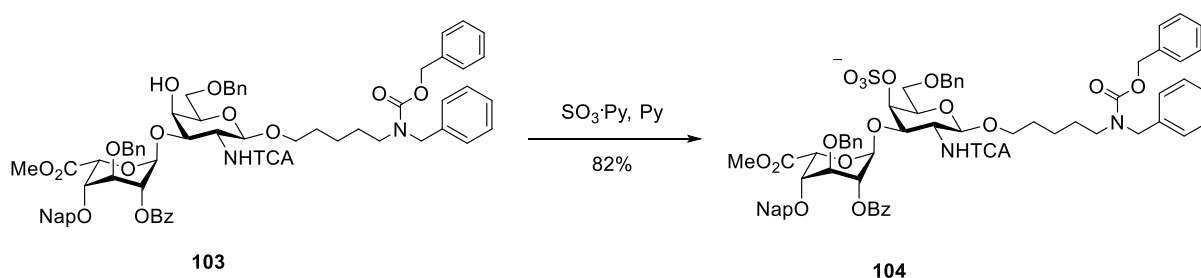
Synthesis of compound 103



To a solution of **102** (0.61 g, 0.52 mmol) in pyridine (15 mL) a 1M solution of hydrazine hydrate (10 μL) in pyridine/acetic acid (3:2) was added at 0°C . The reaction was allowed to warm up to room temperature and stirred for 5 hours. Then, 5 mL of acetone was added, all the volatiles were removed under vacuum. The residue was diluted with DCM, washed with NaHCO_3 , brine, dried over MgSO_4 , concentrated and subjected for column chromatography (Silica; Hexane/Ethyl acetate) to give **103**. Yield 90% (0.50 g).

Analytical data for **103**: ^1H NMR (400 MHz, cdCl_3) 8.14 – 8.07 (m, 2H), 7.80 – 7.70 (m, 2H), 7.55 – 7.41 (m, 4H), 7.39 – 7.19 (m, 21H), 5.94 (d, $J = 6.0$ Hz, 1H), 5.34 (d, $J = 3.2$ Hz, 1H), 5.31 (d, $J = 1.5$ Hz, 1H), 5.27 – 5.21 (m, 1H), 5.15 (d, $J = 2.0$ Hz, 1H), 5.00 (s, 2H), 4.94 – 4.80 (m, 5H), 4.73 (d, $J = 11.4$ Hz, 1H), 4.56 (d, $J = 5.8$ Hz, 2H), 4.42 – 4.37 (m, 1H), 4.35 – 4.25 (m, 3H), 4.22 – 4.00 (m, 4H), 3.95 – 3.90 (m, 1H), 3.80 (s, 3H), 3.75 – 3.69 (m, 1H), 3.58 – 3.54 (m, 1H), 2.88 – 2.78 (m, 2H), 1.35 – 1.27 (m, 3H).

Synthesis of compound 104



To a solution of **103** (25.0 mg, 0.023 mmol) in anhydrous pyridine (5.0 mL), was added $\text{SO}_3\cdot\text{pyridine}$ (0.12 g). The reaction mixture was stirred at RT for 24 h, quenched by the addition of MeOH (1.5 mL) and triethylamine (0.2 mL), and concentrated. The residue was purified by a Sephadex LH-20 chromatography (MeOH– CH_2Cl_2 , 1:1, vol/vol). The obtained product was converted into the Na salt by passing through a column of Dowex 50WX8 (Na^+) in MeOH– H_2O (9:1, vol/vol) to give **104** (22 mg, 82%).

Analytical data for **104**: ^1H NMR (400 MHz, cdCl_3) 8.13 – 8.07 (m, 2H), 7.82 – 7.71 (m, 2H), 7.56 – 7.42 (m, 4H), 7.40 – 7.19 (m, 21H), 5.97 – 5.92 (dm, 1H), 5.37 (d, $J = 3.1$ Hz, 1H), 5.30 (d, $J = 1.3$ Hz, 1H), 5.27 – 5.19 (m, 2H), 5.14 (d, $J = 1.8$ Hz, 1H), 5.03 (s, 2H), 4.945 – 4.85 (m, 4H), 4.74 (d, $J = 11.2$ Hz, 1H), 4.54 (d, $J = 5.6$ Hz, 2H), 4.44 – 4.38 (m, 1H), 4.36 – 4.22 (m, 4H), 4.19 – 4.05 (m, 3H), 3.97 – 3.91 (m, 1H), 3.82 (s, 3H), 3.77 – 3.72 (m, 1H), 3.60 – 3.54 (m, 1H), 2.86 – 2.779 (m, 2H), 1.36 – 1.27 (m, 3H).

4.8.4 Automated synthesis of dermatan sulfate oligosaccharides

4.8.4.1 General materials and methods

All solvents used were HPLC-grade. The solvents used for the building block, activator, TMSOTf and capping solutions were taken from an anhydrous solvent system (jcmeyer-solvent systems). The building blocks were co-evaporated three times with chloroform and dried for 1 h on high vacuum before use. Activator, deprotection, acidic wash and building block solutions were freshly prepared and kept under argon during the automation run. All yields of products obtained by AGA were calculated on the basis of resin loading. Resin loading was determined by **Method 2** (described in Chapter 2).

4.8.4.2 Preparation of stock solutions

- **Building Block:** 0.0625 mmol of building block was dissolved in 1 mL of DCM.
- **Fmoc deprotection solution:** A solution of 20% Et₃N in DMF (v/v) was prepared.
- **TMSOTf Solution:** TMSOTf (0.45 mL) was added to DCM (40 mL).

4.8.4.3 Modules for automated synthesis

Module A: Resin Preparation for Synthesis (20 min)

All automated syntheses were performed on 0.0125 mmol scale. Resin was placed in the reaction vessel and swollen in DCM for 20 min at room temperature prior to synthesis. During this time, all reagent lines needed for the synthesis were washed and primed. Before the first glycosylation, the resin was washed with the DMF, THF, and DCM (three times each with 2 mL for 25 s).

Module B: Acidic Wash with TMSOTf Solution (20 min)

The resin was swollen in 2 mL DCM and the temperature of the reaction vessel was adjusted to -20°C. Upon reaching the low temperature, TMSOTf solution (1 mL) was added drop wise to the reaction vessel. After bubbling for 3 min, the acidic solution was drained and the resin was washed with 2 mL DCM for 25 s.

Action	Cycles	Solution	Amount	T (°C)	Incubation time
Cooling	-	-	-	-20	(15 min)
Deliver	1	DCM	2 mL	-20	-
Deliver	1	TMSOTf solution	1 mL	-20	3 min

Wash	1	DCM	2 mL	-20	25 s
------	---	-----	------	-----	------

Module C: Phosphate Glycosylation (35 min)

The building block solution (0.0625 mmol of BB in 1 mL of DCM per glycosylation) was delivered to the reaction vessel. After the set temperature was reached, the reaction was started by drop wise addition of the activator solution (1.0 mL, excess). The glycosylation conditions are building block dependent (we report the most common set of conditions). After completion of the reaction, the solution is drained and the resin was washed with DCM (three times, each with 2 mL for 25 s). The procedure is repeated twice. Afterwards the temperature of the reaction vessel is increased to 25 °C for the next module.

Action	Cycles	Solution	Amount	T (°C)	Incubation time
Cooling	-	-	-	-20	-
Deliver	1	BB solution	1 mL	-20	-
Deliver	1	Activator solution	1 mL	-20	-
Reaction time	1			-20 to 0	5 min 20 min
Wash	3	DCM	2 mL	0	5 s
Heating	-	-	-	25	-
Wash	2	DCM	2 mL	> 0	25 s

Module D: Fmoc Deprotection (14 min)

The resin was washed with DMF (three times with 2 mL for 25 s) and the temperature of the reaction vessel was adjusted to 25 °C. 2 mL of Fmoc deprotection solution was delivered into the reaction vessel. After 15 min, the reaction solution was drained and the resin washed with DMF (three times with 3 mL for 25 s) and DCM (five times each with 2 mL for 25 s). The procedure is repeated three times. The temperature of the reaction vessel is decreased to -20 °C for the next module.

Action	Cycles	Solution	Amount	T (°C)	Incubation time
Heating	-	-	-	25	(5 min)*

Wash	3	DMF	2 mL	25	25 s
Deliver	1	Fmoc depr. solution	2 mL	25	5 min
Wash	1	DMF	2 mL		
Cooling	-	-	-	-20	-
Wash	3	DMF	2 mL	< 25	25 s
Wash	5	DCM	2 mL	< 25	25 s

4.8.4.4 Post-synthesizer manipulations

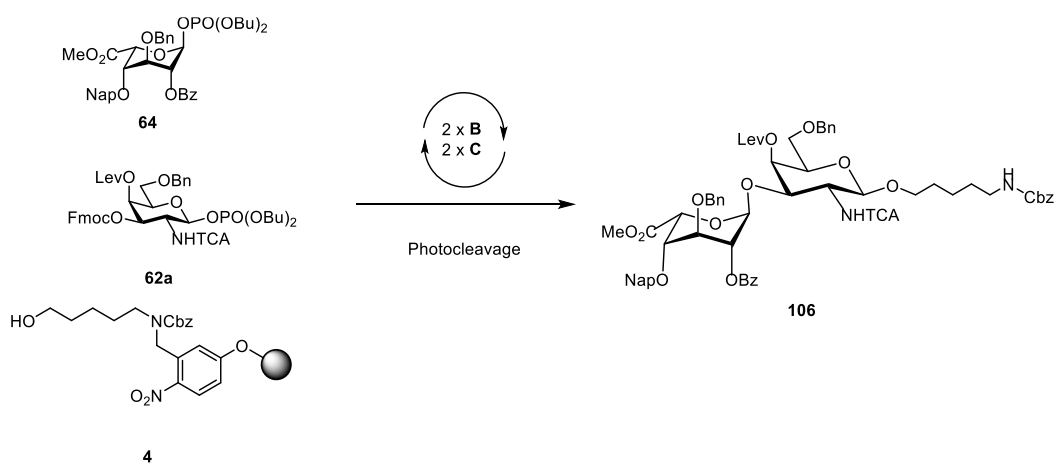
Cleavage from Solid Support

After automated synthesis, the oligosaccharides were cleaved from the solid support using a continuous-flow photoreactor as described previously.⁹¹

Purification

Solvent is evaporated *in vacuo* and the crude products were analyzed and purified using analytical and preparative HPLC (Agilent 1200 Series spectrometer).

Synthesis of disaccharide



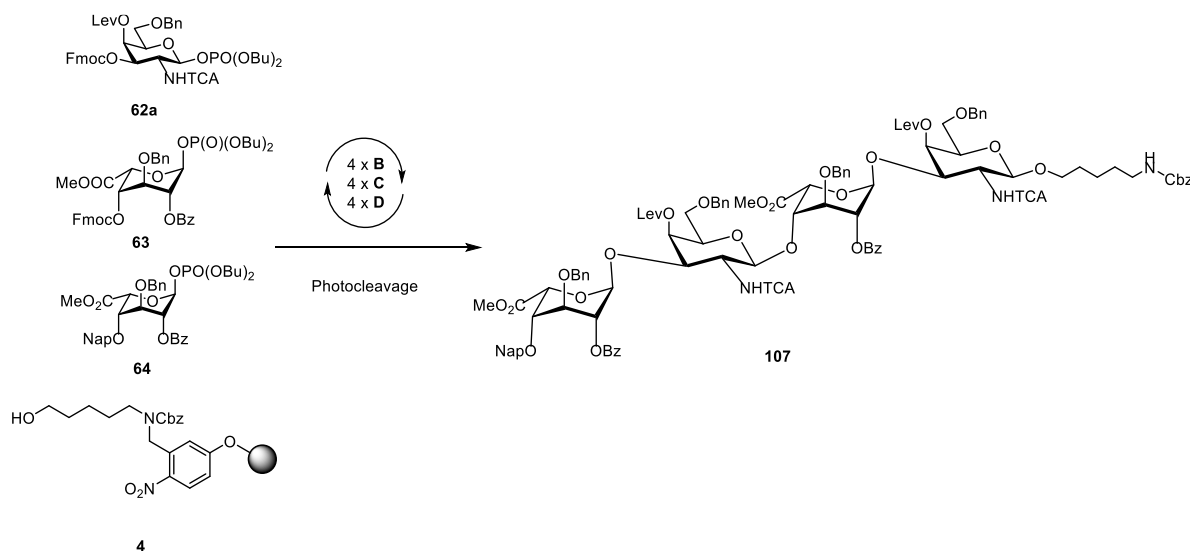
Module	Conditions
A: Resin Preparation for Synthesis	
B: Acidic Wash with TMSOTf Solution	
C: Phosphate Glycosylation	2x 62a 5 eq (-20°C for 5 min, 0°C for 20 min)
D: Fmoc Deprotection	
B: Acidic Wash with TMSOTf Solution	
C: Phosphate Glycosylation	2x 64 5 eq (-20°C for 5 min, 0°C for 20 min)

min)

Cleavage from the solid support as described in *Post-synthesizer manipulation* followed by purification using preparative HPLC afforded compound **106** (28.3 mg, 66%).

Analytical data for **106**: ^1H NMR (400 MHz, Chloroform-*d*) δ 8.13 (d, $J = 8.6$ Hz, 1H), 8.03 (m, $J = 2\text{H}$), 7.91–7.87 (m, 1H), 7.85 (d, $J = 8.3$ Hz, 1H), 7.63 – 7.49 (m, 4H), 7.45 – 7.41 (m, 3H), 7.39 – 7.27 (m, 15H), 6.97 (d, $J = 7.2$ Hz, 1H), 5.52 (d, $J = 3.2$ Hz, 1H), 5.27 (d, $J = 2.5$ Hz, 1H), 5.20 (s, 1H), 5.18 – 5.14 (m, 1H), 5.09 (d, $J = 4.6$ Hz, 1H), 5.02 (s, 2H), 4.99 (d, $J = 2.0$ Hz, 1H), 4.90 (d, $J = 8.3$ Hz, 1H), 4.79 – 4.64 (m, 2H), 4.54 (d, $J = 10.8$ Hz, 1H), 4.48 (d, $J = 2.1$ Hz, 2H), 3.93 – 3.87 (m, 1H), 3.82 (d, $J = 10.8$ Hz, 2H), 3.78 (s, 3H), 3.72 – 3.61 (m, 1H), 3.58 – 3.54 (m, 1H), 3.53 – 3.41 (m, 2H), 3.18 – 3.14 (m, 2H), 2.57 – 2.54 (m, 1H), 2.46 – 2.42 (m, 1H), 2.32 – 2.29 (m, 1H), 2.19 – 2.09 (m, 1H), 2.08 (s, 3H), 1.65 – 1.56 (m, 2H), 1.56 – 1.45 (m, 2H), 1.43 – 1.32 (m, 2H); ^{13}C NMR (101 MHz, Chloroform-*d*) δ 205.3, 172.7, 169.9, 169.8, 168.7, 164.9, 163.2, 157.2, 138.2, 137.4, 136.3, 134.0, 133.6, 133.3, 131.1, 129.8, 129.7, 129.0, 128.8, 128.5, 128.4, 128.4, 128.1, 127.9, 127.8, 127.7, 127.6, 126.8, 126.4, 125.6, 123.8, 100.8, 99.2, 75.3, 73.8, 72.2, 72.0, 71.8, 69.8, 69.3, 68.2, 67.9, 67.2, 66.3, 66.1, 56.2, 52.9, 42.7, 36.4, 31.6, 28.5, 27.4, 27.0, 23.1, 20.3. MS (ESI) m/z calcd for $\text{C}_{65}\text{H}_{69}\text{Cl}_3\text{N}_2\text{O}_{17}$ $[\text{M}+\text{Na}]^+$ 1289.6. Found 1289.3.

Synthesis of tetrasaccharide **107**



Module

Conditions

A: Resin Preparation for Synthesis

B: Acidic Wash with TMSOTf Solution

C: Phosphate Glycosylation **2x62a** 5 eq (-20° for 5 min, 0° for 20 min)

D: Fmoc Deprotection

B: Acidic Wash with TMSOTf Solution

C: Phosphate Glycosylation **2x63** 5 eq (-20° for 5 min, 0° for 20 min)

D: Fmoc Deprotection

B: Acidic Wash with TMSOTf Solution

C: Phosphate Glycosylation **2x62a** 5 eq (-20° for 5 min, 0° for 20 min)

D: Fmoc Deprotection

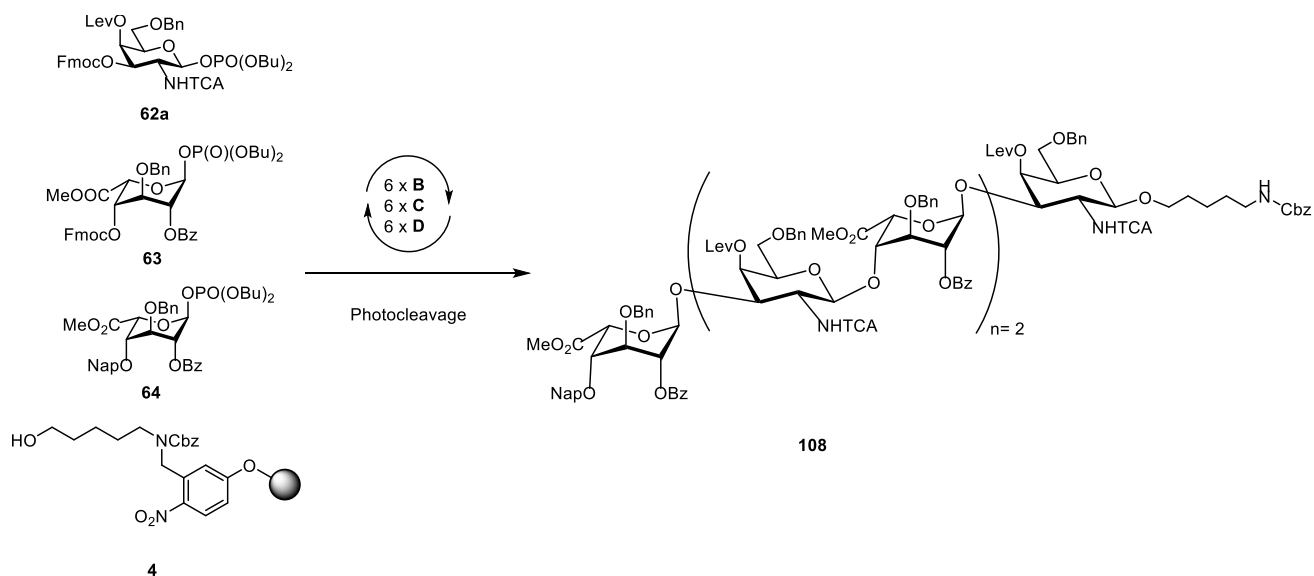
B: Acidic Wash with TMSOTf Solution

C: Phosphate Glycosylation **2x64** 5 eq (-20° for 5 min, 0° for 20 min)

Cleavage from the solid support as described in *Post-synthesizer manipulation* followed by purification using preparative HPLC afforded compound **107** (36 mg, 42%).

Analytical data for **107**: ¹H NMR (400 MHz, CDCl₃) δ: 8.20–7.85 (m, 4H), 7.66 – 7.56 (m, 1H), 7.54 – 7.20 (m, 35H), 7.06 (d, *J* = 7.4 Hz, 1H), 6.86 (d, *J* = 7.8 Hz, 1H), 5.52 (d, *J* = 3.0 Hz, 1H), 5.34 (d, *J* = 3.0 Hz, 1H), 5.23 – 5.17 (m, 2H), 5.13 – 5.04 (m, 4H), 5.01 (s, 2H), 4.96–4.79 (m, 4H), 4.79 – 4.61 (m, 4H), 4.55 – 4.40 (m, 3H), 4.36 (q, *J* = 11.8 Hz, 3H), 4.24 (dd, *J* = 10.2, 3.5 Hz, 1H), 4.06 (dd, *J* = 9.6, 5.2 Hz, 2H), 3.91 (dd, *J* = 9.2, 5.9 Hz, 1H), 3.83 – 3.74 (m, 2H), 3.71 (s, 3H), 3.73 – 3.61 (m, 8H), 3.56 (dd, *J* = 10.0, 6.0 Hz, 1H), 3.48 (dd, *J* = 10.0, 6.2 Hz, 2H), 3.18 (m, 3H), 2.38–2.16 (m, 2H), 2.12 – 2.04 (m, 2H), 2.00 (s, 3H), 1.98 (s, 3H), 1.85 - 1.72 (m, 3H), 1.58 – 1.52 (m, 3H), 1.50 – 1.42 (m, 2H), 1.33 – 1.26 (m, 2H). ¹³C NMR (101 MHz, CDCl₃) δ 206.2, 206.0, 171.9, 171.8, 169.7, 169.6, 168.7, 165.0, 164.6, 162.1, 162.0, 156.3, 137.9, 137.9, 137.7, 137.6, 136.5, 134.0, 133.5, 133.3, 133.1, 129.9, 129.8, 129.7, 129.6, 129.0, 128.5, 128.4, 128.4, 128.3, 128.3, 128.2, 128.2, 128.0, 127.8, 127.8, 127.8, 127.7, 127.7, 127.7, 127.5, 126.6, 126.2, 125.4, 123.7, 101.0, 101.0, 100.7, 99.2, 92.2, 92.2, 77.2, 76.3, 75.2, 74.1, 73.8, 73.5, 73.4, 72.8, 72.7, 72.5, 72.3, 69.8, 69.4, 68.9, 68.3, 68.2, 67.8, 66.9, 66.8, 66.7, 66.5, 66.4, 56.1, 55.3, 54.3, 52.4, 52.3, 40.8, 37.7, 37.5, 31.7, 29.6, 29.5, 28.8, 27.6, 27.2, 23.2, 20.5. m/z (MALDI-TOF) m/z calcd for C₁₀₆H₁₁₁Cl₆N₃O₃₁ [M+Na]⁺ 2158.730. Found 2158.452.

Synthesis of hexasaccharide 108



Module	Conditions
A: Resin Preparation for Synthesis	
B: Acidic Wash with TMSOTf Solution	
C: Phosphate Glycosylation	2x62a 5 eq (-20° for 5 min, 0° for 20 min)
D: Fmoc Deprotection	
B: Acidic Wash with TMSOTf Solution	
C: Phosphate Glycosylation	2x63 5 eq (-20° for 5 min, 0° for 20 min)
D: Fmoc Deprotection	
B: Acidic Wash with TMSOTf Solution	
C: Phosphate Glycosylation	2x62a 5 eq (-20° for 5 min, 0° for 20 min)
D: Fmoc Deprotection	
B: Acidic Wash with TMSOTf Solution	
C: Phosphate Glycosylation	2x63 5 eq (-20° for 5 min, 0° for 20 min)
D: Fmoc Deprotection	

B: Acidic Wash with TMSOTf Solution

C: Phosphate Glycosylation **2x62a** 5 eq (-20° for 5 min, 0° for 20 min)

D: Fmoc Deprotection

B: Acidic Wash with TMSOTf Solution

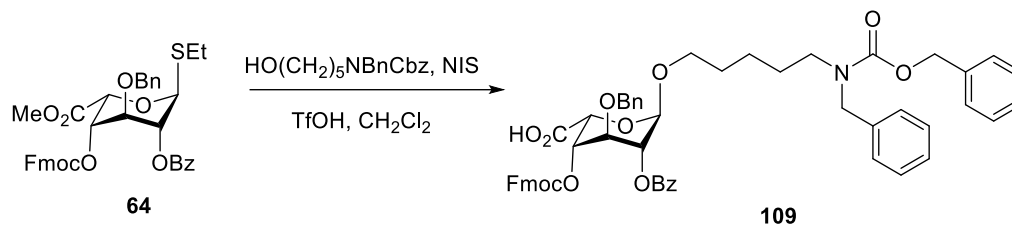
C: Phosphate Glycosylation **2xBB** 5 eq (-20° for 5 min, 0° for 20 min)

Cleavage from the solid support as described in *Post-synthesizer manipulation* followed by purification using preparative HPLC afforded compound **108** (44 mg, 28%).

Analytical data for **108**: ¹H NMR (400 MHz, CDCl₃) δ: 8.19–7.81 (m, 4H), 7.63 – 7.56 (m, 1H), 7.54 – 7.22 (m, 50H), 7.12 (d, *J* = 7.4 Hz, 1H), 6.91 (d, *J* = 7.6 Hz, 1H), 5.50 (d, *J* = 3.0 Hz, 1H), 5.34 (d, *J* = 3.0 Hz, 1H), 5.27 (d, *J* = 3.0 Hz, 1H), 5.25 – 5.16 (m, 3H), 5.12 – 5.02 (m, 6H), 5.00 (s, 2H), 4.98–4.80 (m, 7H), 4.80 – 4.63 (m, 5H), 4.58 – 4.32 (m, 10H), 4.26 – 4.08 (m, 4H), 3.91 – 3.61 (m, 16H), 3.58 – 3.42 (m, 6H), 3.22 – 3.16 (m, 5H), 2.44–2.14 (m, 6H), 2.13 – 2.00 (m, 6H), 1.99 – 1.96 (m, 9H), 1.63 – 1.48 (m, 2H), 1.54 – 1.44 (m, 2H), 1.38 – 1.23 (m, 2H). ¹³C NMR (101 MHz, CDCl₃) δ 207.3, 206.4, 171.9, 171.8, 171.7, 170.2, 169.6, 169.4, 168.8, 166.2, 165.4, 165.2, 163.8, 162.5, 162.3, 162.2, 158.9, 137.9, 137.8, 137.7, 137.6, 137.4, 137.2, 134.9, 134.6, 133.8, 133.6, 133.2, 130.9, 129.9, 129.8, 129.2, 129.1, 128.9, 128.0, 127.9, 127.6, 127.5, 127.3, 127.2, 127.1, 126.9, 126.8, 126.5, 126.4, 125.2, 124.6, 101.9, 101.6, 101.4, 98.3, 94.4, 94.2, 78.5, 78.3, 78.2, 75.5, 74.4, 73.9, 73.6, 73.5, 72.7, 72.6, 72.4, 70.6, 70.4, 69.9, 69.5, 69.3, 68.8, 68.6, 67.8, 66.6, 66.5, 66.3, 66.2, 66.0, 65.8, 64.2, 56.6, 55.8, 55.3, 54.8, 54.3, 42.6, 36.9, 35.9, 34.8, 34.2, 29.8, 28.9, 28.6, 28.5, 26.9, 22.4, 21.8. *m/z* (MALDI-TOF) *m/z* calcd for C₁₄₇H₁₅₃Cl₉N₄O₄₅ [M+Na]⁺ 3037.862. Found 3035.228.

4.8.5 Synthesis of disulfated iduronic acid.

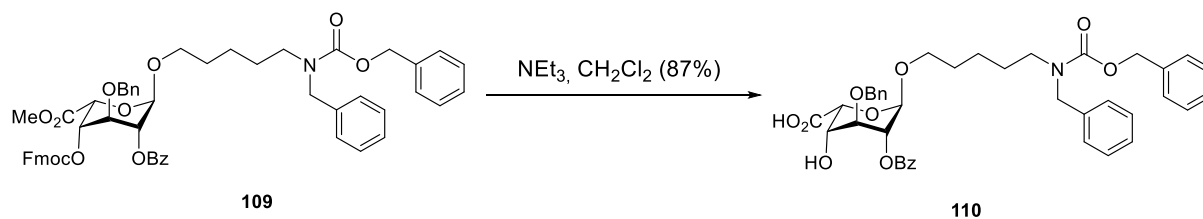
Synthesis of Methyl N-benzyl-(benzyloxycarbonyl)-5-aminopentyl 2-O-benzoyl-3-O-benzyl-4-fluorenylmethyloxycarbonyl- α -L-idopyranosyl urinate 109



To a solution of **64** (110 mg, 0.16 mmol) and (HO)(CH₂)₅NBnCBz (269 mg, 0.82 mmol) in anhydrous DCM (20 mL) molecular sieves (4 Å, powder) were added. The mixture was stirred for 10 minutes before NIS (56 mg, 0.25 mmol) was added. After stirring for 20 minutes the reaction mixture was cooled down to -15°C before TFOH (0.015 mL, 0.16 mmol) was added dropwise to the reaction mixture. The reaction mixture was stirred for 20 minutes and allowed to warm to room temperature. The reaction was successively quenched by saturated NaHCO₃ solution (15 mL) and saturated Na₂S₂O₃ solution. The organic layer was washed with brine (3x 15 mL), dried over Na₂SO₄ and concentrated in vacuum. The crude product was purified by column chromatography (silica gel, hexane – EtOAc, 1:5 to 1:1), giving **109** (120 mg, 0.128 mmol, 78%) as white crystallizing syrup R_f = 0.82 (hexane – EtOAc, 1:1).

Analytical data for **109**: ¹H NMR (400 MHz, CDCl₃) δ 8.12 (d, *J* = 7.1 Hz, 2H), 7.74 (d, *J* = 7.6 Hz, 1H), 7.72 – 7.68 (m, 1H), 7.59 (d, *J* = 7.5 Hz, 1H), 7.49 – 7.11 (m, 23H), 5.23 – 4.98 (m, 5H), 4.83 (d, *J* = 11.6 Hz, 1H), 4.77 – 4.67 (m, 1H), 4.47 (d, *J* = 7.3 Hz, 2H), 4.34 (dd, *J* = 10.3, 8.0 Hz, 1H), 4.22 (dd, *J* = 10.3, 7.3 Hz, 1H), 4.04 – 3.97 (m, 2H), 3.82 – 3.68 (m, 1H), 3.79 (s, 3H), 3.49 (d, *J* = 20.1 Hz, 1H), 3.18 (d, *J* = 27.2 Hz, 2H), 1.65 – 1.45 (m, 4H), 1.35 – 1.20 (m, 2H). MS (ESI) *m/z* calcd for C₅₆H₅₅NO₁₂ [M+Na]⁺ 956.4. Found 956.2

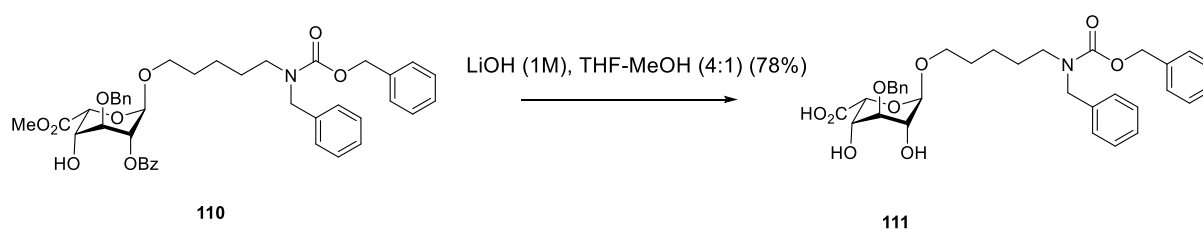
Synthesis of Methyl N-benzyl-(benzyloxycarbonyl)-5-aminopentyl 2-O-benzoyl-3-O-benzyl- α -L-idopyranosyl uronate 110



To a solution of **109** (68 mg, 0.073 mmol) in DCM (50 mL), Et₃N (1 mL, 7.16 mmol) was added dropwise. The reaction mixture was stirred for 5 hours. Then, all the volatiles were evaporated in vacuum, the residue was dissolved in DCM (20 mL), washed with brine (3x 10 mL), dried over Na₂SO₄ and concentrated in vacuum. The crude product was purified by column chromatography (silica gel, hexane – EtOAc, 1:3 to 1:1), giving **S9** (45 mg, 0.063 mmol, 87%) as yellow syrup. R_f = 0.61 (hexane – EtOAc, 1:1).

Analytical data for **110**: ¹H NMR (400 MHz, CDCl₃) δ 7.99 (dd, *J* = 8.4, 1.2 Hz, 2H), 7.59 (t, *J* = 7.4 Hz, 1H), 7.47 – 7.42 (m, 2H), 7.39 – 7.13 (m, 15H), 5.24 – 5.13 (m, 3H), 5.11 – 5.05 (m, 1H), 4.89 (s, 1H), 4.82 (d, *J* = 11.1 Hz, 1H), 4.63 (d, *J* = 11.7 Hz, 1H), 4.47 (d, *J* = 9.8 Hz, 2H), 4.10 (d, *J* = 10.2 Hz, 1H), 3.82 (s, 3H), 3.77 (s, 1H), 3.46 (d, *J* = 14.7 Hz, 2H), 3.26 – 3.11 (m, 2H), 1.67 – 1.43 (m, 4H), 1.37 – 1.22 (m, 2H). MS (ESI) *m/z* calcd for C₄₁H₄₅NO₁₀ [M+Na]⁺ 734.3. Found 734.0

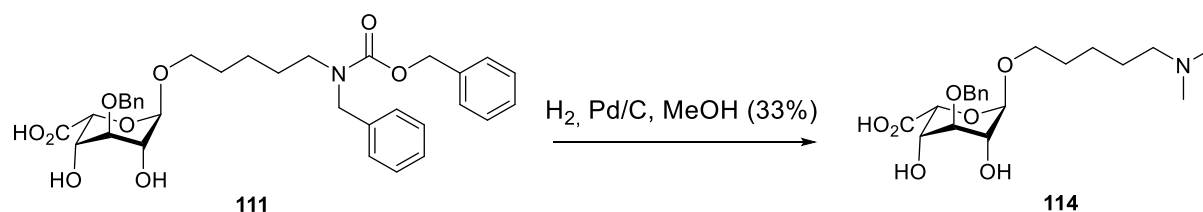
Synthesis of *N*-Benzyl-(benzyloxycarbonyl)-5-aminopentyl 3-*O*-benzyl- α -L-idopyranosyluronate **111**



To a solution of **110** (45 mg, 0.063 mmol) MeOH/THF (15 mL, 1:4), LiOH (0.4 mL, 0.4 mmol, 1 M in solvent) was added. The reaction was stirred for 30 minutes. Afterwards all volatiles were evaporated in vacuum yielding crude **111** (30 mg, 0.050 mmol, 78%) as a white powder. The compound was used in the next step without further purification.

MS (ESI) *m/z* calcd for C₃₃H₃₉NO₉ [M+Na]⁺ 616.3. Found 616.0

Synthesis of *N,N*-Dimethyl-5-aminopentyl α -L-idopyranosyluronate **114**



Argon was bubbled through a solution of **111** (20 mg, 0.033 mmol) in methanol (10 mL) for 10 minutes. To this solution Pd/C (20 mg, 0.019 mmol, 10wt%) was added. Argon was bubbled through this slurry for 10 minutes, before hydrogen was bubbled through the slurry for 10 minutes. The reaction mixture was stirred at for 48 h under hydrogen

atmosphere. The suspension was filtered over Celite®, concentrated in vacuum and purified by size-exclusion column chromatography (Sephadex® LH-20, water) giving compound 114 (4.4 mg, 0.011 mmol, 33%) as slightly yellow solid after lyophilization.

Analytical data for **114**: ^1H NMR (400 MHz, CD_3OD) δ 4.73 – 4.64 (m, 1H), 4.32 – 4.23 (m, 1H), 3.92 – 3.81 (m, 1H), 3.75 – 3.67 (m, 1H), 3.67 – 3.61 (m, 1H), 3.61 – 3.46 (m, 2H), 3.36 – 3.34 (m, 1H), 3.28 – 3.20 (m, 1H), 2.72 (s, 6H), 1.77 – 1.59 (m, 4H), 1.55 – 1.40 (m, 2H). ^{13}C NMR (CD_3OD) 175.72, 100.51, 72.93, 72.12, 71.16, 70.88, 67.97, 57.90, 42.43, 28.31, 24.21, 22.68. MS (ESI) m/z calcd for $\text{C}_{13}\text{H}_{25}\text{NO}_7$ $[\text{M}+\text{H}]^+$ 308.2. Found 308.2

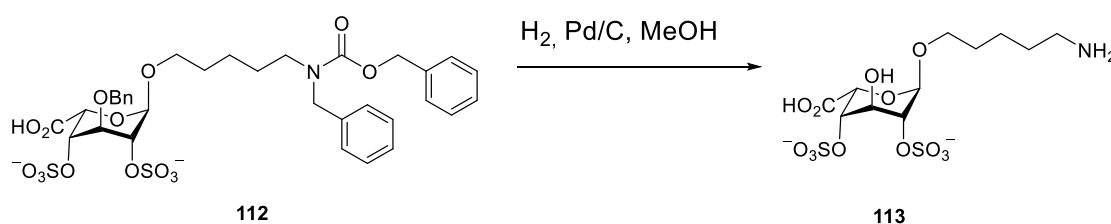
Synthesis of compound 112



To a solution of **111** (60.0 mg) in anhydrous pyridine (4.0 mL), was added SO_3 ·pyridine (0.16 g). The reaction mixture was stirred at RT for 24 h, quenched by the addition of MeOH (0.5 mL) and triethylamine (0.1 mL), and concentrated. The residue was purified by a Sephadex LH-20 chromatography (MeOH– CH_2Cl_2 , 1:1, vol/vol). The obtained product was converted into the Na salt by passing through a column of Dowex 50WX8 (Na^+) in MeOH– H_2O (9:1, vol/vol) to give **112** (64 mg, 85%).

Analytical data for **112**: ^1H NMR (CD_3OD) δ 7.38–7.07 (m, 15H), 5.20–5.05 (m, 3H), 4.87–4.64 (m, 4H), 4.50–4.35 (m, 4H), 3.61 (br, 1H), 3.44 (br, 1H), 3.13 (br, 4H), 1.08–1.66 (m, 6H). MS (ESI) m/z calcd. $[\text{M}^{3-}+2\text{H}]^-$ 616.3, found 616.3.

Synthesis of compound 113



A solution of **112** (39.0 mg) in MeOH– H_2O (2:1, vol/vol, 3 mL) was bubbled by Ar for 10 min. To the solution, was added 10% Pd/C (16 mg). The mixture was bubbled by Ar for 10 min then by H_2 for 15 min, and stirred at RT for 24 h. The suspension was filtered and concentrated to give **113** (21.7 mg, 96%) as a colorless foam.

Analytical data for **113**: ^1H NMR (D_2O) δ 4.98 (br s, 1H), 4.45 (br, 2H), 4.37 (br s, 1H), 4.07 (br s, 1H), 3.61 (br, 1H), 3.53 (br, 1H), 2.87 (br, 2H), 1.55 (br, 4H), 1.33 (br, 2H). ^{13}C NMR (D_2O) δ 174.8, 98.3, 74.6, 73.5, 68.2, 66.4, 66.3, 39.4, 27.8, 26.3, 22.2. $[\text{M}^{3+}+2\text{H}]^-$ 438.0, found 438.0.

5 References

1. A. C. Varki, R. D. E., J. D., Freeze, H. H.; Stanley, P; Bertozzi, C. R.; Hart, G. W.; Etzler, M. E.; Eds., *Essentials of Glycobiology* **2009**, (Cold Spring Harbor, NY).
2. Buléon, A.; Colonna, P.; Planchot, V.; Ball, S., Starch granules: structure and biosynthesis. *International Journal of Biological Macromolecules* **1998**, *23* (2), 85-112.
3. Augustat, S.; Whistler, R. L.; Paschall, E. F., Starch Chemistry and Technology. *Academic Press, New York and London* **1965**, *19* (1), 24-25.
4. Roach, P. J.; Depaoli-Roach, A. A.; Hurley, T. D.; Tagliabracci, V. S., Glycogen and its metabolism: some new developments and old themes. *The Biochemical journal* **2012**, *441* (3), 763-787.
5. Klemm, D.; Heublein, B.; Fink, H.-P.; Bohn, A., Cellulose: Fascinating Biopolymer and Sustainable Raw Material. *Angewandte Chemie International Edition* **2005**, *44* (22), 3358-3393.
6. Cohen, E., Chitin synthesis and inhibition: a revisit. *Pest Management Science* **2001**, *57* (10), 946-950.
7. Ward, H. D.; Alroy, J.; Lev, B. I.; Keusch, G. T.; Pereira, M. E., Identification of chitin as a structural component of Giardia cysts. *Infection and Immunity* **1985**, *49* (3), 629-634.
8. Dwek, R. A., Glycobiology: Toward Understanding the Function of Sugars. *Chemical Reviews* **1996**, *96* (2), 683-720.
9. Boltje, T. J.; Buskas, T.; Boons, G.-J., Opportunities and challenges in synthetic oligosaccharide and glycoconjugate research. *Nature Chemistry* **2009**, *1*, 611.
10. Bertozzi, C. R.; Kiessling; L., L., Chemical Glycobiology. *Science* **2001**, *291* (5512), 2357-2364.
11. Imperiali, B.; O'Connor, S. E., Effect of N-linked glycosylation on glycopeptide and glycoprotein structure. *Current Opinion in Chemical Biology* **1999**, *3* (6), 643-649.
12. Heinz, E., *Plant glycolipids: Structure, isolation and analysis*. 2012; p 211-332.
13. Wormald, M. R.; Petrescu, A. J.; Pao, Y.-L.; Glithero, A.; Elliott, T.; Dwek, R. A., Conformational Studies of Oligosaccharides and Glycopeptides: Complementarity of NMR, X-ray Crystallography, and Molecular Modelling. *Chemical Reviews* **2002**, *102* (2), 371-386.
14. Yang, L.; Zhang, L.-M., Chemical structural and chain conformational characterization of some bioactive polysaccharides isolated from natural sources. *Carbohydrate Polymers* **2009**, *76* (3), 349-361.

15. Grindley, T. B., Structure and Conformation of Carbohydrates. In *Glycoscience: Chemistry and Chemical Biology*, Fraser-Reid, B. O.; Tatsuta, K.; Thiem, J., Eds. Springer Berlin Heidelberg: Berlin, Heidelberg, 2008; pp 3-55.
16. Rao, V. S. R.; Qasba, P. K.; Balaji, P. V.; Chandrasekaran, R., *Conformation of Carbohydrates*. Harwood Academic Publishers,: 1998; Vol. 41.
17. Edward, J. T., Stability of glycosides to acid hydrolysis. *Chem. Ind. Eng.* **1955**, 1102-1104.
18. Tvaroška, I.; Bleha, T., Anomeric and Exo-Anomeric Effects in Carbohydrate Chemistry. In *Advances in Carbohydrate Chemistry and Biochemistry*, Tipson, R. S.; Horton, D., Eds. Academic Press: 1989; Vol. 47, pp 45-123.
19. Valcarcel, J.; Novoa-Carballal, R.; Pérez-Martín, R. I.; Reis, R. L.; Vázquez, J. A., Glycosaminoglycans from marine sources as therapeutic agents. *Biotechnology Advances* **2017**, *35* (6), 711-725.
20. Wilson, R.; Diseberg, A. F.; Gordon, L.; Zivkovic, S.; Tatarczuch, L.; Mackie, E. J.; Gorman, J. J.; Bateman, J. F., Comprehensive Profiling of Cartilage Extracellular Matrix Formation and Maturation Using Sequential Extraction and Label-free Quantitative Proteomics. *Molecular & Cellular Proteomics : MCP* **2010**, *9* (6), 1296-1313.
21. Widyaningsih, T. D.; Rukmi, W. D.; Sofia, E.; Wijayanti, S. D.; Wijayanti, N.; Ersalia, R.; Rochmawati, N.; Nangin, D., Extraction of Glycosaminoglycans Containing Glucosamine and Chondroitin Sulfate from Chicken Claw Cartilage. *2017* **2017**, *3* (3), 9.
22. Volpi, N., Dermatan sulfate from beef mucosa: structure, physicochemical and biological properties of fractions prepared by chemical depolymerization and anion-exchange chromatography. *Carbohydrate Research* **1994**, *255* (Supplement C), 133-144.
23. Roughley, P. J.; White, R. J., The dermatan sulfate proteoglycans of the adult human meniscus. *Journal of Orthopaedic Research* **1992**, *10* (5), 631-637.
24. Lin, N.; Mo, X.; Yang, Y.; Zhang, H., Purification and sequence characterization of chondroitin sulfate and dermatan sulfate from fishes. *Glycoconjugate Journal* **2017**, *34* (2), 241-253.
25. Calabrò, M. L.; Galtieri, V.; Cutroneo, P.; Tommasini, S.; Ficarra, P.; Ficarra, R., Study of the extraction procedure by experimental design and validation of a LC method for determination of flavonoids in Citrus bergamia juice. *Journal of Pharmaceutical and Biomedical Analysis* **2004**, *35* (2), 349-363.
26. Pelkonen, S.; Häyrynen, J.; Finne, J., Polyacrylamide gel electrophoresis of the capsular polysaccharides of Escherichia coli K1 and other bacteria. *Journal of Bacteriology* **1988**, *170* (6), 2646-2653.
27. Hufnagel, M.; Hancock, L. E.; Koch, S.; Theilacker, C.; Gilmore, M. S.; Huebner, J., Serological and Genetic Diversity of Capsular Polysaccharides in

- Enterococcus faecalis. *Journal of Clinical Microbiology* **2004**, *42* (6), 2548-2557.
28. Volpi, N., Application of high-performance capillary electrophoresis to the purification process of Escherichia coli K4 polysaccharide. *Journal of Chromatography B* **2004**, *811* (2), 253-256.
29. Sears, P.; Wong, C.-H., Toward Automated Synthesis of Oligosaccharides and Glycoproteins. *Science* **2001**, *291* (5512), 2344-2350.
30. Li, L.; Liu, Y.; Ma, C.; Qu, J.; Calderon, A. D.; Wu, B.; Wei, N.; Wang, X.; Guo, Y.; Xiao, Z.; Song, J.; Sugiarto, G.; Li, Y.; Yu, H.; Chen, X.; Wang, P. G., Efficient chemoenzymatic synthesis of an N-glycan isomer library. *Chemical Science* **2015**, *6* (10), 5652-5661.
31. Varki, A. C., R. D.; Esko, J. D., Freeze, H. H.; Stanley, P; Bertozzi, C. R.; Hart, G. W.; Etzler, M. E.; Eds., *Essentials of Glycobiology*. Cold Spring Harbor, NY: 2009.
32. Murata, T.; Usui, T., Enzymatic synthesis of oligosaccharides and neoglycoconjugates. *Biosci Biotechnol Biochem* **2006**, *70* (5), 1049-59.
33. Chen, C.; Zhang, Y.; Xue, M.; Liu, X.-w.; Li, Y.; Chen, X.; Wang, P. G.; Wang, F.; Cao, H., Sequential one-pot multienzyme (OPME) synthesis of lacto-N-neotetraose and its sialyl and fucosyl derivatives. *Chemical Communications* **2015**, *51* (36), 7689-7692.
34. Muthana, M. M.; Qu, J.; Li, Y.; Zhang, L.; Yu, H.; Ding, L.; Malekan, H.; Chen, X., Efficient one-pot multienzyme synthesis of UDP-sugars using a promiscuous UDP-sugar pyrophosphorylase from *Bifidobacterium longum* (BLUSP). *Chemical Communications* **2012**, *48* (21), 2728-2730.
35. Chen, Y.; Thon, V.; Li, Y.; Yu, H.; Ding, L.; Lau, K.; Qu, J.; Hie, L.; Chen, X., One-pot three-enzyme synthesis of UDP-GlcNAc derivatives. *Chemical Communications* **2011**, *47* (38), 10815-10817.
36. Yu, H.; Li, Y.; Zeng, J.; Thon, V.; Nguyen, D. M.; Ly, T.; Kuang, H. Y.; Ngo, A.; Chen, X., Sequential One-Pot Multienzyme Chemoenzymatic Synthesis of Glycosphingolipid Glycans. *The Journal of Organic Chemistry* **2016**, *81* (22), 10809-10824.
37. Koenigs, W.; Knorr, E., Ueber einige Derivate des Traubenzuckers und der Galactose. *Berichte der deutschen chemischen Gesellschaft* **1901**, *34* (1), 957-981.
38. Paulsen, H., Advances in Selective Chemical Syntheses of Complex Oligosaccharides. *Angewandte Chemie International Edition in English* **1982**, *21* (3), 155-173.
39. J. Martin, T.; R. Schmidt, R., Efficient sialylation with phosphite as leaving group. *Tetrahedron Letters* **1992**, *33* (41), 6123-6126.
40. Kondo, H.; Ichikawa, Y.; Wong, C. H., .beta.-Sialyl phosphite and phosphoramidite: synthesis and application to the chemoenzymic synthesis of CMP-sialic acid and sialyl oligosaccharides. *Journal of the American Chemical Society* **1992**, *114* (22), 8748-8750.

41. Hashimoto, S.-i.; Honda, T.; Ikegami, S., A rapid and efficient synthesis of 1,2-trans-[small beta]-linked glycosides via benzyl- or benzoyl-protected glycopyranosyl phosphates. *Journal of the Chemical Society, Chemical Communications* **1989**, (11), 685-687.
42. Rademann, J.; Geyer, A.; Schmidt, R. R., Solid-Phase Supported Synthesis of the Branched Pentasaccharide Moiety That Occurs in Most Complex Type N-Glycan Chains. *Angewandte Chemie International Edition* **1998**, 37 (9), 1241-1245.
43. Teruaki, M.; Takashi, N.; Shin-ichiro, S., An efficient glucosylation of alcohol using 1-thioglycoside derivative. *Chemistry Letters* **1979**, 8 (5), 487-490.
44. Liang, R.; Yan, L.; Loebach, J.; Ge, M.; Uozumi, Y.; Sekanina, K.; Horan, N.; Gildersleeve, J.; Thompson, C.; Smith, A.; Biswas, K.; Still, W. C.; Kahne, D., Parallel Synthesis and Screening of a Solid Phase Carbohydrate Library. *Science* **1996**, 274 (5292), 1520-1522.
45. Ferrier, R. J.; Hay, R. W.; Vethaviasar, N. A potentially versatile synthesis of glycosides. *Carbohydrate Research* **1973**, 27 (1), 55-61.
46. Davis, B. G.; Ward, S. J.; Rendle, P. M., Glycosyldisulfides: a new class of solution and solid phase glycosyl donors. *Chemical Communications* **2001**, (2), 189-190.
47. Mehta, S.; Mario Pinto, B., Phenylselenoglycosides as novel, versatile glycosyl donors. Selective activation over thioglycosides. *Tetrahedron Letters* **1991**, 32 (35), 4435-4438.
48. Kochetkov, N. K.; Klimov, E. M.; Malysheva, N. N., Novel highly stereospecific method of 1,2-cis-glycosylation. Synthesis of α -D-glucosyl-D-glucoses. *Tetrahedron Letters* **1989**, 30 (40), 5459-5462.
49. Fraser-Reid, B.; Merritt, J. R.; Handlon, A. L.; Andrews, C. W., The chemistry of N-pentenyl glycosides: Synthetic, theoretical, and mechanistic ramifications. In *Pure and Applied Chemistry*, 1993; Vol. 65, p 779.
50. Hanessian, S.; Banoub, J., Chemistry of the glycosidic linkage. O-glycosylations catalyzed by stannic chloride, in the D-ribofuranose and D-glucopyranose series. *Carbohydrate Research* **1977**, 59 (1), 261-267.
51. Tietze, L.-F.; Fischer, P.; Guder, H.-J., Einfache und stereoselektive synthese von α - und β -phenylglykosiden. *Tetrahedron Letters* **1982**, 23 (45), 4661-4664.
52. Kochetkov, N. K.; Backinowsky, L. V.; Tsvetkov, Y. E., Sugar thio orthoesters as glycosylating agents. *Tetrahedron Letters* **1977**, 18 (41), 3681-3684.
53. Pougny, J.-R., Anomeric Xanthates: A New Activation of the Anomeric Center for Rapid Glycosylation. *Journal of Carbohydrate Chemistry* **1986**, 5 (3), 529-535.
54. Garcia, B. A.; Poole, J. L.; Gin, D. Y., Direct Glycosylations with 1-Hydroxy Glycosyl Donors using Trifluoromethanesulfonic Anhydride and

- Diphenyl Sulfoxide. *Journal of the American Chemical Society* **1997**, *119* (32), 7597-7598.
55. Halcomb, R. L.; Danishefsky, S. J., On the direct epoxidation of glycals: application of a reiterative strategy for the synthesis of .beta.-linked oligosaccharides. *Journal of the American Chemical Society* **1989**, *111* (17), 6661-6666.
56. Hanessian, S.; Huynh, H. K.; Reddy, G. V.; Duthaler, R. O.; Katopodis, A.; Streiff, M. B.; Kinzy, W.; Oehrlein, R., Synthesis of Gal determinant epitopes, their glycomimetic variants, and trimeric clusters—relevance to tumor associated antigens and to discordant xenografts. *Tetrahedron* **2001**, *57* (16), 3281-3290.
57. Briner, K.; Vasella, A., Glycosylidene Carbenes a new approach to glycoside synthesis. Part 1. Preparation of glycosylidene-derived diaziridines and diazirines. *Helvetica Chimica Acta* **1989**, *72* (6), 1371-1382.
58. Demchenko, A. V., General Aspects of the Glycosidic Bond Formation. In *Handbook of Chemical Glycosylation*, Wiley-VCH Verlag GmbH & Co. KGaA: 2008; pp 1-27.
59. Komarova, B. S.; Orekhova, M. V.; Tsvetkov, Y. E.; Nifantiev, N. E., Is an acyl group at O-3 in glucosyl donors able to control α -stereoselectivity of glycosylation? The role of conformational mobility and the protecting group at O-6. *Carbohydrate Research* **2014**, *384* (Supplement C), 70-86.
60. Li, Z.; Zhu, L.; Kalikanda, J., Development of a highly α -selective galactopyranosyl donor based on a rational design. *Tetrahedron Letters* **2011**, *52* (43), 5629-5632.
61. Mong, K.-K. T.; Nokami, T.; Tran, N. T. T.; Nhi, P. B., Solvent Effect on Glycosylation. In *Selective Glycosylations: Synthetic Methods and Catalysts*, Wiley-VCH Verlag GmbH & Co. KGaA: 2017; pp 59-77.
62. Ishiwata, A.; Munemura, Y.; Ito, Y., Synergistic solvent effect in 1,2-cis-glycoside formation. *Tetrahedron* **2008**, *64* (1), 92-102.
63. Zhang, Z.; Ollmann, I. R.; Ye, X.-S.; Wischnat, R.; Baasov, T.; Wong, C.-H., Programmable One-Pot Oligosaccharide Synthesis. *Journal of the American Chemical Society* **1999**, *121* (4), 734-753.
64. Yang, B.; Yoshida, K.; Huang, X., Strategies for one-pot synthesis of oligosaccharides. In *Glycochemical Synthesis*, John Wiley & Sons, Inc.: 2016; pp 155-187.
65. Lee, J.-C.; Greenberg, W. A.; Wong, C.-H., Programmable reactivity-based one-pot oligosaccharide synthesis. *Nature Protocols* **2007**, *1*, 3143.
66. Ritter, T. K.; Wong, C.-H., Carbohydrate-Based Drug Discovery in the Battle against Bacterial Infections: New Opportunities Arising from Programmable One-Pot Oligosaccharide Synthesis. In *Carbohydrate-Based Drug Discovery*, Wiley-VCH Verlag GmbH & Co. KGaA: 2005; pp 899-932.
67. Lahmann, M.; Oscarson, S., One-Pot Oligosaccharide Synthesis Exploiting Solvent Reactivity Effects. *Organic Letters* **2000**, *2* (24), 3881-3882.

68. Ye, X.-S.; Wong, C.-H., Anomeric Reactivity-Based One-Pot Oligosaccharide Synthesis: A Rapid Route to Oligosaccharide Libraries. *The Journal of Organic Chemistry* **2000**, *65* (8), 2410-2431.
69. Ritter, T. K.; Mong, K.-K. T.; Liu, H.; Nakatani, T.; Wong, C.-H., A Programmable One-Pot Oligosaccharide Synthesis for Diversifying the Sugar Domains of Natural Products: A Case Study of Vancomycin. *Angewandte Chemie International Edition* **2003**, *42* (38), 4657-4660.
70. Manabe, S.; Ishii, K.; Ito, Y., N-Benzyl-2,3-oxazolidinone as a Glycosyl Donor for Selective α -Glycosylation and One-Pot Oligosaccharide Synthesis Involving 1,2-cis-Glycosylation. *Journal of the American Chemical Society* **2006**, *128* (33), 10666-10667.
71. Ley, S. V.; Priepke, H. W. M., A Facile One-Pot Synthesis of a Trisaccharide Unit from the Common Polysaccharide Antigen of Group B Streptococci Using Cyclohexane-1, 2-diacetal (CDA) Protected Rhamnosides. *Angewandte Chemie International Edition in English* **1994**, *33* (22), 2292-2294.
72. Huang, X.; Huang, L.; Wang, H.; Ye, X.-S., Iterative One-Pot Synthesis of Oligosaccharides. *Angewandte Chemie International Edition* **2004**, *43* (39), 5221-5224.
73. Wang, Z.; Xu, Y.; Yang, B.; Tiruchinapally, G.; Sun, B.; Liu, R.; Dulaney, S.; Liu, J.; Huang, X., Preactivation-Based, One-Pot Combinatorial Synthesis of Heparin-like Hexasaccharides for the Analysis of Heparin-Protein Interactions. *Chemistry – A European Journal* **2010**, *16* (28), 8365-8375.
74. Gao, J.; Guo, Z., Synthesis of a Tristearoyl Lipomannan via Preactivation-Based Iterative One-Pot Glycosylation. *The Journal of Organic Chemistry* **2013**, *78* (24), 12717-12725.
75. Wang, Z.; Zhou, L.; El-Boubbou, K.; Ye, X.-s.; Huang, X., Multi-Component One-Pot Synthesis of the Tumor-Associated Carbohydrate Antigen Globo-H Based on Preactivation of Thioglycosyl Donors. *The Journal of Organic Chemistry* **2007**, *72* (17), 6409-6420.
76. Bouhall, S. K.; Sucheck, S. J., In situ preactivation strategies for the expeditious synthesis of oligosaccharides: A review. *Journal of carbohydrate chemistry* **2014**, *33* (7-8), 347-367.
77. Wu, Y.; Xiong, D. C.; Chen, S. C.; Wang, Y. S.; Ye, X. S., Total synthesis of mycobacterial arabinogalactan containing 92 monosaccharide units. *Nat Commun* **2017**, *8*, 14851.
78. Xiong, D.-C.; Yang, A.-Q.; Yu, Y.; Ye, X.-S., 2-Pyridyl glycoside: an alternative glycosyl donor in preactivation protocol. *Tetrahedron Letters* **2015**, *56* (1), 211-214.
79. Peng, P.; Xiong, D.-C.; Ye, X.-S., ortho-Methylphenylthioglycosides as glycosyl building blocks for preactivation-based oligosaccharide synthesis. *Carbohydrate Research* **2014**, *384* (Supplement C), 1-8.
80. Machida, K.; Hirose, Y.; Fuse, S.; Sugawara, T.; Takahashi, T., Development and Application of a Solution-Phase Automated Synthesizer,

- ‘ChemKonzert’. *Chemical and Pharmaceutical Bulletin* **2010**, *58* (1), 87-93.
81. Tanaka, H.; Matoba, N.; Tsukamoto, H.; Takimoto, H.; Yamada, H.; Takahashi, T., Automated Parallel Synthesis of a Protected Oligosaccharide Library Based upon the Structure of Dimeric Lewis X by One-Pot Sequential Glycosylation. *Synlett* **2005**, *2005* (05), 0824-0828.
82. Tang, S.-L.; Pohl, N. L. B., Automated Solution-Phase Synthesis of β -1,4-Mannuronate and β -1,4-Mannan. *Organic Letters* **2015**, *17* (11), 2642-2645.
83. Song, E.-H.; Osanya, A. O.; Petersen, C. A.; Pohl, N. L. B., Synthesis of Multivalent Tuberculosis and Leishmania-Associated Capping Carbohydrates Reveals Structure-Dependent Responses Allowing Immune Evasion. *Journal of the American Chemical Society* **2010**, *132* (33), 11428-11430.
84. Jaipuri, F. A.; Pohl, N. L., Toward solution-phase automated iterative synthesis: fluorous-tag assisted solution-phase synthesis of linear and branched mannose oligomers. *Organic & Biomolecular Chemistry* **2008**, *6* (15), 2686-2691.
85. Toshiki Nokami, R. H., Yoshihiro Saigusa, Akihiro Shimizu, Chih-Yueh Liu, Kwok-Kong Tony Mong, and Jun-ichi Yoshida, Automated Solution-Phase Synthesis of Oligosaccharides via Iterative Electrochemical Assembly of Thioglycosides. *Org. Lett.* **2013**, *15* (17), 4520-4523.
86. Isoda, Y.; Sasaki, N.; Kitamura, K.; Takahashi, S.; Manmode, S.; Takeda-Okuda, N.; Tamura, J.-i.; Nokami, T.; Itoh, T., Total synthesis of TMG-chitotriomycin based on an automated electrochemical assembly of a disaccharide building block. *Beilstein Journal of Organic Chemistry* **2017**, *13*, 919-924.
87. Manmode, S.; Sato, T.; Sasaki, N.; Notsu, I.; Hayase, S.; Nokami, T.; Itoh, T., Rational optimization of the mannoside building block for automated electrochemical assembly of the core trisaccharide of GPI anchor oligosaccharides. *Carbohydrate Research* **2017**, *450* (Supplement C), 44-48.
88. Nokami, T.; Isoda, Y.; Sasaki, N.; Takaiso, A.; Hayase, S.; Itoh, T.; Hayashi, R.; Shimizu, A.; Yoshida, J.-i., Automated Electrochemical Assembly of the Protected Potential TMG-chitotriomycin Precursor Based on Rational Optimization of the Carbohydrate Building Block. *Organic Letters* **2015**, *17* (6), 1525-1528.
89. Guedes, N.; Czechura, P.; Echeverria, B.; Ruiz, A.; Michelena, O.; Martin-Lomas, M.; Reichardt, N. C., Toward the solid-phase synthesis of heparan sulfate oligosaccharides: evaluation of iduronic acid and idose building blocks. *J Org Chem* **2013**, *78* (14), 6911-34.
90. Kandasamy, J.; Schuhmacher, F.; Hahm, H. S.; Klein, J. C.; Seeberger, P. H., Modular automated solid phase synthesis of dermatan sulfate oligosaccharides. *Chem Commun (Camb)* **2014**, *50* (15), 1875-7.

91. Eller, S.; Collot, M.; Yin, J.; Hahm, H. S.; Seeberger, P. H., Automated solid-phase synthesis of chondroitin sulfate glycosaminoglycans. *Angew Chem Int Ed Engl* **2013**, *52* (22), 5858-61.
92. Dallabernardina, P.; Schuhmacher, F.; Seeberger, P. H.; Pfrengle, F., Mixed-Linkage Glucan Oligosaccharides Produced by Automated Glycan Assembly Serve as Tools To Determine the Substrate Specificity of Lichenase. *Chemistry* **2017**, *23* (13), 3191-3196.
93. Schmidt, D.; Schuhmacher, F.; Geissner, A.; Seeberger, P. H.; Pfrengle, F., Automated synthesis of arabinoxylan-oligosaccharides enables characterization of antibodies that recognize plant cell wall glycans. *Chemistry* **2015**, *21* (15), 5709-13.
94. Senf, D.; Ruprecht, C.; de Kruijff, G. H.; Simonetti, S. O.; Schuhmacher, F.; Seeberger, P. H.; Pfrengle, F., Active Site Mapping of Xylan-Deconstructing Enzymes with Arabinoxylan Oligosaccharides Produced by Automated Glycan Assembly. *Chemistry* **2017**, *23* (13), 3197-3205.
95. Routenberg Love, K.; Seeberger, P. H., Automated solid-phase synthesis of protected tumor-associated antigen and blood group determinant oligosaccharides. *Angew Chem Int Ed Engl* **2004**, *43* (5), 602-5.
96. Hahm, H. S.; Liang, C. F.; Lai, C. H.; Fair, R. J.; Schuhmacher, F.; Seeberger, P. H., Automated Glycan Assembly of Complex Oligosaccharides Related to Blood Group Determinants. *J Org Chem* **2016**, *81* (14), 5866-77.
97. Werz, D. B.; Castagner, B.; Seeberger, P. H., Automated Synthesis of the Tumor-Associated Carbohydrate Antigens Gb-3 and Globo-H: Incorporation of α -Galactosidic Linkages. *Journal of the American Chemical Society* **2007**, *129* (10), 2770-2771.
98. Seeberger, P. H., The logic of automated glycan assembly. *Acc Chem Res* **2015**, *48* (5), 1450-63.
99. Rodrigo B. Andrade, O. J. P., Luis G. Melean, and Peter H. Seeberger, Solid-Phase Oligosaccharide Synthesis: Preparation of Complex Structures Using a Novel Linker and Different Glycosylating Agents. *Org. Lett.* **1999**, *1* (11), 1811-1814.
100. Kröck, L.; Esposito, D.; Castagner, B.; Wang, C.-C.; Bindschädler, P.; Seeberger, P. H., Streamlined access to conjugation-ready glycans by automated synthesis. *Chemical Science* **2012**, *3* (5), 1617.
101. Wilsdorf, M.; Schmidt, D.; Bartetzko, M. P.; Dallabernardina, P.; Schuhmacher, F.; Seeberger, P. H.; Pfrengle, F., A traceless photocleavable linker for the automated glycan assembly of carbohydrates with free reducing ends. *Chem Commun (Camb)* **2016**, *52* (66), 10187-9.
102. Haase, P. H. S. a. W.-C., Solid-Phase Oligosaccharide Synthesis and Combinatorial Carbohydrate Libraries. *Chem. Rev.* **2000**, *100*, 4349-4393.
103. de Jong, A. R.; Volbeda, A. G.; Hagen, B.; van den Elst, H.; Overkleeft, H. S.; van der Marel, G. A.; Codée, J. D. C., A Second-Generation Tandem

- Ring-Closing Metathesis Cleavable Linker for Solid-Phase Oligosaccharide Synthesis. *European Journal of Organic Chemistry* **2013**, 2013 (29), 6644-6655.
104. Codee, J. D.; Krock, L.; Castagner, B.; Seeberger, P. H., Automated solid-phase synthesis of protected oligosaccharides containing beta-mannosidic linkages. *Chemistry* **2008**, 14 (13), 3987-94.
105. Liu, X.; Wada, R.; Boonyarattanakalin, S.; Castagner, B.; Seeberger, P. H., Automated synthesis of lipomannan backbone alpha(1-6) oligomannoside via glycosyl phosphates: glycosyl tricyclic orthoesters revisited. *Chem Commun (Camb)* **2008**, (30), 3510-2.
106. Esposito, D.; Hurevich, M.; Castagner, B.; Wang, C. C.; Seeberger, P. H., Automated synthesis of sialylated oligosaccharides. *Beilstein J Org Chem* **2012**, 8, 1601-9.
107. Geissner, A.; Seeberger, P. H., Glycan Arrays: From Basic Biochemical Research to Bioanalytical and Biomedical Applications. *Annual Review of Analytical Chemistry* **2016**, 9 (1), 223-247.
108. Schumann, B.; Hahm, H. S.; Parameswarappa, S. G.; Reppe, K.; Wahlbrink, A.; Govindan, S.; Kaplonek, P.; Pirofski, L.-a.; Witzenrath, M.; Anish, C.; Pereira, C. L.; Seeberger, P. H., A semisynthetic *Streptococcus pneumoniae* serotype 8 glycoconjugate vaccine. *Science Translational Medicine* **2017**, 9 (380).
109. Parameswarappa, Sharavathi G.; Reppe, K.; Geissner, A.; Ménová, P.; Govindan, S.; Calow, Adam D. J.; Wahlbrink, A.; Weishaupt, Markus W.; Monnanda, Bopanna P.; Bell, Roland L.; Pirofski, L.-A.; Suttorp, N.; Sander, Leif E.; Witzenrath, M.; Pereira, Claney L.; Anish, C.; Seeberger, Peter H., A Semi-synthetic Oligosaccharide Conjugate Vaccine Candidate Confers Protection against *Streptococcus pneumoniae* Serotype 3 Infection. *Cell Chemical Biology* **2016**, 23 (11), 1407-1416.
110. Seeberger, P. H.; Pereira, C. L.; Khan, N.; Xiao, G.; Diago-Navarro, E.; Reppe, K.; Opitz, B.; Fries, B. C.; Witzenrath, M., A Semi-Synthetic Glycoconjugate Vaccine Candidate for Carbapenem-Resistant *Klebsiella pneumoniae*. *Angewandte Chemie International Edition* **2017**, 56 (45), 13973-13978.
111. Lisboa, M. P.; Khan, N.; Martin, C.; Xu, F.-F.; Reppe, K.; Geissner, A.; Govindan, S.; Witzenrath, M.; Pereira, C. L.; Seeberger, P. H., Semisynthetic glycoconjugate vaccine candidate against *Streptococcus pneumoniae* serotype 5. *Proceedings of the National Academy of Sciences* **2017**, 114 (42), 11063-11068.
112. Naresh, K.; Schumacher, F.; Hahm, H. S.; Seeberger, P. H., Pushing the limits of automated glycan assembly: synthesis of a 50mer polymannoside. *Chemical Communications* **2017**, 53 (65), 9085-9088.
113. Fair, R. J.; Hahm, H. S.; Seeberger, P. H., Combination of automated solid-phase and enzymatic oligosaccharide synthesis provides access to alpha(2,3)-sialylated glycans. *Chem Commun (Camb)* **2015**, 51 (28), 6183-5.

114. Lai, C. H.; Hahm, H. S.; Liang, C. F.; Seeberger, P. H., Automated solid-phase synthesis of oligosaccharides containing sialic acids. *Beilstein J Org Chem* **2015**, *11*, 617-21.
115. Hahm, H. S.; Schlegel, M. K.; Hurevich, M.; Eller, S.; Schuhmacher, F.; Hofmann, J.; Pagel, K.; Seeberger, P. H., Automated glycan assembly using the Glycoener 2.1 synthesizer. *Proc Natl Acad Sci U S A* **2017**, *114* (17), E3385-E3389.
116. Dallabernardina, P.; Schuhmacher, F.; Seeberger, P. H.; Pfrengle, F., Automated glycan assembly of xyloglucan oligosaccharides. *Org Biomol Chem* **2016**, *14* (1), 309-13.
117. Hahm, H. S.; Hurevich, M.; Seeberger, P. H., Automated assembly of oligosaccharides containing multiple cis-glycosidic linkages. *Nat Commun* **2016**, *7*, 12482.
118. Calin, O.; Eller, S.; Seeberger, P. H., Automated polysaccharide synthesis: assembly of a 30mer mannoside. *Angew Chem Int Ed Engl* **2013**, *52* (22), 5862-5.
119. Gude, M.; Ryf, J.; White, P. D., An accurate method for the quantitation of Fmoc-derivatized solid phase supports. *Letters in Peptide Science* **2002**, *9* (4), 203-206.
120. Il'ichev, Y. V.; Schwörer, M. A.; Wirz, J., Photochemical Reaction Mechanisms of 2-Nitrobenzyl Compounds: Methyl Ethers and Caged ATP. *Journal of the American Chemical Society* **2004**, *126* (14), 4581-4595.
121. Guillier, F.; Orain, D.; Bradley, M., Linkers and Cleavage Strategies in Solid-Phase Organic Synthesis and Combinatorial Chemistry. *Chemical Reviews* **2000**, *100* (6), 2091-2158.
122. Holmes, C. P., Model Studies for New o-Nitrobenzyl Photolabile Linkers: Substituent Effects on the Rates of Photochemical Cleavage. *The Journal of Organic Chemistry* **1997**, *62* (8), 2370-2380.
123. Chatterjee, M. N.; Kay, E. R.; Leigh, D. A., Beyond Switches: Ratcheting a Particle Energetically Uphill with a Compartmentalized Molecular Machine. *Journal of the American Chemical Society* **2006**, *128* (12), 4058-4073.
124. Hattori, K.; Sajiki, H.; Hirota, K., Pd/C(en)-Catalyzed Chemoselective Hydrogenation with Retention of the N-Cbz Protective Group and its Scope and Limitations. *Tetrahedron* **2000**, *56* (43), 8433-8441.
125. Blanchard, J. E.; Withers, S. G., Rapid screening of the aglycone specificity of glycosidases: applications to enzymatic synthesis of oligosaccharides. *Chemistry & Biology* **2001**, *8* (7), 627-633.
126. Ebrahimi, M.; Placido, L.; Engel, L.; Ashaghi, K. S.; Czermak, P., A novel ceramic membrane reactor system for the continuous enzymatic synthesis of oligosaccharides. *Desalination* **2010**, *250* (3), 1105-1108.
127. Seeberger, P. H.; Pereira, C. L.; Govindan, S., Total synthesis of a *Streptococcus pneumoniae* serotype 12F CPS repeating unit hexasaccharide. *Beilstein Journal of Organic Chemistry* **2017**, *13*, 164-173.

128. Kinnaert, C.; Daugaard, M.; Nami, F.; Clausen, M. H., Chemical Synthesis of Oligosaccharides Related to the Cell Walls of Plants and Algae. *Chemical Reviews* **2017**, *117* (17), 11337-11405.
129. Bernlind, C.; Bennett, S.; Oscarson, S., Synthesis of a d,d- and l,d-heptose-containing hexasaccharide corresponding to a structure from *Haemophilus ducreyi* lipopolysaccharides. *Tetrahedron: Asymmetry* **2000**, *11* (2), 481-492.
130. Daragics, K.; Fügedi, P., Synthesis of glycosaminoglycan oligosaccharides. Part 5: Synthesis of a putative heparan sulfate tetrasaccharide antigen involved in prion diseases. *Tetrahedron* **2010**, *66* (40), 8036-8046.
131. Hahm, H. S.; Broecker, F.; Kawasaki, F.; Mietzsch, M.; Heilbronn, R.; Fukuda, M.; Seeberger, P. H., Automated Glycan Assembly of Oligo-*N*-Acetylglucosamine and Keratan Sulfate Probes to Study Virus-Glycan Interactions. *Chem* **2** (1), 114-124.
132. Yu, Y.; Kononov, A.; Delbianco, M.; Seeberger, P. H., A Capping Step During Automated Glycan Assembly Enables Access to Complex Glycans in High Yield. *Angew. Chem., Int. Ed.* **2017**, *Under review*.
133. Case, D. A. D., T. A.; Cheatham, T. E.; Simmerling, C. L.; Wang, J.; Duke, R. E.; Luo, R.; Walker, R. C.; Zhang, W.; Merz, K. M.; Roberts, B.; Hayik, S.; Roitberg, A.; Seabra, G.; Swails, J.; Goetz, A. W.; Kolossváry, I.; Wong, K. F.; Paesani, F.; Vanicek, J.; Wolf, R. M.; Liu, J.; Wu, X.; Brozell, S. R.; Steinbrecher, T.; Gohlke, H.; Cai, Q.; Ye, X.; Wang, J.; Hsieh, M. J.; Cui, G.; Roe, D. R.; Mathews, D. H.; Seetin, M. G.; Salomon-Ferrer, R.; Sagui, C.; Babin, V.; Luchko, T.; Gusarov, S.; Kovalenko, A.; Kollman, P. A. *AMBER* **12**, 2012.
134. Wang, J.; Wolf, R. M.; Caldwell, J. W.; Kollman, P. A.; Case, D. A., Development and testing of a general amber force field. *J. Comput. Chem.* **2004**, *25* (9), 1157-74.
135. Kirschner, K. N.; Yongye, A. B.; Tschampel, S. M.; Gonzalez-Outeirino, J.; Daniels, C. R.; Foley, B. L.; Woods, R. J., GLYCAM06: a generalizable biomolecular force field. *Carbohydrates. J. Comput. Chem.* **2008**, *29* (4), 622-55.
136. Xu, B.; Unione, L.; Sardinha, J.; Wu, S.; Ethève-Quellejeu, M.; Pilar Rauter, A.; Blériot, Y.; Zhang, Y.; Martín-Santamaría, S.; Díaz, D.; Jiménez-Barbero, J.; Sollogoub, M., gem-Difluorocarbadiaccharides: Restoring the exo-Anomeric Effect. *Angew. Chem., Int. Ed.* **2014**, *53* (36), 9597-9602.
137. Cremer, D.; Pople, J. A., General definition of ring puckering coordinates. *J. Am. Chem. Soc.* **1975**, *97* (6), 1354-1358.
138. Sattelle, B. M.; Almond, A., Microsecond kinetics in model single- and double-stranded amylose polymers. *Phys. Chem. Chem. Phys.* **2014**, *16* (17), 8119-8126.
139. French, A. D., Chapter 2 - Combining Computational Chemistry and Crystallography for a Better Understanding of the Structure of Cellulose. In *Adv.*

Carbohydr. Chem. Biochem., Horton, D., Ed. Academic Press: 2012; Vol. 67, pp 19-93.

140. Unione, L.; Alcalá, M.; Echeverria, B.; Serna, S.; Ardá, A.; Franconetti, A.; Cañada, F. J.; Diercks, T.; Reichardt, N.; Jiménez-Barbero, J., Fluoroacetamide Moieties as NMR Spectroscopy Probes for the Molecular Recognition of GlcNAc-Containing Sugars: Modulation of the CH– π Stacking Interactions by Different Fluorination Patterns. *Chem. – Eur. J.* **2017**, *23* (16), 3957-3965.

141. Hoogewerf, A. J.; Kuschert, G. S. V.; Proudfoot, A. E. I.; Borlat, F.; Clark-Lewis, I.; Power, C. A.; Wells, T. N. C., Glycosaminoglycans Mediate Cell Surface Oligomerization of Chemokines. *Biochemistry* **1997**, *36* (44), 13570-13578.

142. Cai, S.; Liu, Y.; Zheng Shu, X.; Prestwich, G. D., Injectable glycosaminoglycan hydrogels for controlled release of human basic fibroblast growth factor. *Biomaterials* **2005**, *26* (30), 6054-6067.

143. Varghese, S.; Hwang, N. S.; Canver, A. C.; Theprungsirikul, P.; Lin, D. W.; Elisseeff, J., Chondroitin sulfate based niches for chondrogenic differentiation of mesenchymal stem cells. *Matrix Biology* **2008**, *27* (1), 12-21.

144. Afratis, N.; Gialeli, C.; Nikitovic, D.; Tseggenidis, T.; Karousou, E.; Theocharis, A. D.; Pavão, M. S.; Tzanakakis, G. N.; Karamanos, N. K., Glycosaminoglycans: key players in cancer cell biology and treatment. *FEBS Journal* **2012**, *279* (7), 1177-1197.

145. Raghuraman, A.; Mosier, P. D.; Desai, U. R., Understanding Dermatan Sulfate–Heparin Cofactor II Interaction through Virtual Library Screening. *ACS Medicinal Chemistry Letters* **2010**, *1* (6), 281-285.

146. Zhang, X.; Pagadala, V.; Jester, H.; Lim, A. M.; Pham, T. Q.; Goulas, A. M. P.; Liu, J.; Linhardt, R. J., Chemoenzymatic synthesis of heparan sulfate and heparin oligosaccharides and NMR analysis: paving the way to a diverse library for glycobiochemists. *Chemical Science* **2017**, *8* (12), 7932-7940.

147. Jeyakumar Kandasamy, F. S., Heung Sik Hahm, James C. Kleina and Peter H. Seeberger, Modular automated solid phase synthesis of dermatan sulfate oligosaccharides. *Chem. Commun.* **2014**, *50*, 1875-1877.

148. Bongat, A. F. G.; Demchenko, A. V., Recent trends in the synthesis of O-glycosides of 2-amino-2-deoxysugars. *Carbohydrate Research* **2007**, *342* (3), 374-406.

149. Jekishan R. Parikh, W. v. E. D., Sulfur Trioxide in the Oxidation of Alcohols by Dimethyl Sulfoxide. *J. Am. Chem. Soc.* **1967**, *89*, 5505.

150. Matsushita, K.; Nakata, T.; Tamura, J.-i., The application of 2,2,2-trichloroethyl sulfate to the synthesis of chondroitin sulfate C and D. *Carbohydrate Research* **2015**, *406* (Supplement C), 76-85.

151. Nonaka, M.; Bao, X.; Matsumura, F.; Götze, S.; Kandasamy, J.; Kononov, A.; Broide, D. H.; Nakayama, J.; Seeberger, P. H.; Fukuda, M., Synthetic di-sulfated iduronic acid attenuates asthmatic response by blocking T-cell

recruitment to inflammatory sites. *Proceedings of the National Academy of Sciences* **2014**, *111* (22), 8173-8178.